PNNL-11777
M9805142 UC-2030

Composition and Quantities of Retained Gas Measured in Hanford Waste Tanks 241-U-103, S-106, BY-101, and BY-109

L. A. Mahoney
Z. I. Antoniak
J. M. Bates

December 1997

Prepared for the U.S. Department of Energy
under Contract DE-AC06-76RLO 1830

PNNL-11777

PACIFIC NORTHWEST NATIONAL LABORATORY
operated by
BATTELLE
for the
UNITED STATES DEPARTMENT OF ENERGY
under Contract DE-AC06-76RLO 1830

Printed in the United States of America

Available to DOE and DOE contractors from the Office of Scientific and Technical Information, P.O. Box 62, Oak Ridge, TN 37831; prices available from (615) 576-8401.

Available to the public from the National Technical Information Service, U.S. Department of Commerce, 5285 Port Royal Rd., Springfield, VA 22161

PNNL-11777
UC-2030

Composition and Quantities of Retained Gas Measured in Hanford Waste Tanks 241-U-103, S-106, BY-101, and BY-109

L. A. Mahoney
Z. I. Antoniak
J. M. Bates

December 1997

Prepared for
the U.S. Department of Energy
under Contract DE-AC06-76RLO 1830

Pacific Northwest National Laboratory Richland,
Washington 99352

Preface

This report was prepared to satisfy the DOE-RL milestone T22-97-006, "Complete RGS Data Analysis for 4 of 4 Flammable Gas SSTs." This task supported the deployment of the Retained Gas Sampler (RGS) system in Flammable Gas Watch List Tanks.

The emphasis of this report is on presenting the measurements resulting from retained gas sampling of Tanks U-103, S-106, BY-101, and BY-109, not on interpreting the effects of the findings on understanding tank behavior or on the safety issues. The retained gas sampling information is a direct measurement of the amount and composition of gas retained in these tanks. This information will be combined with information from other sources to develop a better understanding of the mechanisms for gas generation, retention, and release, which will lead to resolution of the Flammable Gas Safety Issue and provide a more detailed understanding of tank behavior to support retrieval operations.

Executive Summary

This report provides the results obtained for the single-shell tanks (SSTs) sampled with the Retained Gas Sampler (RGS) during 1997: Tanks 241-U-103, 241-S-106, 241-BY-101, and 241-BY-109. (Hereafter these tanks will be referred to without the "241-," following standard practice.) The RGS is a modified version of the core sampler used at Hanford. It is designed specifically to be used in concert with the gas extraction equipment in the hot cell to capture and extrude a gas-containing waste sample in a hermetically sealed system. The retained gases are then extracted and stored in small gas canisters. The composition of the gases contained in the canisters is measured by mass spectroscopy. The total gas volume in the sample is obtained from analyzing the extraction process, as discussed in detail throughout this report.

The following are the findings of this research:

- The RGS has been confirmed as a viable approach for measuring the composition of retained gases in SSTs at Hanford.
- The retained gas inventories calculated from the local measurements of gas volume fraction made by the RGS can differ significantly from the total gas inventories estimated by the barometric pressure effect (BPE) or surface level rise (SLR) methods. These discrepancies occur together with irregular waste layers and other strong indications of lateral inhomogeneity in the waste. Because the RGS samples are localized they capture little of this variation. Therefore, the BPE or SLR methods, which are related to the overall gas in the tank, must be used to supplement RGS measurements in estimating the gas inventories in high-waste-variability tanks.
- Nitrogen, an inert gas, was found to be a major component of the retained gas (more than 20 vol%) in each of the tanks that were sampled.
- In two of the tanks sampled, the ratios of hydrogen to nitrous oxide were observed to be significantly higher than 1; i.e., these tanks are fuel-rich. However, U-103 samples contained as much as 52% nitrous oxide and as little as 14% hydrogen.
- Segment 2 of U-103 contained 44 vol% of gas under in-situ conditions. This measurement was confirmed by a large gas volume shown in the sampler x-rays.
- The four SSTs that have undergone successful RGS sampling (U-103, S-106, BY-109, and A-101) in FY 1996 and FY 1997 have all shown different retained gas characteristics. Tank A-101 had a high gas fraction in an upper layer and had unusually high H_2 and NH_3 content; U-103 had a very high near-surface gas fraction, with low H_2 and high N_2O content; S-106 had unusually low NH_3 content; and BY-109 showed a composition and gas fraction that were about average for the tanks that have been RGS-sampled. Thus no single trend is immediately apparent in SST gas retention.
- BY-109, a tank that has recently been salt-well pumped, had in-situ gas fractions of 7.3 to 12% in samples taken below the interstitial liquid level (ILL), demonstrating that substantial gas fractions can be retained in pumped tanks.

- The failure of RGS sampler valves to close led to the loss of samples in FY 1997, as in FY 1996. In addition, waste impenetrability often prevented sample acquisition. Both problems contributed to our failure to obtain BY-101 RGS samples. Accordingly, the sampler design is being modified to provide stronger valve closure, to increase the likelihood of obtaining samples even from hard waste.

- The equilibration of ammonia in the RGS extractor was so slow that it was difficult to estimate the total ammonia in the sample, whether by adding a $^{15}NH_3$ standard or by mass balance methods. Despite improved process models and procedures that make it possible to account for more of the sample ammonia than in previous work (Shekarriz et al. 1997), the ammonia in the sample is still being underestimated, primarily because of slow equilibration. Further procedural improvements are being put in place to provide better ammonia estimates.

Based on this experience, the RGS will continue to be used to sample for retained gases in several SSTs at Hanford.

The remaining sections of this summary describe the RGS findings for the four tanks tested during 1997. The results are described in the order in which the tanks were sampled, to reflect the increasing experience on which RGS methods were based.

Tank 241-U-103 (U-103) Results

Tank U-103 was the sixth tank sampled using the RGS system to measure the retained gases. It is on the Flammable Gas and Organic Watch Lists. The waste in this tank was 422 cm (166 inches) deep and showed substantial variation between the two risers. At riser 7, near one wall of the tank, there was about 145 cm (57 in.) of liquid at the top of the waste, with the lower layer being saltcake. At riser 13, at the center of the tank, the top 30 cm (12 in.) was sludge slurry that contained no drainable liquid; salt slurry and saltcake made up the rest of the waste in the core.

Four samples were taken with the RGS from riser 7 in this tank. We had planned to take further samples from riser 2, but the drill string was blocked by an obstacle or hard waste. One RGS sample was taken from riser 13 but was lost because the sampler valve could not be opened for extrusion.

Retained gas measurements and estimated solubilities showed three major constituents in the gas/vapor phase (free gas): 36 mol% nitrogen, 22 mol% hydrogen, and 40 mol% nitrous oxide. (The low H_2/N_2O ratio in the retained gas, 0.55, is in accord with that measured in the dome space, which ranged from 0.7 to 0.79 in July 1995 and October 1997.)(a) The remainder of the gas content comprised ammonia, methane, and other hydrocarbons. The measured local ammonia concentrations in U-103 ranged from 2,300 to 76,000 µmol/L of waste. Integrating the local concentrations led to a total amount, if it were vapor (which is improbable), of 1500 m^3 (52,000 ft^3) of ammonia at standard temperature and pressure (STP). Based on estimated solubility, more than 99.7% of the ammonia was dissolved in the liquid. (Details of the integration are in Section 3.6.1 of the report.)

(a) Brothers JW. 1997. Composition data from samples U-103-0725-95-1505, U-103-0727-95-1425, U-103-0731-95-1410, U-103-10-22-97-1403. Pacific Northwest National Laboratory, Richland, Washington.

Based on estimated solubilities and RGS measurements of gas concentrations, about 20% by volume (in situ) of the waste in the tank was filled with free gas. The in-situ gas volume fraction ranged between 7.7 and 44%; the high value was a single measurement for the waste just under the surface. (There were indications that this high-gas region might extend beyond the single riser at which samples were successfully taken.) Because of the waste variability from one riser to another and the availability of only four RGS samples from one riser, the best estimate of the total gas inventory was considered to be that based on the BPE method, 200 ± 60 m^3 of gas at in-situ conditions, or 260 ± 70 m^3 (STP). By comparison, the inventory estimated from the RGS data was 420 ± 210 m^3 (STP). The RGS inventory was larger than the BPE inventory, perhaps because the RGS inventory was biased by a single high-gas measurement (which was taken from a riser near the tank periphery).

Two results were obtained from examining the x-ray images of various segments. First, the exceptionally high gas content (44%) of the topmost sample (segment 7-2) was confirmed by observing a large gas space in the x-ray of the sampler. The high gas content was probably not localized to the riser 7 area, because segment 13-4 (at an elevation about 48 cm below 7-2) had an equally large gas gap. Second, much of the retained gas volume (up to a gas volume fraction of about 5%) was found to be smaller than the detection threshold (<~1 mm) of the current x-ray imaging system. It was also noted that in most of the samples the waste was strong enough and cohesive enough to form a "stalactite" hanging from the piston at the top of the sampler.

Tank 241-S-106 (S-106) Results

Tank S-106 was the seventh tank sampled for measurement of the retained gases in the waste. The waste consisted of two distinct layers, an upper liquid layer ranging from 40 to 200 cm in thickness, and a lower, high-solids saltcake layer also of varying thickness (260 to 420 cm). There was also a thick, dry crust around the perimeter of the tank. The waste properties were not consistent between the two risers, suggesting that the waste was not laterally uniform in the tank.

The RGS was used in risers 7 and 8 of S-106 to sample four segments, two from each riser. Both of these risers were near the tank center. There were no RGS samples from either the perimeter crust or the upper liquid layer; such sampling was attempted but was not successful because of hard waste and sampler valve closure problems.

Retained gas measurements and estimated solubilities showed three major low-solubility constituents in the gas/vapor phase (free gas) of the high-solids layer: 24 mol% nitrogen, 63 mol% hydrogen, and 11 mol% nitrous oxide. The remainder of the gas content comprised ammonia, methane, and other hydrocarbons. The drill-string gas in S-106 had an H_2/N_2O ratio of 4.0, somewhat lower than the average RGS value of 5.7.[a] The measured local ammonia concentrations in Tank S-106 ranged from 1,100 to 6,200 µmol/L of waste, and more than 99.7% of the ammonia was dissolved in the liquid. Integrating the local concentrations led to a total amount, if it were vapor (which is improbable), of approximately 84 m^3 (3,000 ft^3) of ammonia at STP present in the high-solids layer. (Details of the integration are in Section 3.6.1.)

Based on the estimated solubilities and RGS measurements of gas concentrations, about 10% by volume (in situ) of the high-solids layer was filled with free gas. The in-situ gas volume fraction ranged between 7.3 and 14%. Because of the waste variability from one riser to another and the availability of only two RGS samples from each riser, the best estimate of the total gas

---

(a) Brothers JW. 1997. Composition data from sample S-106 riser 7 (received at the mass spectrometry lab 2/25/97). Pacific Northwest National Laboratory, Richland, Washington.

inventory was considered to be that based on the BPE method, 410 ± 130 m^3 at in-situ conditions, or 580 ± 190 m^3 (STP). By comparison, the inventory estimated from the RGS data was 230 ± 120 m^3 (STP). The RGS inventory was smaller than the BPE inventory, perhaps because the RGS inventory was biased by samples being taken only near the tank center.

X-ray images of the samplers revealed that the high-solids layer contained a number of gas pockets and gas-filled fractures. The largest bubbles, ranging from 1 cm to more than 2.5 cm across, were found in the sample taken nearest the bottom. Another sample contained 11% gas, of which all was less than the detection threshold (<~1 mm) of the current x-ray imaging system.

Tank 241-BY-101 (BY-101) Results

Tank BY-101 was the eighth tank sampled for retained gases. One RGS sample was taken at each of two risers, but further sampling was impossible because of obstructions at both risers. The samplers contained no waste that was visible in x-ray images, and upon extraction the samples proved to contain no retained gas, only air. The samples provided no useful information on the composition or quantity of the gas retained in BY-101.

Tank 241-BY-109 (BY-109) Results

Tank BY-109 was the ninth tank sampled for retained gases. The total depth of waste in BY-109 was 310 to 343 cm; it is composed of saltcake and sludge. The liquid level was below the surface because of recent salt-well pumping. The ILL was 279 cm. The waste varied between the two risers that were sampled; at riser 12C, most of the waste was sludge or salt/sludge slurry under a thin (20 cm) layer of moist saltcake, while at riser 10B the top 150 cm of waste was all saltcake and the remaining lower layer was sludge slurry or sludge.

Three segments were taken with the RGS in two risers within this tank. Both risers were located about halfway between the tank center and the tank wall, on opposite sides of the tank from each other. No RGS samples were taken above the ILL; two had been planned but were lost because of damaged piston seals. One other sample at the bottom of riser 12C had also been planned but was blocked by impenetrable waste.

Retained gas measurements and estimated solubilities showed three major constituents in the gas/vapor phase (free gas) of the waste below the ILL: 29 mol% nitrogen, 50 mol% hydrogen, and 18 mol% nitrous oxide. The remainder of the gas was composed of ammonia, methane, and other hydrocarbons. The drill-string gas in BY-109 had an H_2/N_2O ratio of 3.4, somewhat higher than the average RGS value of 2.8.[a] The measured local ammonia concentrations in BY-109 were found to range from 6,100 to 14,000 µmol/L of waste, of which more than 99.8% was dissolved in the liquid. Integrating the local concentrations led to a total amount, if it were vapor (which is improbable), of approximately 250 m^3 (9,000 ft^3) of ammonia at STP that was present in the waste below the ILL. (Details of the integration are in Section 3.6.1.)

Based on the estimated solubilities and RGS measurements of gas concentrations, about 9% by volume (in situ) of the waste below the ILL was filled with free gas. The gas volume

(a) Brothers JW. 1997. Composition data from sample BY-109-6-17-97-0350. Pacific Northwest National Laboratory, Richland, Washington.

fractions based on RGS data ranged between 7.3 and 12%. The total gas inventory, based on the RGS data alone, was 110 ± 50 m^3 at in-situ conditions, or 140 ± 70 m^3 (STP). (The BPE method could not be used because the liquid in this tank was all subsurface.)

X-ray images of the samplers showed both small (a few mm in diameter) and large bubbles (more than 2.5 cm across). The waste characteristically contained bands and swirls of denser material, indicating that the solids did not all have the same composition. A maximum of 8% volume fraction of gas was in a form that was less than the detection threshold (<~1 mm) of the current x-ray imaging system.

Overall Summary for all Tanks

Table S.1 summarizes the gas volume fractions, gas volumes, and hydrogen fractions of the tanks discussed in this report. The values in the table are derived from RGS data alone.

Table S.1. Overview of Tank Gas Contents Based on RGS Data (all values derived from RGS data alone)

	Average In-Situ Void Fraction	Maximum In-Situ Void Fraction	Average Mol% H_2 [a]	Total STP Free Gas (m^3)
U-103 (whole tank)	0.20[b] ± 0.10	0.44 ± 0.041	22 ± 4.7	420 ± 210[b]
S-106 (high-solids layer)	0.10[b] ± 0.05	0.14 ± 0.012	63 ± 6.3	230 ± 120[b]
BY-101	RGS samples were compromised by air inleakage. No results are available for this tank.			
BY-109 (layer below ILL)	0.09 ± 0.05	0.12 ± 0.014	50 ± 4.9	140 ± 70

(a) The error bands on the average composition only represent the instrument error because there are too few samples to define the spatial variability of gas compositions. Lateral variation is not included.
(b) The RGS gas inventories and average gas volume fractions are considered highly uncertain because of the limited number of samples on which the estimates are based. The inventories and average volume fractions obtained using the BPE method are considered to be the "best estimates" for these tanks at this time.

Reference

Shekarriz A, DR Rector, LA Mahoney, MA Chieda, JM Bates, RE Bauer, NS Cannon, BE Hey, CG Linschooten, FJ Reitz, and ER Siciliano. 1997. *Composition and Quantities of Retained Gas Measured in Hanford Waste Tanks 241-AW-101, A-101, AN-105, AN-104, and AN-103.* PNNL-11450 Rev. 1, Pacific Northwest National Laboratory, Richland, Washington.

Acknowledgments

The authors would especially like to acknowledge the instrumental role played in implementation of the Retained Gas Sampler System by the following Project Hanford Management Contract staff: Dennis Graves, Jerry Johnson, Bruce Hey, Jim Person, Scott Cannon, Bob Kowitz, and Jim Weber. Many thanks to Milt Goheen and Larry Pederson at Pacific Northwest National Laboratory and Bill Kubic at the Los Alamos National Laboratory. Also, we would like to thank Chuck Stewart, Dave Hedengren, and Joe Brothers for reviewing the document and Reza Shekarriz for his management and guidance.

Contents

Figures

Tables

1.0 Introduction

The key phenomena of the Flammable Gas Safety Issue are the generation of the gas mixture, the modes of gas retention, and the mechanisms causing release of the gas. An understanding of the mechanisms of these processes is required for final resolution of the safety issue. Central to understanding is gathering information from such sources as historical records, tank sampling data, tank process data (temperatures, ventilation rates, etc.), and laboratory evaluations conducted on tank waste samples.

Gas generation processes must be understood well enough to estimate the generation rate and gas composition. The generation rates of the major fuel (hydrogen, ammonia, methane) and diluent species (nitrogen) determine the minimum tank ventilation rate required to prevent the buildup of a flammable mixture in the head space of a tank. A knowledge of gas generation processes also aids in assessing the long-term behavior of tank wastes and will support analyses of potential changes in waste storage conditions. Knowledge of the composition is needed to assess postulated deflagrations. The presence of such gases as ammonia, methane, and nitrous oxide can have a significant influence on the burn characteristics of a gas mixture.

Evaluation of the stored gas to date has been through analysis of tank level data and temperature profiles, detailed modeling activities, and in-situ measurements using the void fraction instrument (VFI) and retained gas sampler (RGS). VFI measurements have been conducted on double-shell tanks (DSTs), but the same method will not work for the single-shell tanks (SSTs), where the waste is either sludge or saltcake. Therefore, the RGS is to be used in selected SSTs to directly determine the gas composition and gas volume fraction. This report provides the results for the four SSTs sampled with RGS during 1997: 241-U-103, 241-S-106, 241-BY-101, and 241-BY-109.(a)

The four tanks represent several different types of flammable gas SSTs. Tank U-103 is on the Flammable Gas Watch List (FGWL) and is one of the highest-priority group of SSTs that show evidence of significant gas retention (Stewart et al. 1996a). Tank S-106, though not a FGWL tank, has a uniquely high barometric pressure response and continuing rapid surface level rise, indicating a large and increasing volume of retained gas. Tanks BY-101 and BY-109 are not on the FGWL but were chosen to test the effect of recent salt-well pumping on gas retention.

Section 2 of this report provides an overview of the process by which retained gases in the Hanford tanks are sampled and analyzed. A detailed description of the procedure used to reduce and analyze the data is provided in Section 3. Tank-by-tank results are covered in Section 4 (with the data presented in the order in which the tanks were sampled), and an RGS system performance overview is given in Section 5. Section 6 presents our conclusions from these analyses and recommendations for further research. The cited references are listed in Section 7. Appendix A describes the procedures used to extract gas and ammonia from the samples, Appendix B contains detailed laboratory data from each of the tanks, and Appendix C gives field sampling data.

(a) Hanford waste tanks are numbered beginning with the prefix 241-. Hereafter, in this report, the prefix will not be used, as is common practice when referring to the tanks at Hanford..

2.0 Retained Gas Sampler Processing

The RGS is a version of the universal core sampler specifically designed for sampling waste that contains gas. An overview of the procedure by which the data obtained using the RGS were analyzed and interpreted is provided in this section. Figure 2.1 provides a graphical diagram of the flow of material and information from the tanks sampled to the end product (this report). The RGS system, the sampler preparation, deployment, and retrieval, and the analytical procedure are detailed in Appendix A of Shekarriz et al. (1997). Details on the core sampler and modifications and operational constraints of the RGS are contained in Webb (1994).

To obtain an RGS sample, an RGS is installed in the drill string, lowered into the correct vertical position in the tank, and the sample taken by holding the sampler piston in position while pushing the rest of the sampler and drill string down through the waste. When the piston contacts the top end of the sampler, a spring is triggered that closes the sampler ball valve—hermetically sealing the waste sample solids, liquids, and gases in a chamber approximately 2.8 cm (1.125 in.) in diameter and 48 cm (19 in.) long.

The sampler is then removed from the tank and transferred to the x-ray cart for imaging. The x-ray images provide information about the void structure (bubble shape, etc.) and density of the waste and also allow a semi-quantitative estimate of the amount of gas present. After being x-rayed, the sampler is placed in a transport cask for delivery to the hot cell facilities for extrusion and gas extraction. To extract the gases, the sampler is loaded into the hot cell and installed on a previously evacuated extraction system. (A photograph of the extrusion and extraction system is provided in Figure 2.2.) The sampler ball valve is opened, and the extruder's hydraulic ram pushes the sampler piston all the way forward to move the sampler contents into the extractor. The sample waste is then stirred at the ambient temperature, after which sample gas is transferred from the extractor to collector gas sample canisters using a mercury transfer pump. During this process the sampler and canister pressures and temperatures are monitored and recorded in computer files for further data reduction and analysis. The extracted gases are analyzed with a mass spectrometry system.

A data analysis procedure (derived in Section 3) was formulated that uses the temperature, pressure, and volumes during extraction as well as the mass spectrometry data on species concentration as input. The model outputs are the mole fraction of gas constituents, total volume of each gas, vapor phase versus dissolved percentages for all species, and void fraction for each elevation at which the gas was sampled. The analysis also provides an estimate of the gas inventory in the sampled layers within the tank. The x-ray images are analyzed to provide, in addition to qualitative observations, quantitative information on the density and distribution of the phases in the sampler immediately after the sample is removed from the tank (see Section 3.8).

Shekarriz (1994) performed a series of flow visualization tests to examine the effectiveness of the RGS drill bit in capturing bubbles in the sludge during sampling. A transparent simulant with rheological properties similar to the sludges in the DSTs was used for these tests. Based on these tests, we concluded that a 60° drill bit provides the optimal conditions for minimizing disturbance of the bubbles and the waste during sampling. Comprehensive studies were performed to quantify the uncertainty in measuring retained gases using the RGS (Cannon and Knight 1995; Cannon 1996). In these acceptance tests, the procedures for sampling both insoluble (low-solubility) gases and ammonia were calibrated. We found that, while the insoluble components could be measured with high accuracy, ammonia was more problematic because it is absorbed within the system. The tank-by-tank results are given in the order in which sampling was carried out to reflect the increasing experience on which RGS methods were based. The details of the difficulties with ammonia measurements are given in Sections 3.7 and 5.4.

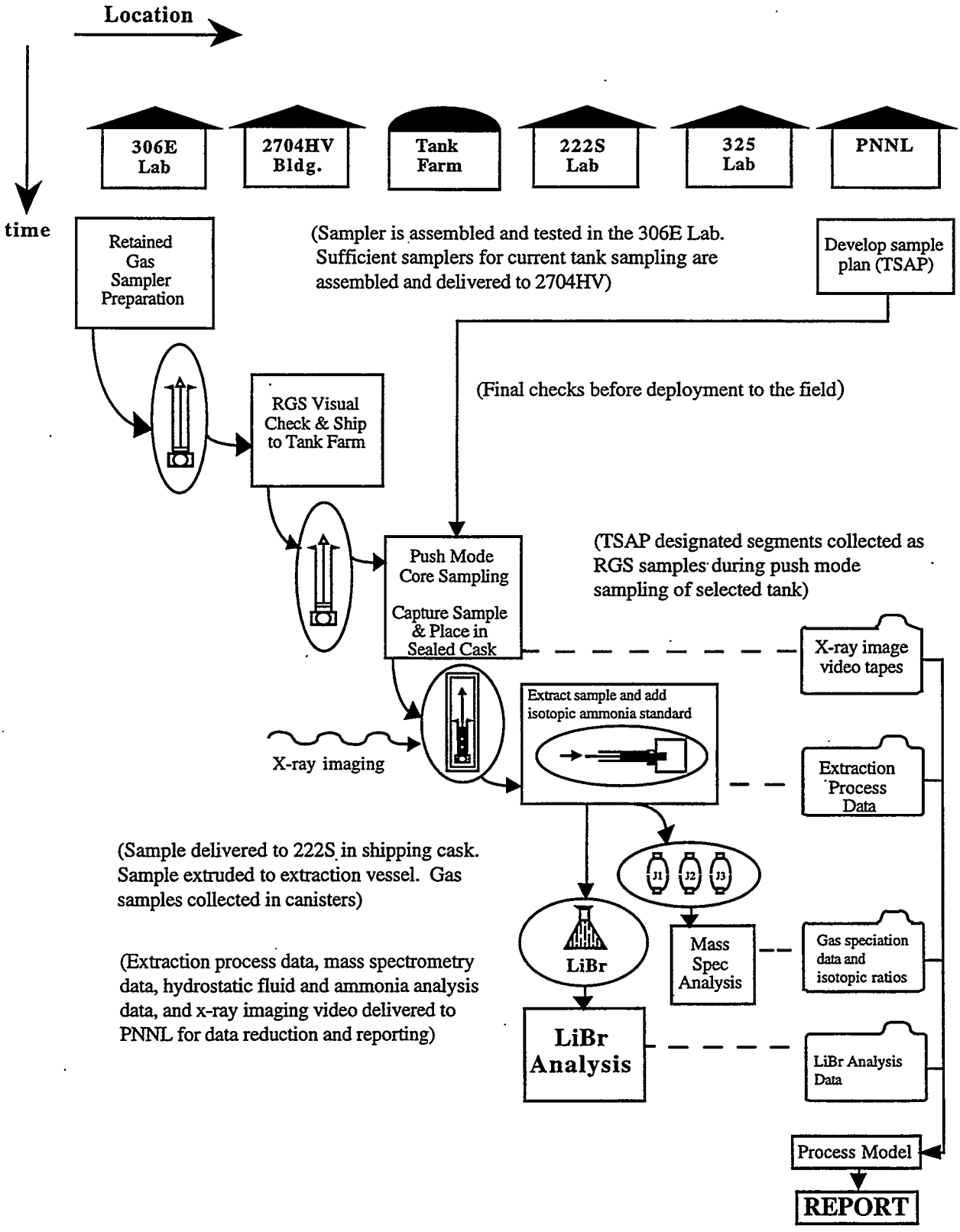

Figure 2.1. RGS Process Flow Diagram

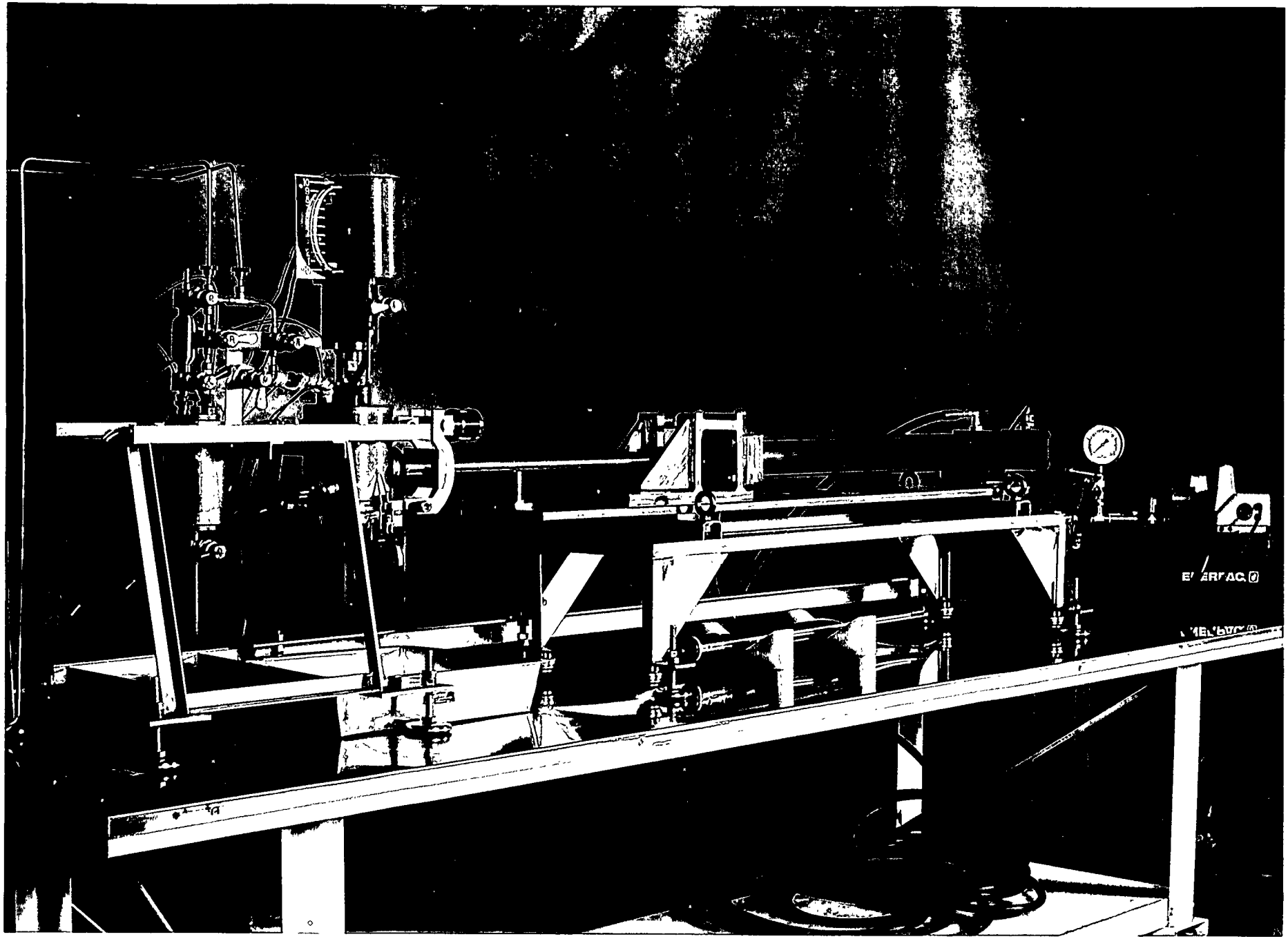

Figure 2.2. Photograph of the RGS Extrusion and Extraction System

3.0 Data Analysis

This section sets forth the analysis method that is used on the raw data to determine the total concentrations of low-solubility gas ("insoluble gas") and ammonia in an RGS waste sample, to calculate the in-tank void fraction at each sampled elevation, and to estimate the total tank gas inventory. The section describes the inputs, assumptions, and procedures related to each of the analysis tasks. A tank-by-tank discussion of the analysis results is presented in Section 4 and in the appendixes.

The total gas in the sample includes that in the gas/vapor in the collection canisters and that left behind in the headspace of the extractor after collection. The total ammonia includes that in the gas/vapor phase of the collection canisters; that in the condensed phase in the same canisters; and the residual, which remains in the sample after the "insoluble gases" have been extracted. Both extractor and collector pressures and temperatures are used to establish the mass balances that are necessary to calculate the sample ammonia content.

Section 3.1 derives expressions, in terms of extractor-side pressures, that describe the amounts of insoluble gas, ammonia vapor, and water vapor that are removed from the extractor by pumping. Section 3.2 completes the mass balance by deriving expressions, in terms of collector pressures, for the gas/vapor-phase and condensed moles in the collector. Section 3.3 derives the equations used to calculate the partitioning of ammonia and water between phases in the collector, based on the collector pressure and the dry gas/vapor composition determined by mass spectrometry. Section 3.4 gives the analysis methods used to tie together the derivations from the preceding sections. These methods vary depending on exactly what extraction procedure was used (for example, whether or not an isotopic ammonia standard was added to the system to determine residual ammonia).

The concentrations of gases and ammonia in the sample, which are determined by the methods given in Sections 3.1 through 3.4, are then used to find the distribution of the constituents between vapor/gas and liquid phases under in-tank conditions, employing methods described in Section 3.5. These results, which include the in-tank gas volume fraction, are then used to determine the total tank inventory of gases in the liquid and vapor phases, as described in Section 3.6. A description of the procedure for x-ray images is presented in Section 3.8.

The assumptions used in the analysis are stated briefly in the derivation sections, Sections 3.1 through 3.6. The justifications of the assumptions and the estimates of their significance are reserved for Section 3.7 to maintain the flow and clarity of the derivation.

3.1 Material Removed From the Extractor

The objective of this derivation is to determine the concentration of low-solubility (sometimes called "insoluble") gases in each waste sample as received. A "sample" consists of one 48-cm (19-in.) waste segment (the words "sample" and "segment" are used interchangeably in this report). A sample, as received, may contain not only native tank waste but hydrostatic head fluid (HHF) and entrained gases (potentially a combination of air with the argon gas used to purge the drill string). These possible contaminants are discussed in Section 3.6.

An RGS gas/vapor extraction begins with the sample fully extruded into the previously evacuated extractor vessel and the extractor vessel valved into the lines that connect it to the rest of the system, including the collection canisters. This allows the sample to approach equilibrium with the entire gas/vapor volume of the system. Next, the extractor and collector sides are disconnected from one another. Once that has been done, the only way gas and vapor can be transferred from

the extractor side of the system to the collector side is by cycling the mercury pump (which is essentially a displacement vacuum pump). The collection canisters (or J canisters) may be "unpumped"—that is, filled during the initial approach to equilibrium, while collector and extractor are connected—or "pumped," that is, filled by pumping. Other "grab-sample" canisters ("PQ" or "C" canisters, depending on the sample point) may also be filled by connecting previously evacuated canisters to various valves on the extractor side of the system. The collection and grab-sample canisters are subjected to mass spectrometry to determine the dry mole fractions of insoluble gases and ammonia. (More details of the extraction procedure are given in Appendix A. The dry mole fraction results are presented in Table B.n.1. Here "n" is a tank identification index from 1 through 4; it refers to the order in which tanks were analyzed and corresponds to the order in which tank results are discussed in Section 4.)

Each stroke of the RGS mercury pump (where the pump stroke counter is called i) removes $P_{xi}V_s/RT$ moles (of water plus NH_3 plus "insoluble" gas) from the extractor. The extractor pressure, P_{xi}, can be expressed as

$$P_{xi} = P_{xwi} + P_{xAi} + P_{xgi} \qquad (3.1.1)$$

where P_{xi} = the total extractor pressure just before the mercury pump is sealed off from the extractor for stroke i+1; that is, just before the collector pressure begins to rise as the pump is closed during stroke i+1. The subscript i = 0 denotes the point in time before the first stroke; i=1 means the point after the first and before the second stroke, and so on. P_{xi} is measured by pressure transducers.

P_{xwi} = the water partial pressure in the extractor before stroke i+1.

P_{xAi} = the ammonia partial pressure in the extractor before stroke i+1.

P_{xgi} = the gas partial pressure in the extractor before stroke i+1.

V_s = the volume of the pump stroke (assumed constant for all strokes). Vs is a known quantity.

T = the system temperature, an average of the extractor-side and collector-side temperatures (assumed constant for all strokes). The temperatures that are averaged to provide T are measured.

R = ideal gas constant

The stroke-by-stroke water partial pressure, P_{xwi}, can be assumed constant for all strokes if T is constant and if the water concentration in the sample is constant. For the latter to be a good assumption, the water evaporated from the sample must be a negligible part of the total water content, the extraction of ammonia and gas must have a negligible effect on the water vapor pressure, and the water in the sample and in the vapor volume must be in equilibrium. With this assumption, we can say

$$P_{xwi} = P_{xw} \qquad (3.1.2)$$

where P_{xw} = the water vapor pressure over the waste sample. This is an unknown to be solved for.

The moles of water removed from the extractor by each pump stroke are therefore equal to the following:

$$n_{xwi} - n_{xwi-1} = P_{xw}V_s/RT \qquad (3.1.3)$$

To find the gas partial pressure, P_{xgi}, assume the solubility of all the gas constituents (H_2, N_2, N_2O, CH_4, etc.) is so low that the amount dissolved in the waste is negligible. Also assume

that no gas pockets are trapped in the waste and that the gas is uniformly mixed throughout the extractor side. Finally, assume that all of the gas in the pump goes to the collector, and none of it leaks back to the extractor at any time. Given these assumptions, each pump stroke removes a fraction $[V_s/(V_s + V_x)]$ of the gas present in the extractor and transfers all of it to the collector. Then the moles of gas removed from the extractor by stroke i are equal to

$$\begin{aligned} n_{xgi} - n_{xgi-1} &= 0 && \text{for } i = 0 \\ n_{xgi} - n_{xgi-1} &= n_{xg0}\, F_v\, (1-F_v)^{i-1} && \text{for } i > 0 \end{aligned} \qquad (3.1.4)$$

and the moles of gas remaining on the extractor side are

$$n_{xgi} = n_{xg0}\, (1-F_v)^i \qquad \text{for } i \geq 0 \qquad (3.1.5)$$

where

F_v = $V_s/(V_s + V_x + V_2)$, the fractional gas removal per stroke.

V_x = the effective volume of the extractor vessel. This equals the volume of the empty extractor, which is a known quantity, minus the liquid/solid volume of the sample. The latter is equal to the sampler volume minus the fraction of the sampler that is occupied by gas and vapor under in-situ conditions. V_x must be calculated iteratively; a value assumed, the sample gas content calculated and from that the in-situ gas/vapor volume fraction (per Section 3.5). The gas volume fraction is then used to obtain a new value for V_x. This volume determination depends on the assumption that the sampler was completely filled with tank waste (100% sample recovery).

V_2 = the volume of the second-volume vessel and associated lines. This is a known quantity, which, like other system volumes, is determined by pressurizing the system with a known quantity of gas.

n_{xg0} = the initial moles of insoluble gas in the extractor vessel, second volume, and associated line volume. This is an unknown to be solved for. It is not equal to the sample gas content because it does not include insoluble gas in the collector side or in any grab sample canisters that may be mounted (whether at the PQ or the C valve, as described in Appendix A). However, once n_{xg0} has been determined, the sample gas content can be back-calculated using the ideal gas law and ratios of known volumes.

It follows from Equation (3.1.5) that the extractor gas pressure after stroke i is

$$P_{xgi} = \frac{n_{xg0}(1-F_v)^i RT}{V_s + V_x + V_2} \qquad \text{for } i \geq 0 \qquad (3.1.6)$$

Having modeled the water and gas partial pressures in the extractor, the ammonia partial pressure, P_{xAi}, remains. Assume that the ammonia vapor is in equilibrium with the ammonia in the sample; that all of the ammonia in the pump goes into the collector, and none is returned to the extractor; that there is negligible condensation in the extractor; that ammonia is dilute enough in the sample for a Henry's Law approach to be valid; and that the K_{HA} (the Henry's Law constant for ammonia) is constant for all strokes. Then the ammonia partial pressure in the extractor is

$$P_{xAi} = c_{Ai}/K_{HA} \qquad (3.1.7)$$

where

K_{HA} = Henry's Law constant for ammonia in the sample, expressed in terms of moles of NH_3 in solution per volume of gas-free waste per unit partial pressure of NH_3. This is an unknown.

c_{Ai} = the dissolved concentration of ammonia, expressed per volume of gas-free waste.

Summing the liquid (waste) and the vapor contributions, the total moles of ammonia in the extractor after stroke i are

$$n_{xAi} = V_w c_{Ai} + (V_s+V_x+V_2)P_{xAi}/RT \qquad (3.1.8)$$

where

V_w = the volume of the liquid/solids in the sample; V_w is assumed constant for all strokes. V_w is the same sample volume that is subtracted from the empty extractor volume to obtain V_x, as noted under Equation (3.1.5).

Equation (3.1.7) can be substituted into Equation (3.1.8) to give the partial pressure of ammonia in the extractor after stroke i as

$$P_{xAi} = \frac{n_{xAi}}{V_w K_{HA} + (V_s + V_x + V_2)/RT} \qquad \text{for } i > 0 \qquad (3.1.9)$$

Equation (3.1.9) is analogous to the expression for the partial pressure of gas in the extractor, which is

$$P_{xgi} = \frac{n_{xgi}}{(V_s + V_x + V_2)/RT} \qquad (3.1.10)$$

Comparing Equations (3.1.9) and (3.1.10), assuming that ammonia reaches equilibrium at every stroke, and using the development of the gas partial pressure model in Equations (3.1.4) and (3.1.6) as an analogy, we can define a fractional ammonia removal factor, F_A, analogous to (and always less than) F_V:

$$F_A = \frac{V_s/RT}{V_w K_{HA} + (V_s + V_x + V_2)/RT} = \frac{F_v}{1 + V_w K_{HA} RT/(V_s + V_x + V_2)} \qquad (3.1.11)$$

Note that the factor F_A is an unknown, unlike the factor F_V. Now we can say that the moles of ammonia removed from the extractor by stroke i equal

$$n_{xA0}\, F_A\, (1\text{-}F_A)^{i-1} \qquad \text{for } i > 0 \qquad (3.1.12)$$

and the ammonia partial pressure in the extractor after stroke i is

$$P_{xAi} = \frac{n_{xA0} F_A (1 - F_A)^i RT}{V_s} \qquad \text{for } i \geq 0 \qquad (3.1.13)$$

where n_{xA0} = the initial moles of ammonia in the extractor. This is an unknown to be solved for.

Now all the partial pressures have been defined in Equations (3.1.2), (3.1.6), and (3.1.13), and the total pressure in the extractor after stroke i and before stroke (i+1) is found to be

$$P_{xi} = P_{xw} + \frac{n_{xA0} F_A (1-F_A)^i RT}{V_s} + \frac{n_{xg0} (1-F_v)^i RT}{V_s + V_x + V_2} \tag{3.1.14}$$

3.2 Material Added to The Collector

The total moles of all the species that have been pumped to the collector, when pumping is completed after stroke N, can be found by adding Equations (3.1.3), (3.1.4), and (3.1.12), and summing over all pump strokes from stroke i to stroke N:

$$n_{cN} = \left(n_{cw0} + \frac{N P_{xw} V_s}{RT} \right) + \left(n_{cA0} + n_{xA0} F_A \sum_{i=1}^{N} (1-F_A)^{i-1} \right) + \\ + \left(n_{cg0} + n_{xg0} F_v \sum_{i=1}^{N} (1-F_v)^{i-1} \right) \tag{3.2.1}$$

where

n_{cw0} = the initial moles of water in the collector (before any pumping is done). This value is not an independent unknown; it can be found in terms of n_{xw0} by performing a full process mass balance that takes into account the sequence in which the collector and the PQ and/or C canisters were opened to the sample, which parts of the system were evacuated before this canister was opened, and other details that depend on the extraction procedure. Procedures are discussed in Appendix A.

n_{cA0} = the initial moles of ammonia in the collector (before any pumping is done). Like n_{cw0}, this value is not an independent unknown (see above).

n_{cg0} = the initial moles of insoluble gas in the collector (before any pumping is done). Like n_{cw0}, this value is not an independent unknown (see above).

In Equation (3.2.1) the variables P_{xw}, n_{xg0}, n_{xA0}, and F_A are unknowns.

Not all of the moles in the collector are in the gas phase; some moles of ammonia and water condense in the J canister and the lines of the collector. The presence of condensation is reflected in the fact that the pressure measured in the collector at the end of pumping is much lower than that which would be measured if all the ammonia and water were in the gas phase. A measure of the extent of condensation is the parameter r, which is defined by

$$r = \frac{P_{cN}}{(n_{cN} RT / (V_{cl} + V_J))} \tag{3.2.2}$$

where

V_{cl} = the volume of the collector lines. This is a known quantity.

V_J = the volume of the J canister. This is a known quantity.

P_{cN} = the final collector pressure (after stroke N).

Here r is the fraction of moles in the collector side that are in the gas/vapor phase, and (1-r) is the fraction of moles in the condensate. It has been assumed that the volume of condensate is negligible compared with the collector volume, V_c, where $V_c = V_J + V_{cl}$. The collector volumes, determined by pressurizing the system with a known quantity of gas, are listed in Appendix B (Tables B.n.2), and the tank-specific extractor and collector pressures as a function of pump cycle are presented in Tables B.n.3–5.

3.3 Phase Partitioning In The Collector

The amounts of water and ammonia that condense in the collector are not measured but must be known before the water, ammonia, and gas content of the sample can be determined. The condensation can be calculated based on solution thermodynamics.

Among the known quantities are the following:

P_{cN} = the total pressure in the J canister after pumping is complete, which is the same as the total pressure in the collector at large.
T = the system temperature (absolute).
Y_A = the mole fraction of ammonia in the gas/vapor phase in the J canister (collector) on a dry basis (water excluded). This is the ammonia mole fraction that is measured by mass spectrometry. The temperature at which the mole fraction is measured is assumed to be negligibly different from that at which the gas sample was collected (room temperature), meaning that the equilibrium concentrations are the same.

The unknowns include

y_A = the mole fraction of ammonia in the gas in the collector, on a wet basis
y_w = the mole fraction of water in the collector gas, on a wet basis
x_A = the mole fraction of ammonia in the collector condensate
x_w = the mole fraction of water in the collector condensate
v_A = the moles of ammonia in the gas/vapor phase in the collector
v_w = the moles of water in the collector gas/vapor phase
L_A = the moles of ammonia in the collector condensate
L_w = the moles of water in the collector condensate.

It is clear from the definitions of the variables that

$$y_A = Y_A (1 - y_w) \tag{3.3.1}$$

Assuming that other dissolved gases (including N_2O) can be neglected, we can also say that

$$x_w = 1 - x_A \tag{3.3.2}$$

If the ammonia and water vapor in the canister (collector) are in equilibrium with the condensate, then the fugacities are equal in the liquid and vapor phases. Then

$$x_A p_A \gamma_A = y_A P_{cN} = Y_A (1-y_w) P \tag{3.3.3}$$

$$(1-x_A)p_w\gamma_w = y_w P_{cN} \tag{3.3.4}$$

where

p_A = the vapor pressure of pure ammonia at temperature T
p_w = the vapor pressure of pure water at temperature T
γ_A = the activity coefficient of ammonia in the ammonia-water condensate
γ_w = the activity coefficient of water in the ammonia-water condensate.

The following expressions can be used to find the pure-component vapor pressures (in units of kPa) and the solution activity coefficients:

$$p_A = 100 \exp(45.327 - 4104.67/T - 5.146 \ln T + 6.15 p_A/T^2) \tag{3.3.5}$$

$$p_w = 22120 \exp[(1/T_r)(-7.76451(1-T_r) + 1.45838(1-T_r)^{1.5} - 2.7758(1-T_r)^3 - 1.23303(1-T_r)^6)] \tag{3.3.6}$$

$$\ln \gamma_A = (1-x_A)\left(\frac{\Lambda_{Aw}}{x_A + \Lambda_{Aw}(1-x_A)} - \frac{\Lambda_{wA}}{x_A\Lambda_{wA} + (1-x_A)}\right) - \ln(x_A + \Lambda_{Aw}(1-x_A)) \tag{3.3.7}$$

$$\ln \gamma_w = -x_A\left(\frac{\Lambda_{Aw}}{x_A + \Lambda_{Aw}(1-x_A)} - \frac{\Lambda_{wA}}{x_A\Lambda_{wA} + (1-x_A)}\right) - \ln((1-x_A) + \Lambda_{wA}x_A) \tag{3.3.8}$$

where

T_r = the reduced collector temperature, T /647.3 (the critical temperature for water is 647.3 K).
Λ_{Aw}= 0.6777/exp ([-908.30 + 2.0723 x_AT/x_w]/T), the correlating parameter for ammonia in an ammonia/water system.
Λ_{wA}= 1.476/exp ([77.584 + 0.041975 x_wT/x_A]/T), the correlating parameter for water in an ammonia/water system.

The pure-component vapor pressures came from Reid et al. (1987), while the activity coefficients were estimated by fitting ammonia/water composition/vapor pressure data (found in AIChE [1984]) to a variant of the Wilson equation (p. 234, Prausnitz et al. [1986]). A least-squares fit was used to find the optimum parameters over 40 data points that fell in a range of dissolved ammonia concentrations between 0 and 40 mol% and temperatures between 15 and 40°C. In this range, the correlation predicts ammonia mole fractions within 7% error and water mole fractions within 10% error.

Equations (3.3.3) and (3.3.4) constitute two equations in two unknowns (x_A and y_w). These equations can be solved iteratively, allowing the compositions of the phases, y_A, y_w, x_A, and x_w, to be determined. First, the moles of ammonia, water, and insoluble gas must be stated in terms of the unknowns:

$$v_A = y_A P_{cN}(V_{cl}+V_J)/RT \tag{3.3.9}$$

$$v_w = y_w P_{cN}(V_{cl}+V_J)/RT \tag{3.3.10}$$

$$n_{cgN} = (1 - y_w - y_A)P_{cN}(V_{cl}+V_J) / RT \quad (3.3.11)$$

The next step is to find the amounts of ammonia and water in the gas and condensed phases. By definition, the total collected moles of ammonia and water are the sum of the gas and liquid contributions, and r is the ratio of gas to total moles in the collector:

$$n_{cAN} = v_A + L_A \quad (3.3.12)$$

$$n_{cwN} = v_w + L_w \quad (3.3.13)$$

$$r = \frac{n_{cgN} + v_A + v_w}{n_{cgN} + v_A + v_w + L_A + L_w} \quad (3.3.14)$$

where

n_{cAN} = total moles ammonia in the collector at the end of pumping
n_{cwN} = total moles water in the collector at the end of pumping.

It follows that

$$r = \frac{P_{cN}(V_{cl}+V_J)/RT}{P_{cN}(V_{cl}+V_J)/RT + L_A(1+(1-x_A)/x_A)} = \frac{1}{1+L_A(RT/x_A P_{cN}(V_{cl}+V_J))} \quad (3.3.15)$$

From this it can be shown, by substituting Equation (3.2.2) into Equation (3.3.15), that

$$L_A = (1 - r)\, x_A n_{cN} \quad (3.3.16)$$

This finding can be carried through to find L_w, n_{cAN}, and n_{cwN}:

$$L_w = x_w\,(1-r)\, n_{cN} \quad (3.3.17)$$

$$n_{cAN} = y_A P_{cN}(V_{cl}+V_J) / RT + L_A \quad (3.3.18)$$

$$n_{cwN} = y_w P_{cN}(V_{cl}+V_J) / RT + L_w \quad (3.3.19)$$

3.4 Final Determination of Sample Contents

At this point, we have four unknown variables: P_{xw} (water vapor pressure in the extractor), n_{xg0} (initial "insoluble" gas moles in the extractor), n_{xA0} (initial ammonia moles in the extractor), and F_A (the per-stroke ammonia transfer factor, from which the Henry's Law constant for ammonia can be derived). Of these variables, two are easy to find once the thermodynamic manipulations of Section 3.3 are complete:

$$P_{xw} = \frac{(n_{cwN} - n_{cw0})RT}{NV_s} \quad (3.4.1)$$

$$n_{xg0} = \frac{n_{cgN} - n_{cg0}}{F_v \sum_{i=1}^{N} (1-F_v)^{i-1}} \quad (3.4.2)$$

As was already noted, once n_{xg0} is known the original sample gas content n_{Sg} is easily back-calculated by including whatever gas was removed in grab-sample canisters and partial system evacuations. The residual gas left in the extractor after pumping can also be calculated (with Equation [3.1.5]). The amounts of gas in each J canister and the per-canister composition can be found in Tables B.n.6 and B.n.7.

The moles of each gas constituent are equal to

$$n_{Si} = \left(\sum_{j=1}^{M} \frac{n_{dgN,j} Y_{i,j}}{1 - Y_{A,j}} \right) + \frac{n_{Rg} Y_{i,M}}{1 - Y_{A,M}} \qquad (3.4.3)$$

where

n_{Si} = original sample moles of constituent i.

$n_{dgN,j}$ = moles of insoluble gas removed from the system in each container j, where there are a total of M containers. Most of the gas is in collection canisters whose pressure, temperature, and composition are measured so the moles of gas can be calculated as in Sections 3.1–3.3. A small amount of gas leaves the system in grab-sample canisters and system evacuations. In these cases, calculations use measured system pressures and volumes and the measured composition of the gas in the collection canister taken just before or after the grab sample (or evacuation).

$Y_{i,j}$ = the dry mole fraction of constituent i in container j, as measured by mass spectrometry.

$Y_{A,j}$ = the dry mole fraction of ammonia vapor in container j, as measured by mass spectrometry.

n_{Rg} = moles of insoluble gas present in the system when the extraction is complete. This quantity is found by calculating $n_{xgN,M}$ for the last pumped canister using Equation (3.1.5).

There are a number of different ways to complete the ammonia calculation. The choice of method depends heavily on mass-balance considerations, which, in turn, depend on the details of the extraction procedure. In addition, some samples were analyzed using an injection of isotopically labeled ammonia to estimate the residual ammonia (that which is left on the extractor side when gas extraction is complete). The different methods that may be used to finish the ammonia determination are described in Sections 3.4.1 through 3.4.3.

The original sample contents of each constituent are then divided by the sampler volume to give the concentration of each low-solubility gas species per liter of waste under in-tank conditions (see Section 4 for results). This assumes that the sampler is filled up to the piston with tank waste (gas/vapor and slurry).

3.4.1 Ammonia Determination by the Isotopic Method

The laboratory technique used for the isotopic method is as follows. After gas extraction is complete and the gas collection canisters have been valved out, new collection canisters are attached and the whole system (except for the extractor system) is evacuated. The ammonia remaining in the extractor is called the residual ammonia and includes both the ammonia vapor in the extractor headspace and the ammonia dissolved in the waste sample.

A canister containing a known amount of $^{15}NH_3$ (ammonia in which all the nitrogen is the ^{15}N isotope) is then attached to the extractor side and valved in. The isotopically labeled ammonia

(which is added as vapor) is allowed to come to equilibrium with the residual ammonia, whose nitrogen is quantitatively the ^{14}N isotope. The equilibrated ammonia is then extracted from the sample via mercury pumping. Mass spectrometry is used to determine the molar ratio, $^{14}N/^{15}N$. The end result of the mass-spectrometric analysis is the $^{14}N/^{15}N$ ratio. (This ratio, provided to us by the mass-spectrometry analysts, is corrected for the small fraction of ^{15}N that is naturally present in the sample ammonia, so that the ratio is equal to residual/injected ammonia moles.)

The amount of labeled ammonia (^{15}N ammonia) that is added is determined using the ideal gas law. The volume and temperature of the system to which it is added are known, and the pressure increase produced by adding the labeled ammonia is also measured. Then the residual ammonia is

$$n_{RA} = Q n_{LA} \tag{3.4.4}$$

where

n_{RA} = the moles of residual ammonia (both the vapor and dissolved ammonia that is in the extractor vessel after gas extraction).
Q = the molar ratio ($^{14}N/^{15}N$ ratio corrected for natural ^{15}N).
n_{LA} = the moles of isotopically labeled ammonia.

The initial ammonia in the extractor, n_{xA0}, is found by using mass-balance methods to account for all the ammonia that was removed from the extractor side between the time the extractor was sealed off from the collector, before the first pump stroke, and the time when the residual was determined. These moles of ammonia removed are added to the residual to obtain n_{xA0}.

Once n_{xA0} is known, the factor F_A is found by iteratively solving the equation

$$F_A \sum_{i=1}^{N} (1-F_A)^{i-1} = \frac{n_{cAN} - n_{cA0}}{n_{xA0}} \tag{3.4.5}$$

Then Equation (3.1.11) is used to calculate K_{HA}, based on F_A.

3.4.2 Ammonia Determination by Mass Balance Comparison

This method calculates the total initial ammonia in the sample, and the residual ammonia is found by subtracting all the ammonia that has been extracted from the sample. The method is used when there are two pumped canisters.

First, the amounts of ammonia that were collected in the canisters are expressed in terms of F_A and the original moles of ammonia in the sample, n_{SA}:

$$n_{cAN,1} = n_{cA0,1} + (n_{SA} - \Delta_{xA0,1}) F_A \sum_{i=1}^{N_1} (1-F_A)^{i-1} \tag{3.4.6}$$

$$n_{cAN,2} = n_{cA0,2} + (n_{SA} - \Delta_{xA0,2}) F_A \sum_{i=1}^{N_2} (1-F_A)^{i-1} \tag{3.4.7}$$

where

$n_{cAN,1}$ = the moles of ammonia in the collector after pumping is completed for collection canister 1. The moles are found using the collector pressure and temperature, the condensation ratio r

derived from extractor and collector pressures as defined in Section 3.2 and the phase partitioning relationships in Section 3.3.

$n_{cA0,1}$ = the moles of ammonia in collection canister 1 before pumping is begun. The moles are found using the collector pressure and the canister-1 composition determined by mass spectrometry.

$\Delta_{xA0,1}$ = the moles of ammonia that were removed from the extractor side of the system by the time pumping began on canister 1. This typically includes the contents of grab samples and the initial collector side contents. $\Delta_{xa0,1}$ can be calculated as a function of n_{SA} by using volume ratios and the ideal gas law.

N_1 = the number of pump strokes used on collection canister 1.

$n_{cAN,2}$ = the moles of ammonia in the collector after pumping is completed for collection canister 2.

$n_{cA0,2}$ = the moles of ammonia in collection canister 2 before pumping is begun. The moles are found using the collector pressure and the canister 1 composition determined by mass spectrometry.

$\Delta_{xA0,2}$ = the moles of ammonia that were removed from the extractor side of the system by the time pumping began on canister 2. This includes the contents of grab sample canisters, collection canister 1, and the collector side contents just before collection canister 2 is pumped. $\Delta_{xA0,1}$ can be calculated as a function of n_{SA} by using volume ratios and the ideal gas law.

N_2 = the number of pump strokes used on collection canister 2.

Equations (3.4.6) and (3.4.7) constitute two equations in two unknowns and can be solved for n_{SA} and F_A.

3.4.3 Ammonia Determination from a Known Henry's Law Constant

In some cases, for example, when there is only one pumped canister for a sample, it may be necessary to calculate the residual ammonia based on a Henry's Law constant that comes from data for other samples. For example, it might be possible to use a Henry's Law constant K_{HA} that is the average of values found for other, more completely extracted samples from the same tank. F_A can then be calculated from Equation (3.1.11), and the approach described in Section 3.4.2 provides the original sample ammonia, n_{SA}.

3.5 Phase Distribution and Gas Volume Fraction

Once the concentrations of low-solubility gases and high-solubility vapors have been determined, the distribution of the different components between the liquid (or slurry) and gas/vapor phases must be determined for each waste sample under in-tank conditions. The quantity of gases in the gas/vapor phase determines the in-situ gas volume fraction of the sample.

The phase distribution of the gas constituents is based on the effective Henry's Law constants that are calculated for in-situ conditions using the Weisenberger and Schumpe gas solubility model, which is described in Section 3.5.1. The in-tank pressure for each sample is calculated as a hydrostatic pressure based on the measured waste densities. An iterative procedure is used that matches the sum of partial pressures of all the gas constituents with the in-tank pressure. This procedure is described in Section 3.5.2.

The analysis procedures described in this section require input from a variety of sources. The total gas concentrations are determined using the procedures described in Sections 3.1 through 3.4. Several tank waste properties are used in the analysis; these were obtained from a variety of sources, including the Tank Characterization Reports (tank-specific references are given in Sections 4 and 7 and Appendix B). These properties include the following:

- Molar ion concentrations in the waste solution, used to calculate Henry's Law constants
- Solid volume fractions and weight fraction of water in solution, used to calculate effective Henry's Law constants per liter of waste
- Average bulk densities of the different layers, used to calculate the in-tank hydrostatic pressures at each elevation.

Other inputs include

- Elevations from which the samples were taken (from the sampling plan)
- Location and thickness of the different layers and crust
- Temperature at each sample elevation
- Water vapor pressure at each sample location.

3.5.1 In-Situ Solubility Model

The distribution of gases and ammonia vapor between the vapor and slurry phases of the waste is determined by a parameter referred to as a Henry's Law constant, K_H, which is defined as

$$K_H = c_i / p_i \tag{3.5.1}$$

where p_i is the partial pressure of a component in atmospheres and c_i is the concentration of the component expressed in terms of moles per liter of waste. This equation differs from the normal definition of the Henry's Law constant because it is in terms of unit volume of gasless waste rather than mass of solvent (water) in the waste. The distribution of a component between both the vapor and slurry phases can be determined under any set of conditions if the total moles of component and the effective Henry's Law expression have been determined.

The Henry's Law constant for a gas depends on several variables, including the solution temperature and ion concentrations. A number of expressions have been developed to calculate the Henry's Law constant; these have been reviewed by Norton and Pederson (1994, 1995). (A word of caution: there are two different conventions for expressing the Henry's Law constant; one is the inverse of the other. Our discussion uses the expression that is defined in Equation [3.5.1] and is consistent with Norton and Pederson [1994, 1995].) The Schumpe model is given by

$$\log(c_{G,o} / c_G) = \log\left(\frac{K_{H,G}(\text{water})}{K_{H,G}(\text{solution})}\right) = \sum_i (h_i + h_G)\, s_i \tag{3.5.2}$$

where $c_{G,o}$ and c_G denote the gas solubility of gas G in pure water and salt solution, respectively; h_i and h_G are the ion and gas-specific coefficients, respectively; and s_i is the concentration of ion i in

the salt solution. The gas-specific constant, h_G, is assumed to be a linear function of temperature

$$h_G = h_{G,o} + h_T(T - 298.15K) \tag{3.5.3}$$

where $h_{G,o}$ is the reference value, and h_T is the temperature-specific coefficient.

The solubility of ammonia is at least two orders of magnitude greater than that of the next highest solubility species, nitrous oxide. The Henry's Law constants that were calculated from the Schumpe model to determine phase distributions in the tanks can be found in Tables B.n.11.

The Henry's Law constant obtained using Equations (3.5.2) and (3.5.3) must be converted from a molal basis, moles of solute per kg of solvent (water) in solution, to a basis of moles per volume of gas-free waste (both solution and solids). The conversion is accomplished by calculating

$$K_H \text{, L waste basis} = (K_H \text{, kg water basis})\,(1 - x_s)\rho_L\omega_L \tag{3.5.4}$$

where x_S is the volume fraction of solids in the gas-free waste, ω_L is the weight fraction of water in the solution, and ρ_L is the solution density. Solids volume fractions are either taken from core sample data (when available) or estimated based on solution density, intrinsic solid density ρ_S (also known as particle density), and gasless bulk waste density, ρ_b:

$$x_s = \frac{\rho_b - \rho_L}{\rho_S - \rho_L} \tag{3.5.5}$$

Values for the solids fractions and densities used in Equations (3.5.4) and (3.5.5) are given in Tables B.n.9 and the surrounding text. The weight fraction of water in the solution is taken from analyses of core extrusions that were obtained in the same sampling campaign as the RGS samples.

3.5.2 In-Situ Gas/Vapor Distribution

The gas volume fraction (phase distribution) analysis begins by determining the in-tank gas pressure, p_Z, at each sample elevation. It is assumed to be equal to the hydrostatic pressure, which is obtained by multiplying the average waste density for each layer by the thickness of each layer above that elevation and summing. Next, the effective Henry's law constant at the in-tank temperature is calculated for each sample elevation using the procedure described in Section 3.5.1.

The distribution of each gas constituent between the slurry and vapor phases can be determined using Henry's Law if the concentration of the gas constituent, the total gas volume fraction, and the effective Henry's Law constant for that constituent are known. The portion of each gas constituent, i, in the vapor phase is given by the expression

$$\frac{n_{i,v}}{n_{i,tot}} = \frac{\alpha/RT}{\alpha/RT + (1-\alpha)K_{H,i}} \tag{3.5.6}$$

where α is the gas volume fraction. The partial pressure for each gas constituent is given by the expression

$$p_i = \frac{n_{i,tot}/V_{tot}}{\left[\frac{\alpha}{RT} + (1-\alpha)\cdot K_{H,i}\right]} \qquad (3.5.7)$$

The system is constrained by the fact that the sum of all the gas constituent partial pressures must equal the dry hydrostatic pressure in the tank at that elevation

$$p_{hyd} = p_{H_2O} + \sum p_i \qquad (3.5.8)$$

The gas volume fraction can be calculated using the ideal gas law:

$$\alpha = \frac{\sum n_{i,v} RT}{p_{hyd} V} \qquad (3.5.9)$$

Note that the in-situ gas volume fraction is not known *a priori*. It is required to calculate the phase distributions using Equation (3.5.6). As a result, an iterative procedure has been developed that begins with an estimated total gas volume fraction. The phase distribution for each gas component is calculated, and the partial pressures are summed. This sum is compared with the in-tank hydrostatic pressure, and the gas volume fraction is adjusted accordingly. This iteration continues until the sum of partial pressures is within 0.001% of the specified in-tank pressure.

3.6 Tank Inventories and Data Interpretation

The data analysis tasks in Sections 3.1 through 3.5 provide gas concentration data and in-situ gas volume fraction values at the points where samples were successfully taken. These results require further interpretation to provide overall tank waste properties such as gas inventories and to account for types of sample contamination that might have made the concentration data not fully representative of actual undisturbed tank waste.

3.6.1 Estimating Gas Inventory from RGS Data

Once the phase distribution of each of the gas constituents has been determined, the total tank inventory of free and dissolved gases can be calculated. The analysis consists of calculating the average in-situ gas volume fraction in each of the layers from which samples were taken, calculating the average gas composition in each layer, estimating the total number of moles of each gas constituent in both layers, and summing to determine the total gas inventory. The analysis also provides the average gas location and pressure in the tank.

The analysis procedures described in this section require input from a variety of sources. The free and dissolved gas concentrations at the various sampling locations are determined using the procedure described in Sections 3.1 through 3.5. Other inputs include

- Location, thickness, and volume of the different layers, including estimated variation (uncertainty) in layer thicknesses and location; layers are distinguished from one another by their temperature profiles, core sample physical properties, and gas retention capacities.

- Elevations at which samples were taken.
- Temperature at each sample elevation (obtained from multifunction instrument trees [MITs] or thermocouple [TC] profiles).
- Pressure at each sample elevation (calculated in Section 3.3).

In generating RGS inventories, three calculation methods may be used on RGS concentration data. Where only one RGS sample is available in a layer, its data are used directly. The species concentrations of the single sample are assumed to extend throughout the layer. The gas volume for the layer is calculated from the single gas concentration and the average pressure in the layer (usually the hydrostatic pressure at the layer midpoint).

When more than one sample is available for a low-solids layer, the layer is assumed to be well mixed. An arithmetic average of the samples' concentrations is used to determine the average gas concentrations (mol/L) for the layer. In this case, too, the in-situ gas volume is based on the average pressure in the layer.

When more than one sample is available for a high-solids layer, the concentrations are integrated over depth to find the average. In addition, the mass-average pressure and temperature of the gas in the layer are found from integrating the temperatures and pressures at sample locations (multiplied by gas concentration). The STP gas volume for the layer is calculated from the averaged concentration, temperature, and pressure using the ideal gas law to adjust from tank conditions to standard conditions.

The integration method assumes that the concentrations of all the gases are piece-wise linear continuous between samples, within a layer. (The discontinuities between layers are preserved so that, for example, the low gas concentration in a low-solids layer does not "pull down" the higher average concentration in a high-solids layer.) The assumption of piece-wise linearity allows Simpson's Rule to be used for integration, with the concentrations between sample centers linearly interpolated. Figure 3.1 shows an example integration for one layer of waste from which three samples (segments 5, 6, and 10, the closed circles) have been taken. The concentrations at the bottom of the layer are set equal to the concentrations from the lowest sample within the layer, and similarly for the top of the layer. The four integration intervals are unequal in size, reflecting the different distances between data locations.

3.6.2 Best Estimate Inventory and Uncertainty

The RGS extraction system provides sufficient data to determine the total gas volume in an individual sampler to within about 10%. However, since only three or four segments were successfully extracted in each of the three tanks studied, and since core extrusions show high lateral nonuniformity in the waste in these tanks, there is a very large uncertainty in using these sparse data to derive the total tank gas inventory. A statistically sound estimate of the uncertainty cannot be made because there are too few samples to quantify the spatial variability of gas retention. However, methods other than the RGS can sometimes be used in the same tank to provide a better estimate of the retained gas volume and to assess the uncertainty in RGS-derived inventory.

Local gas fractions were measured in several of the DSTs with both the RGS and the void fraction instrument (VFI) in 1995–96 (Stewart et al. 1996a, b). The VFI provides many more measurements and therefore defines the gas fraction profile in much greater detail than the RGS. In comparing the calculated gas inventory (standard temperature and pressure [STP]) in the nonconvective layers of the four tanks with both RGS and VFI measurements, the volume derived from

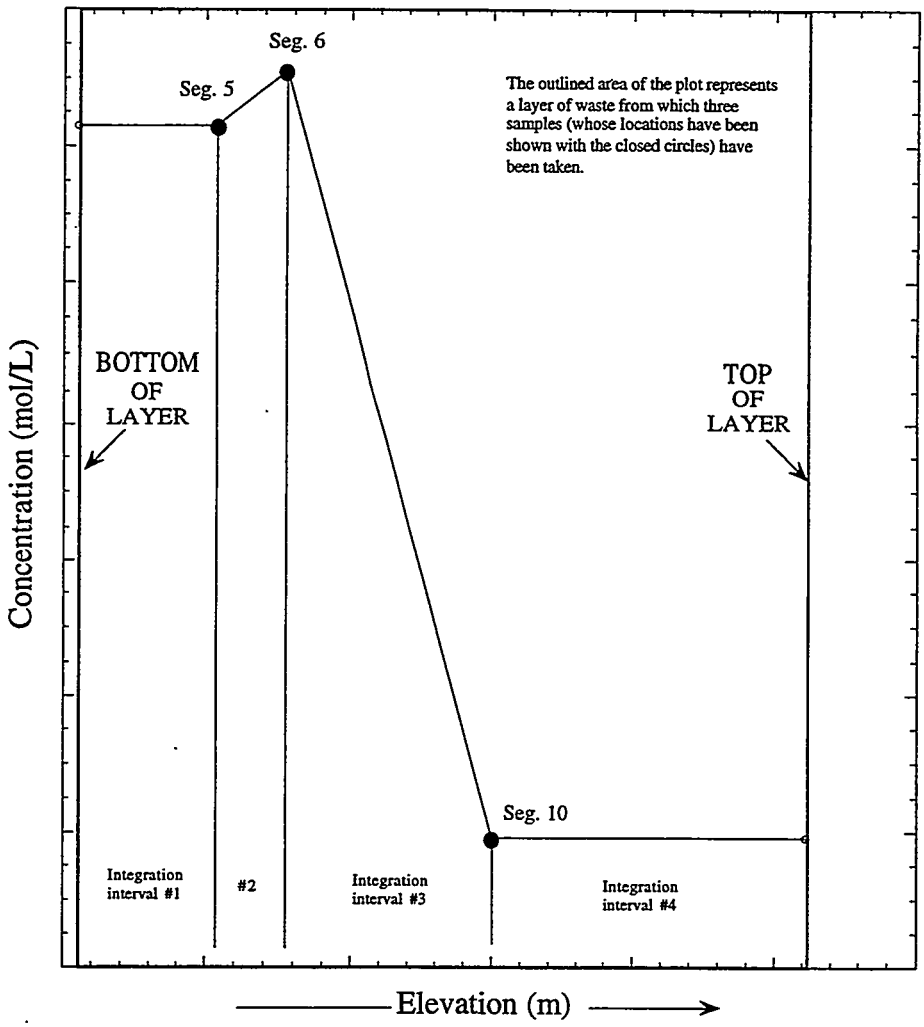

Figure 3.1. Example of Integration Scheme for Averaging RGS Concentrations

RGS measurements was almost 40% low in two tanks and about 10% high in two others (Shekarriz et al. 1997). The comparison is summarized in Table 3.1. The root-mean-square (rms) average of the differences is 27%. The VFI and RGS data for AW-101 are overlaid in Figure 3.2 as an example of how the RGS samples missed the high gas fraction region in the waste.

The representativeness of a single RGS sample might be comparable to that of a single VFI measurement. The standard error of a single VFI gas fraction measurement with respect to the average is quite high even in DSTs, as evidenced by the scatter in the VFI data in Figure 3.2. Statistical analysis of the VFI data from five DSTs gives uncertainties from 25% to over 60% of the mean (Meyer et al. 1997) with an rms average of 48%.(a) This implies that the uncertainty of an average of four such measurements would be at least 24%.

(a) That is, a single measurement represents the mean with an error of 25% to 60%. Though individual measurements have a high uncertainty, the uncertainty of the average is much lower because many data are included.

Table 3.1. Comparison of RGS and VFI Nonconvective Layer Gas Inventory in Four DSTs

Tank	Number of RGS Nonconvective Layer Samples	Nonconvective Layer Gas Volume		
		RGS (STP m^3)	VFI (STP m^3)	(VFI-RGS)/VFI
AN-103	2	216	363 ± 10	36%
AN-104	5	202	197 ± 12	-9%
AN-105	6	156	148 ± 24	-12%
AW-101	5	69	115 ± 12	37%

The gas inventory derived from the VFI data set is also uncertain since it represents the waste in the immediate vicinity of just two risers. However, where it can be applied, the barometric pressure effect (BPE) method can be used to compute the total gas inventory directly. The BPE method is derived in detail in Meyer et al. (1997), and a method to filter out the effects of waste strength is discussed in Whitney et al. (1996). It is based on the correlation between barometric pressure fluctuations and changes in the waste surface level, which are attributed to expansion and compression of retained gas.

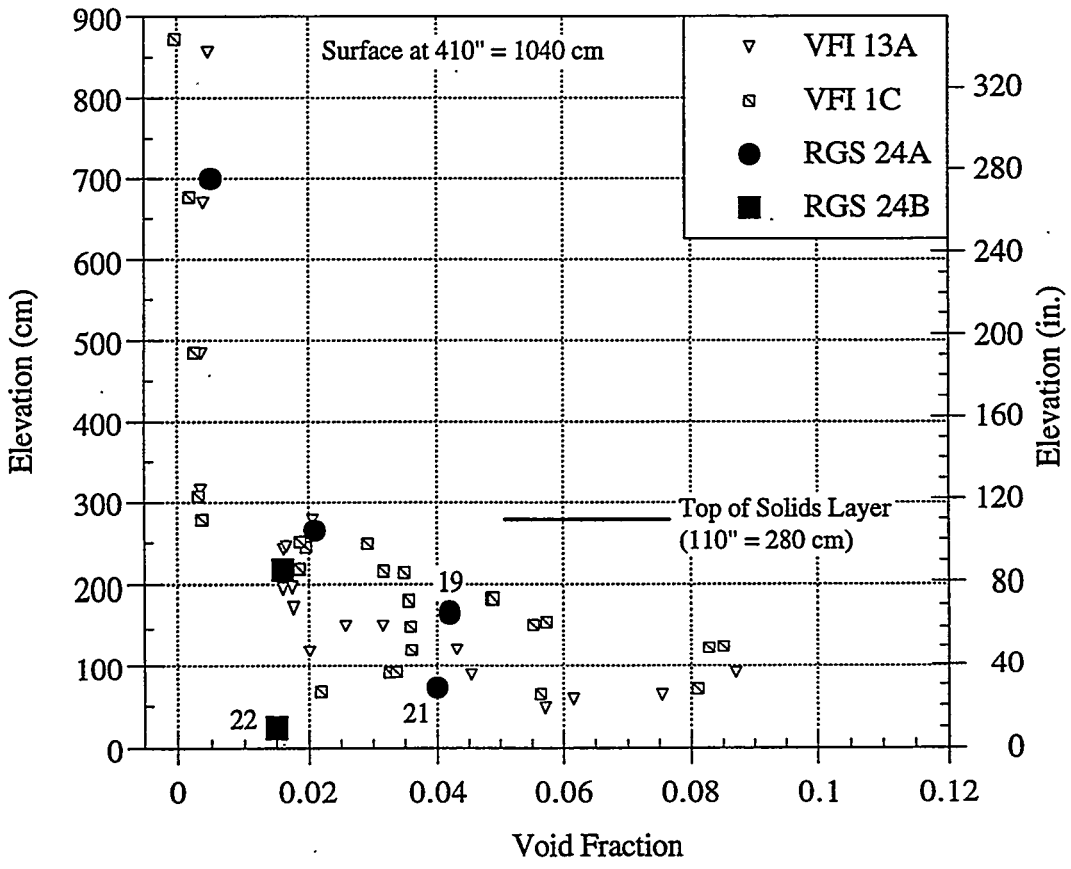

Figure 3.2. VFI and RGS Gas Fraction Data for AW-101

The in-situ gas volume, V_G, can be estimated from the level-to-pressure correlation, dL/dP, by

$$V_G = -AP_{eff}\, dL/dP \tag{3.6.1}$$

where A is the tank cross-sectional area and P_{eff} is the effective pressure at which the gas is stored. The effective pressure can be calculated based on the gas distribution implied by the RGS measurements, by assuming each RGS sample represents a point on the gas fraction profile. The gas fraction at the top of the gas-bearing region is assumed equal to the gas fraction in the highest RGS sample, and the gas fraction at the tank bottom is assumed to be equal to that of the lowest RGS sample. Then the average gas fraction in the tank defined for N RGS segments is given by

$$\bar{\alpha} = \frac{\sum_{i=1}^{N} \alpha_i H_i}{L} \tag{3.6.2}$$

where α_i is the in-situ gas volume fraction in RGS segment i, L is the total height of the gas-bearing region, and the effective heights assigned to each RGS segment, H_i, are defined using Simpson's rule integration as

$$H_N = L - \tfrac{1}{2}(z_N + z_{N-1}),$$
$$H_i = \tfrac{1}{2}(z_{i+1} - z_{i-1}), \quad \text{for } 1 < i < N, \text{ and}$$
$$H_1 = \tfrac{1}{2}(z_2 + z_1)$$

The determination of the total height, L, depends (somewhat subjectively) on what waste layers were sampled and on the conditions in the tank. In BY-109, L is taken to be the interstitial liquid level (ILL) because the waste above that level is not saturated with liquid and cannot retain flammable gas; and because the waste above the ILL was not sampled. For U-103, L is the waste surface height at riser 7. In S-106, two of the cores show a definite supernatant liquid layer that cannot store gas, the bottom of which is estimated to average 152 in. in elevation and which was not sampled. This corresponds to the top of the highest RGS segment.

The effective pressure for BPE calculations is determined by (Meyer et al. 1997):

$$P_{eff} = \frac{\sum_{i=1}^{N} \alpha_i H_i}{\sum_{i=1}^{N} \frac{\alpha_i}{P_i} H_i} \tag{3.6.3}$$

where P_i is the in-situ hydrostatic pressure in segment i estimated from the bulk densities of segments above it. The effective dL/dP correlation implied by the RGS data can also be calculated by

$$\left(\frac{dL}{dP}\right)_{RGS} = -\sum_{i=1}^{N} \frac{\alpha_i}{P_i} H_i \tag{3.6.4}$$

The gas inventory estimated from VFI measurements matches the volumes calculated with the BPE model within one standard deviation of the VFI volume. The results for five DSTs (from Meyer et al. [1997]) are summarized in Table 3.2.(a)

Though the comparison was done only for DSTs, the BPE method can also be applied effectively in other tanks with a sufficiently accurate and frequent surface level measurement (daily readings with an automatic Food Instrument Corporation (FIC®) contact probe suffice, hourly readings with an Enraf® buoyancy gauge are best) to provide a clean level-pressure correlation (dL/dP) with reasonably low uncertainty. The level reading must represent the entire waste volume. This requires that the waste be 'wet' (i.e., the ILL nearly equal to the surface level) to transmit hydrostatic pressure uniformly and that the level measurement be away from any hard deposits attached to the tank wall. In this study, both S-106 and U-103 meet these criteria; BY-109 does not because it has no measurable dL/dP correlation and the ILL is ~30 cm (12 in.) below the waste surface.

The foregoing discussion indicates that the gas inventory estimated from RGS data in DSTs might be off from 24% (based on VFI scatter) to almost 40% (Table 3.1). Since the waste in the SSTs appears to be much more nonuniform, the uncertainty in the gas inventory is likely higher still. We think that, in an SST whose cores exhibit high lateral variability in the waste, and which lacks other information on the total gas volume, the uncertainty in the inventory estimated by RGS data alone should be set at 50%. But, if a good level-pressure correlation exists for the tank, and it is a high-variability tank, the BPE method should be used to estimate the gas inventory, with the effective gas pressure defined based on RGS data. (The surface level rise in the tank may be useful as an ancillary corroboration.) Though the uncertainty in the BPE volume estimate may also approach 50%, we are more confident that it captures the mean in tanks with highly variable waste. Hence the "best estimate" gas inventories and their uncertainties for S-106 and U-103 are computed with the BPE method. Only the BY-109 gas inventory is based solely on RGS data, with an uncertainty therefore assigned at 50%.

Table 3.2. Comparison of DST Gas Inventories from VFI Data and the BPE Model

Tank	VFI In-Situ Volume (m^3)	BPE In-Situ Volume (m^3)	(VFI-BPE)/VFI
AN-103	229 ± 41	265 ± 76	-16%
AN-104	132 ± 33	115 ± 38	13%
AN-105	101 ± 34	111 ± 38	-10%
AW-101	89 ± 30	100 ± 31	-12%
SY-103	99 ± 56	100 ± 77	-1%

(a) The VFI gas volumes in this comparison are at in-situ conditions, include estimates of gas retained in the floating solids layer, and are based on the gas volume fraction data set that includes both VFI and RGS measurements. Hence the difference between Tables 3.1 and 3.2.

3.6.3 Corrections for Contamination

Shekarriz et al. (1997) found concentrations of oxygen and argon that were significantly higher than the essentially zero values that were anticipated. This contamination was believed to occur during the sampling process because the leading end of the sampler trapped air and argon (used as a drill-string purge gas).

A separate laboratory measurement of the maximum air volume at STP suggested that a maximum of 6.1 cc of air/argon could be trapped in the nose piece (Cannon 1997). To reduce this source of contamination, procedural changes in sampler preparation were instituted for Tanks U-103, S-106, BY-101, and BY-109. Each sampler's ball valve assembly was backfilled with helium and sealed with grease before the sampler was deployed (Cannon 1997). This step considerably decreased the contamination from gas entrainment. However, contamination by air gases from RGS system inleakage and from isotopic ammonia addition cylinders has been apparent. The air contamination results from Tanks U-103, S-106, and BY-109 are discussed further in Section 5.

The gas concentration results measured by RGS extraction are corrected to in-tank concentrations based on the assumption that all the argon and oxygen in the sample are from the entrained drill-string gases and air inleakage. The argon and oxygen are removed, and the nitrogen is reduced based on the nitrogen-to-oxygen ratio for standard atmospheric air, $N_2/O_2 = 3.73$.

Another type of sample contamination could result from the HHF, the fluid used during the sampling procedures to balance hydrostatic head, seeping into the sampler and replacing some of the waste volume. If such contamination occurred, the RGS measurements would misrepresent the pure waste in four ways (in order of diminishing importance): 1) for a given volume percent of HHF, the calculated gas content of the waste is reduced by about the same percentage, just as if incomplete sample recovery had occurred; 2) the HHF contains dissolved air constituents with which it contaminates the waste gas; 3) the HHF dilutes the ammonia in the sample, reducing its measured partial pressure (measured by the PQ canister grab sample during extraction) below that of pure waste; 4) the HHF may decrease the ionic strength of the waste liquid, increasing the solubility of ammonia and leading to a further underestimate of the partial pressure of ammonia. However, this depends on whether the solids in the waste are still present and in equilibrium with the solution; if so, the solution concentration will be essentially the same as if no HHF had been added.

The HHF was marked with trace amounts of lithium bromide so a chemical analysis could indicate whether contamination has occurred. Chemical analysis results, which are further discussed on a tank-by-tank basis in Section 4, show that HHF (bromide ion), when it was detectible at all, was present in the waste in concentrations that usually corresponded to HHF contamination of 10% or less. Concentrations were often below the Br^- detection limit, which ranged from 3 to 15 vol% depending on the amount of solids in the waste; in most cases the detection limit was less than 8 vol%. The average contamination of 1997 samples was about 7 vol% HHF when detection limits were included in the average as if they were measurements. The actual contamination could be substantially less, because the detection limit represents the maximum amount of HHF that could be present without being measurable, not the actual amount.

3.7 Review of Assumptions Made in RGS Analysis

The preceding sections have derived models for interpreting RGS extraction data to calculate the insoluble gas and ammonia content of the original sample, and for incorporating those data into estimates of in-situ gas volume fractions and gas inventories. Section 3.7.1 provides a review of the assumptions used in deriving the models. Section 3.7.2 compares the assumptions used in this report with those used in the previous RGS report (Shekarriz et al. 1997).

3.7.1 Current Assumptions

Assumption: The available sampler volume (back to the piston) is filled with tank waste (gas/vapor and slurry). That is, 100% sample recovery is assumed. This assumption (used in Section 3.4) is not necessarily true; it depends on the resistance to movement of the waste during sampling, which may be due either to the cohesive strength of the waste or to drag along the walls of the sampler. This effect might result in the waste not filling the sampler and leaving a void at the top of the sample.(a) However, the assumption of 100% recovery is unavoidable because, lacking a method for measuring pressure in the sampler and comparing it with in-situ pressure, we cannot tell whether the void spaces in x-ray images result from retained gas volume or from incomplete sample recovery. Thus we cannot quantify the impact of this assumption, but we believe it leads to less than 10% underestimation of gas content in samples with less than complete sample recovery. This statement is based on a semi-quantitative review of x-ray images of samplers and a comparison of the void in them with the extracted gas content (see Sections 4.n.4).

Assumption: The gas/vapor species behave like ideal gases under the temperatures (25 to 70°C) and pressures (0.02 to 3 atm) applicable to the RGS extraction process and to in-situ conditions. This assumption (used in all the preceding sections) holds for ammonia vapor as well as for the low-solubility species; ammonia's critical pressure and temperature are 112.5 atm and 132.5°C. The reduced pressure ($P/P_c < 0.01$) is so low that the compressibility factor of ammonia is effectively unity.

Assumption: The gas/vapor in the interconnected parts of the RGS system is well mixed such that its composition is the same everywhere. The assumption (used in Sections 3.1 and 3.2) depends on the mixing on both the extractor and the collector side that comes from sudden volume changes caused by pumping.

Assumption: The volume of condensate trapped in the J canister is negligible because the density of the liquid is so much greater than that of the vapor. This assumption (used in Section 3.3) is based on calculations that indicate that less than 0.3% of the canister volume (or 0.3 mL) is taken up by condensate.

Assumption: The low-solubility gases are completely extracted from the sample to the collector or the extractor headspace; no significant amount is lost as a result of deposition on equipment surfaces, dissolution in the canister condensate, or dissolution in the waste sample. The mole fraction information, provided in Tables B.n.7 as mass spectrometry results, shows the extent to which the assumption of complete gas extraction (e.g., low solubility) that is used in Sections 3.1–3.4 is consistent with the data. For truly insoluble gases, the relative composition of the insoluble gases (excluding ammonia) will be the

(a) Shekarriz A and JD Norton. 1995. *Retained Gas Sampler System Analysis.* PNLFGP:091595, Pacific Northwest Laboratory, Richland, Washington.

same for all canisters of a sample. The results of this comparison are presented in Appendix B (Tables B.n.7). Given the measurement uncertainties, the values for hydrogen, nitrogen, oxygen, and argon are relatively constant as a percentage of total. However, it does appear that the fractions of nitrous oxide, methane, and the other hydrocarbons increase as the insoluble gases are removed from the sample, indicating the possibility of a solubility effect. The effect is sufficiently small, however, that it will not significantly affect the total composition results.

Assumption: No significant amount of ammonia is lost because of deposition on equipment surfaces. This assumption is used in Sections 3.1–3.4. RGS system tests have been made using gas standards with low ammonia concentrations and no water. The preliminary findings are that approximately 50 μmol of ammonia are lost. This finding is order-of-magnitude consistent with the maximum of 20 μmol of NH_3 that could be held by a monolayer in the apparatus whose surface area is 0.6 m^2 (± 50%). Based on preliminary tests, the ammonia lost to surfaces (in the absence of condensation) would cause no more than a 10% underestimation for most samples, as review of the ammonia totals in Tables B.n.6 confirms. However, the percentage losses may have been more substantial for S-106 samples because their ammonia content was so small (less than that of any other tank). In addition, the apparent holdover of $^{15}NH_3$ from sample to sample is evidence that absorption occurs. The issue of ammonia absorption is further discussed in Section 5.

Assumption: The ammonia solubility for the waste sample, represented by the effective Henry's Law constant, is assumed not to change significantly as a result of extraction of ammonia. This assumption is used in Sections 3.1 through 3.4.

Assumption: The ammonia in the waste sample is assumed to reach equilibrium with the extractor headspace before every stroke of the mercury pump. This assumption, used in Sections 3.1 through 3.4, is partially incorrect, because pressure-time plots for the extractor show that, after a pump stroke takes gas and vapor out of the extractor and so decreases the pressure, the pressure does not rise all the way to a steady value before the next pump stroke. The impact of this error is unclear. The method of calculating residual (and so total) ammonia does not use a predetermined value for ammonia solubility but only assumes that the solubility is constant throughout extraction. As long as the pump strokes tend (on average) to always truncate the ammonia equilibration at about the same "distance" from equilibrium, the effect will be that the ammonia will behave as though it had a falsely low partial pressure (high solubility). This by itself might not contribute significantly to the error as long as the false solubility is constant. However, another type of nonequilibrium situation must also be considered. If an ammonia concentration gradient exists within the sample (which is not being stirred for most of the extraction), it could cause a significant (as yet unquantified) underestimation of the residual ammonia. Ammonia equilibration is discussed further in Section 5.

Assumption: Gases are in equilibrium between the gas/vapor and slurry phases under tank conditions, and both phases are at the same temperature. This assumption, which is used in Section 3.5, should hold true for undisturbed waste. The effect on equilibrium of the disturbance caused by the sampling process cannot be quantified.

Assumption: The Schumpe model provides an accurate estimate of the Henry's Law constants for each gas constituent in salt solution as long as the correct concentrations of ions are used in the waste solution. This assumption is used in Section 3.5. Norton and Pederson (1995) provide information on the accuracy of this solubility model in predicting oxygen, nitrogen, hydrogen, methane, nitrous oxide, and ammonia solubility in heterogeneous and homogeneous simulants of SY-101 waste. It appears that the Schumpe model predicts solubilities of low-solubility gases with less than a factor of 2 error, while it underpredicts ammonia solubility by a factor of as much as 3 at 60–70°C. (For all species the model error increases with temperature.) The effect of this error is discussed in the next item in terms of the overall impact of solubility errors whether caused by solubility models or poor concentration data.

Assumption: The ionic concentrations of the waste solutions are uniform throughout the tank. This assumption is used in Section 3.5. The concentrations were taken from analyses of drainable liquid from the 1997 core samples and are probably the best concentration data available. The effect of nonuniformity in the solution salt concentration is greatest for ammonia and depends on the ammonia concentration in the tank. In a high-ammonia tank, of which A-101 is the only known example, doubling the total salt concentration can increase the void fraction by as much as 50% because ammonia becomes less soluble in the higher-salt solution and thus enters the gas phase, increasing its volume. In a low-ammonia tank, doubling the salt increases the void fraction by no more than 5% of its value. In both types of tanks, doubling the salt multiplies the ammonia concentration in the vapor phase by a factor of 4 and halving the concentration has substantially less effect than doubling it. The range of variation of the solubility when the total salt is doubled or halved is a factor of 4 to 16, depending on the dissolved species.

Assumption: The hydrostatic head (in-situ pressure) can be calculated with sufficient accuracy by treating each layer as having a uniform density equal to its average density. This assumption is used in Section 3.5. (Waste layers are distinguished from each other, for the purposes of this report, by their thermal behavior [temperature profiles], their physical properties as found in core samples, and their gas retention characteristics. Tank-specific layering details are presented in Section 4.) A typical error in calculating hydrostatic head might involve having 1 m less or more of a layer than had been anticipated at a calculated pressure of 1.5 atm. Then the difference in pressure might be 400 kg/m^3 (a typical difference between slurry and liquid densities) times the depth difference times gravity, or about 4 kPa (0.04 atm). Thus the errors from density and layer depth variation probably cause an error contribution of less than 5% of the void fraction (which is inversely proportional to pressure).

Assumption: The pressure experienced by the bubbles is that of atmospheric pressure plus the hydrostatic head of the bulk waste. That is, the bubbles are supporting both the particles and the liquid above them, and the capillary pressure is not significant. This assumption is used in Section 3.5. In the alternative case, the bubbles are confined to the pores of the waste and support only the liquid in the pores; the particles are self-supporting. In this latter case, bubbles experience hydrostatic pressure from the liquid alone. Because most of the waste in the five tanks is fine-grained and the pores are small, the gas bubbles are expected to be particle-supporting (as assumed in calculations). However, bubbles could be confined to pores in three situations: 1) bubbles in extremely strong waste; 2) bubbles near the tank bottom; or 3) bubbles more than 50 cm (20 in.) deep in coarse saltcake (Stewart et al. 1996b, Section 3.1). We do not have enough information on particle size and waste strength to confirm the assumption of particle-supporting bubbles in all cases. If bubbles in coarse saltcake were not particle-supporting, the in-situ void fraction would be underestimated by less than 15%.

Assumption: All variables are radially uniform; variation between risers is not accounted for in calculations. This assumption (used in Section 3.6) is necessary because there are too few measurements to allow a sound statistical assessment of the effects of lateral variability. Calculating "alternative" inventories based on each riser alone would have little meaning because there would be only one or two samples per layer per riser. Shekarriz et al. (1997) showed that RGS and VFI gas volume estimates could differ by as much as 50%, and the scatter in VFI data for DSTs (Stewart et al. 1996a, b) indicated uncertainties of 20–30% in the gas volume fractions between two risers. Thus tanks that display substantial differences between risers are noted qualitatively on a tank-by-tank basis (in Section 4), and lateral variability estimates are discussed therein on a tank-by-tank basis.

Assumption: The low-solids layer is assumed to be well mixed, so temperature and gas concentration (mol/L) are vertically uniform. This assumption (used in Section 3.6) is equivalent to assuming a void fraction that varies with the inverse of depth. In most cases this assumption is necessary because samples were concentrated in the high-solids layer of the tank, where most of the gas is retained, and at most one sample was taken from the low-solids layer.

Assumption: Concentration within the high-solids layer varies linearly between the vertical locations at which samples were taken (the elevations of the sampler centers). Again, we have no data to permit any more accurate assumptions than this one (which is used in Section 3.6). VFI results for earlier tanks (Shekarriz et al. 1997) suggest that total gas concentrations (void fractions) may not behave monotonically.

In summary, the assumptions under which the low-solubility gas data analysis is conducted are believed to bias the sample gas concentrations on the low side. The total underestimation is probably 10% or less, owing to incomplete sample recovery in a few cases, but this cannot be well quantified. The sample ammonia concentrations are probably further underestimated because of

incomplete ammonia equilibration during extraction, but the degree of this underestimation is not known. Further work is planned to gather more complete ammonia data and to improve ammonia estimation methods to put ammonia on the same footing as the low-solubility gases.

The assumptions in the in-situ gas volume fraction method have less than a ±10% effect on the gas volume fraction in tanks with low ammonia content, such as S-106. However, errors in the ammonia solubility could easily increase or decrease the void fraction by 20% in high-ammonia tanks (U-103 is the best example of the three tanks in this report). The in-situ ammonia vapor concentrations are also sensitive to the solubility (proportional to it), in all the tanks measured to date.

The uncertainty in determining the number of moles of each species for each J canister is a function of the uncertainty in the canister pressure measurement, volume measurement, canister temperature measurement, and the mole fraction measurements provided by mass spectrometry. The uncertainty in the pressure measurement is ± 2% of the full range of the instrument, 101 kPa (1 atm), or an uncertainty of approximately ± 2.0 kPa. The uncertainty in the temperature measurement is approximately ± 2.2°C. The cumulative uncertainty is found using the rms approach of Klein and McClintock as described in Holman (1978).

3.7.2 Assumptions Used in Previous RGS Analyses

Certain assumptions that are no longer necessary were made in the RGS analyses that were carried out for Tanks AW-101, A-101, AN-105, AN-104, and AN-103 (Shekarriz et al. 1997). These were as follows:

- In the current model (Section 3.3), the water vapor pressure in the pumped J canisters is calculated as the water vapor pressure over an ammonia-water solution. In the previous model, the water was assumed to have the vapor pressure of pure water. The resulting underestimation of gas and ammonia vapor was estimated to be 5% or less in cases where the in-situ gas volume fraction was greater than 2%. In samples from low-solids layers, which retain much less gas and produce lower total canister pressures, the under-estimation of low-solubility gas and ammonia vapor resulting from this assumption was estimated to be 10% or less.

- In the current model (Sections 3.1 through 3.4), the water vapor pressure for unpumped J canisters is assumed to be the vapor pressure over the waste, which is calculated based on RGS extraction data. In the previous model, the water vapor pressure over the waste was calculated based on correlations from simulant data (Mahoney and Trent 1995, Equation 6.2 and Table 6.2). This model tends to predict lower vapor pressures than have been calculated from RGS data and led to an overestimation of the gas and ammonia vapor in the sample. However, these relatively low-pressure unpumped canisters typically do not contribute much of the total extracted gas for a sample, so a typical 10% error in gas content of an unpumped canister produced an overestimation of only 1 or 2% in the total sample gas.

- The current model accounts for the gas and ammonia vapor that leave the RGS system in grab samples and partial evacuations. The previous model did not account for these losses, resulting in an underestimation of less than 2% of the gas and ammonia vapor in the system.

- In the current model, the ammonia dissolved in water condensate on the canister (collector) side of the vacuum pump is accounted for. The previous model did not include the condensed ammonia, which caused the total sample ammonia to be underestimated by a factor of about 1.5 to 3.

The experimental procedures used during RGS extractions have also changed. Some of the most noteworthy changes are the following:

- A $^{15}NH_3$ vapor standard is introduced into the system to allow the residual (post-pumping) ammonia in the waste to be determined; the ratio of the isotopic to the normal ^{14}N ammonia in the waste is measured by the mass spectrometer. This method has not resulted in the clear determination of residual ammonia that had been hoped, owing primarily to the long time that seems to be required for equilibration of the isotopic ammonia with the ammonia in the waste. Holdover of the isotopic ammonia from sample to sample has also been evident. These matters are further discussed in Section 5.

- The sample no longer undergoes thermal cycling during extraction. Therefore, temperature-related ammonia solubility changes have not been an issue, and the solubility of ammonia can more confidently be assumed not to change during extraction.

- Administrative and scheduling problems made it impossible to carry out "wet-chemistry" grab-sample analyses. In past work, these measurements provided direct data for the ammonia partial pressure under laboratory conditions and gave a useful cross-check on ammonia determination. They typically showed higher partial pressures of ammonia than did other RGS methods.

3.8 X-Ray Image Analysis

Analyses of x-ray images are expected to yield several pieces of information that will assist in data interpretation and understanding of the waste behavior. The most notable parameter that can be extracted from these images is density. In a less quantitative fashion, the phase distribution can be obtained from these images as well. Furthermore, information on where the gas phase is concentrated or how it is distributed, the structure of the solid matrix/particle agglomerates, and the amount of gas can be inferred. The procedure is essentially the same as that described in Shekarriz et al. (1997), with minor changes.

3.8.1 General Background on X-Ray Image Processing

The current approach yields line-of-sight averaged information on the density of the material that fills the sampler. Such information does not offer the ability to obtain local information along the line-of-sight; the system has no "depth perception." As such, the phases might be distributed in many different ways and still produce the same results. For instance, we can see that there is a void in the waste and measure its size, but we cannot tell where, front to back, the void is. Thus the x-ray image analysis technique offers a two-dimensional map of phase distributions in the core sampler.

Immediately after sampling, each segment is radiographed using the x-ray imaging system described in Appendix A of Shekarriz et al. (1997), and the radiographs are recorded on video tape. The video for each segment is then transferred to a digital image format for analysis. The analysis begins by preparing the calibration standards and extracting the core sample regions of interest from the full-frame video images. Attenuation coefficients for the waste and the water standard are then calculated by applying a logarithmic relationship derived from Beer's law (see Shekarriz et al. 1997 for more details). Density (in terms of specific gravity) of the waste is then obtained by dividing the attenuation coefficients of the waste by the mean attenuation coefficient for water obtained from the calibration sample.

Successful analysis of x-ray images depends heavily on the invariance of the radiography system between imaging the standards and the waste sample. If either the x-ray source energy or the iris on the x-ray imaging camera are adjusted between the radiography of the standards and completion of the waste radiography, the standards may no longer be valid and analysis may not yield reliable results. The air standard is required to effectively compensate for the attenuation of the steel RGS sampler walls. The water standard is used to derive the waste density from the attenuation coefficients.

The entire analysis procedure has been described in detail in Shekarriz et al. (1997). This procedure continues to be used with some minor changes that are summarized in Table 3.3.

Table 3.3. Differences Between Past and Present X-Ray Image Analysis Techniques

Past Method/Equipment	Present Method/Equipment	Reason for Change
PC	MacIntosh	Availability
Image Pro Plus 2.0	NIH Image 1.62b7f from the National Institute of Health(a)	Availability; good image processing capabilities
Averaging of 8 frames	Single frame	Image quality not substantially improved by averaging
50 Line averaging of air and water calibrations	20–50 line averaging	Calibration image size is smaller; it limits averaging over larger area
Creation of composite image	No composite image	Time-consuming task that adds no new information
Creation and application of correction matrix	Not used	Separate correction matrix not available; past use indicated little effect on results
Grayscale images with inverted density scale	False color images with darkness proportional to density	Improvement in image comprehensibility; low-density bubbles now appear lighter than higher-density waste
(a) Analysis performed on a Macintosh computer using the public domain NIH Image 1.62b7f program (developed at the U.S. National Institute of Health and available on the Internet at http://rsb.info.nih.gov/nih-image/)".		

3.8.2 Guide for Viewing X-Ray Images

This subsection is provided as a guide to interpret the x-ray images in Section 4. Figure 3.3 shows the image subsegments, which are marked with Roman numerals to more conveniently identify their relative position in the sampler, with I typically corresponding to an image elevation of 1.5 ft and VI to an elevation of 0.25 ft, given a typical increment between images of 0.25 ft. These identifiers and elevations should be referred to when looking at the tank-specific images in Sections 4.1 through 4.4. Note that the lower part of the piston usually appears in subsegment I and the top of the valve housing usually shows up in subsegment VI. Also, the cable for the valve trigger mechanism occasionally shows up in the images.

Several additional points have a bearing on the information that can be obtained from the density images. First, only features containing several pixels (where a typical pixel is about 0.25 mm in size) can be interpreted as being real. That is, individual pixels embedded in a matrix of a different color do not necessarily imply the presence of very local large density gradients. This is consistent with our earlier estimate of minimum resolvable feature size being on the order of 0.5 mm. Second, the errors associated with image analysis are greatest near the sampler wall, and in the subsequent reporting of average density, we have therefore elected to discard the first 10 pixel rows on both the right and left sides of the image. This means that effectively only the central ~80% of the density image is used in the average density measurements, as reported in Section 4. Therefore, in viewing and interpreting the density images, caution needs to be exercised regarding the density and features present near the wall. Third, the accuracy of these reported measurements is estimated to be within about 5% of the true value.

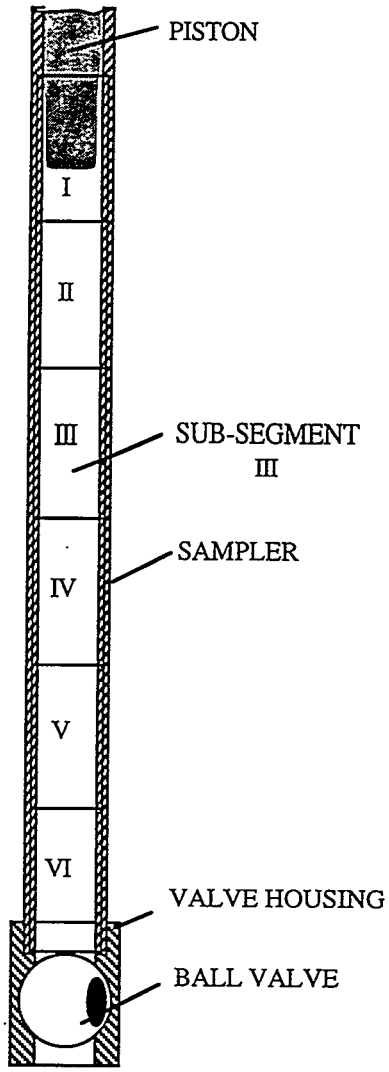

Figure 3.3. Schematic Diagram of X-Ray Subsegments

4.0 Tank-by-Tank RGS Results

This report primarily focuses on the RGS results from the four tanks that underwent RGS sampling during calendar year 1997. In Section 5, the 1997 results are compared with those from samples taken in 1996.

The samples underwent extraction (by procedures that are described generically in Appendix A and specifically [with sample-by-sample variations] in Appendix B). The physical models (algorithms) described in Section 3 were applied to the extraction data to calculate the species concentrations in each sample and then to find the tank inventories. The results of these calculations are found in this section.

The results are presented separately for each tank. (Intercomparisons are reserved for Section 5.) First the tanks are characterized with respect to sample locations and timing, waste and layer levels, waste densities and types, and temperatures (Sections 4.n and 4.n.1, where n is the tank sequence number, 1 for U-103, 2 for S-106, 3 for BY-101, and 4 for BY-109). Then, in Sections 4.n.2 and 4.n.3, the compositions and gas volume fractions are given, along with gas inventory estimates. The features of the waste that were visible in x-ray images of the RGS samplers are described in Sections 4.n.4, and the features visible during extrusion of other core samples are briefly described and illustrated in Sections 4.n.5. Unusual or unprecedented results (when there are any) are highlighted in Sections 4.n.6. Finally, Section 4.5 provides an overview of the retained gas compositions that have been found in all the tanks that have been sampled, emphasizing the tanks sampled in 1997.

4.1 Tank U-103

Tank U-103 was the sixth tank and the second SST sampled with the RGS. This tank was selected as representing the highest-priority group of SSTs that show evidence of significant gas retention (Stewart et al. 1996a). Tank U-103 is on the Flammable Gas and Organic Watch Lists, exhibiting high concentrations of H_2 and NH_3 in the dome space. It is part of a group of tanks (Cluster 13 in Stewart et al. [1996b]) that have fairly high radioactivity, fairly low temperatures, high nitrite concentrations, and about 0.1% total organic carbon (TOC). Historical tank content estimates indicate that the primary waste stored in U-103 was saltcake from evaporator campaign S1, and the secondary waste was salt slurry from evaporator campaign S2 (Remund et al. 1995).

Push-mode sampling was done in risers 7 and 13 in February 1997 and April 1997, respectively.(a) Sampling was also attempted in riser 2 in October 1996, but the waste (or some object imbedded in it) proved impenetrable. The approximate locations of the risers are depicted in Figure 4.1.1. Core segments were taken at various elevations in each riser, as shown in Figure 4.1.2.

The total depth of waste in Tank U-103 is approximately 422 ± 1.5 cm (166 ± 0.5 in.). Figure 4.1.2 shows the expected tank content layering as derived from sample data taken in the late 1970s (Brevick 1994). On this basis, a partial crust was believed to be about 36 cm (14 in.) thick, and a salt slurry layer 48 cm (19 in.) thick lies under the crust. Saltcake was believed to form most

(a) Bates JM and R Shekarriz. October 1996. *Sampling Plan for Tank 241-U-103 Retained Gas Sampler Deployment.* TWSMIT:091896 Rev. 2, Pacific Northwest National Laboratory, Richland, Washington.

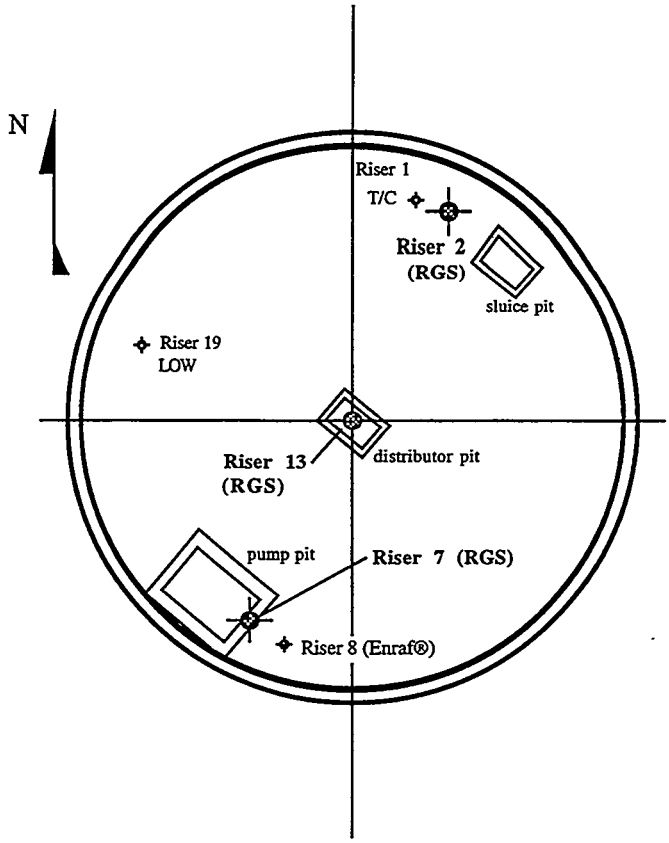

Figure 4.1.1. Schematic Diagram of Riser Locations in Tank U-103

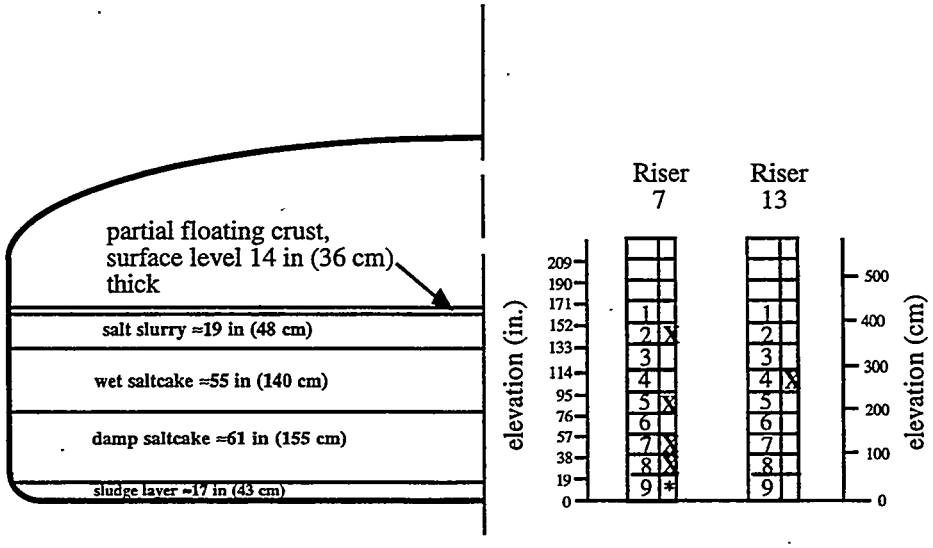

Figure 4.1.2. Diagram of Expected Waste Layering and RGS Sample Elevations for U-103 (segment 9 of riser 7 could not be taken because the waste was too hard or the tank bottom was reached. Sampling was attempted but abandoned in riser 2 because an obstacle or hard waste blocked the drill string)

of the balance of the contents; the upper 140 cm (55 in.) of the saltcake was described as "wet," while the lower 155 cm (61 in.) was "damp." A 43-cm (17-in.)-thick sludge layer was believed to occupy the bottom of the tank. Eight full sampler cores and one partial sampler core were taken; of these, the crust occupied the partial core in segment 1 (not an RGS segment). The elevations of the RGS segments are depicted in Figure 4.1.2.

Figure 4.1.3 is a temperature profile from the thermocouple tree in riser 1. The large squares show the average temperature measured between May and August 1996; the temperature minima and maxima at each thermocouple (TC) are also shown. The low temperature and small temperature difference indicate relatively low heat load. The temperature profile shows the parabolic shape characteristic of conduction heat transfer with generation. No significant convective layer, which would appear as a uniform temperature or a sharp slope change in the profile, is indicated. However, the temperature profile at this riser may not be representative of most of the waste because the riser is so close to the wall (Figure 4.1.1).

The most recent information on tank content layering comes from the core observations made in 1997, which are presented in Figure 4.1.4.(a) The thickness of the top layer of liquid varies from one to three segments over the three risers. Another sign of lateral waste variability is the presence of sludge slurry at the top of riser 13 but not the other risers. The core samples from riser 13 roughly match the layering that was expected before the 1997 sampling was carried out (see Figure 4.1.2). The major difference is the presence of sludge slurry as the top layer and the absence of sludge at the bottom. ("Sludge slurry" is a term based on core extrusion observations, not chemical analysis. "Sludge" denotes a core that has a muddy, slimy appearance, rather than the gritty, sandy appearance of "salt" materials. "Slurry" indicates that the core is wet enough to slump under its own weight.) Riser 13 also appears to contain subsurface liquid (segments 8 and 9) that was not part of the expected layering. The liquid in these segments is not an artifact of HHF intrusion, based on the low bromide concentrations in the samples.

Preliminary densities for the liquid and bulk solids in Tank U-103 were available from cores taken in 1997.(a) The density of drainable liquid varied from 1345 to 1500 kg/m^3, with an average and standard deviation of 1420 ± 49 kg/m^3. The bulk density of the samples with high solids concentrations varied from 1490 to 2370 kg/m^3, with an average and standard deviation of 1730 ± 150 kg/m^3.

For the purpose of in-situ inventory and average composition calculations, the liquid density was set at 1420 kg/m^3, and the remainder of the tank waste was given a bulk density of 1730 kg/m^3. A waste depth of 422 cm (166 in.) was used in the calculations, and the waste was treated as a single layer.

4.1.1 Sampling and Extraction Information

The segments analyzed are listed in Table 4.1.1. Riser 13 segment 4, the only RGS sample from riser 13, was lost because the sampler valve froze closed after the sample was taken and could only be opened slightly. Some of the gas that leaked out through the valve was collected, but a complete extraction was impossible. Only x-ray data and insoluble gas composition data were obtained; these data show a gas composition and a sampler gas space (a rough measure of gas quantity) that are consistent with the high-gas content findings for segment 2 of riser 7.

(a) Sasaki L. April 21, 1997. Transmittal from L. Sasaki to LA Mahoney (PNNL) of data collected for the U-103 TCR (document in preparation). Lockheed Martin Hanford Corporation, Richland, Washington.

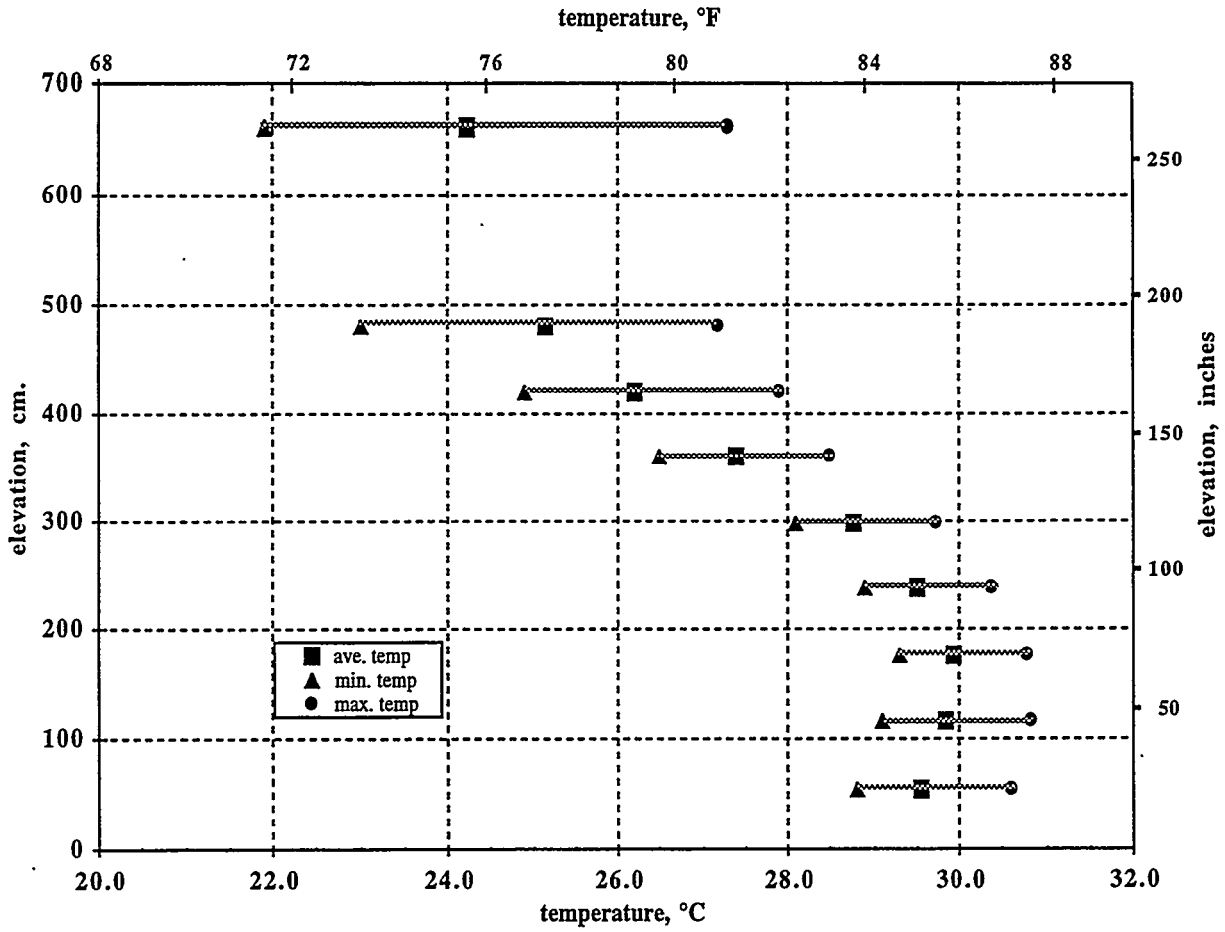

Figure 4.1.3. Profile of Temperature in Tank U-103 Taken with TC Tree

Table 4.1.1. Lag Times for Processing RGS Samples from Tank U-103

Sample	Acquisition Date	Processing Date	Lag (days)
7-2	January 21, 1997	February 4, 1997	14
7-5	January 22, 1997	February 6, 1997	15
7-7	January 22, 1997	February 12, 1997	21
7-8	January 22, 1997	February 13, 1997	22
13-4	April 2, 1997	April 23, 1997	21

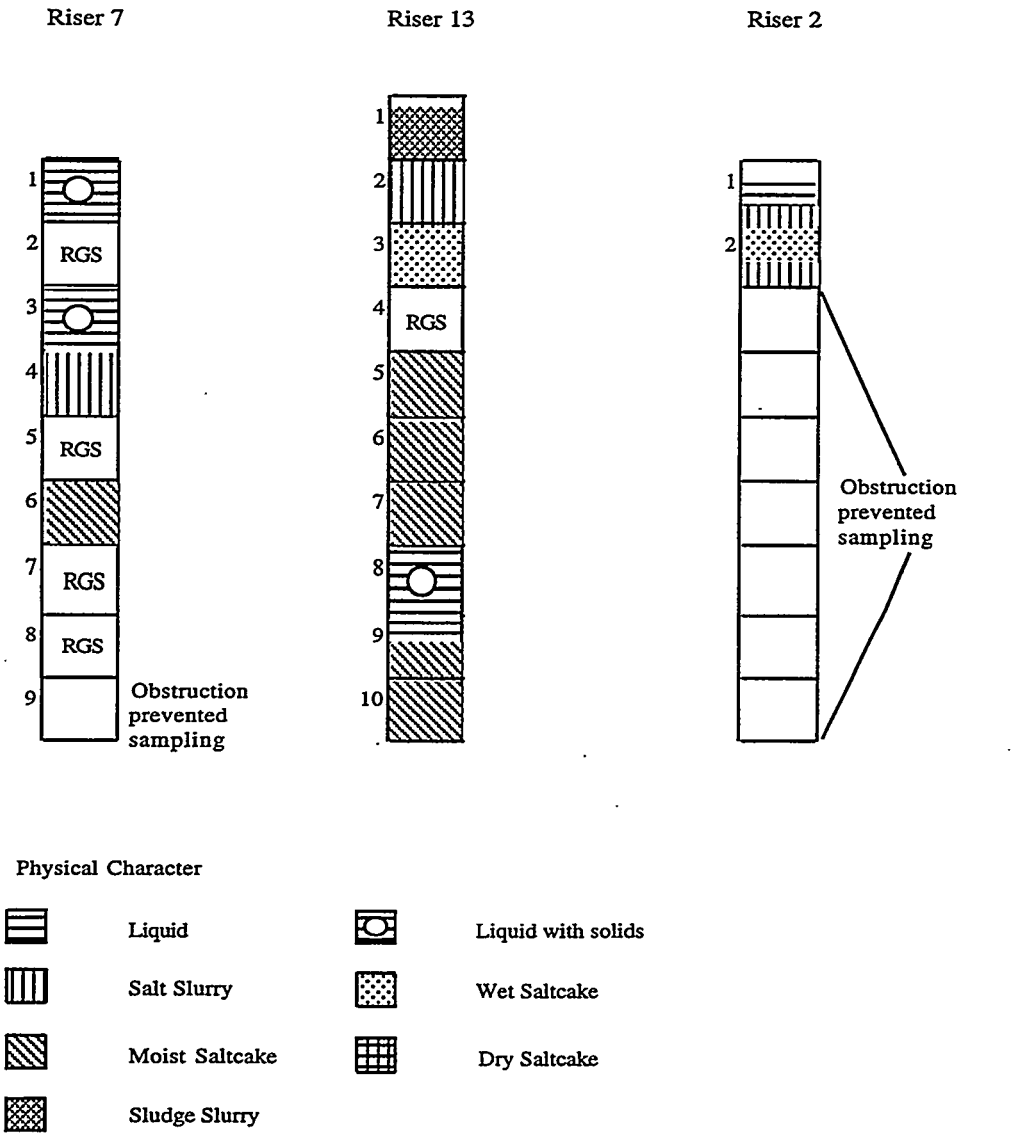

Figure 4.1.4. Most Recent Core Profile for the Push-Mode Sampling Risers in Tank U-103(a)

Table 4.1.1 also shows the lag times (delay between sample acquisition and processing) for these samples. This information was provided to allow data users to correlate the lag time between sampling and extrusion with the concentrations of the various constituents, to test for decomposition or other chemical reactions. One such correlation (of oxygen plus other contamination gases versus lag time) is discussed in Section 5.

As is discussed in Section 3.6.2, the HHF used during sampling may enter the sampler in place of some of the waste. The HHF is a solution of LiBr; the Br^- ion that is not present in waste is used as the HHF tracer. Table 4.1.2 shows the volume percentage contamination by HHF of

(a) Personal communication, AP Mousel (LATA) to LA Mahoney. May 23, 1997. "U-103 PMCS Core Profile." File U103.CRD, revised April 22, 1997. Los Alamos Technical Associates, Richland, Washington.

Table 4.1.2. Hydrostatic Head Fluid Contamination in Riser 7 Samples

Sample	HHF Contamination (vol%)
7-1	< 3.7
7-2 (RGS)	no data
7-3	9.0
7-4	6.8
7-5 (RGS)	< 7.9
7-6	< 14.6
7-7 (RGS)	4.2
7-8 (RGS)	4.9
7-9	10.5

samples in riser 7, from which all the RGS samples were taken. Some of these samples (7-1, 7-5, and 7-6) contained bromide below the detection limit. Averaging the HHF contamination over all the riser 7 samples and treating the below-detection samples as if at the detection limit gives an average contamination of 7.1 vol%. This value is used to calculate a reduced effective sampler volume for RGS samples 7-2 (no bromide data) and 7-5 (bromide below the detection limit). The actual measured HHF contamination percentages are used for RGS samples 7-7 and 7-8.

All of these samplers were helium-backfilled and sealed with vacuum grease before they were deployed. This method virtually eliminated air and argon contamination from gases entrained during sampling. The helium backfill results are discussed in considerable detail by Cannon (1997) and summarized in Section 5 of this report.

The data analysis calculations were carried out as described in Section 3 of this report, with a method that calculates the condensed ammonia in the canisters as well as the ammonia in the vapor phase. In addition, one U-103 sample (segment 2) was injected (after gas extraction) with an ^{15}N-labeled ammonia standard to determine how much ammonia was still dissolved in the sample after the extraction of other gases was complete. The results of this residual ammonia analysis are discussed in Section 5.

4.1.2 Retained Gas Composition

Table 4.1.3 presents the estimated concentrations of the insoluble gases in each RGS sample taken from U-103, without corrections for air and argon entrainment and helium backfill. The corrections consist of removing all the oxygen, argon, and helium and subtracting (3.73) · (O_2) from the nitrogen, consistent with the molar N_2/O_2 ratio in atmospheric air. The corrected concentrations are given in Table 4.1.4. Segment 13-4 is not shown in Table 4.1.4 because a full extraction could not be performed; its H_2/N_2O ratio was 1.2, higher than the values for the other segments of U-103 but lower than the ratios for other tanks.

Table 4.1.3. Concentrations of Insoluble Constituents (μmol/L of waste) in Tank U-103 Without Gas Entrainment Correction

Segment	N_2	H_2	N_2O	O_2	CH_4	He	Ar	Other Nit. Ox	C_2H_x	C_3H_x	Other Hyd.
7-2	7000±590	4300±350	7500±600	63±23	75±7.0	520±120	13±2.6	2.3±2.3	76±9.7	0.02±0.02	6.7±2.5
7-5	1600±380	700±170	2700±640	11±2.5	12±4.2	390±90	2.2±0.6	0±0	11±5.4	1.9±1.1	3.8±1.3
7-7	2500±430	1400±240	2000±340	5.8±1.1	34±10	480±80	2.0±0.4	8.5±4.6	46±9.8	0.01±0.01	4.8±1.6
7-8	1600±300	1400±250	1400±270	9.7±1.9	32±9.0	430±80	3.0±0.5	19±5.2	49±11	0.78±0.43	5.1±1.6

Table 4.1.4. Concentrations of Insoluble Constituents (μmol/L of waste) in Tank U-103 With Gas Entrainment Correction

Segment	N_2	H_2	N_2O	O_2	CH_4	He	Ar	Other Nit. Ox	C_2H_x	C_3H_x	Other Hyd.
7-2	6700±600	4300±350	7400±600	0	74±7.0	0	0	2.3±2.3	76±9.7	0.02±0.02	6.7±2.5
7-5	1600±380	700±170	2700±640	0	12±4.2	0	0	0±0	11±5.4	1.9±1.1	3.8±1.3
7-7	2500±430	1400±240	2000±340	0	34±10	0	0	8.5±4.6	46±9.8	0.01±0.01	4.8±1.6
7-8	1600±300	1400±250	1400±270	0	32±9.0	0	0	19±5.2	49±11	0.78±0.43	5.1±1.6

Table 4.1.5 presents the total ammonia concentration per liter of waste under in-tank conditions. The "extracted NH_3" column gives the total moles of ammonia, both condensed and vapor-phase, that were pumped out of the samples into the "J" collection canisters. "Residual NH_3" refers to the ammonia remaining in the waste after pumping. It was possible to calculate the extracted ammonia with more accuracy than was possible for the residual ammonia; therefore, the latter is shown separately in the table.

However, the residual ammonia was easier to estimate for segment 7-2, the sole segment for which labeled ammonia was injected to determine the residual. It should be noted that the labeled-ammonia method has not yet been fully tested on standard waste simulants; until such tests have been completed, the method should be considered unverified. A further discussion of the ammonia calculations is given in Section 5.

The ammonia concentration of segment 7-2 is significantly lower than that of the other samples, possibly because the sample volume was occupied by so much gas and solids that there was little liquid, which usually contains essentially all of the ammonia. Another possibility is that the isotopically labeled ammonia, which was used to determine the residual ammonia, did not have enough time to reach equilibrium with the ammonia dissolved in the waste and therefore caused the residual ammonia to be underestimated. The latter theory seems unlikely to be the full explanation because the extracted, as well as the residual, ammonia is low in 7-2.

Table 4.1.5. Total Ammonia Concentrations in Tank U-103

Segment	Extracted NH_3 (μmol/L)	Residual NH_3 (μmol/L)	Total NH_3 (μmol/L)
7-2	600 ±120	1700 ± 540[a]	2300 ± 660[a]
7-5	11000 ± 1600	38000 ± 38000[b]	49000 ± 40000[b]
7-7	21000 ± 3100	55000 ± 55000	76000 ± 59000
7-8	14000 ± 3200	29000 ± 29000	43000 ± 31000

(a) The residual NH_3 for segment 2 was calculated by the labeled standard method.
(b) The residual NH_3 for segment 5 was calculated by assuming that the Henry's Law constant for the segment was equal to the average of Henry's Law constants for segments 2, 7, and 8.

The variation in the ammonia concentrations of the other samples is less than the measurement error band; thus the differences among the ammonia contents of segments 7-5, 7-7, and 7-8 may be more apparent than real. The average and standard deviation of the ammonia concentrations over segments 7-5, 7-7, and 7-8 are 56,000 ± 18,000 μmol/L waste (0.17 wt% NH_3 dissolved in the liquid).

Table 4.1.6 contains the composition of the gas/vapor phase in each sample and the integrated average composition for Tank U-103. The sample compositions in the table have been calculated using the in-situ solubility method described in Section 3.5.2. The tank average composition is the result of integrating RGS species concentrations over the waste layer and multiplying those concentrations by the waste volume. The integration method is described in Section 3.6.

Table 4.1.6. Sample and Overall Average Compositions of Retained Gas in Tank U-103 With Gas Entrainment Correction

Segment	N_2 (mol%)	H_2 (mol%)	N_2O (mol%)	NH_3 (mol%)	Other (mol%)
7-2	36 ± 4.4	23 ± 2.7	40 ± 4.6	0.22 ± 0.07	0.86 ± 0.14
7-5	31 ± 11	14 ± 4.9	52 ± 18	2.8 ± 2.4	0.58 ± 0.27
7-7	40 ± 10	23 ± 6.0	32 ± 8.2	3.9 ± 3.1	1.5 ± 0.51
7-8	35 ± 9.7	30 ± 8.3	30 ± 8.2	2.0 ± 1.5	2.3 ± 0.76
Average in tank waste[a]	36 ± 7.6	22 ± 4.7	40 ± 8.5	1.2 ± 1.2	1.0 ± 0.3

(a) The error bands on the average composition, as for the individual sample compositions, only represent the instrument error because there are too few samples to define the spatial variability of gas concentration.

4.1.3 Gas Inventory

The method by which the in-situ gas volume fractions were calculated is given in Section 3; the results are presented in Table 4.1.7, showing the difference between in-situ gas volume fractions that were and were not corrected for the presence of entrained and backfilled gases. The table also contains the average gas volume fraction and the average pressure experienced by the gas. All of the averages are in-situ volume averages and are calculated by Simpson's Rule integration, as described in Section 3.6.

The four ammonia concentration measurements in U-103 integrate to a total (vapor and dissolved) ammonia inventory that would have an STP volume of 1500 m^3 (52,000 ft^3). The error band on the ammonia inventory should be considered to be at least 50%.

Table 4.1.8 gives estimates of the STP volume of gas in the waste in Tank U-103. The RGS gas inventory was calculated by integrating RGS total gas concentrations (four data points) over the waste layer and multiplying the average gas concentration by the volume of the waste. The integration method is described in Section 3. The RGS volumes in Table 4.1.8 all include corrections to remove the entrained air, argon, and the backfilled helium. In all cases, as is further discussed in Section 5, the correction for entrained gas was insignificant, and the amount of helium present was found to be equivalent to the air/argon entrainment that had been contained in samples taken from tanks sampled previously (Shekarriz et al. 1997).

The gas inventory calculation for U-103 is complicated by the extremely high corrected gas fraction of 0.44 in segment 7-2. This brings the average gas fraction based on RGS data to 0.20 ± 0.10, which corresponds to a total in-situ gas inventory of 420 ± 210 m^3. The measured dL/dP correlation for U-103 is -0.48 ± 0.13 in./in.-Hg,(a) which translates into an average gas fraction of 0.11 ± 0.03 and an in-situ gas volume of 200 ± 60 m^3. If the segment 7-2 value is ignored, the average gas fraction calculated from RGS data comes down to 0.095 ± 0.05, an in-situ gas volume of 160 ± 80 m^3.

Table 4.1.7. In-Situ Gas Volume Fractions in Tank U-103

Segment	Sample Central Height (cm)	Hydrostatic Pressure (atm)	Temperature (°C)	Corrected Gas Volume Fraction (in-tank conditions)	Uncorrected Gas Volume Fraction (in-tank conditions)
7-2	362	1.06	27.4	0.441 ± 0.042	0.460
7-5	217	1.26	29.7	0.100 ± 0.018	0.110
7-7	121	1.41	29.8	0.110 ± 0.018	0.120
7-8	72	1.48	29.7	0.077 ± 0.014	0.085
Average in waste		1.19 ± 0.04		0.20 ± 0.10	

(a) Whitney PD, PA Gauglitz, PA Meyer, and NE Miller. April 1997. *Estimating Retained Gas Volumes in the Hanford Tanks Using Waste Level Measurements: Progress.* TWSFG97.33, Pacific Northwest National Laboratory, Richland, Washington.

Table 4.1.8. U-103 Gas Inventory Corrected for Gas Entrainment

Quantity	RGS	Best Estimate (BPE)
Avg. Gas Fraction	0.20 ± 0.10	0.11 ± 0.03
Gas Volume (m^3) In-Situ STP	 350 ± 175 420 ± 210	 200 ± 60 260 ± 70
dL/dP (in./in.-Hg)	-0.95 ± 0.48	-0.48 ± 0.13
P_{eff} (atm)	1.19 ± 0.04	1.31 ± 0.06 [(a)]
(a) The effective pressure P_{eff} for computing the gas volume from the measured dL/dP was determined with the high segment 7-2 gas fraction ignored. Otherwise, the effective pressure would have been underestimated.		

The surface level measurement in U-103 is via an Enraf buoyancy gauge in riser 8. This riser is near the tank wall adjacent to riser 7 from which the usable RGS samples were taken. Segments 1 and 3 from riser 7 contained a high fraction of liquid, and no hard saltcake was penetrated at the surface. Riser 13 waste was also moist, although there was no free liquid in the upper layers. We conclude that, though the level gauge is near the tank wall, there is no attached "shelf" to prevent it from sensing level fluctuations, and there is free liquid in the vicinity to transmit waste expansion/compression from elsewhere in the tank.

While the BPE value is higher than the 0.095 obtained by ignoring the high segment 7-2 datum, it is much lower than assuming the high value represents the entire upper layer of the tank. Similarly, there is no indication from surface level rise (SLR) that such a high gas content is present. The waste surface level has risen about 3 inches since 1981. If an additional 6-in. rise is allowed for pre-existing gas inventory and evaporation (Hodgson et al. 1996), the resulting gas fraction is only 0.06 ± 0.04. The low inventories indicated by BPE and SLR imply that the high gas fraction measured by RGS in segment 7-2 does not extend over the whole upper layer of the tank, though there is more gas in the upper region than in the other three segments.

Because the RGS data were taken in only one riser, near the tank periphery, and the waste shows signs of lateral variability, we choose the predictions of the BPE method as the best estimate for the gas inventory of U-103. These calculations are summarized in Table 4.1.8.

Figure 4.1.5 shows the corrected gas volume fractions (Table 4.1.7) and the entrainment-corrected compositions (Table 4.1.4) in the samples from U-103. The compositions represent the mole fraction of the species in the insoluble gas. Water and ammonia are not included. Figure 4.1.5 also shows data taken from core extrusion analyses, as a way of tying those observations together with RGS. The lines and symbols in the rightmost plot indicate the fraction of the sample mass that was drainable liquid; the remainder is wet solids. The bulk densities measured for the wet solids in each sample are also noted on the figure.

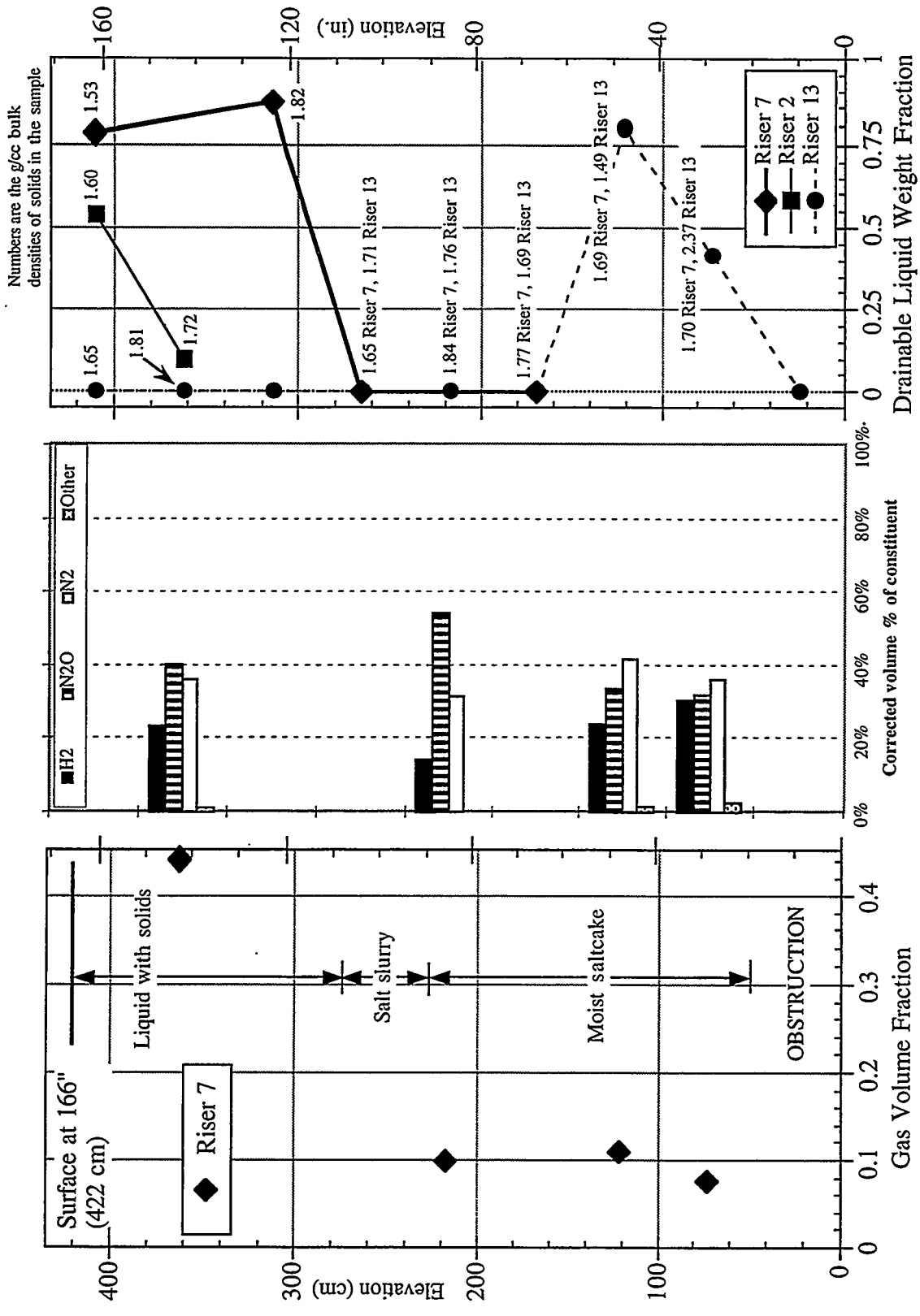

Figure 4.1.5. Gas Volume Fractions, Compositions, and Liquid Contents in Tank U-103

4.1.4 X-Ray Results

Table 4.1.9 summarizes all the available radiography observations, including segment 4 from riser 13. (The segment 4 sampler had a frozen ball valve that made RGS extraction impossible, but the radiographs are valid.) There were no standard air/water density profiles for two of the five samples for which x-ray images were recorded (segments 7-5 and 13-4). The standard air/water density profiles for segment 7-8 were used for segment 7-5 because they were x-rayed on the same day. The profiles for segment 14-2 from Tank S-106 were used for segment 13-4 from U-103 for the same reason.

The error bands of the visible gas volume fractions that are given in Table 4.1.9 are unknown but are believed to be larger than the errors in the gas volume fractions calculated from gas extraction. (The "visible" gas volume fraction refers to the gas that has separated from the solids and liquid such that its volume can be calculated based on the image. The uncorrected gas fractions from extraction are used for comparison to reflect the presence of entrained air in the sampler.) A comparison of x-ray-derived gas volume fractions and extraction-derived gas volume

Table 4.1.9. Summary of Observations from X-Ray Images of Tank U-103

Segment	Comments/Observations
7-2	The waste in this sample occupies only the bottom 25 cm (10.1 in.). The waste is homogeneous in appearance with a flat meniscus and a 23 cm (8.9 in.) gas gap below the piston. No waste was attached to the piston. The visible gas fraction is therefore 0.47. (Compare with the uncorrected gas volume fraction of 0.460 ± 0.04 in Table 4.1.7 obtained by gas extraction.)
7-5[a]	This sample contained barely visible gas bubbles. There is a slightly curved top surface and a 2.5 cm (1 in.) gas gap below the piston, to which a large lump of waste is attached. The visible gas volume fraction (not counting bubbles, and excluding the volume of the waste on the piston) is therefore 0.052. (Compare with the uncorrected gas volume fraction of 0.110 ± 0.02 in Table 4.1.7 obtained by gas extraction.)
7-7	This sample contained barely visible gas bubbles. There is a lumpy top surface and a 6.1 cm (2.4 in.) gas gap below the piston, to which a large lump of waste is attached. The visible gas volume fraction (not counting bubbles, and excluding the volume of the waste on the piston) is therefore 0.114. (Compare with the uncorrected gas volume fraction of 0.120 ± 0.02 in Table 4.1.7 obtained by gas extraction.)
7-8	This sample contained barely visible gas bubbles, mostly near the top. There is a smooth slanting top surface and a 7.4 cm (2.9 in.) gas gap below the piston, to which a sampler-spanning lump of waste is attached. The visible gas volume fraction (not counting bubbles, and excluding the volume of the waste on the piston) is therefore 0.116. (Compare with the uncorrected gas volume fraction of 0.085 ± 0.02 in Table 4.1.7 obtained by gas extraction.)
13-4[b]	This sample showed bubble structure, with many mostly round bubbles of diameter up to about 1 cm. It was about 25 cm (10 in) full. The top surface of the waste is uneven. No image of the piston was available, so it is not known whether waste was attached to it. The visible gas volume fraction is 0.47, roughly equal to that of segment 7-2, but there are no RGS extraction data for comparison.
(a) This segment lacked standard air/water density profiles; used data from segment 7-8 taken the same day. (b) This segment lacked standard air/water density profiles; used data from segment 14-2 of Tank S-106 taken the same day.	

fractions, which is given in Table 4.1.9, shows that sample recovery was about 95% for segments 7-2, 7-7, and 7-8, and about 100% for segment 7-5. (The visibly bubbly waste in segments 7-5, 7-7, and 7-8 is estimated to contain about 5% gas.) The 5% or less underestimate caused by incomplete sample recovery is within the gas fraction measurement error.

Table 4.1.10 provides a summary of the waste densities that have been estimated from radiographic data. The radiographic densities include the gas in the waste and are given for several locations within each sample to show density trends.

Table 4.1.10. Densities of U-103 Samples from Radiography and Core Samples

Riser-Segment Number	Distance from Bottom of Sampler (ft)	Calculated Mean Density (g/cc)	Calculated Standard Deviation (g/cc)	Gas-Free Density Above and Below the RGS Sample (from cores) (g/cc)
7-2	0.25	1.38	0.29	density above, 1.53 g/cc solid 1.42 g/cc liquid
	0.50	1.44	0.27	density below, 1.82 g/cc solid 1.42 g/cc liquid
	0.75	1.37	0.26	
7-5[a]	0.25	1.48	0.26	density above, 1.65 g/cc
	0.50	1.60	0.24	
	0.75	1.55	0.24	density 1.84 g/cc
	1.00	1.36	0.27	
	1.25	1.24	0.25	density below, 1.77 g/cc
7-7	0.25	1.23	0.31	density above, 1.77 g/cc
	0.50	1.27	0.29	
	0.75	1.30	0.28	density 1.69 g/cc
	1.00	1.40	0.30	
	1.25	1.50	0.30	density below, 1.70 g/cc
7-8	0.25	1.40	0.23	density above, 1.69 g/cc
	0.50	1.44	0.24	
	0.75	1.44	0.30	density 1.70 g/cc
	1.00	1.34	0.24	
	1.25	1.46	0.24	
	waste on piston	1.37	0.24	
13-4[b]	0.50	1.20	0.28	density above, 1.80 g/cc
	0.75	1.18	0.32	
	1.00	1.15	0.31	density below, 1.71 g/cc

(a) This segment lacked standard air/water density profiles; used data from segment 7-8 taken the same day.
(b) This segment lacked standard air/water density profiles; used data from segment 14-2 of Tank S-106 taken the same day.

Table 4.1.10 also shows the densities that were measured for the core samples that lay above and below each RGS sample; these are gas-free densities. (In some cases densities were also available for RGS segments because the samples underwent further analysis after RGS processing was complete.) The x-ray methods gives consistently lower results, even when the extracted gas content of the x-rayed samples is accounted for, and even for the samples that had air/water density profiles.

Figure 4.1.6 shows density images calculated from the x-rays of segment 7-7. The bubble structure in the waste has been enhanced with color. In these images, features that are only a few pixels in size are probably noise and should be ignored. The waste attached to the piston is clearly evident at the upper left, as is the lumpy surface of the waste. The piston cables are also visible.

4.1.5 Core Extrusion Results

Figure 4.1.7 shows some samples of U-103 waste. The RGS samples comprised segments 2, 5, 7, and 8 from riser 7 (Core 176). Segments 1 and 3 from riser 7 contained liquid (see Figure 4.1.5) and are not shown. The remaining samples from riser 7, segments 4 and 6, are shown in Figure 4.1.7. Both samples were dark gray to brown in color. Sample 7-4 had the appearance of salt slurry, soggy and partly collapsed with its own weight, while sample 7-6 was visibly stiffer, more solid and drier, without a liquid film on its surface—characteristics of moist saltcake. Neither extrusion showed the pockmarks or cavities that would mark gas bubbles. The bubbles in the riser 7 RGS samples (Table 4.1.9) were also barely visible, and the x-rays showed that the waste adhered to the piston, suggesting strong, "sticky" waste in riser 7.

The figure also shows some samples from riser 13, from which no RGS samples were taken successfully. The riser 13 samples were like those in riser 7 in color and texture. Samples 13-1 (pictured), 13-2 (pictured), and 13-3 were brown to dark gray and wetter than samples 7-4 and 7-6; their texture was between the sandy appearance of saltcake and the muddy, slimy appearance of sludge. Large bubble pocks marked these three samples, most of them in segment 13-1. This is consistent with the bubble structure that appeared in the unsuccessful RGS sample 13-4 (Table 4.1.9).

Segments 13-5, 13-6, and 13-7 (13-7 is pictured) were all very alike. They were much darker, drier, and stiffer than the top three segments of the riser 13 core (Core 182). They showed no visible bubble pocks, although they were at about the same elevation as RGS sample 7-5 (gas volume fraction of 0.100). Segment 13-7 broke into smaller fragments than 13-5 and 13-6 on extrusion and probably contained the stiffest waste of the three; it also appeared slightly drier.

Sample 13-8 (pictured) and the upper half of 13-9, however, were almost entirely liquid (as shown in Figure 4.1.5). RGS sample 7-7, at the same level, showed no sign of free liquid in its x-ray (Figure 4.1.6); the top surface of the waste was a lumpy, rather than smooth, liquid meniscus. The next lower samples were the lower half of 13-9 and the upper half of 13-10, which resembled the dark moist salt of sample 13-5 except that some small bubble pocks were present. These were at about the same elevation as RGS sample 7-8, with its relatively low gas volume fraction of 0.077.

At the very bottom of the core, in the bottom half of segment 13-10, was a stiff, solidly packed, moist material, most of which was nearly black in color, though the bottom 2 or 3 inches were brown. No bubble marks were evident in this bottom material.

The few segments from riser 2 (Core 175, which is not included in Figure 4.1.7) contained coarse-textured moist gray salt and salt slurry that was lighter colored in segment 1 than segment 2 and not as stiff as the riser 7 material. Drainable liquid was present in segment 1, but not lower.

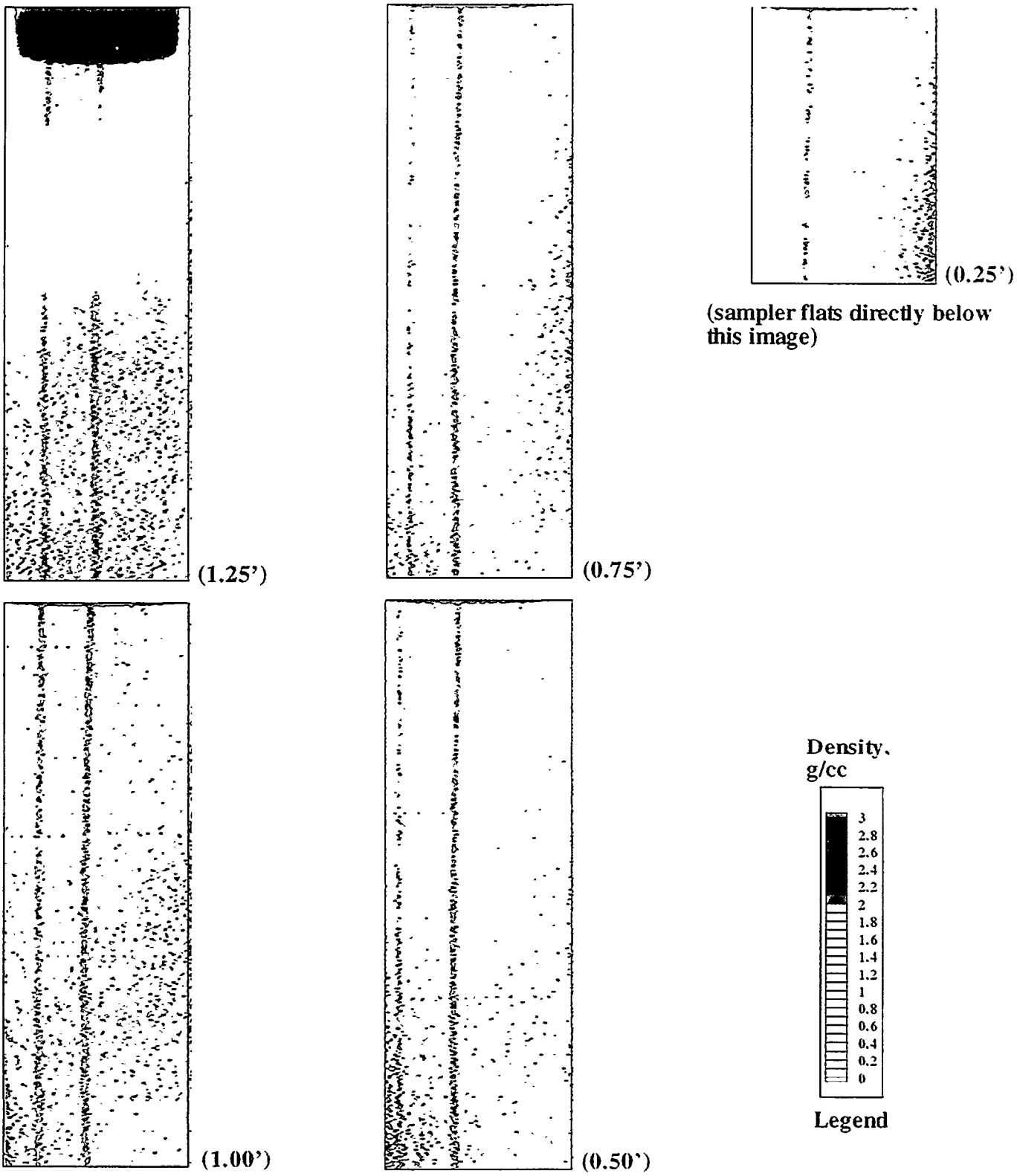

Figure 4.1.6. Density Images Calculated from X-Rays of Sample 7-7 from Tank U-103

U-103 Core 182, Riser 13, Segment 1

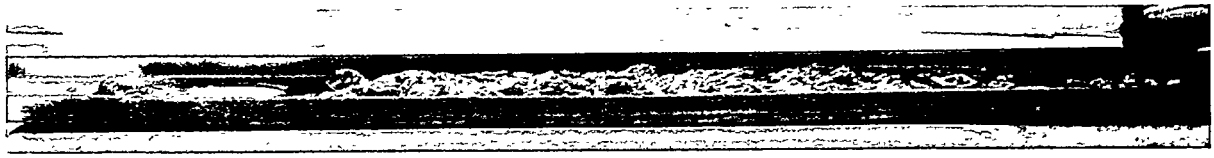

U-103 Core 182, Riser 13, Segment 2

U-103 Core 176, Riser 7, Segment 4

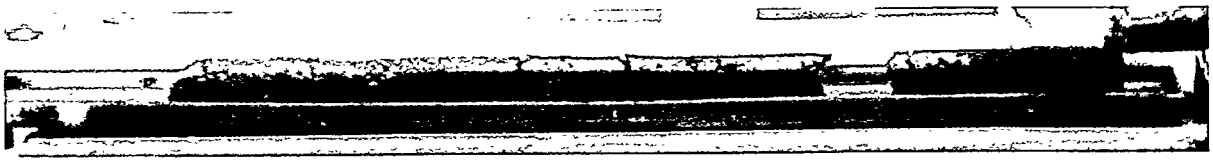

U-103 Core 176, Riser 7, Segment 6

U-103 Core 182, Riser 13, Segment 7

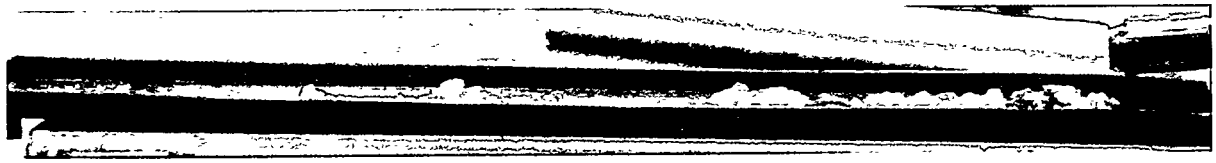

U-103 Core 182, Riser 13, Segment 8

Figure 4.1.7. Core Sample Extrusion Photos from Tank U-103

4.1.6 Unique Features of U-103 RGS Results

An unusually large amount of gas was extracted from segment 7-2 of U-103. The in-situ gas volume fraction calculated from RGS extraction data was 0.44 for this sample, which was supposed to be located in a salt slurry layer beneath a partial crust. The high gas content found by extraction was confirmed by the large (approximately 22.9-cm [9-in.]) gap that was seen in the sampler x-rays. The gas in segment 7-2 had much the same composition as that in the other samples, except for its low ammonia content. (This is consistent with the high gas volume fraction, since nearly all of the tank ammonia is in the liquid rather than the vapor phase.)

The gas in segment 7-2 contained essentially no oxygen, which was also the case for the other U-103 samples. There is, therefore, little reason to believe that segment 7-2 was part of a crust that contained large amounts of trapped air or whose pores were open to the air in the dome space. One remaining possible explanation for the high gas content is that there were sufficient local solids in the mostly liquid salt slurry layer to trap gas that had risen from below. This explanation is supported to some extent by the U-103 core profile,(a) which shows that a segment at the same elevation (segment 2 of riser 2) was composed partly of moist salt and partly of liquid.

Another possible explanation is that the top layer at the RGS riser, riser 7, has a closed pore structure that severely restricts gas migration, and the high gas content has accumulated from below. This is not inconsistent with the fact that essentially zero force was required to push the drill string into the waste at riser 7. A closed pore structure does not necessarily imply great structural strength. (Sampling was discontinued at riser 2, segment 2, because the waste was impenetrable; in this case, the core is believed to have been blocked not by hard waste but by a submerged object. Therefore, the riser 2 observation neither proves nor disproves the existence of a hard, closed top layer.)

The high gas content of segment 7-2 is probably not local to riser 7. One piece of evidence for this is the x-ray of the RGS sample from segment 13-4, which had a visible gas volume fraction of 0.47, not counting numerous bubbles. This sample came from the center of the tank at an elevation about one segment-length, or 48 cm (19 in.), lower than segment 7-2. (For completeness, it should be noted that segment 13-4 was taken about nine weeks later than the riser 7 samples; the S-106 samples were taken in the interim.)

Another sign that the high-gas region near the top of the waste is probably present in locations other than the riser 7 area is that when sampling was attempted at riser 2 unusually high flammable gas concentrations (relative to the lower flammable limit [LFL]) were measured in the dome space.(b) Sampling at riser 2, which was the first riser sampled in U-103, was terminated because of obstruction in or by the waste, and there was about a 2-1/2 month delay before riser 7 was sampled. The delay resulted from flammable gas concerns that temporarily halted all the tank-intrusive work in the tank farms.

At 1400 hr on October 1, 1996, the two combustible gas meters (CGMs) that were used by the industrial hygiene organization to sniff the dome space at riser 7 indicated flammable gas concentrations of 10% (meter #1) and 13% (meter #4) of the lower flammability limit (LFL). No

---

(a) Mousel A. 1997. "U-103 PMCS Core Profile." File U103.CRD, created April 22, 1997, transmitted to LA Mahoney (PNNL) May 23, 1997. Los Alamos Technical Associates, Richland, Washington.

(b) Electronic communications: GA Stanton Jr. to LM Sasaki (WHC), October 3 1996; LM Sasaki (LMHC) to LA Mahoney (PNNL), November 7 1997. Industrial Hygiene Direct Reading Instrument Survey sheets for October 1 1996, sheet ID #96-1766 and #96-1985. Westinghouse Hanford Company, Richland, Washington.

work was done in the tank on day shift. At 2000 hr, the flammable gas concentration was 12% of LFL on CGM #1 and 18% of LFL on CGM #4. A vapor sample was taken from the dome space at this time (at a riser about 12 m from the sniff riser); it showed 0.22% hydrogen, or 5.5% of LFL. This is consistent with the CGM #1 reading, because the CGMs are calibrated with pentane and therefore are expected to read the hydrogen concentration at least 100% high (Wilkins and Bauer 1996). At 2140 hr, after core sampling segments 1 and 2 from riser 2, the flammable gas readings were 13% of LFL on CGM #1 and 19% of LFL on CGM #4. The post-swing-shift calibration showed CGM #1 was within calibration, but CGM #4 was about 15% high. The standard hydrogen monitoring system (SHMS) was out of service and could not provide comparison measurements. Considering that CGM #4 was out of calibration and that CGM #1 and the dome space sample were roughly consistent, the peak flammable gas concentration in the U-103 dome was probably about 6% of LFL in the period of interest.

The flammable gas concentrations seen in U-103 at that time were unusually high (though not hazardous), suggesting that a significant amount of gas was present in a releasable form. The measured high gas concentrations near the top of the waste are a possible source. Note that the peak flammable gas concentrations occurred before as well as during riser 2 core sampling, so it is not clear to what extent the riser 2 operations contributed, and to what extent high gas concentrations might exist in the riser 2 waste.

4.2 Tank S-106

Tank S-106 was the seventh tank, and the third SST, that was sampled. S-106 was selected for RGS sampling for its uniquely high barometric pressure response and continuing rapid surface level rise, both of which indicate a large and increasing volume of retained gas. It is part of a group of tanks (Cluster 20 in Stewart et al. [1996b]) that have high radioactivity, moderate nitrite concentrations (0.1-0.16 M), and low TOC, 0.03–0.05%. Historical tank content estimates indicate that the primary waste stored in S-106 was salt cake from evaporator campaign S1, and the secondary waste was aluminum cladding Redox wastes from 1961 to 1967 (Remund et al. 1995).

Push-mode sampling was carried out in risers 7 and 8 in March 1997.(a) Sampling was also attempted in riser 14, but the waste (or some object imbedded in it) proved impenetrable. The approximate locations of the risers are depicted in Figure 4.2.1. Core segments were taken at various elevations, as shown in Figure 4.2.2.

The Tank Characterization Plan (Homi 1995) describes Tank S-106 (S-106) as a passively ventilated sound SST awaiting interim stabilization. Tank S-106 has a capacity of about 750,000 gallons and contains about 543,000 gallons, of which 162,000 gallons are pumpable liquid.

Automatic FIC surface level measurements through riser 3 showed an increasing trend in waste level from about 1989 to 1993. Riser 4 liquid observation well (LOW) measurements showed a relatively stable liquid level from March 1989 through 1993. The best available data show that the total depth of waste at the locations of risers 7 and 8 is about 460 cm (181 in.) (see WHC 1994). Waste depth at the location of riser 14 is estimated as ~235 in., indicating a non-uniform waste surface level. A further indication of waste surface level variations is that surface level measurements by the FIC in riser 3 indicate levels of ~181 in. RGS sampling elevations for each riser are shown in relation to the expected contents layering in Figure 4.2.2.

(a) Bates JM and R Shekarriz. October 1996. *Sampling Plan for Tank 241-S-106 Retained Gas Sampler Deployment.* TWSMIT:091896 Rev. 2, Pacific Northwest National Laboratory, Richland, Washington.

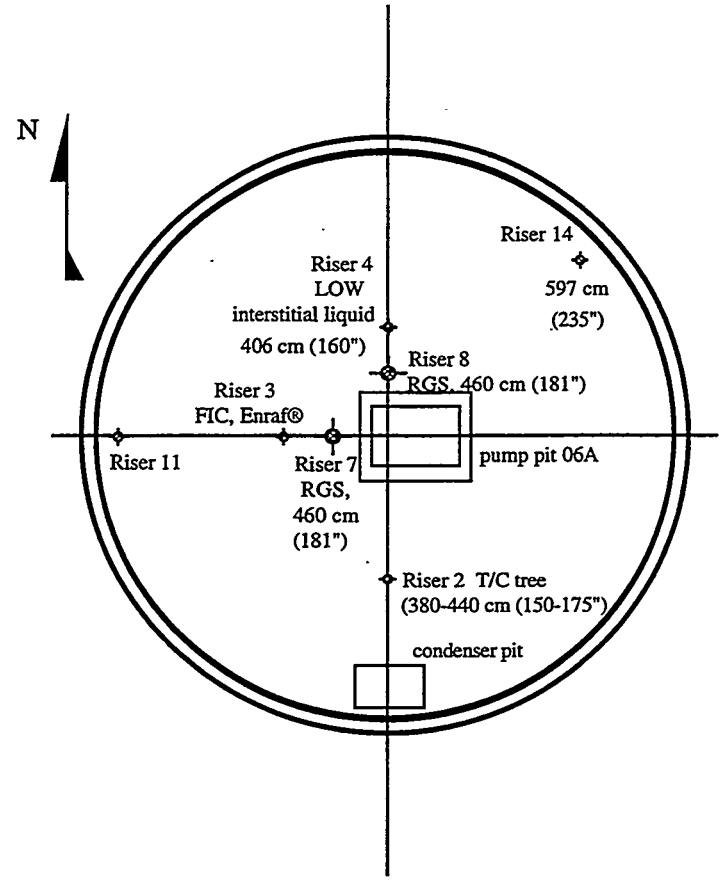

Figure 4.2.1. Schematic Diagram of Riser Locations in Tank S-106 (waste surface elevations are given in inches for several of the risers)

Figure 4.2.3 is a temperature profile from the TC tree in riser 2. The large squares show the average temperature measured between September and October 1996; the temperature minima and maxima at each TC are also shown. The low temperature and small temperature difference indicate relatively low heat load. The temperature profile shows the parabolic shape characteristic of conduction heat transfer with generation. No significant convective layer, which would appear as a uniform temperature or a sharp slope change in the profile, is indicated.

The most recent information on tank content layering (derived from the core observations made in 1997) is presented in Figure 4.2.4. Note the strongly varying extents and levels of the layers at risers 7 and 8. This is especially remarkable because risers 7 and 8 are near each other in the center portion of the tank. According to these observations, a substantial solids fraction was probably present in all four of the RGS samples that were taken successfully (riser 7, segments 3 and 5, and riser 8, segments 6 and 10). The upper layer, which is predominantly liquid, was not RGS-sampled because of sampler failures. A depth of 371 ± 51 cm (146 ± 20 in.) was used in calculating the in-situ inventory and average gas composition for the sampled high-solids layer. This is probably about equal to the depth of the high-solids layer at riser 7 and is greater than the layer depth at riser 8.

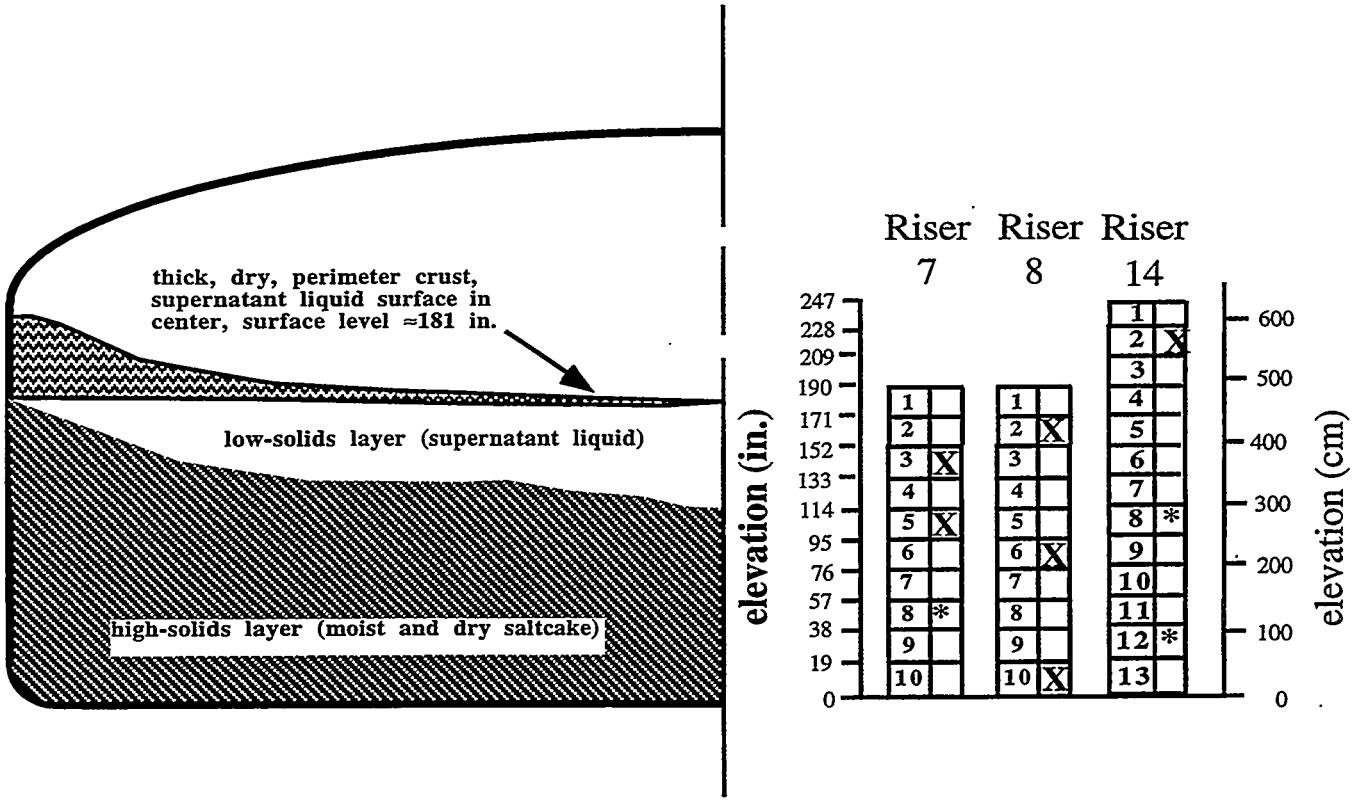

Figure 4.2.2. Diagram of Expected Waste Layering and RGS Sample Elevations for Tank S-106 (segments marked by * could not be taken because the waste was too hard)

Preliminary densities for the liquid and bulk solids in S-106 were available from cores taken in 1997.(a) The density of drainable liquid varied from 1390 to 1470 kg/m^3, with an average and standard deviation of 1420 ± 29 kg/m^3. The bulk density of the samples with high solids concentrations varied from 1640 to 1920 kg/m^3, with an average and standard deviation of 1780 ± 120 kg/m^3.

(a) Transmittal from R Esch (LMHC) to LA Mahoney (PNNL) of data to be included in the S-106 TCR (in preparation), May 13, 1997. Lockheed Martin Hanford Corporation, Richland, Washington.

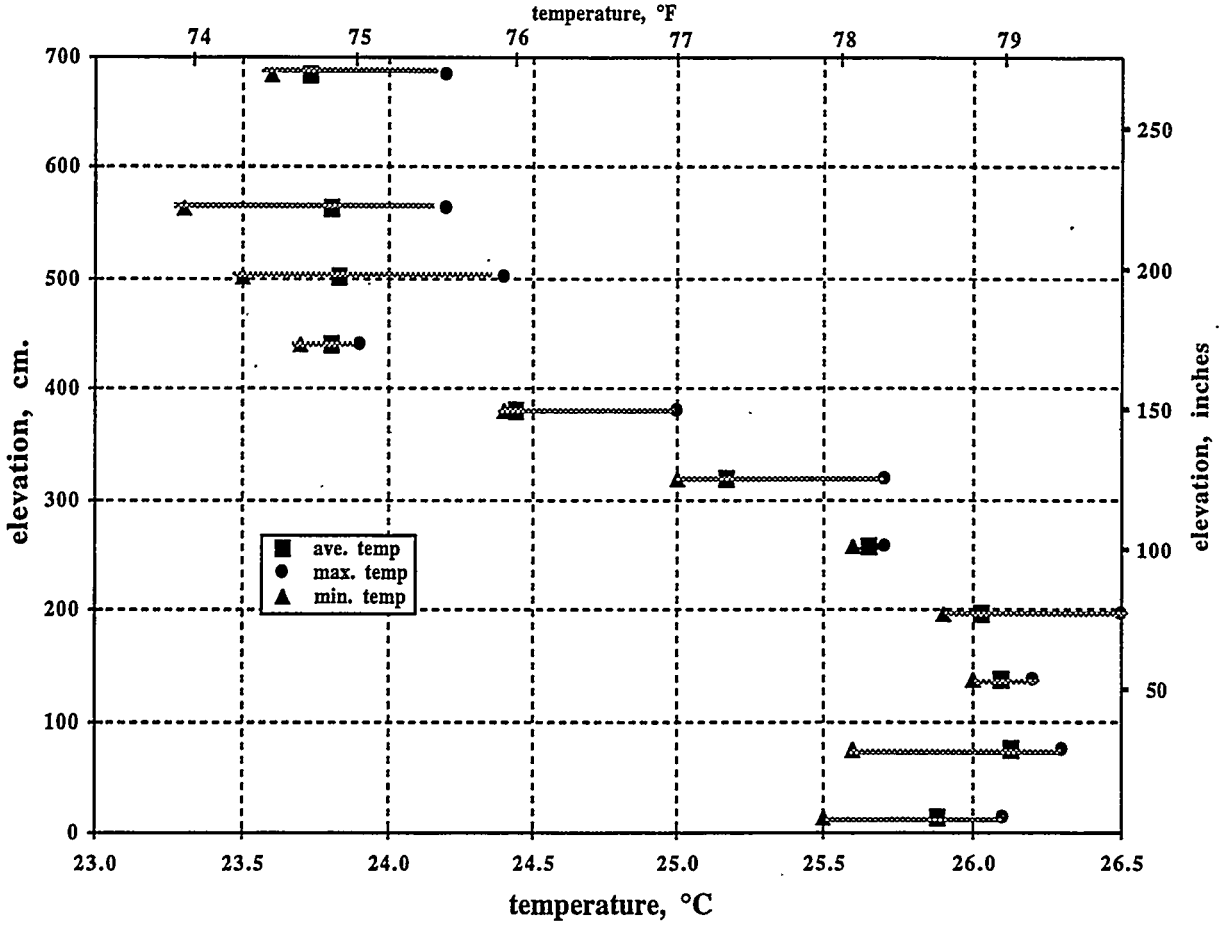

Figure 4.2.3. Recent Profile of Temperature in Tank S-106 Taken in Riser 2 (TC)

For the purpose of in-situ inventory and average gas composition calculations, the density of solids-free liquid was set at 1420 kg/m^3, the liquid-layer density was set at 1420 kg/m^3, and the remainder of the waste was given a layer density of 1780 kg/m^3.

4.2.1 Sampling and Extraction Information

The segments analyzed are listed in Table 4.2.1. Two samples, riser 8, segment 2 and riser 14, segment 2, were discarded because the sampler valves had not closed completely. As a result of these sampling difficulties, no samples were taken successfully in the low-solids supernatant layer that apparently occupied the topmost two to five segments of risers 7 and 8. The valve springs have been changed to exert stronger valve closure force in future sampling.

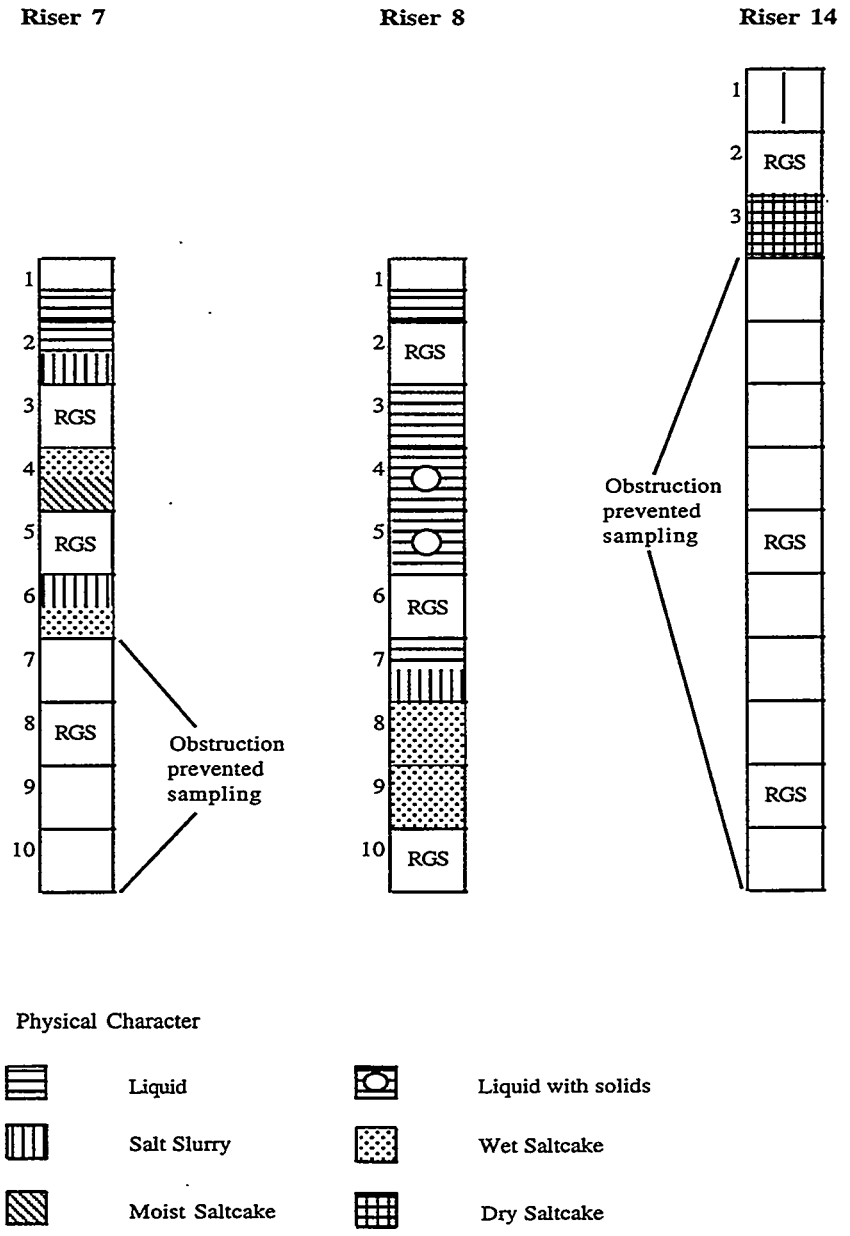

Figure 4.2.4. Most Recent Core Profile for the Three Selected Push-Mode Sampling Risers in Tank S-106(a)

Table 4.2.1 also shows the lag times (delay between sample acquisition and processing) for these samples. This piece of information was provided to allow data users to correlate the lag time between sampling and extrusion with the concentrations of the various constituents, in order to test for decomposition or other chemical reactions. One such correlation (oxygen plus other contamination gases versus lag time) is discussed in Section 5.

(a) Personal communication, AP Mousel (LATA) to LA Mahoney. May 23, 1997. "S-106 PMCS Core Profile." File S106.CRD, revised April 4, 1997. Los Alamos Technical Associates, Richland, Washington.

Table 4.2.1. Lag Times for Processing RGS Samples from Tank S-106

Sample	Acquisition Date	Processing Date	Lag (days)
7-3	February 24, 1997	March 20, 1997	24
7-5	February 25, 1997	March 18, 1997	21
8-2	February 12, 1997	compromised	---
8-6	February 18, 1997	March 11, 1997	21
8-10	February 21, 1997	March 13, 1997	20
14-2	March 20, 1997	compromised	---

As is discussed in Section 3.6.2, the HHF used during sampling may enter the sampler in place of some of the waste. Table 4.2.2 shows the volume percentage contamination by HHF of samples for which bromide measurements were made (these did not include any RGS samples). The bromide concentration was used as the HHF tracer. Some of these samples (7-1, 7-2, 8-1, 8-5, 8-8, and 8-9) contained bromide below the detection limit. Averaging the HHF contamination over the samples, and treating the below-detection samples as if at the detection limit, gives an average contamination of 6.6 vol%. This value is used to calculate a reduced effective sampler volume for the RGS samples.

All of these samplers were backfilled with helium and sealed with vacuum grease before they were deployed. This method virtually eliminated air and argon contamination from gases entrained during sampling. The helium backfill results are discussed in considerable detail by Cannon (1997) and are summarized in Section 5.

Table 4.2.2. Hydrostatic Head Fluid Contamination in S-106 Samples

Sample	HHF Contamination (vol%)
7-1	< 2.6
7-2	< 3.6
7-4	5.4
8-1	< 3.2
8-3	4.6
8-4	11.5
8-5	< 10.1
8-7	17.4
8-8	< 2.8
8-9	< 5.2

The data analysis calculations were carried out as described in Section 3 of this report, with a method that calculates the condensed ammonia in the canisters as well as the ammonia in the vapor phase. In addition, all of the S-106 samples were injected (after gas extraction) with an ^{15}N-labeled ammonia standard to determine how much ammonia was still dissolved in the sample after the extraction of other gases was complete. The results of this residual ammonia analysis are discussed in Section 5.

4.2.2 Retained Gas Composition

Table 4.2.3 presents the estimated concentrations of the insoluble gases in each RGS sample taken from S-106. The corrections consist of removing all the oxygen, argon, and helium and subtracting $(3.73) \cdot (O_2)$ from the nitrogen, consistent with the molar N_2/O_2 ratio in atmospheric air. The corrected concentrations are given in Table 4.2.4.

Table 4.2.5 presents the total ammonia concentration per liter of waste under in-tank conditions. The "extracted NH_3" column gives the total moles of ammonia, both condensed and vapor-phase, that were pumped out of the samples into the "J" collection canisters. "Residual NH_3" refers to the ammonia remaining in the waste after pumping. The extracted ammonia has a different accuracy than the residual ammonia; therefore, the contribution of the residual is shown separately in the table. (It should be noted that the labeled ammonia method has not yet been fully tested on standard waste simulants; until such tests have been completed, the method should be considered unverified. A further discussion of the ammonia calculations is given in Section 5.)

Table 4.2.3. Concentrations of Insoluble Constituents (µmol/L of waste) in Tank S-106 Without Air Entrainment Correction

Segment	N_2	H_2	N_2O	O_2	CH_4	He	Ar	Other Nit. Ox	C_2H_x	C_3H_x	Other Hyd.
7-3	1400±120	2500±200	360±31	17±5.7	17±6.4	490±51	12±1.2	0.8±0.8	5.0±3.1	2.1±0.8	2.3±1.0
7-5	1300±120	3200±230	770±58	30±12	0.4±0.2	480±39	4.2±0.9	3.5±3.5	9.9±5.0	5.9±3.7	6.7±2.1
8-6	1100±120	2500±250	440±52	23±2.1	21±11	400±41	5.2±1.0	5.1±5.1	19±12	9.5±9.5	3.0±1.5
8-10	2400±180	6100±260	1100±50	80±28	16±1.6	520±25	6.0±1.7	3.0±2.2	18±10	10±9.0	2.0±1.6

Table 4.2.4. Concentrations of Insoluble Constituents (µmol/L of waste) in Tank S-106 with Air Entrainment Correction

Segment	N_2	H_2	N_2O	O_2	CH_4	He	Ar	Other Nit. Ox	C_2H_x	C_3H_x	Other Hyd.
7-3	1400±130	2500±200	360±31	0	17±6.4	0	0	0.8±0.8	5.0±3.1	2.1±0.8	2.3±1.0
7-5	1200±130	3200±230	770±58	0	0.4±0.2	0	0	3.5±3.5	9.9±5.0	5.9±3.7	6.7±2.1
8-6	1000±120	2500±250	440±52	0	21±11	0	0	5.1±5.1	19±12	9.5±9.5	3.0±1.5
8-10	2100±210	6100±260	1100±50	0	16±1.6	0	0	3.0±2.2	18±10	10±9.0	2.0±1.6

Table 4.2.5. Total Ammonia Concentrations in Tank S-106

Segment	Extracted NH_3 (μmol/L)	Residual NH_3 (μmol/L)	Total NH_3 (μmol/L)
7-3	240 ± 55	840 ± 300	1100 ± 360
7-5	1900 ± 280	4300 ± 1600	6200 ± 1800
8-6	530 ± 130	1300 ± 450	1800 ± 580
8-10	850 ± 160	1100 ± 380	1900 ± 550

The average and standard deviation of the ammonia concentrations over samples 7-3, 8-6, and 8-10 are 1,600 ± 450 μmol/L waste (0.0036 wt% NH_3 dissolved in the liquid). The variation in the ammonia concentrations of these samples is about the same as the measurement error band; thus the differences among the ammonia contents of samples 7-3, 8-6, and 8-10 could be more apparent than real. However, sample 7-5 shows a significantly higher ammonia content than the other three samples from S-106.

Table 4.2.6 contains the composition of the gas/vapor phase in each sample and the integrated average composition for the high-solids layer of Tank S-106. The sample compositions in the table have been calculated using the in-situ solubility method described in Section 3.5.2.

The tank average composition is the result of integrating RGS species concentrations over the high-solids layer of the waste and multiplying those concentrations by the layer volume. The integration method is described in Section 3.6.

Table 4.2.6. Sample and Overall Average Compositions of Retained Gas in Tank S-106 with Gas Entrainment Correction

Segment	N_2 (mol%)	H_2 (mol%)	N_2O (mol%)	NH_3 (mol%)	Other (mol%)
7-3	32 ± 4.0	59 ± 6.8	8.1 ± 1.0	0.027 ± 0.009	0.64 ± 0.29
7-5	22 ± 3.0	62 ± 6.9	15 ± 1.6	0.38 ± 0.11	0.51 ± 0.28
8-6	25 ± 4.0	63 ± 9.6	11 ± 1.8	0.10 ± 0.032	1.4 ± 0.98
8-10	23 ± 2.4	65 ± 4.6	11 ± 0.8	0.095 ± 0.025	0.52 ± 0.27
Average in the high-solids layer[a]	24 ± 3.0	63 ± 6.3	11 ± 1.2	0.14 ± 0.02	0.73 ± 0.43

(a) The error bands on the average composition, as for the individual sample compositions, only represent the instrument error because there are too few samples to define the spatial variability of gas concentration.

4.2.3 Gas Inventory

The method by which the in-situ gas volume fractions were calculated is given in Section 3. The results are presented in Table 4.2.7, showing the difference between in-situ gas volume fractions that were and were not corrected for the presence of entrained and backfilled gases. The table also contains the average gas volume fraction in the high-solids layer of S-106 and the average pressure experienced by the gas. All of the averages are in-situ volume averages and are calculated by Simpson's Rule integration, as described in Section 3.6.

Table 4.2.8 gives estimates of the STP volume of gas in the high-solids layer of the waste in Tank S-106. The RGS gas inventory was calculated by integrating RGS total gas concentrations (four data points) over the high-solids layer and multiplying the average gas concentration by the volume of the layer. The integration method is described in Section 3. The RGS volumes in Table 4.2.8 all include corrections to remove the entrained air, argon, and the backfilled helium. In all cases, as is further discussed in Section 5, the correction for entrained gas was insignificant, and the amount of helium present was found to be equivalent to the air/argon entrainment that had been contained in samples taken from tanks sampled previously (Shekarriz et al. 1997).

The gas inventory calculated for S-106 based on RGS data is significantly lower than the gas volume indicated by the BPE method and surface level rise. The average gas fraction based on RGS data is 0.10 ± 0.05, which corresponds to a total in-situ gas inventory of 160 ± 80 m^3. The measured dL/dP correlation for S-106 is one of the highest in any Hanford tank: -0.91 ± 0.30 in./in.-Hg.(a) This corresponds to an average gas fraction of 0.26 ± 0.08 and an in-situ gas volume of 410 ± 130 m^3.

Table 4.2.7. In-Situ Gas Volume Fractions in Tank S-106

Segment	Sample Central Height (cm)	Hydrostatic Pressure (atm)	Temperature (°C)	Corrected Gas Volume Fraction (In-Tank Conditions)	Uncorrected Gas Volume Fraction (In-Tank Conditions)
7-3	362	1.14	25.1	0.092 ± 0.009	0.105
7-5	265	1.29	25.7	0.099 ± 0.011	0.111
8-6	217	1.36	25.8	0.073 ± 0.009	0.082
8-10	24	1.66	25.9	0.138 ± 0.012	0.152
Average in the high-solids layer		1.43 ± 0.07		0.10 ± 0.05	

(a) Whitney PD, PA Gauglitz, PA Meyer and NE Miller. 1997. *Estimating Retained Gas Volumes in the Hanford Tanks Using Waste Level Measurements: Progress.* Letter report TWSFG97.33, Pacific Northwest Laboratory, Richland, Washington.

Table 4.2.8. Gas Inventory (corrected for gas entrainment) in the High-Solids Layer of S-106

Quantity	RGS	Best Estimate (BPE)
Avg. Gas Fraction	0.10 ± 0.05	0.26 ± 0.08
Gas Volume (m^3)		
In-Situ	160 ± 80	410 ± 130
STP	230 ± 120	580 ± 190
dL/dP (in./in.-Hg)	-0.36 ± 0.18	-0.91 ± 0.30
P_{eff} (atm)	1.43 ± 0.07	1.43 ± 0.07

The surface level measurement in S-106 is via an Enraf buoyancy gauge in riser 3. This riser is in the central part of the tank near risers 7 and 8, from which the usable RGS samples were taken. Segments 1 and 2 from riser 7 and segments 1, 3, 4, and 5 from riser 8 contained a high fraction of liquid, and the sampler did not penetrate hard material at the surface. Level data for this tank are recorded hourly, which enables the most precise determination of the dL/dP correlation. We conclude that, because the level gauge is in the central portion of the tank and there is evidence of a liquid layer to transmit waste expansion/compression, the BPE method can be confidently applied to this tank.

The SLR method also confirms that high gas volume is present. The waste surface level has risen steadily more than 17 in. since 1981. If an additional 9 in. rise is allowed for pre-existing gas inventory (Hodgson et al. 1996), and discounting evaporation since no free liquid surface was present, the resulting gas fraction is 0.15 ± 0.05. The higher gas inventories calculated by the BPE and SLR methods imply that the RGS segments missed a high gas-fraction region, possibly in the lower levels or away from the center of the tank. Both the RGS risers were near the tank center and the pump pit.

Because the RGS data were taken only in risers near the tank center, and the waste shows signs of lateral variability, we choose the predictions of the BPE method as the best estimate for the gas inventory of S-106. These calculations are summarized in Table 4.2.8.

The four ammonia concentration measurements in the high-solids layer of S-106 integrate to a total (vapor and dissolved) ammonia inventory that would have an STP volume of 84 m^3 (3,000 ft^3). The error band on the ammonia inventory should be considered to be at least 50%. (Note that this is not an ammonia inventory for the entire tank because it does not include the supernatant layer, for which measurements were lacking.)[a]

Figure 4.2.5 shows the corrected gas volume fractions (Table 4.2.7) and the entrainment-corrected compositions (Table 4.2.4) in the samples from S-106. The compositions represent the

(a) The ammonia content of the supernatant layer can be estimated by assuming an ammonia concentration in the liquid that is an average of the ammonia concentrations in the waste liquid in the four samples. Corrections can be made for the volumes of solids and gas in the samples based on the estimated solid density and gas volume fractions. When these corrections are made, the maximum ammonia concentration for the four samples is 16,000 µmol/L liquid, and the arithmetic average over the four samples is 6,900 µmol/L liquid. When these values are used to represent the ammonia concentration in the supernatant layer, their error bands cannot be readily quantified but must be considered substantially higher than the 50% value given for the gas inventory.

mole fraction of the species in the insoluble gas; water and ammonia are not included. Figure 4.2.5 also shows data taken from core extrusion analyses, as a way of tying those observations together with RGS. The lines and symbols in the rightmost plot indicate the fraction of the sample mass that was drainable liquid; the remainder is wet solids. The bulk densities measured for the wet solids in each sample are also noted on the figure.

4.2.4 X-Ray Results

Table 4.2.9 summarizes all the available radiography observations, including segment 2 from riser 8. (The segment 8-2 sampler had a slightly-open ball valve that compromised RGS extraction processing, but because the radiographs were taken immediately after sampling, before much leakage could occur, the qualitative features of the sample are expected to be valid.) There were no standard air/water density profiles for two of the five samples for which x-ray images were recorded (segments 8-6 and 8-10). The standard profiles for segment 8-2 were used for those samples because all three samples were x-rayed at about the same time.

The error bands of the visible gas volume fractions that are given in Table 4.2.9 are unknown but are believed to be larger than the errors in the gas volume fractions calculated from gas extraction. (The "visible" gas volume fraction refers to the gas that has separated from the solids and liquid such that its volume can be calculated based on the image. The uncorrected gas fractions from extraction are used for comparison to reflect the presence of entrained air in the sampler.) A comparison of x-ray-derived gas volume fractions and extraction-derived gas volume fractions, which is given in Table 4.2.9, shows that the samples all have visible gas volume fractions that are slightly less than or equal to the extracted gas volume (at in-situ temperature and pressure). Therefore, it appears that sample recovery was close to 100% for S-106.

Segment 7-5, uniquely, contains no gas gap (observed gas under the piston) and only one bubble in the waste. Thus its visible gas volume fraction is zero. However, its uncorrected gas volume fraction was 0.111 (based on gas extraction). This suggests that the gas was predominantly present either in solution or in bubbles too small to be recognized in the x-ray (0.5 mm or less). Recall that segment 7-5 was also unique in having an ammonia concentration that was significantly higher than that in the other samples. It would be worth considering what waste characteristics might explain both these observations.

Segment 8-10 also shows unique behavior. None of the other samples show any sign of separation of the solids and liquids, but in segment 8-10 supernatant layers appear to have formed under the gas gaps. It seems possible that the liquid layers came into existence because the solids settled out of them (forming, for example, the flat bottom of the liquid layer that underlies the largest visible bubble). Some of the liquid may also have come from drainage from of the solids above the larger bubbles. However, such drainage may be a questionable mechanism because core extrusion observations showed no drainable liquid in the two segments above this one.

Segment 14-2 appears to have had high gas content, but it is also possible that the sample recovery was not complete. Unfortunately, the sample was compromised, and it was therefore impossible to determine how much of the apparent gas volume in the sampler was real gas. Segment 14-1 contained no liquid or solids, so it is possible that segment 14-2 was the top waste and partly filled with air. However, there is another possibility. Because the sample was taken near the top of the tank in a riser near the tank wall, like segment 7-2 of U-103, we can speculate that segment 14-2 of S-106 also contained a high gas fraction. If there were higher gas fractions in the waste in the tank periphery than in the center, it would explain why RGS (whose successful samples were only in the center) estimated a lower gas inventory for S-106 than the BPE method did (a less localized approach).

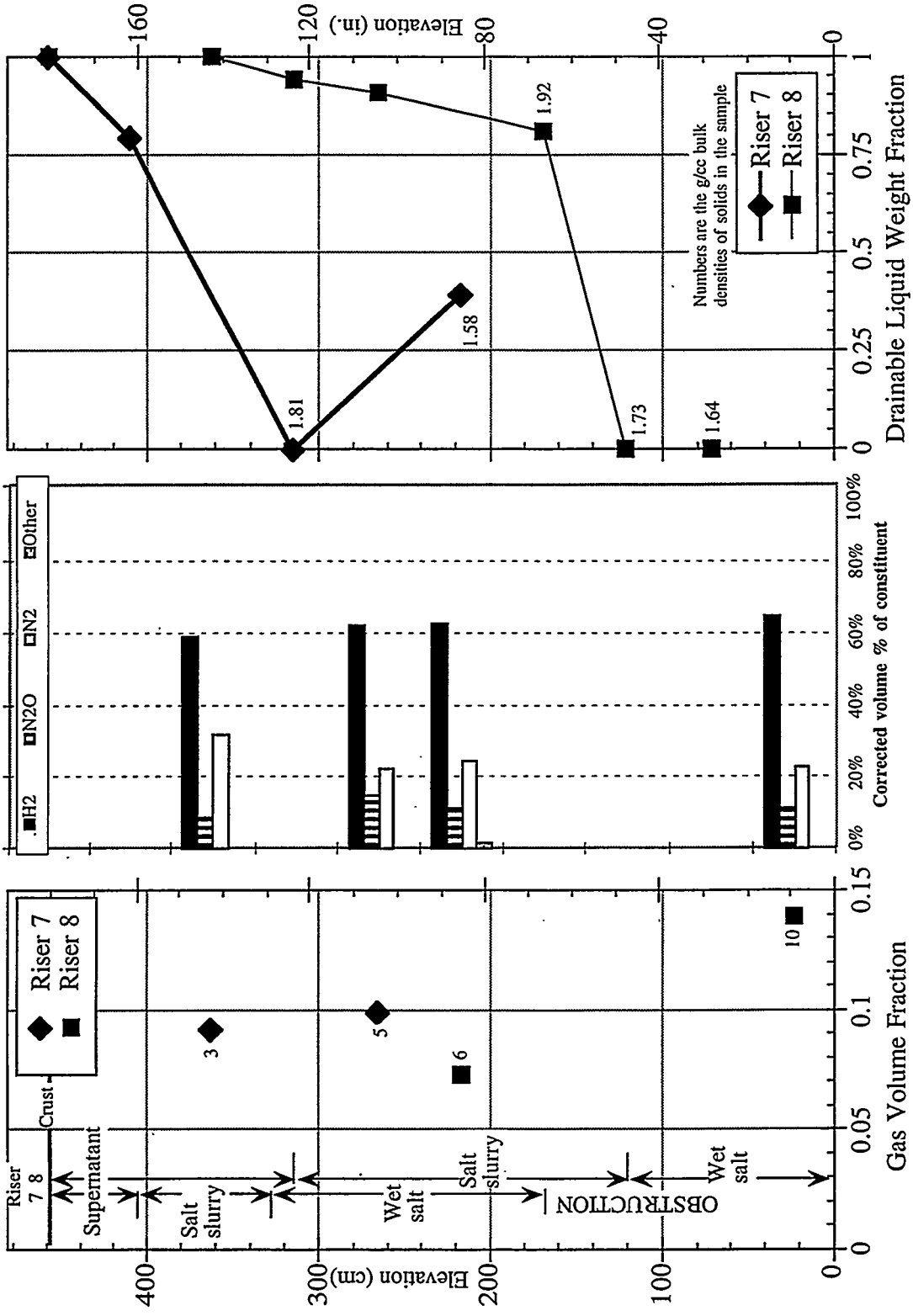

Figure 4.2.5. Gas Volume Fractions, Compositions, and Liquid Contents in Tank S-106

Table 4.2.9. Summary of Observations from X-Ray Images of Tank S-106

Segment	Comments/Observations
7-3	Mostly featureless, with a flat meniscus and no waste hanging down from the piston. In the lower third of the sampler, a few barely perceptible lower-density features, probably gas bubbles; round, about 4 mm in diameter. The gas gap under the piston is 4.3 cm (1.7 in.), for a visible volume fraction of 0.089. (Compare with the gas volume fraction of 0.105 ± 0.009 in Table 4.2.7 obtained by gas extraction.)
7-5	Mostly featureless, with the sampler completely filled (no gas gap). One irregular (worm-like) lower-density feature, probably a bubble, about 2 mm wide by 7 mm long. The visible volume fraction is 0. (Compare with the gas volume fraction of 0.111 ± 0.010 in Table 4.2.7 obtained by gas extraction.)
8-2	Completely featureless, with a flat meniscus and no waste hanging down from the piston. The gas gap is 1.7 cm (0.7 in.), for a visible volume fraction of 0.035.
8-6	Several definite lower-density and higher-density features (oval, about 4 mm diameter) in one image in the lower third of the sampler; otherwise featureless. The lower-density features are probably bubbles; the nature of the higher-density features is unknown. The meniscus is flat and there is no waste attached to the piston. The gas gap is 2.8 cm (1.1 in.), for a visible volume fraction of 0.058. (Compare with the gas volume fraction of 0.082 ± 0.009 in Table 4.2.7 obtained by gas extraction.)
8-10	Several large (1 cm and larger) flat-bottomed bullet-shaped gas features. Also, in the lower third of the sampler, a gas gap all the way across the sampler width (though probably not across its whole depth). This large gas space is also bullet-shaped and flat-bottomed. Its base appears to be a layer (about 3 cm deep) of waste with a slightly lower density than most of the sample. The bottom of this possibly liquid layer is also flat, and beneath it is the denser (and more typical) waste. There is also a thin layer (about 5 mm deep) of "liquid" at the top of the waste. Both its upper interface (with gas) and its lower one (with denser material) are flat. The gas gap at the top of the waste is about 3.8 cm (1.5 in.), giving a gap volume fraction of 0.079. The embedded bullet-shaped bubbles add roughly 0.02 volume fraction of gas, bringing the visible gas volume fraction to about 0.11. (Compare with the gas volume fraction of 0.152 ± 0.011 in Table 4.2.7 obtained by gas extraction.)
14-2	Only 18 cm (7 in.) of waste, which shows much bubble structure and also some higher-density blobs. The top waste surface is lumpy, or perhaps frothy, definitely not a liquid meniscus. There is no waste attached to the piston. The gas gap is 30.5 cm (12 in.), for a visible gas (or void) volume fraction of 0.63. (Because the sampler valve had not fully closed and the sample was compromised, there is no extraction-based gas volume fraction for comparison.)

Table 4.2.10 provides a summary of the waste densities that have been estimated from radiographic data. The radiographic densities include the gas in the waste and are given for several locations within each sample to show density trends. The table also shows the gas-free densities that were measured for the core samples that lay above and below each RGS sample. The two methods give reasonably consistent results for four of the five segments, considering the differences that can be expected because of the effect of retained gas on the radiographic densities of the RGS samples, the fact that RGS are adjacent to standard core samples rather than collocated, and the partial unavailability of x-ray calibration records. Segment 8-10 appears to be underexposed and therefore to give an inaccurately high range of densities.

Table 4.2.10. Densities of S-106 Samples from Radiography and Core Samples

Riser-Segment Number	Distance from the bottom of the sampler (ft)	Calculated Mean Density (g/cc)	Calculated Standard Deviation (g/cc)	Gas-Free Density Above and Below the RGS Sample (from cores) (g/cc)
7-3	0.25	1.56	0.28	density above, 1.39 g/cc (liquid)
	0.50	1.56	0.38	
	0.75	1.49	0.32	
	1.00	1.47	0.34	
	1.25	1.46	0.30	density below, 1.81 g/cc (solids)
7-5	0.25	1.33	0.25	density above, 1.81 g/cc (solids)
	0.50	1.39	0.24	
	0.75	1.37	0.23	
	1.00	1.51	0.25	
	1.25	1.60	0.26	no sample below
8-2	0.25	1.35	0.25	density above, 1.41 g/cc (liquid)
	0.50	1.44	0.29	
	0.75	1.46	0.26	
	1.00	1.38	0.27	
	1.25	1.29	0.26	density below, 1.40 g/cc (liquid)
8-6[a]	0.25	1.36	0.22	density above, 1.47 g/cc (liquid)
	0.50	1.69	0.31	
	0.75	1.50	0.25	
	1.00	1.48	0.27	density below, 1.42 g/cc (liquid)
	1.25	1.48	0.30	1.92 g/cc (solids)
8-10[a]	0.25	2.27	0.32	density above, 1.64 g/cc
	0.50	1.89	0.68	
	0.75	2.23	0.41	
	1.00	2.27	0.39	
	1.25	2.30	0.36	tank bottom below
14-2[b]	0.25	0.94	0.37	no liquids or solids collected above
	0.50	0.89	0.32	dry crumbly salt below

(a) These segments lacked standard air/water density profiles; used data from segment 8-2, taken at almost the same time. Segment 8-10 is probably underexposed.
(b) This image was unusually blurry.

One more feature of interest in the x-rays is the density trend in segments 7-3 and 7-5. The radiographic density of segment 7-3 appears to consistently decrease from the top to the bottom of the sample, while the density of segment 7-5 consistently increases from top to bottom. Interestingly, the core sample in between (segment 7-4) showed qualitative differences between its upper and lower halves. Its upper half was a dark gray wet salt containing some large crystals; its lower half was a moist green-gray salt. Thus the density behavior shown by the x-rays may reflect differences in solids composition or gas retention in this part of the waste.

Figures 4.2.6 and 4.2.7 show density images calculated from the x-rays of segments 8-6 and 8-10. False color has been used to enhance the bubble structure in the waste. In these images, features that are only a few pixels in size are probably noise and should be ignored.

Figure 4.2.6 shows the nearly featureless waste in segment 8-6. Some oval features, the largest of which is about 3 mm (1/8 in.) across, can be seen near the bottom of the 0.50-ft subsegment. The gas gap at the top of the sampler has been cropped and is not visible in the figure.

Figure 4.2.7 shows the rather dramatic structures in segment 8-10. Gas bubbles that span the width of the sampler are clearly evident. The largest such bubble, in the 0.50-ft image, shows a gas dome above a layer of low-density waste, probably separated liquid. Other large bubbles in this segment also have domed tops and flat bottoms (suggesting some liquid at the bottom). Smaller bubbles are also visible throughout most of the waste.

4.2.5 Core Extrusion Results

Figure 4.2.8 shows some samples of S-106 waste. The RGS samples comprised segments 3 and 5 from riser 7 (Core 184) and segments 6 and 10 from riser 8 (Core 183).

In riser 7, segments 1 and 2 (not pictured) were almost entirely liquid (see Figure 4.2.5). Segment 4 of riser 7, which is shown in Figure 4.2.8, lay between RGS samples 7-3 and 7-5. Segment 4 showed considerably more liquid in its upper half, a dark gray wet salt, than in its lower half, a moist gray-green salt. The lower half of segment 4 was the driest part of the riser 7 core and abutted on RGS sample 7-5, which contained a gas volume fraction of about 0.11 in a form that was not visible on x-rays. Segment 7-6 (not pictured) had about the same color and apparent liquid content as the top of segment 7-4. The waste in riser 7 did not show any clear bubble pockmarks, but its wetness might have tended to erase such small irregularities.

Riser 8 material (which is represented by segments 8 and 9 in Figure 4.2.8) was superficially similar to riser 7 waste, although in riser 8 the top five (rather than the top two) samples contained predominantly liquid. Segment 8-7, located immediately below RGS sample 8-6 (whose gas content was lower than that of the other RGS samples), was a wet dark green salt; as extruded, it lay in several separated parts. Segments 8-8 and 8-9 (both pictured) both contained dark green-gray wet salt that showed what might be gas pockmarks and cavities on the surface. Below these samples was the RGS sample 8-10, which (as seen in Figure 4.2.7) contained two or three sampler-spanning gas bubbles that gave it the highest gas content of the RGS samples. The presence of such large bubbles in 8-10 suggests that the gaps observed in extruded sample 8-7 originally might have been filled with gas. If so, the gas content of 8-7 could have been higher than that of 8-10 (a gas volume fraction of 0.139).

The only riser 14 material that was successfully sampled was that in segment 3. This was a very dry, crumbly gray-white salt, with no drainable liquid. As shown in Figure 4.2.4, segment 3 was located at an elevation above any of the segments in risers 7 and 8.

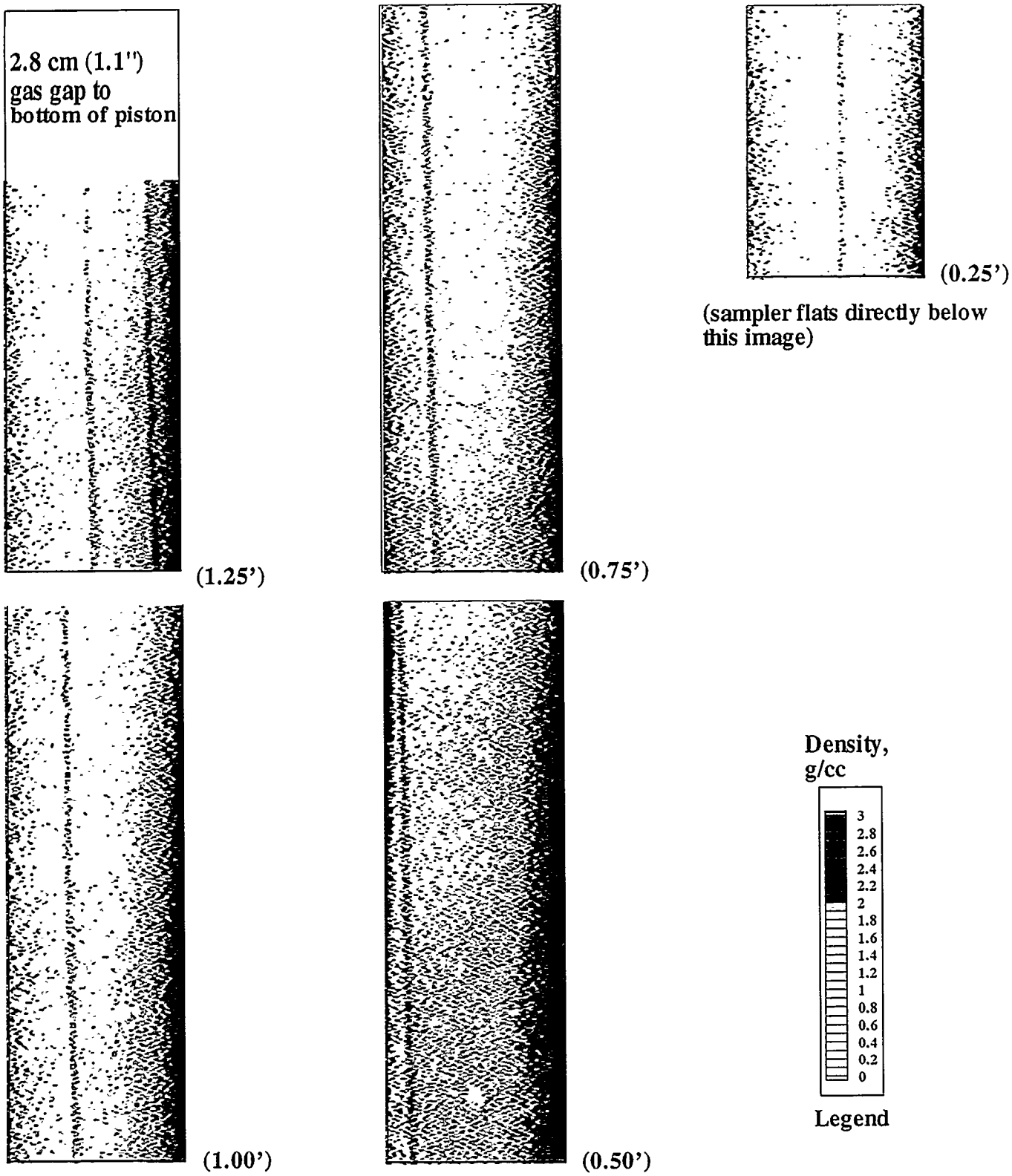

Figure 4.2.6. Density Images Calculated from X-Rays of Sample 8-6 from Tank S-106

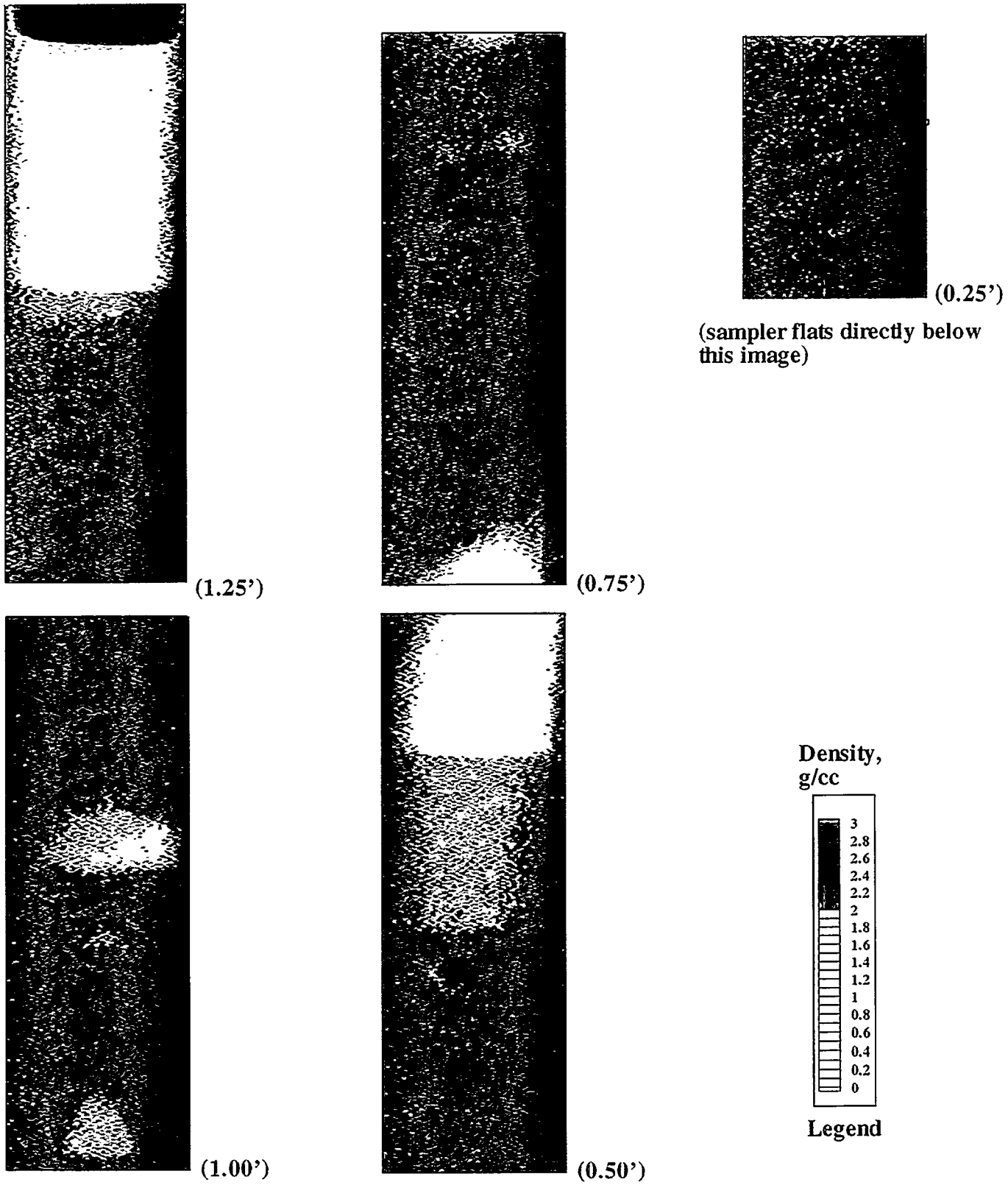

Figure 4.2.7. Density Images Calculated from X-Rays of Sample 8-10 from Tank S-106

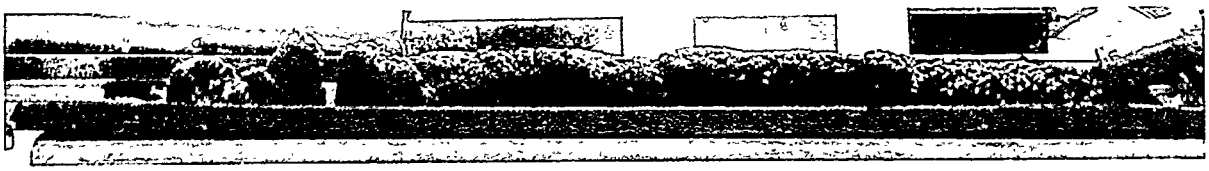

S-106 Core 184, Riser 7, Segment 4

S-106 Core 183, Riser 8, Segment 8

S-106 Core 183, Riser 8, Segment 9

Figure 4.2.8. Core Sample Extrusion Photos from Tank S-106

4.3 Tank BY-101

Tank BY-101 was the eighth tank and the fourth SST sampled with the RGS. The methods of RGS sampler preparation, sample acquisition, and sample gas extraction were the same as those used for the other tanks that were sampled in FY 1997.

Two samples were taken from BY-101: riser 10B, segment 3, and riser 10D, segment 2. Further sampling was impossible because of obstructions at both risers. The samples contained no retained gas and provide no useful information on the composition or quantity of retained gas. The supporting evidence and additional details are as follow:

- Mass spectrometry analyses show that only air and helium were present in the two BY-101 samples. The typical retained waste gases, hydrogen, nitrous oxide, methane, and ammonia, were found in quantities of less than 0.01 mol% each.

- X-rays showed no visible waste in the samplers,(a) although the samples were taken well below the waste surface level of 345 cm (135.8 in.). The observations made during RGS system cleanup, which was carried out after the attempted gas extraction, also confirmed that the samplers contained no solid/liquid waste.

- Helium was present at about 1 mol% in the samples, representing roughly 3 cc (at STP) of gas trapped in the sampler's leading edge. This quantity of helium is consistent with the findings for Tanks U-103 and S-106.

(a) Mousel A. 1997. Sampling field log spreadsheet "tk1data.xls," received by LA Mahoney, June 26, 1997. Los Alamos Technical Associates, Richland, Washington.

When the samples were extruded into the evacuated RGS system (whose total volume was 1575 cc), the resulting pressures were 20.04 kPa for segment 10D-2 and 20.42 kPa for segment 10B-3. Applying the ideal gas law shows that the sample pressure (in the 308-cc sampler volume) must have been 103 kPa, or roughly 1 atm. This atmospheric pressure, in conjunction with the composition of the sample gas, suggests that the samples contain dome space gas.

4.4 Tank BY-109

Tank BY-109 was the ninth tank and the fifth SST sampled with the RGS. An important factor in choosing this tank for RGS sampling was to assess the effect of salt-well pumping on gas retention. BY-109 had its supernatant liquid removed in 1985 and was partially salt-well pumped in 1996 just before sampling, leaving the ILL about 20 in. below the waste surface. Push-mode sampling was done in risers 10B and 12C of BY-109. The approximate locations of the risers are depicted in Figure 4.4.1. Core segments were taken at various elevations in each riser, as shown in Figure 4.4.2.

Historical Tank Content Estimate for the Northeast Quadrant of the Hanford 200 Area (Consort et al. 1996) describes Tank BY-109 as a sound SST with interim stabilization completed in June 1985. Tank BY-109 has a capacity of about 758,000 gallons and currently contains about 423,000 gallons, of which 340,000 gallons is saltcake and 83,000 gallons is sludge-type waste. Salt-well pumping was carried out in 1996, removing the supernatant liquid, but about 32,000 gallons of interstitial liquid remains in the saltcake and sludge. BY-109 is part of a group of tanks

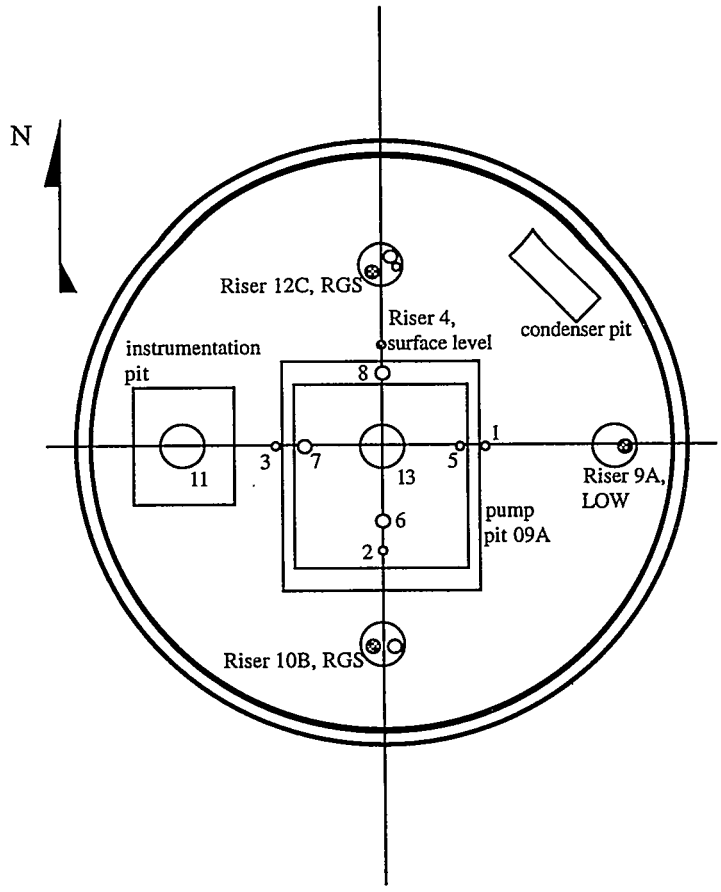

Figure 4.4.1. Schematic Diagram of Riser Locations in Tank BY-109

(Cluster 15 in Stewart et al. [1996b]) that have fairly high radioactivity, nitrite concentrations around 0.25 M, and low TOC, about 0.05%. Historical tank content estimates indicate that the primary waste stored in BY-109 was saltcake from evaporator campaign BY, and the secondary waste was metals from the bismuth phosphate process, 1944 to 1951 (Remund et al. 1995).

Surface level measurements through riser 4, as catalogued on the Tank Characterization Database, show that the level has remained steady with readings fluctuating between 357.6 and 348.2 cm (140.8 and 137.1 in.). Riser 9A LOW measurements showed an interstitial liquid elevation of 279.1 cm (109.9 in.) as of January 21, 1997. Zip-cord measurements taken March 6, 1997, indicate waste depth under riser 10B as 342.6 cm (134.9 in.).(a) For riser 12C, the second selected for core sampling, zip-cord measurements indicate a waste depth of 311.6 cm (122.7 in.). (Both zipcord measurements are referenced to tank bottom at tank center.) RGS sampling locations for each riser are shown in relation to the expected tank contents profile in Figure 4.4.2.

Current temperature data are not available for Tank BY-109. The TC tree in the tank appears to have become unusable sometime during the late 1970s and was not replaced after it malfunctioned. A report, *Thermocouple Status: Single Shell and Double Shell Waste Tanks* (Tran 1993), which is used to find TC elevation data, does not give locations for this TC tree.

The most recent historical temperature datum (from TC#1 in 1991, before salt-well pumping) gave a local temperature of 87.2°F. This temperature is used for all the in-situ calculations throughout the tank, because no recent temperature profile data are available.

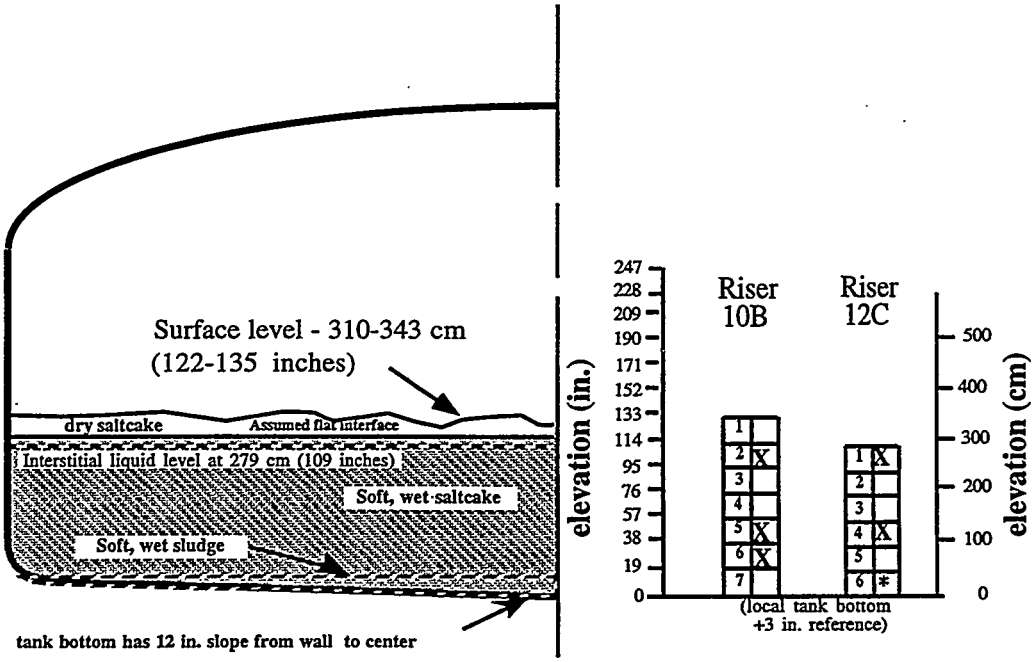

Figure 4.4.2. Diagram of Expected Waste Layering and RGS Sample Elevations for Tank BY-109 (* indicates a planned sample could not be obtained because the waste could not be penetrated)

(a) cc:Mail communication, BC Simpson (LMHC) to JM Bates (PNNL), April 16, 1997.

The best available information on tank content layering is derived from the core observations made in 1997, which are presented in Figure 4.4.3.(a) Note the variation in the nature of the layers at risers 12C and 10B. According to these observations, sludge slurry probably made up much or all of the three RGS samples that were taken successfully (riser 12C, segment 4, and riser 10B, segments 5 and 6). It should be noted that the RGS samples were observed after RGS gas extraction, which may have homogenized, dried, or otherwise modified their appearance.

Preliminary density data for the liquid and bulk solids in BY-109 were available from cores taken in 1997.(a) The density of drainable liquid from two samples was 1500 kg/m^3 in both cases. The bulk density of the samples with high solids concentrations varied from 1610 to 2000 kg/m^3, with an average and standard deviation of 1730 ± 110 kg/m^3.

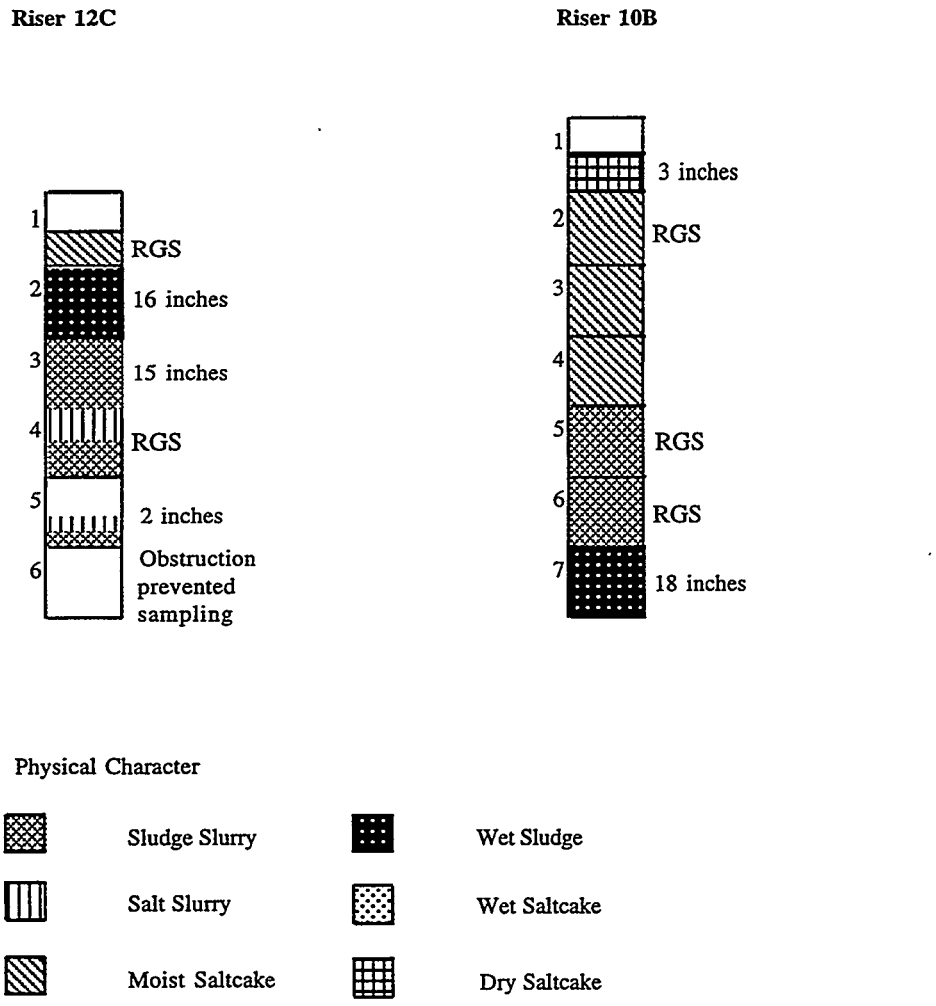

Figure 4.4.3. Most Recent Core Profiles for the Push-Mode Sampling Risers in Tank BY-109

(a) Transmittal from R Esch (LMHC) to LA Mahoney (PNNL) of data for the BY-109 TCR (document in preparation). July 29, 1997, and August 6, 1997. Lockheed Martin Hanford Corporation, Richland, Washington.

For the in-situ inventory and average gas composition calculations, the density of solids-free liquid was set at 1500 kg/m^3, the gas-free bulk density of the zone above the ILL was set at 1730 kg/m^3, and the remainder of the waste was also given a gas-free density of 1730 kg/m^3.

4.4.1 Sampling and Extraction Information

The segments analyzed are listed in Table 4.4.1. Two samples, riser 12C, segment 1 and riser 10B, segment 2, were discarded because the piston cables and seals were damaged, allowing post-sampling leakage to compromise the samples. As a result of these sampling difficulties, no samples were taken successfully in the zone of waste above the ILL. The successful samples were of reduced volume, because the sampler piston was not fully withdrawn. The reduced effective sampler volumes were taken into account in calculating the gas concentrations in the waste; the piston positions were found by examining the x-ray images (Section 4.4.4).

Table 4.4.1 also shows the lag times (delay between sample acquisition and processing) for these samples. This information was provided to allow data users to relate the lag time between sampling and extrusion to the concentrations of the various constituents to test for decomposition or other chemical reactions. One such relationship (oxygen plus other contamination gases versus lag time) is discussed in Section 5. The maximum lag time allowed by the sampling plan is 24 days, based on sampler leakage rates measured during acceptance testing. The hold times for samples 10B-5 and 10B-6 exceeded this limit, but the samples were accepted based on calculations that indicated the estimated leakage was still negligible.

As is discussed in Section 3.6.2, the HHF used during sampling may enter the sampler in place of some of the waste. Table 4.4.2 shows the volume percentage contamination by HHF of samples taken from BY-109. Some of these samples (12C-4, 12C-5, 10B-3, 10B-4, 10B-5, 10B-6, and 10B-7) contained bromide below the detection limit. The actual measured HHF contamination percentages (or, rather, the upper bounds set by the detection limit) are used for RGS samples 12C-4, 10B-5, and 10B-6. All of these samplers were backfilled with helium and sealed with vacuum grease before they were deployed. This method virtually eliminated air and argon contamination from gases entrained during sampling. The helium backfill results are summarized in Section 5.

Table 4.4.1. Lag Times for Processing RGS Samples from Tank BY-109

Sample	Acquisition Date	Processing Date	Lag (days)
12C-1[(a)]	June 6, 1997	June 25, 1997	19
12C-4	June 12, 1997	July 1-7, 1997	19
10B-2[(a)]	June 16, 1997	July 9, 1997	23
10B-5	June 16, 1997	July 11-15, 1997	25
10B-6	June 17, 1997	July 16-17, 1997	29
(a) Discarded because of air inleakage.			

Table 4.4.2. Hydrostatic Head Fluid Contamination in BY-109 Samples

Sample	HHF Contamination (vol%)
12C-1 (RGS)	15.7
12C-2	15.7
12C-3	no data
12C-4 (RGS)	< 8.6
12C-5	< 6.2
10B-1	10.7
10B-2 (RGS)	16.7
10B-3	< 5.7
10B-4	<9.2
10B-5 (RGS)	< 6.7
10B-6 (RGS)	<7.0
10B-7	<11.3

The data analysis calculations were carried out as described in Section 3, with a method that calculates the condensed ammonia in the canisters as well as the ammonia in the vapor phase. In addition, all of the BY-109 samples were injected (after gas extraction) with an ^{15}N-labeled ammonia standard to determine how much ammonia was still dissolved in the sample after the extraction of other gases was complete. Some of these analyses were carried out over several days, as shown in Table 4.4.1, to test the effect of giving the injected ammonia a longer time to equilibrate with the sample ammonia. The details of the residual ammonia analysis are discussed in Section 5.

4.4.2 Retained Gas Composition

Table 4.4.3 presents the estimated concentrations of the insoluble gases in each RGS sample taken from BY-109. No corrections have been made for air and argon entrainment and helium backfill. The corrections consist of removing all the oxygen, argon, and helium and subtracting $(3.73) \cdot (O_2)$ from the nitrogen, consistent with the molar N_2/O_2 ratio in atmospheric air. The corrected concentrations are given in Table 4.4.4.

Table 4.4.5 presents the total ammonia concentration per liter of waste under in-tank conditions. The "extracted NH_3" column gives the total moles of ammonia, both condensed and vapor-phase, that were pumped out of the samples into the "J" collection canisters. "Residual NH_3" refers to the ammonia remaining in the waste after pumping. The extracted ammonia has a different accuracy than the residual ammonia; therefore, the contribution of the residual is shown separately in the table. (It should be noted that the labeled ammonia method has not yet been fully tested on standard waste simulants; until such tests have been completed, the method should be considered unverified. A further discussion of the ammonia calculations is given in Section 5.)

Table 4.4.3. Concentrations of Insoluble Constituents (μmol/L of waste) in Tank BY-109 Without Air Entrainment Correction

Segment	N_2	H_2	N_2O	O_2	CH_4	He	Ar	Other Nit. Ox	C_2H_x	C_3H_x	Other Hyd.
12C-4	2400 ± 220	1300 ± 80	800 ± 50	260±48	37 ± 5.7	1700±260	32±4.9	0.8±0.8	31±6.9	6.6±1.0	40±8.5
10B-5	1500 ± 120	2300± 160	770 ± 50	60 ± 12	31 ± 2.9	450 ± 30	12±1.2	0.7±0.7	31±3.0	5.5±1.0	40±5.4
10B-6	1800 ± 110	3800± 220	1200 ± 70	52 ± 10	59 ± 3.3	360 ± 21	16±1.3	0.9±0.9	89±9.7	9.8±1.5	77±12

Table 4.4.4. Concentrations of Insoluble Constituents (μmol/L of waste) in Tank BY-109 with Air Entrainment Correction

Segment	N_2	H_2	N_2O	O_2	CH_4	He	Ar	Other Nit. Ox	C_2H_x	C_3H_x	Other Hyd.
12C-4	1500 ± 290	1300 ± 80	800 ± 50	0	37 ± 5.7	0	0	0.8±0.8	31±6.9	6.6±1.0	40±8.5
10B-5	1300 ± 130	2300± 160	770 ± 50	0	31 ± 2.9	0	0	0.7±0.7	31±3.0	5.5±1.0	40±5.4
10B-6	1600 ± 120	3800± 220	1200 ± 70	0	59 ± 3.3	0	0	0.9±0.9	89±9.7	9.8±1.5	77±12

Table 4.4.5. Total Ammonia Concentrations in Tank BY-109

Segment	Extracted NH_3 (μmol/L)	Residual NH_3 (μmol/L)	Total NH_3 (μmol/L)
12C-4	1200 ± 460	11000 ± 2500	12000 ± 3000
10B-5	2000 ± 620	12000 ± 2900	14000 ± 3500
10B-6	1400 ± 490	4700 ± 1100	6100 ± 1500

The average and standard deviation of the ammonia concentrations over samples 12C-4, 10B-5, and 10B-6 are 11,000 ± 4,000 μmol/L waste (0.025 wt% NH_3 dissolved in the liquid). The variation in the ammonia concentrations of these samples is not much larger than the measurement error band; thus the difference between the ammonia contents of samples 12C-4 and 10B-5 (which were both taken at the same elevation) could be more apparent than real. However, sample 10B-6 shows a significantly lower ammonia content than the other two samples from BY-109.

Table 4.4.6 contains the composition of the gas/vapor phase in each sample and the integrated average composition for Tank BY-109. The sample compositions in the table have been calculated using the in-situ solubility method described in Section 3.5.2. The tank average composition is the result of integrating RGS species concentrations over the layer below the ILL and multiplying those concentrations by the layer volume. The integration method is described in Section 3.6.

Table 4.4.6. Sample and Overall Average Compositions of Retained Gas in Tank BY-109 with Gas Entrainment Correction

Segment	N_2 (mol %)	H_2 (mol %)	N_2O (mol %)	NH_3 (mol %)	Other (mol %)
12C-4	40 ± 7.4	35 ± 4.2	21 ± 2.6	0.52 ± 0.14	3.2 ± 0.7
10B-5	29 ± 3.5	52 ± 5.3	16 ± 1.7	0.57 ± 0.14	2.4 ± 0.3
10B-6	23 ± 3.7	56 ± 7.0	17 ± 2.2	0.25 ± 0.10	3.4 ± 0.7
Average in waste below the ILL (a)	29 ± 3.8	50 ± 4.9	18 ± 1.8	0.41 ± 0.09	3.1 ± 0.5

(a) The error bands on the average composition, as for the individual sample compositions, only represent the instrument error because there are too few samples to define the spatial variability of gas concentration.

4.4.3 Gas Inventory

The method by which the in-situ gas volume fractions were calculated is given in Section 3. The results are presented in Table 4.4.7, showing the difference between in-situ gas volume fractions that were and those that were not corrected for the presence of entrained and backfilled gases. (The temperature used throughout the tank was the TC#1 measurement made in 1991, as discussed in Section 4.4.) The table also contains the average gas volume fraction in the layer below the ILL and the average pressure experienced by the gas. All of the averages are in-situ volume averages and are calculated by Simpson's Rule integration, as described in Section 3.6.

Table 4.4.8 shows estimates of the STP volumes of gas constituents in the interstitial liquid layer in Tank BY-109. The gas inventories were calculated by integrating the RGS constituent concentrations (three data points) over the volume of the layer to obtain an average concentration, using Simpson's Rule, and multiplying those averages by the volume of the interstitial liquid layer. Because samples 12C-4 and 10B-5 were taken from the same elevation in different risers the data from these two samples were averaged into a single point, which was then used in the standard integration. The integration method is described in Section 3.

Table 4.4.7. In-Situ Gas Volume Fractions in Tank BY-109

Segment	Sample Central Height (cm)	Hydrostatic Pressure (atm)	Temperature (°C)	Corrected Gas Volume Fraction (in-tank conditions)	Uncorrected Gas Volume Fraction (in-tank conditions)
12C-4	121	1.3	30.7	0.073 ± 0.011	0.132
10B-5	121	1.3	30.7	0.084 ± 0.012	0.098
10B-6	72	1.4	30.7	0.121 ± 0.014	0.132
Average in waste below the ILL		1.35 ± 0.05		0.09 ± 0.05	

Table 4.4.8. Gas Inventory (corrected for gas entrainment) in the Interstitial Liquid Layer of BY-109

Quantity	RGS	Best Estimate (RGS)
Avg. Gas Fraction	0.09 ± 0.05	0.09 ± 0.05
Gas Volume (m^3)		
In-Situ	110 ± 50	110 ± 50
STP	140 ± 70	140 ± 70
dL/dP (in./in.-Hg)	-0.25 ± 0.13	-0.25 ± 0.13
P_{eff} (atm)	1.35 ± 0.05	1.35 ± 0.05

The values in Table 4.4.8 all include the effect of corrections to remove the entrained air, argon, and the backfilled helium. In samples 10B-5 and 10B-6, as is further discussed in Section 5, the correction for entrained gas was insignificant, and the amount of helium present was found to be equivalent to the air/argon entrained volumes that had been contained in samples taken from tanks sampled previously (Shekarriz et al. 1997). (The helium and air contamination in sample 12C-4 is rather high but can be traced to known procedure changes that were in effect only for this sample; see Section 5 for more detail.)

The gas inventory calculation for BY-109 is based solely on RGS data; the BPE method is not applicable in this tank, and surface level rise yields no information because of recent salt-well pumping. Since segment 4 in riser 12C and segment 6 in riser 10B were at the same elevation, their gas fractions were averaged to represent a single datum. Because so few measurements are available in this tank and they cover only the lower half of the waste, the assigned 50% uncertainty may be too low.

The average gas fraction based on RGS data is 0.09 ± 0.05, which corresponds to a total in-situ gas inventory of 140 ± 70 m^3. The barometric pressure response correlation calculated from the RGS data is -0.25 ± 0.13 in./in.-Hg, and the effective pressure is 1.35 ± 0.05 atm. These calculations are summarized in Table 4.4.8.

The three ammonia concentration measurements in the interstitial liquid layer of BY-109 integrate to a total (vapor and dissolved) ammonia inventory with an STP volume of 250 m^3 (9,000 ft^3). The error band on the ammonia inventory should be considered to be at least 50%.

Figure 4.4.4 shows the corrected gas volume fractions (Table 4.4.7) and the entrainment-corrected compositions (calculated from Table 4.4.4) in the samples from BY-109. The compositions represent the mole fraction of the species in the insoluble gas; water and ammonia are not included. Two composition plots appear to show the two samples (12C-4 and 10B-5) that are both at the same elevation. Figure 4.4.4 also shows data taken from core extrusion analyses, as a way of tying those observations together with RGS. The lines and symbols in the rightmost plot indicate the fraction of the sample mass that was drainable liquid; the remainder is wet solids. The bulk densities measured for the wet solids in each sample are also noted on the figure.

Note that the gas volume fractions in samples 12C-4 and 10B-5, which were located at the same elevation, are different by an amount that is about equal to their error bands. This may indicate that the gas distribution is similar for both two risers. However, the compositions of the two samples from the same riser (10B) at different elevations are more similar to one another than

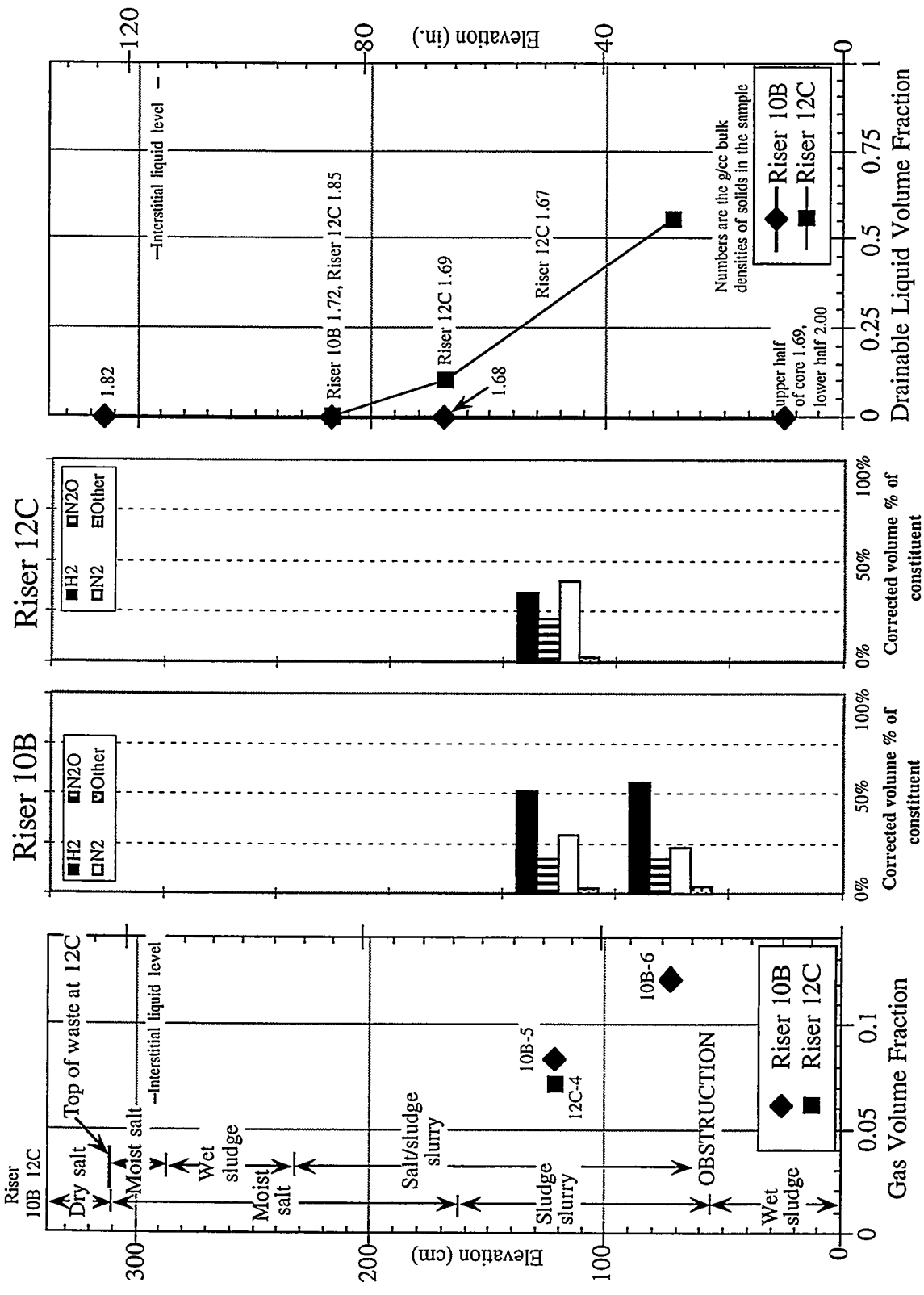

Figure 4.4.4. Gas Volume Fractions, Compositions, and Liquid Contents in Tank BY-109

are the compositions of the two samples from the same elevation but different risers (see Figure 4.4.4). Thus the evidence of lateral uniformity in the retained gas is not conclusive.

4.4.4 X-Ray Results

Table 4.4.9 summarizes all the available radiography observations, including segment 1 from riser 12C and segment 2 from riser 10B. (These samplers had piston seating problems that compromised RGS extraction processing but, because the radiographs were taken immediately after sampling, before much leakage could occur, the qualitative features of the sample are expected to be valid.) There were no standard air/water density profiles for one of the five samples for which x-ray images were recorded (segment 12C-4). The standard air/water density profiles for segment 12C-3R1 were used for this sample because 12C-4 and 12C-3R1 were x-rayed on the same day.

The error bands of the visible gas volume fractions that are given in Table 4.4.9 are unknown but are believed to be larger than the errors in the gas volume fractions calculated from gas extraction. (The "visible" gas volume fraction refers to the gas that has separated from the solids and liquid, such that its volume can be calculated based on the image. The uncorrected gas fractions from extraction are used for comparison to reflect the presence of entrained air in the sampler.) A comparison of x-ray-derived gas volume fractions and extraction-derived gas volume fractions, which is given in Table 4.4.9, shows that sample recovery was greater than 95% for BY-109. The 5% or less underestimation caused by incomplete sample recovery is within the gas fraction measurement error.

Table 4.4.10 provides a summary of the waste densities that have been estimated from radiographic data. The radiographic densities include the gas in the waste and are given for several locations in each sample to show density trends. Table 4.4.10 also shows the densities that were measured for the core samples that lay above and below each RGS sample; these are gas-free densities. The two methods give reasonably consistent results, considering the differences that can be expected because of the effect of retained gas on the radiographic densities of the RGS samples, the fact that RGS samples are adjacent to standard core samples rather than collocated, and the partial unavailability of standard x-ray profile images for air and water densities.

Figures 4.4.5 and 4.4.6 show density images calculated from x-rays of segments 10B-5 and 10B-6. False color has been used to enhance the bubble structure in the waste. In these images, features that are only a few pixels in size are probably noise and should be ignored. In Figure 4.4.5, note the sampler-spanning bubble at the bottom of the 0.75-ft image and the darker (denser) striations in the 1- and 1.25-ft images. The overexposure of the 1-ft image is also evident. Similar bubbles and higher-density bands are present in Figure 4.4.6. The piston cables are visible in both figures.

4.4.5 Core Extrusion Results

Figure 4.4.7 shows some samples of BY-109 waste. The successful RGS samples comprised segment 4 of riser 12C (Core 201) and segments 5 and 6 from riser 10B (Core 203). The riser 12C waste tended to become wetter at greater depths, at least down to the lowest sample taken (segment 5). The only riser 12C sample pictured in Figure 4.4.7 is segment 2, a wet brown waste with the typical muddy appearance of sludge. The lower samples in riser 12C contained more saltcake as well as more liquid. The RGS sample 12C-4 lay at the top of the region where salt first began to appear mixed with the sludge. A few bubble marks were visible on the surfaces of segments 12C-2 and 12C-3R1.

Table 4.4.9. Summary of Observations from X-Ray Images of Tank BY-109

Segment	Comments/Observations
12C-1	Only a small amount of waste was recovered; the sampler was virtually empty. No waste was attached to the piston.
12C-3R1[a]	This sample (which was not processed by RGS) contained many gas bubbles, with a "string" of bubbles of about 3 mm (0.13 inch) diameter evident in the lower portion. Density gradients are also present. There is a flat top surface and a 2.5 cm (1 inch) gas gap below the piston, to which no waste is attached. The visible gas volume fraction (not counting bubbles) is therefore 0.052. (This assumes the piston was drawn all the way back, which was not true for some other BY-109 samples.)
12C-4[b]	The lower waste is fairly homogeneous, but becomes increasingly less so toward the top. Some lighter areas/bubbles are visible in the middle third of the sample, with many dark/dense striations evident in the upper third. The light/bubble features are typically about 1 mm in dimension. The dark regions typically extend across the whole sampler. The waste extends all the way to the piston, giving a visible gas volume fraction of 0. (Compare to the gas volume fraction of 0.073 ± 0.011 in Table 4.4.7 obtained by gas extraction.) The piston was about 3.5 in. from its stops, reducing the effective sampler volume by 3.5/19 = 18.4%.
10B-2	The recovered waste only fills about half the sampler volume. A number of low-density inhomogeneities (bubbles) appear in the lowest third of the sampler. The waste becomes less dense toward the top, has a flat top surface, and gives way to a large gas volume region. It is possible that this gas volume region represents gas trapped in the waste, but the more likely explanation for its existence, given the known piston seal problem, is incomplete sample recovery and/or gas leakage.
10B-5[c]	The lower half of the waste shows low-density material, probably gas, including a single large gas "bubble" that appears to span the entire sampler diameter but is relatively flat, being only about 0.6 cm (0.25 in.) or so high. The waste higher up contains decreasing amounts of low-density material, containing instead numerous, large "swirls" of darker/denser material. The waste extends all the way to the piston. The visible gas volume fraction (based on the large bubble) is 0.013, taking into account that the piston was drawn back to about 0.25 in. from the stops. (Compare with the gas volume fraction of 0.098 ± 0.012 in Table 4.4.7 obtained by gas extraction.) The piston was about 0.25 inch from its stops, reducing the effective sampler volume by 0.25/19 = 1.3%.
10B-6[d]	The waste was very similar to segment 10B-5. It also contains lower-density material and has a large single "bubble" of 0.6 cm thickness about mid-way up the sample, but it contains fewer "swirls" than 10B-5 and has some low-density material in the upper sampler region. A large gas gap region exists below the piston, extending about 5.1 cm (2.0 in.). A flat meniscus is visible at the waste/gas interface, and there is no waste attached to the piston. The visible gas volume fraction (based on the large bubble and the gas gap) is 0.123, taking into account that the piston was drawn back to about 0.75 in. from the stops. (Compare with the gas volume fraction of 0.132 ± 0.014 in Table 4.4.7 obtained by gas extraction.) The piston was about 0.75 in. from its stops, reducing the effective sampler volume by 0.75/19 = 3.9%.

(a) Extensive flattening visible at top of the standard air density profile.
(b) This segment lacked standard air/water density profiles; used data from segment 12C-3r-1, taken nearly at the same time.
(c) Some flattening visible at top of standard air density profile; some skewing of water density profile evident. The quality of the x-ray images is uneven, with varying exposure and with several images containing large bright areas outside the sampler. These areas affect the overall brightness level and complicate image processing.
(d) Some flattening visible at top of standard air density profile.

Table 4.4.10. Densities of BY-109 Samples, from Radiography and Core Samples

Riser-Segment Number	Distance from bottom of sampler, (ft)	Calculated Mean Density, (g/cc)	Calculated Standard Deviation, (g/cc)	Gas-free Density Above and Below the RGS Sample (from cores), (g/cc)
10B-2	0.25	1.47	0.22	density above, n/a
	0.50	1.55	0.25	density, 1.66
	0.75	1.46	0.21	density below, 1.72
10B-5[a]	0.25	1.37	0.25	density above, 1.68
	0.50	1.43	0.35	
	0.75	1.46	0.31	density, 1.61
	1.00	1.03	0.32	
	1.25	1.56	0.46	
	1.50	1.64	0.27	density below, 1.69
10B-6	0.25	1.47	0.28	density above, 1.61
	0.50	1.59	0.29	
	0.75	1.64	0.36	density, 1.69
	1.00	1.67	0.34	
	1.25	1.57	0.29	density below, n/a
12C-1	0.25	n/a[b]	n/a[b]	density below, 1.85
12C-3R1	0.25	1.55	0.28	density above, 1.85
	0.50	1.57	0.25	
	0.75	1.63	0.26	density, 1.69
	1.00	1.47	0.26	
	1.25	1.41	0.25	density below, 1.67
12C-4[c]	0.25	1.44	0.30	density above, 1.69
	0.50	1.65	0.36	
	0.75	1.60	0.39	density, 1.67
	1.00	1.85	0.39	
	1.25	2.21	0.49	density below, n/a

(a) The quality of the x-ray images is uneven, with varying exposure and with several images containing large bright areas outside the sampler. These areas affect the overall brightness level and make densities less accurate, as can be seen at the 1-ft level (which is overexposed).
(b) Not enough waste was in the sampler for a meaningful density estimate.
(c) This segment lacked standard air/water density profiles, so the profiles from segment 12C-3R1 were used.

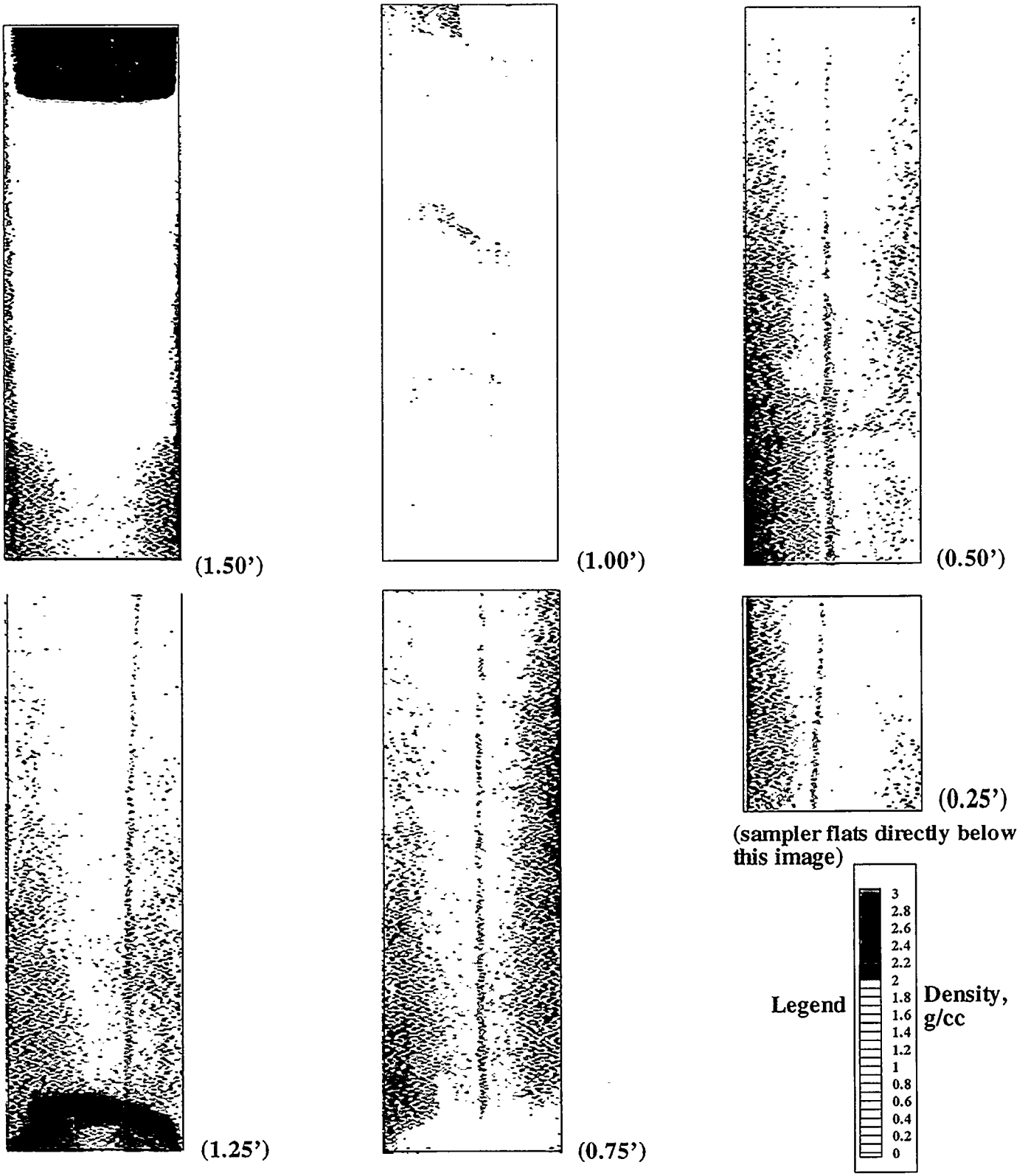

Figure 4.4.5. Density Images Calculated from X-Rays of Sample 10B-5 from Tank BY-109

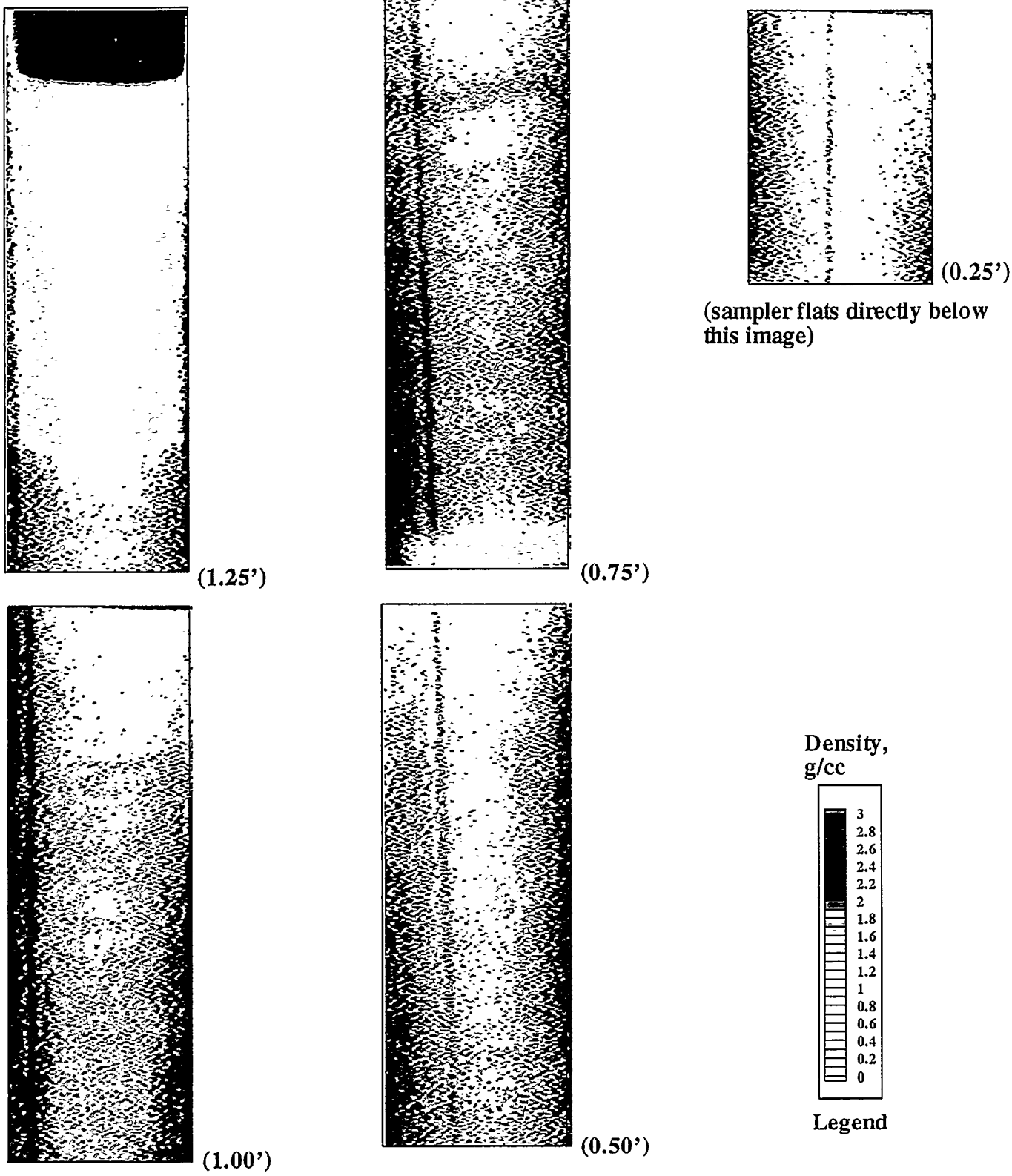

Figure 4.4.6. Density Images Calculated from X-Rays of Sample 10B-6 from Tank BY-109

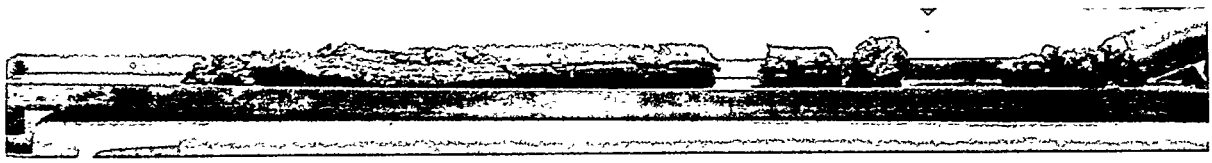

BY-109 Core 201, Riser 12C, Segment 2

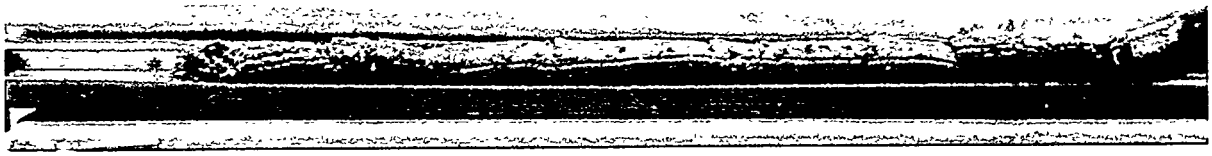

BY-109 Core 203, Riser 10B, Segment 3

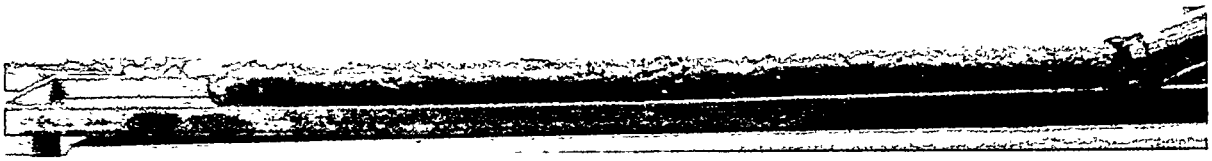

BY-109 Core 203, Riser 10B, Segment 4

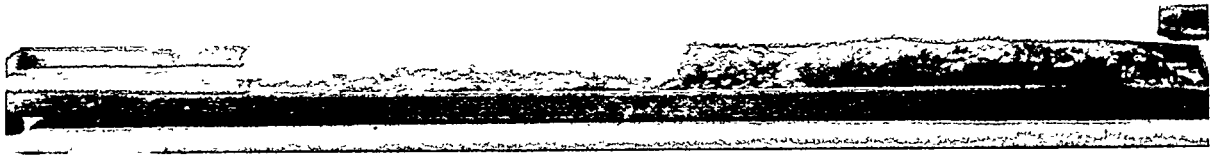

BY-109 Core 203, Riser 10B, Segment 7

Figure 4.4.7. Core Sample Extrusion Photos from Tank BY-109

The waste in riser 10B primarily consisted of moist saltcake, gritty-textured gray material. Unlike the riser 12C waste, the riser 10B waste appeared to become drier with depth, down to the bottom of segment 10B-4. This upper portion of the riser 10B core had enough flexibility to be extruded as a single coherent length, as shown in Figure 4.4.7 for samples 10B-3 and 10B-4, and enough stiffness to retain a number of bubble marks. These two segments are shown in Figure 4.4.7.

The two RGS samples, 10B-5 and 10B-6, lay below this elevation. They seem (based on post-extraction observations) to have contained more sludge than the extruded samples above them, though this could have been an artifact of homogenization during extraction. As shown in Figures 4.4.5 and 4.4.6, the x-rays, the RGS samples contained sampler-spanning bubbles and density striations suggestive of varying composition in the solids. Below the RGS samples was the extruded sample 10B-7, which consisted entirely of sludge but showed a very distinct color difference between its upper and lower halves (as can be seen in Figure 4.4.7). Bubble marks were also present in 10B-7.

4.5 Overview of Gas Compositions

Figure 4.5.1 shows the relationship between the major constituents of the retained low-solubility gas in the eight tanks for which RGS data have been taken to date. This figure plots the normalized mole fraction of hydrogen on the ordinate and the normalized mole fraction of nitrous oxide on the abscissa. So that hydrogen and nitrous oxide are normalized to mole fractions of the major gases, the axes are expressed in terms of $H_2/(H_2 + N_2O + N_2)$ and $N_2O/(H_2 + N_2O + N_2)$. Because of this normalization, the normalized mole fraction of nitrogen can also be read as the distance from the diagonal; the lines of constant nitrogen are marked. All the compositions in the figure have been corrected for contamination by inleakage and entrainment.

As is clear in Figure 4.5.1, many of the data points cluster near the hydrogen axis and away from the N_2O and N_2 axes, indicating that hydrogen is often the dominant constituent in retained gas. (However, hydrogen is generally not dominant for samples with gas retention of less than 1 vol%.) Some clustering can be seen for each tank.

Tank AN-104 gas compositions occupy a relatively broad area near the center of the chart. AW-101 compositions lie near the ordinate because of their relatively high nitrogen content, while U-103 compositions fall uniquely along a line of roughly constant nitrogen mole fraction and high N_2O. The retained gas in Tank S-106 lies in about the same high-H_2 composition cluster as the high retained-gas samples from AN-105 and AN-103. Only Tank A-101 retained gas had higher measured hydrogen fractions. The compositions for Tank BY-109 lie in much the same region of the plot as did AN-105 and AN-104.

Information is available for the composition of dome space gas in U-103 and for drill-string gases during the 1997 sampling of S-106 and BY-109.[a] The gas in the dome space of U-103 had H_2/N_2O ratios that ranged from 0.70 to 0.79, measured in July 1995 and October 1997; the RGS ratios were 0.27 to 0.97. The S-106 drill-string gas (February 1997) had an H_2/N_2O ratio of 4.0, which compares fairly closely to the RGS ratios (which were between 4.2 and 6.9). In BY-109 in June 1997, the drill-string gas had an H_2/N_2O ratio of 3.4; the RGS ratios were 1.6 to 3.2.

(a) Brothers JW. 1997. Composition data from samples U-103-0725-95-1505, U-103-0727-95-1425, U-103-0731-95-1410, U-103-10-22-97-1403, S-106 riser 7 (received at the mass spectrometry lab 2/25/97), and BY-109-6-17-97-0350. Pacific Northwest National Laboratory, Richland, Washington.

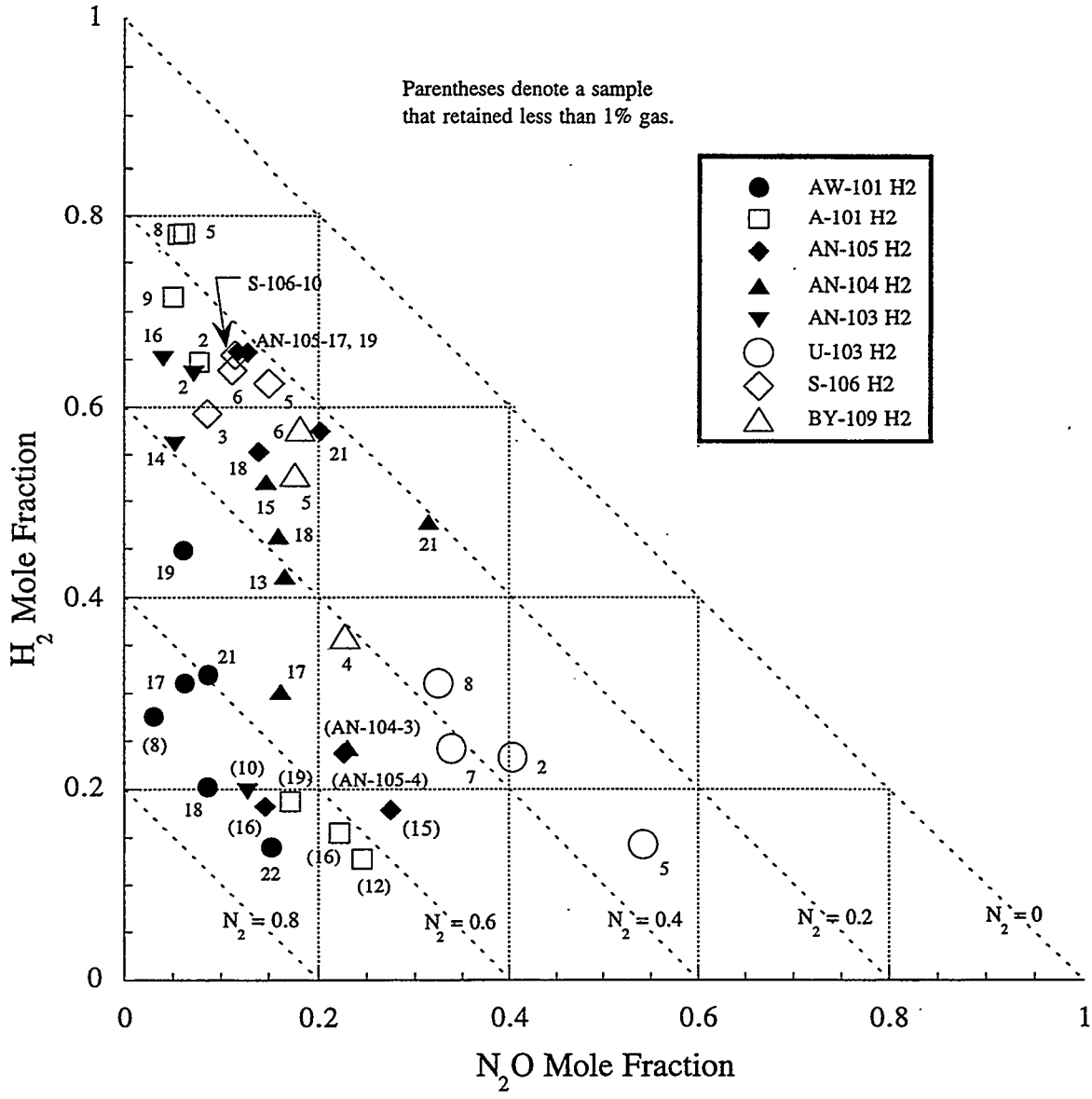

Figure 4.5.1. Compositions of Retained Gas in RGS Samples

5.0 RGS System Performance

This section discusses the performance of the RGS sampling and extraction procedures, equipment, and models. The primary focus is on the tanks successfully sampled during 1997 and on procedure and equipment changes made for the 1997 sampling program. The applicability of these changes—increased sampler valve closure force, sampler helium backfill, condensed ammonia calculations, and isotopic ammonia addition—to the various samples that were taken is shown in Table 5.1.

Section 5.1 summarizes the performance history of the RGS samplers. Section 5.2 covers topics associated with insoluble gas sampling and extraction: helium backfill, inleakage of air gases (N_2 and O_2 in nonatmospheric proportions), and incomplete extraction. Water vapor pressure over the waste is presented in Section 5.2, with a comparison to water vapor pressures that have been measured over waste simulants in other experiments. Ammonia-related procedures and difficulties are discussed in Section 5.4: condensed and residual ammonia determination, ammonia equilibration rate, and isotopic ammonia addition. Each of these sections contains a summary of what has been learned about the possible errors in RGS analyses and their effect on the calculated gas and ammonia concentrations.

Table 5.1. Sampling Procedure Changes in 1997

Sample	Increased Sampler Valve Closure Force	Helium Backfill	Condensed Ammonia Calculation	Isotopic Ammonia Addition
1996 Samples	No	No	No	No
U-103, Riser 7 Seg. 2	No	Yes	Yes	Yes
U-103, Riser 7 Seg. 5	No	Yes	Yes	No
U-103, Riser 7 Seg. 7	No	Yes	Yes	No
U-103, Riser 7 Seg. 8	No	Yes	Yes	No
S-106, Riser 7 Seg. 3	No	Yes	Yes	Yes
S-106, Riser 7 Seg. 5	No	Yes	Yes	Yes
S-106, Riser 8 Seg. 6	No	Yes	Yes	Yes
S-106, Riser 8 Seg. 10	No	Yes	Yes	Yes
BY-101, Riser 10D Seg. 2 (compromised by leak)	Not confirmed	Yes	Yes	Yes
BY-101, Riser 10B Seg. 3 (compromised by leak)	Not confirmed	Yes	Yes	Yes
BY-109, Riser 12C Seg. 4	Yes	Yes	Yes	Yes
BY-109, Riser 10B Seg. 5	Yes	Yes	Yes	Yes
BY-109, Riser 10B Seg. 6	Yes	Yes	Yes	Yes

5.1 Sampler Performance History

Figure 5.1 depicts the RGS sampler performance history to date. (The figure includes the five tanks that were sampled in 1996; other information on these tanks has been given by Shekarriz et al. [1997].) Each box represents a sample. Inside the box, reading from left to right, are the dose rate through the drill string, the sample failure code (if there was a failure), and the riser name. To the right of each box is a code or other description of the push force needed to take the sample (where this information is available). Dashed horizontal lines are used to indicate the approximate location of interfaces between layers.

It can be seen that for the first seven tanks, up through S-106, the predominant cause of sample loss was the failure of the sampler ball valve to close (code "V"). There is no consistent pattern of valve failures being related to layer interfaces, dose rates, or push force.

To prevent further losses, the ball valve was changed so that the valve spring would exert more closure force. After the valve spring change, a previously unseen type of sampler failure occurred on BY-109: the sampler piston did not fully retract, or so much force was needed to retract the piston that its seals were damaged and the sample compromised. Sampler changes that will avoid this difficulty are under consideration.

5.2 Insoluble Gases

Certain assumptions that were discussed in Section 3 (particularly Section 3.7.1) were made in developing the physical model that was used to interpret the RGS extraction data to find the in-situ gas concentrations in the samples. The assumptions that had the most potential effect on calculating the insoluble gas concentration were as follows:

- complete sample recovery
- atmospheric ratios of N_2 to O_2 in contamination, allowing the contamination N_2 to be estimated from the measured O_2
- complete mixing in the extractor side of the RGS system
- complete removal of gases from the sample (i.e., insolubility of gases other than NH_3).

Sample recovery appears, based on the x-ray images discussed in Section 4, to have been 95% or better, so that the quantity of insoluble gas in the waste would be underestimated by 5% or less as a result of this assumption alone.

The N_2/O_2 ratio in gas entrained by the sampler during sampling could be greater than the atmospheric ratio, leading to an overestimation of in-situ nitrogen and of total gas if the entrained oxygen reacted away before RGS extraction took place. The evidence presented in Section 5.2.1, in connection with helium backfill results, does not suggest any significant reaction took place. However, it appears (Section 5.2.2) that the air gases which entered the extractor through inleakage have N_2/O_2 ratios that for unknown reasons are substantially lower than the atmospheric ratio. The resulting overestimation of sample nitrogen is expected to be less than 15% and the overestimation of the total sample gas less than 7%.

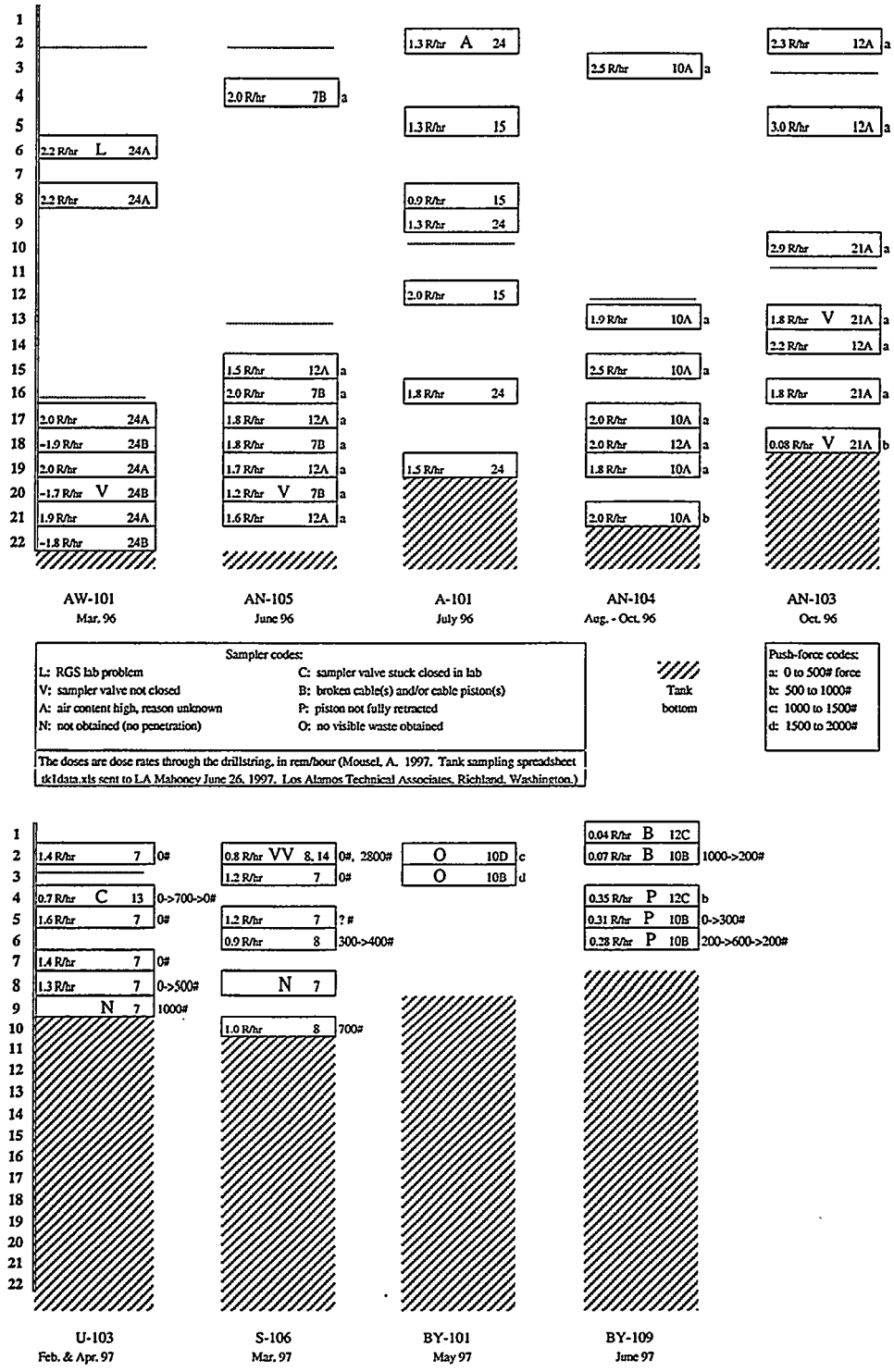

Figure 5.1. RGS Sampling History (as of September 1997)

The extraction of the insoluble gases from the extractor side of the system to the collector canisters appears to have been incomplete (Section 5.2.3), possibly because of gas solubility or incomplete mixing in the gas space. The assumptions of complete mixing and extraction cause an underestimation of insoluble gas by 10% or less.

Thus the overall bias produced by the major assumptions in the insoluble-gas model includes both overestimation and underestimation, and (based on the arguments just presented) is believed to be a maximum of 10% underestimation.

5.2.1 Helium Backfill

The oxygen and argon that have been found in RGS waste samples are believed to have their source not in "native" tank gases but in mechanical entrainment of air and purge gas during sampling. The sampler "interface" volume into which gas can be entrained consists of spaces within the valve body. Laboratory tests, as well as volume calculations from design drawings, estimate a maximum interface volume of ~6 cc. A procedural change, first employed on Tank U-103, was used for all of the samples taken in 1997 and is more fully detailed in other documents (Cannon 1997). Each sampler's ball valve assembly was backfilled with helium and sealed with grease before the sampler was deployed, a procedure change which was designed to minimize entrainment by pre-filling the entrainment volume.

Despite the helium backfill, many of the samples taken during 1997 had oxygen concentrations of about the same magnitude as those found in 1996 samples (50 μmol/L or higher). An examination of the data for these high-O_2 samples shows that most of the oxygen appeared in the canister that was extracted after the isotopic ammonia standard had been introduced into the system. Very little O_2 was present in the canister(s) that preceded the isotopic ammonia addition, as is demonstrated by the data in Table 5.2. Exactly the opposite trend is visible for helium (with one exception, which will be discussed later).

Air appears to have been introduced when the isotopic ammonia standard was added to the RGS extractor, rather than entering the sample by entrainment during sampling. This hypothesis is further supported by mass spectrometric analysis of samples of some of the isotopic ammonia standards, which contained 5% to 21% air gases; the remainder was NH_3. (The term "air gases" refers to N_2-O_2 mixtures that are not in atmospheric proportions. Air gases are further discussed in Section 5.2.2.) The isotopic standard canisters are filled at nearly standard temperature and pressure (STP) and are typically 27 cc or more in volume. The amounts of O_2 (and accompanying N_2) that have been extracted after isotopic ammonia addition would be in the range of 0.4 to 17 cc, under standard canister conditions. These values are roughly consistent with the percentage of air gases found by analysis of the standards.

The helium and air contamination in sample 12C-4 of BY-109 is exceptionally high but can be traced to procedural changes that affected this sample uniquely. A close examination of the extraction data shows that the contamination in the first canister of 12C-4 was comparable to that of the other two samples and to that of U-103 and S-106 samples. All of the extra air and helium appears in the post-isotopic-addition canister of sample 12C-4 and can be traced to procedural causes.

Table 5.2. Contamination Gases Before and After Isotopic Ammonia Addition

Sample	Before isotopic ammonia addition			After isotopic ammonia addition		
	O_2 (cc at STP)	Ar (cc at STP)	He (cc at STP)	O_2 (cc at STP)	Ar (cc at STP)	He (cc at STP)
U-103, 7-2	0.09	0.04	2.96	0.31	0.04	0.33
U-103, 7-5	0.06	0.01	2.51	No $^{15}NH_3$ added		
U-103, 7-7	0.04	0.02	3.15			
U-103, 7-8	0.06	0.02	2.80			
S-106, 7-3	0.03	0.07	2.97	0.08	0.01	0.18
S-106, 7-5	0.03	0.02	2.94	0.16	0.01	0.12
S-106, 8-6	0.14	0.02	2.29	0.01	0.01	0.29
S-106, 8-10	0.03	0.01	3.27	0.49	0.02	0.06
BY-109, 12C-4	0.06	0.05	2.44	1.28	0.12	6.10
BY-109, 10B-5	0.03	0.05	2.64	0.35	0.02	0.20
BY-109, 10B-6	0.03	0.08	2.13	0.29	0.02	0.11

Sample 12C-4 of BY-109 was allowed five days to equilibrate after the isotopic ammonia was added—an unusually long time. During the equilibration period the bulk sample volume determination, which requires helium to be introduced into the extractor, was carried out. This procedure normally takes place after all the sample gas has been extracted, but in this case the usual procedure was thought to be inappropriate because of the five-day delay. Thus the bulk sample volume determination is almost certainly the source of the excess helium (6.1 cc at STP).

The excess air in sample 12C-4 of BY-109 comes from a procedural error. The collector side of the system was, as usual, evacuated before the equilibration delay; however, a line was left open, and over the five-day delay period the collector pressure rose from 0.0 to 3.38 kPa. In a volume of 185 cc (collector-side with canister), this pressure represents 6.2 cc of air at STP. The air contamination (calculated from second canister extraction data) was a total of 6.1 cc at STP, or 4.4–4.7 cc more than was present in the second canisters of the other BY-109 samples. The close agreement of the two calculated air volumes confirms the leak as the air source.

Figure 5.2 shows the volume of "contamination" gas—the helium and argon plus 4.73 times the oxygen (to account for both the oxygen and the nitrogen associated with it in atmospheric air)—that was calculated to be present in the RGS samples from the eight tanks. Correction lines have been put on some of the 1997 sample symbols to show an estimate of what the contamination gas would have been if it were only entrainment, without the contribution from the isotopic addition canister. (The estimate was based on Table 5.2; the O_2, N_2 and Ar from entrainment alone were assumed to be decreased in the same proportion as He from the pre-isotopic to the post-isotopic canister. No such estimate could be made for sample 12C-4 of BY-109; it was too heavily contaminated by inleakage and helium.)

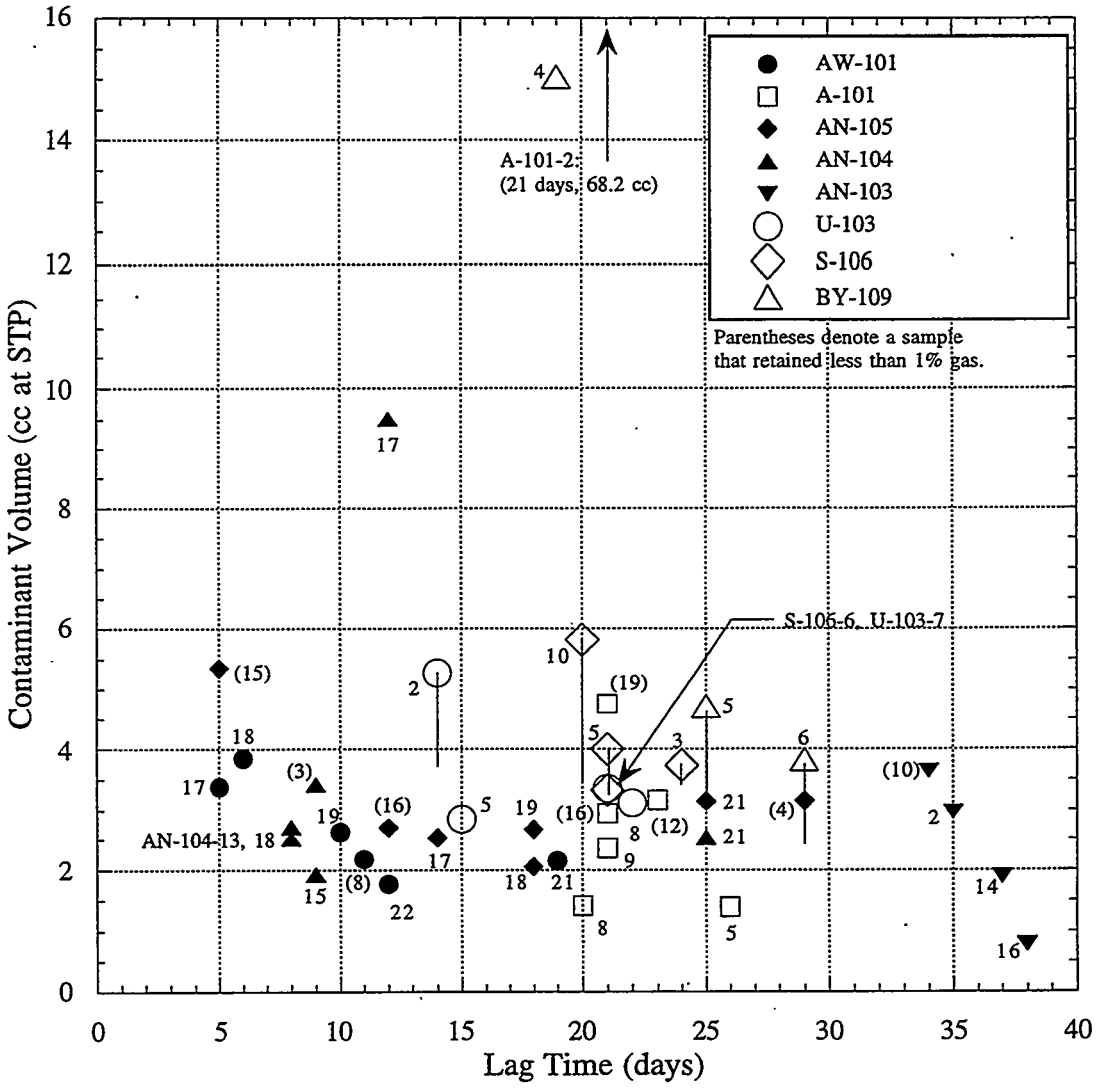

Figure 5.2. Volume of Contamination Gas Related to Lag Time

As discussed by Shekarriz et al. (1997), there is independent evidence that some of the most contaminated 1996 samples, namely AW-101 segment 18, A-101 segment 2, AN-105 segment 15, and AN-104 segment 17, suffered not only from gas entrainment but from air inleakage during sample gas extraction. Thus the highest calculated contamination volume that is not known to be partly explained by inleakage was that of sample A-101 segment 19, at 5.3 cc.

In all cases (except sample 12C-4 of BY-109), the 1997 sample contamination volumes were less than 6 cc at STP even when isotope addition leakage was added in. With the isotopic canister contribution removed (as indicated by the bottoms of the correction lines), the 1997 sample air values typically lie in the middle of the scatter in Figure 5.2.

One of the concerns in estimating the contamination by gases entrained during sampling has been that the entrained oxygen might have partially reacted with the waste. This would have meant that the contaminant N_2 was higher than the $3.73 \cdot O_2$ that was used in correcting RGS measurements for contamination and the true N_2 concentration in the samples was less than the calculated value. If this was the case, Figure 5.2 would have been expected to show that 1997 samples characteristically had larger contamination volumes than 1996 samples and that the difference increased with lag time, becausethe 1997 samples contained almost no entrained air and so underwent no loss of oxygen by reaction. No such trend is evident.

Based on the pre-isotopic-addition extraction results, it can be concluded that the helium backfill procedure has successfully reduced contamination of the RGS samples by entrained air. It also seems likely that reaction of entrained oxygen with the waste caused little error in the nitrogen estimates for the 1996 RGS samples.

5.2.2 Inleakage Air Gases

All of the air contamination that is discussed in this report has been calculated based on measured O_2 concentrations and atmospheric N_2/O_2 ratios. However, there is some indication that the oxygen, nitrogen, and argon mixture that comes from system inleakage does not have the composition of air. The compositions of the isotopic standards that were added to some of the samples were determined by the standard mass spectrometric method. The ratios of the air gas constituents in the standards are given in Table 5.3. (The table also includes the air gases that were sampled from the extractor after segment 12C-4 of BY-109 had been exposed to a system leak through an open line for five days. These data are included as another example of contamination from inleakage.)

Note that for all the samples, the N_2/O_2 ratios are significantly lower than in air. Apparently inleakage, whether into a standard canister or into the system itself, does not necessarily maintain the atmospheric ratios. This non-air composition makes it a bit problematic to estimate the extent of air gas contamination and might cause underestimation of the in-tank nitrogen through correcting for too much contamination nitrogen. At the measured oxygen levels in most of the samples, the difference amounts to less than 1 cc of N_2 at STP, or 150 μmol/L of N_2. This represents a potential underestimation of less than 15% (usually much less than 15%) in the corrected nitrogen concentrations and inventories given in Section 4. A similar degree of nitrogen underestimation may have been present in the 1996 samples that had high air gas inleakage (AW-101 segment 18, A-101 segment 2, AN-105 segment 15, and AN-104 segment 17).

Table 5.3. Composition of Leaked Contamination Gases

Sample	N_2/O_2	Ar/O_2
BY-101, 10B-3, standard 1	2.68	0.041
BY-101, 10D-2, standard 2	2.60	0.040
BY-109, 12C-4, standard	1.97	0.035
BY-109, 12C-4, extractor contents after five-day equilibration and inleakage	2.55	0.15
In the atmosphere	3.73	0.044

5.2.3 Incomplete Extraction of Insoluble Gas

A physical model that is derived and discussed in Section 3 has been used throughout RGS analysis to interpret the extraction data to find the in-situ gas concentrations in the samples. According to the model, the "insoluble" gas in the samples should be transferred from the extractor to the collector according to a simple volume ratio, F_v. This F_v is the ratio of the pump volume to the total gas volume in the extractor plus the pump. It is the fraction of the sample gas volume (and moles) that is extracted to the collector at each pump stroke. The model predicts that the ratio of the extracted gas to the residual gas (for any given canister) should be equal to

$$\frac{n_{res}}{n_{ext}} = \frac{(1-F_v)^N}{1-(1-F_v)^N} \qquad (5.1)$$

where

n_{res} = the moles of residual gas in the extractor after extraction to a canister
n_{ext} = the moles of gas extracted to the canister
N = the number of pump strokes.

The model has been tested by comparing the amount of insoluble gas it predicts to remain after a canister is extracted to the amount of gas that is actually present. The amount that is present is considered to be equal to (actually it is greater than) the amount of gas extracted into the next canister. The test shows that there is consistently much more insoluble gas remaining after extraction than the model predicts. Table 5.4 shows the comparison for samples taken in 1997. (The same excess in residual gas seems to occur for 1996 samples, based on a spot check.)

The excess residual gas cannot be explained by air gas inleakage; the mole percent of O_2 is typically less than 0.1% in the extracted gas and less than 1% in the residual gas. This is too little air to make up the difference. In addition, the error bands on the insoluble gas are about ±15% of the central value or less, so they do not explain the excess residual gas either.

It appears that some of the gas in the extractor side is not fully accessible to pumping, effectively making the gas transfer fraction less than the simple pump/extractor side volume ratio given above as F_v. The cause of this inaccessibility is not known. It might be that the "insoluble" gas is substantially more soluble than believed and is dissolved in the waste liquid, or some of it is mechanically trapped as small bubbles in the waste, or poor mixing in the gas space leaves behind pockets of gas/vapor with higher than average insoluble gas concentrations.

The effect of this unexplained behavior on RGS concentration and inventory estimates can be estimated, for the insoluble gases. The gas that the model predicts to remain after the last canister is extracted (generally less than 5 μmol) can be scaled up by the ratio of actual to modeled residuals (less than 30, except for the high-leakage case) to calculate the amount by which the total gas in a sample is underestimated. The RGS underestimation of insoluble gas might be roughly 10%, judged by this approach.

Table 5.4. Comparison of Modeled and Measured Insoluble Gas Extraction

Sample and Canister	Insoluble gas extracted to the canister (μmol)	Number of pump strokes (N)	Gas transfer fraction (F_v)	Insoluble gas remaining as residual (μmol)	
				Modeled	Actual
U-103, 7-2, can. J2	4642	19	0.207	57	546
U-103, 7-7, can. J1	785	12	0.217	44	111
U-103, 7-8, can. J1	608	13	0.218	26	176
S-106, 7-3, can. J2	1187	21	0.217	7	88
S-106, 7-5, can. J2	1431	21	0.217	8	86
S-106, 8-6, can. J2	1044	20	0.218	8	109
S-106, 8-10, can. J2	2528	21	0.216	16	74
BY-109, 12C-4, can. J1	1004	22	0.212	5	465 (large leak)
BY-109, 10B-5, can. J1	1326	21	0.217	8	145
BY-109, 10B-6, can. J1	1892	21	0.215	12	128

The same unidentified process that slows the gas extraction might also affect the ammonia extraction. Until the physical process is identified, the amount of underestimation (or over-estimation) of the RGS ammonia concentrations cannot be calculated.

5.3 Water Vapor Pressures over the Waste

The algorithm for calculating the moles of condensed ammonia in the collector also calculates the moles of condensed water. Assuming that the water vapor pressure is constant during the extraction process, the moles of water transferred from extractor to collector per stroke are equal for each stroke, and the water vapor pressure in the extractor can be calculated using the ideal gas law. The water vapor pressures that were calculated in this way are given in Table 5.5. It can be seen that the assumption of constant water vapor pressure appears to hold, with a few exceptions.

One exception is the apparent sudden drop of vapor pressure in canister J3 of sample S-106-8-6. The variation may have something to do with the fact that this canister was pumped for only four strokes. However, canister J3 of sample S-106-8-10 was pumped for only three strokes and showed no such water vapor pressure drop. Another exception to the general rule of constancy is the apparent sudden increase of vapor pressure in canister J2 of segment 12C-4 from BY-109.

Table 5.5. Water Vapor Pressures for 1997 Samples at Room Temperature

Collection Canister	Calculated Water Vapor Pressure over Sample (atm)	Approximate Measured Water Vapor Pressure over Sample (atm)
U-103, 7-2, can. J2	0.022 ± 0.0024	
U-103, 7-2, can. J3	0.017 ± 0.0020	
U-103, 7-5, can. J2	0.022 ± 0.0024	
U-103, 7-7, can. J1	0.022 ± 0.0024	
U-103, 7-7, can. J2	0.024 ± 0.0026	
U-103, 7-8, can. J1	0.022 ± 0.0024	
U-103, 7-8, can. J2	0.023 ± 0.0025	
S-106, 7-3 can. J2	0.020 ± 0.0022	
S-106, 7-3 can. J3	0.018 ± 0.0020	
S-106, 7-5 can.J2	0.015 ± 0.0017	
S-106, 7-5 can. J3	0.014 ± 0.0016	
S-106, 8-6 can. J2	0.017 ± 0.0019	
S-106, 8-6 can. J3	0.0075 ± 0.0008	
S-106, 8-10 can. J2	0.011 ± 0.0013	
S-106, 8-10 can. J3	0.012 ± 0.0013	
BY-109, 12C-4 can. J1	0.020 ± 0.0022	0.0086
BY-109, 12C-4 can. J2	0.026 ± 0.0033	0.030
BY-109, 10B-5 can. J1	0.019 ± 0.0021	
BY-109, 10B-5 can. J2	0.017 ± 0.0021	
BY-109, 10B-6 can. J1	0.020 ± 0.0022	
BY-109, 10B-6 can. J2	0.021 ± 0.0024	

For sample 12C-4 of BY-109, mass spectrometry was used to make rough estimates of the amount of water in some of the unpumped sample canisters. These estimates, together with the known extractor pressure at the time the canister was taken, appear in Table 5.5 as approximate measured values of the sample water vapor pressure under laboratory conditions. The predicted and measured values match for J2 but not for J1.

The water vapor pressures calculated from RGS data (Table 5.5) can be compared with water vapor pressures that were measured over waste simulants by Norton and Pederson (1994). The portion of the simulant data set that was in the room-temperature range of RGS extraction is given in Table 5.6. (Note that the simulants with 40 wt% water contained some solids, while the others were solutions.) A comparison of Tables 5.5 and 5.6 shows that, in general, the RGS

Table 5.6. Water Vapor Pressures over Simulants at Room Temperature (Norton and Pederson 1994)

Temperature (°C)	Water (wt%)	NH_3 concentration (mol NH_3/kg water)	Water vapor pressure (atm)
21.1	100	0.00	0.025
21.1	95.3	2.93	0.023
26.5	39.6	0.00	0.015
26.7	100	0.00	0.035
26.7	95.3	2.93	0.033
26.7	66.6	0.00	0.026
27.3	64.0	3.53	0.026
27.3	39.0	2.30	0.013
27.3	38.7	3.30	0.013
27.6	66.0	0.86	0.027
27.7	65.5	1.52	0.027
28.0	65.0	2.23	0.026
29.3	39.3	1.27	0.015

water vapor pressures are consistent with those found for simulants in the temperature range of 25 ± 3°C (the range found in RGS extractions) that contain 30–50 wt% water. This is a reasonable estimate of water content for typical wastes.

Based on this comparison of RGS results and simulant data, we believe that the RGS water vapor pressure is within ±30% of the true value, with no identifiable bias toward overestimation or underestimation. It seems likely that the assumptions the physical model of extraction makes about water—complete equilibrium between sample water and water vapor, and constant water vapor pressure throughout extraction—are not sources of substantial error in data interpretation.

5.4 Ammonia

The physical model that was used to interpret the RGS extraction data to find the in-situ ammonia concentrations in the samples contained assumptions that were discussed in Section 3 (particularly Section 3.7.1) and that should be tested against the observations. The assumptions that had the most potential effect on calculating the ammonia concentration in the sample were

- complete sample recovery
- ammonia in the collector condensate is accounted for
- equilibrium between ammonia vapor and dissolved ammonia
- no significant sorption of ammonia on system surfaces.

Sample recovery appears, based on the x-ray images discussed in Section 4, to have been 95% or better, so that the quantity of ammonia in the waste would be underestimated by 5% or less as a result of this assumption alone.

The condensed ammonia calculation method (Section 5.4.1) has not yet been compared with experimental data for standard samples. However, because it was derived from standard ammonia and water vapor pressure data and predicted vapor pressures within ±7% of those data, this part of the model is not expected to contribute a significant bias to the ammonia concentration results.

Sections 5.4.2 and 5.4.3 review the residual ammonia determination method(s) and the ammonia equilibration rate, respectively. Two methods for finding the residual NH_3 (that which is left in the extractor after extraction) were employed: mass balance and isotopic ammonia ($^{15}NH_3$) addition. Both assumed complete equilibration but depended on different measurements; thus if they had given comparable results, it would have been a good indication that equilibrium had been reached. The two methods did not give comparable results, even after equilibration times of five days, and did not appear to show increasing convergence on a value with increasing equilibration time. Incomplete equilibrium would be expected to cause an underestimation of the amount of ammonia. Because the residual ammonia calculated by the isotopic method is usually greater than that from the mass balance (Table 5.8), it is not clear whether the isotopic method causes an underestimation of ammonia or how great the bias is.

The isotopic method has not only provided a direct indication that ammonia equilibrium is incomplete during RGS extraction, it has demonstrated that ammonia sorption on surfaces plays a part in system behavior. As discussed in Section 5.4.4, $^{15}NH_3$ apparently attaches strongly to surfaces and can remain in the extraction system from one sample to the next. This holdover could cause either overestimation or underestimation of the sample ammonia, probably within a 10% limit.

The overall bias produced by the major assumptions in the ammonia model is primarily underestimation, caused by incomplete equilibrium between ammonia vapor and dissolved ammonia. This underestimation cannot be quantified because of the unavailability of supporting data, such as solution-chemistry analyses of extractor vapor grab samples and post-extraction chemical analyses of the residual ammonia.

5.4.1 Condensed Ammonia Determination

Tanks U-103, S-106, and BY-109 were the first tanks for which the ammonia dissolved in condensed water in the extraction canisters (J canisters) was calculated and included in the results. In the five tanks tested previously, ammonia was underestimated because the ammonia that was extracted and pumped into the collection canisters was treated as though it, and all the ammonia present, was vapor. In fact, the partial pressures of ammonia and water were probably low enough that ammonia and water could have condensed in those canisters that were pumped.

The amount of condensed ammonia and water in each collection canister was found by comparing the actual collector pressure with what would have been measured if none of the gas/vapor transferred from the extractor had condensed. (The transferred gas and vapor were calculated from the known extractor pressures.) The actual collector pressure was lower by an amount proportional to the number of moles that condensed. This condensation ratio, combined with known solution equilibria for ammonia/water mixtures, allowed the partial pressures of ammonia and water in the system to be found, along with the moles of ammonia and water in the condensed phase.

Table 5.7 shows, for each pumped pre-isotopic-addition 1997 sample canister, the fraction of the total collected ammonia that was present in the vapor phase. Because these fractions are typically between 0.4 and 0.5, using the previous ammonia calculation method would have underestimated the ammonia in these tanks by more than a factor of 2. The condensed ammonia ratios are so consistent for the 1997 samples, in spite of the widely varying ammonia contents in the three tanks, that it seems likely the five tanks sampled in 1996 would have had similar ratios. Hence, the extracted ammonia (as distinct from the residual ammonia) in the 1996 samples could probably be multiplied by a factor of 2 to obtain a reasonable estimate of the true extracted ammonia.

5.4.2 Residual Ammonia Determination

For one sample from U-103 (sample 7-2) and all samples from S-106 and BY-109, the residual ammonia was calculated using an injection of an isotopically labeled standard (^{15}N-labeled ammonia). For test purposes, isotopic standards were also injected during the extraction of BY-101 samples, though these samplers were found to contain no waste.

In the isotopic method of residual ammonia determination, a known quantity of ammonia vapor labeled with ^{15}N was injected into the extractor side headspace and allowed some time (Table 5.8) to approach equilibrium with the residual ^{14}N ammonia in the waste sample. Vapor and gas were then pumped from the sample to the collector canister; a mass spectrometry analysis on the collected gas/vapor gave the ratio of ^{14}N to ^{15}N ammonia. The residual ammonia in the extractor (that which is present after the last pre-isotopic canister is collected and before the standard is added) can therefore be found, as discussed in Section 3. The ammonia that was in the

Table 5.7. Fraction of Collected Ammonia Present as Vapor in Gases Extracted from 1997 Samples

Collection Canister	Ratio of Ammonia Vapor to Total Ammonia
U-103, 7-2, can. J2	0.58
U-103, 7-5, can. J2	0.36
U-103, 7-7, can. J1	0.48
U-103, 7-7, can. J2	0.36
U-103, 7-8, can. J1	0.47
U-103, 7-8, can. J2	0.72
S-106, 7-3, can. J2	0.54
S-106, 7-5, can. J2	0.56
S-106, 8-6, can. J2	0.61
S-106, 8-10, can. J2	0.69
BY-109, 12C-4, can. J1	0.50
BY-109, 10B-5, can. J1	0.49
BY-109, 10B-6, can. J1	0.52

extractor before the last pre-isotopic canister was collected is found as the sum of the extracted canister ammonia and the residual ammonia. With the ammonia content and the number of pump strokes known, the Henry's Law constant can be determined.

The mass balance method (described in more detail in Section 3) is based on the fact that all of the samples had two pumped canisters (J1 taken before labeled standard injection, and J2 after). To find the pre-extraction ammonia in the sample and the Henry's Law constant, the moles of ammonia in the collector must be known at the beginning and end of the extraction. The amount of ammonia added to the collector by pumping can be related to both the initial sample content of ammonia and the Henry's Law Constant. With data points from two independent pumped canisters, it is possible to solve for the two unknowns (the initial, or total, sample ammonia and the Henry's Law constant). The sample ammonia content obtained by this mass balance method is shown in Table 5.8. The Henry's Law constants that were obtained by the isotopic method are given in Table 5.9.

The results that were obtained with the labeled standard were cross-checked against those obtained with mass balance methods. Table 5.8 shows the moles of residual ammonia that were calculated for each sample by each method. The samples are arranged in order of increasing equilibration time. For the sample with the longest equilibration time, the mass-balance method gives residual ammonia that is about four times that found isotopically. In all other cases, the mass-balance method gives residual ammonia that is half or less of that found isotopically. It was not possible to solve the mass-balance equations for samples 7-2 of U-103 and 10B-5 of BY-109.

For sample BY-109-10B-5, less ammonia was contained in the post-isotopic canister than in the pre-isotopic canister, even though the addition of the isotopic standard should have provided more ammonia to the post-isotopic canister. This internal inconsistency prevented the mass balance equations from converging on an answer; the reason for the anomaly is not known but seems to be related to low collector pressure. An opposite anomaly appeared for sample U-103-7-2: substantially more ammonia was removed in the post-isotopic canister than was

Table 5.8. Moles of Residual Ammonia in Each 1997 Sample Calculated from Isotopic Ratios Versus Ammonia Mass Balances

Sample	Residual NH_3 in the sample (μmol)		Delay Time Before Pumping (hours)
	Isotopic	Mass balance	
U-103, 7-2	487	not solvable	0.1
S-106, 8-6	361	2.5	0.1
S-106, 8-10	306	4.1	0.17
S-106, 7-3	241	17	1.2
S-106, 7-5	1254	722	2
BY-109, 10B-6	1285	523	21.5
BY-109, 10B-5	3322	not solvable	91
BY-109, 12C-4	2488	11380	139

Table 5.9. Room-Temperature Henry's Law Constants for 1997 Samples

Sample	Henry's Law Constant for Ammonia		
	(mol/L gasless waste/atm)	(mol/kg water/atm)	
	Experimental (isotopic method)	Experimental (isotopic method)	Theoretical (Schumpe model)
U-103, 7-2	5.4	14	5.9
S-106, 8-6	4.9	14	5.3
S-106, 8-10	2.8	8.4	5.6
S-106, 7-3	8.9	12	5.0
S-106, 7-5	4.4	13	5.3
BY-109, 10B-6	5.6	13	5.8
BY-109, 10B-5	9.2	21	6.3
BY-109, 12C-4	18	41	5.7

consistent with the amount of isotopic ammonia added and the removal in the pre-isotopic canister. The reason for this discrepancy is also unknown. (See Sections 5.4.3 and 5.4.4 for descriptions of other observations that indicate unexpected difficulties in applying the isotopic method.)

No clear conclusions can be drawn about why the mass balance and isotopic methods do not provide comparable results; the reasons could lie in errors and sensitivities in either method, or both. The mass-balance method depends on pressure and composition measurements and on the calculated condensed ammonia, and could be sensitive to errors in any of these (a notorious trait of mass balances). The method, in some cases, makes use of small differences between large numbers and can amplify small data changes into large differences in calculated residual ammonia. For the isotopic method, errors may result from ammonia holdover from previous extractions, as well as slow mixing within the RGS system gas volume, as suggested by the observations reviewed in Sections 5.4.4 and 5.2.3. Slow equilibration of ammonia vapor with dissolved ammonia would affect both methods, though not necessarily to the same extent.

5.4.3 Ammonia Standard Equilibration Rate

One of the most basic questions about the isotopic-standard method is whether the injected isotopic ammonia has had enough time to equilibrate with the ammonia in the sample before the ratio of isotopic to native ammonia is measured. If equilibrium has not been reached, the ratio will be too high and the residual ammonia will be underestimated. The time constant for equilibration is unknown.

The response of the extractor-side pressure to the injection of the standard gives some clue about the time constant for equilibration of injected ammonia with the waste in segment 7-2 of U-103. The pressure just before the isotopic ammonia is injected is 2.678 kPa; upon injection, the pressure jumps (within 0.2 minute) to 3.976 kPa, an increase of 1.298 kPa. The pressure then gradually drops off for the next 8 minutes as the excess injected ammonia vapor is absorbed by the

waste. (After 8 minutes, the extraction was carried out and lasted until about 45 minutes after the standard injection. The mixer in the extractor turns at 3 rpm, and would have completed 24 turns over the initial 8-minute period.)

The decrease in the post-injection pressure P_I follows a curve that can be modeled with a relative error of less than 5% by an exponential function:

$P_I = 3.698 + (3.976 - 3.698) \exp(-20.4 \Delta t)$ kPa, where the elapsed time, Δt, is in hours.

According to this correlation, the half-time for pressure equilibration is about 0.065 hour, or 3.9 minutes. It should be noted, however, that the pressure response shows a much more rapid decrease than an exponential function can match, probably meaning that the exponential is not a physically appropriate correlation function.

It is possible to use the pressure response to cross-check the isotopic ratio to find out whether the two isotopes of ammonia have reached equilibrium. If the Henry's Law constant that was estimated from pressure data alone after 8 minutes of approach to equilibrium is equal to the constant estimated from the isotopic ratio, which depends on ammonia extracted over a period of 8 to 45 minutes of equilibration, it is likely that equilibrium had already been reached by 8 minutes. (Or else equilibrium takes so long that 8 and 45 minutes are both relatively short and show the same trivial degree of equilibration.) If the two constants are not equal, there is reason to suspect that equilibration was not complete.

The Henry's Law constant that was calculated from the isotopic ratio is given in Table 5.8 as 5.4 mol/L waste atm. The pressure-based Henry's Law constant is calculated as follows: the addition of 1115 µmol of isotopically labeled NH_3 raised the extractor-side pressure by 1.298 kPa; the subsequent absorption and dissolution of ammonia decreased the pressure by (3.976–3.698) or 0.278 kPa. This must correspond to ammonia absorption of

$(0.278/1.298)\cdot(1115) = 239$ µmol of injected ammonia absorbed.

The Henry's Law constant can be calculated from the observed pressures and the known moles of injected and absorbed ammonia:

$K_{HA} = (239/[1115 - 239]) (V_v/V_L)/RT$
$K_{HA} =$ 0.16 mol/atm L waste for ammonia, based on the pressure response at 8 minutes after injection.

where

K_{HA} = Henry's Law constant of ammonia at 8 minutes (mol/L waste atm)
R = 0.08205 atm L/mol K
T = a temperature of 297 K in the extractor
V_L = the volume of gas-free waste, 154 cc
V_v = the gas volume of the extractor side, 2222 cc (including the extractor vessel, second volume, lines, pump, and standard injection canister volume)

The pressure-based Henry's Law constant is much smaller than the isotopic value for sample U-103-7-2, an observation which suggests that equilibration was far from complete at 8 minutes (and may still have been incomplete at 45 minutes). This interpretation is consistent with the short half-time (3.9 minutes) and the rapid decline of the pressure response, if the initial 8-minute pressure equilibration involved only part of the waste. If so, the $^{15}NH_3$ was absorbed by an outer shell of the waste over 8 minutes, bringing a pressure equilibrium whose timing depended

largely on the mass-transfer rate at the surface of the sample. If that was the case, full equilibration depended on ammonia diffusion within the waste and had not occurred within the 8-minute period.

5.4.4 Ammonia Holdover

One set of difficulties with the isotopic method became apparent midway through the 1997 RGS program because more extensive mass spectrometry analyses were carried out for BY-101 and BY-109 samples than for the earlier tanks. The supplemental data indicate that ammonia (isotopic or normal) may be held over in the system, or in standard canisters or gas-collection canisters. This increases the error in isotopic ammonia determinations.

In one case, the isotopic standard that was used for sample BY-101-10B-3 was found to contain ammonia that was 6.4% $^{14}NH_3$, when there should have been no $^{14}NH_3$ present. This observation suggests that normal ammonia had been held over in the canister containing the standard. (It should be noted that this high level of contamination was not seen in other standards.)

For tanks sampled before BY-101, the $^{15}NH_3/^{14}NH_3$ ratio was measured only for canisters that were taken after standard addition. For BY-101 and BY-109, the $^{15}NH_3/^{14}NH_3$ ratio was measured for gas that was collected from some of the samples *before* any isotopic standard was added to the system. In sample BY-109-12C-4, the ratio was found to be 0.092 for the contents of an unpumped canister; it was 0.052 for the contents of the immediately subsequent pumped canister. It should have been zero in both cases if there was no holdover of $^{15}NH_3$ from earlier extractions.

The records do not show whether the canisters that were used to collect gas from sample BY-109-12C-4 had been used as standard addition canisters for prior tests. Thus holdover in the canisters is a possibility that cannot be verified or ruled out. Another possibility is holdover in the RGS system. Whatever the explanation, no holdover $^{15}NH_3$ appeared in the gas extracted from BY-109 samples 10B-5 and 10B-6, which were processed after 12C-4.

The absolute amount of ammonia holdover may not be large. The $^{15}NH_3$ found in the BY-109-12C-4 pumped canister was about 15 μmol. If this was local (collector-side) contamination, it is of the right order of magnitude to represent ammonia that had been sorbed on the walls of the lines and canisters. (As noted in Section 3.7.1, the sorption in the whole system has been roughly estimated at 50 μmol NH_3.) However, the exact source of the contamination can only be speculated on at this time.

Another possible indication of ammonia holdover was found by analyzing the contents of the standard addition canisters after they had been open to the extractor for some time. The $^{15}NH_3/^{14}NH_3$ ratio in these canisters would have been the same as that in the pumped gas-collection canisters that were taken after the delay period, if the standard had equilibrated with the sample and if the vapor/gas in the standard canister had fully mixed with that in the rest of the extractor side. Table 5.10 shows these ratios, which were equal (within experimental error) in BY-109 sample 12C-4 but were decidedly unequal for sample 10B-6 (with its shorter time for equilibration and mixing). The isotopic ammonia added to 10B-6 apparently lingered disproportionately in its original canister.

Table 5.10. Isotopic Ammonia Ratios in Standard-Addition and Pumped Canisters for 1997 Samples

Sample	$^{15}NH_3/^{14}NH_3$ Ratio		Delay time before pumping (hr)
	Standard-addition canister	Post-addition pumped canister	
Segment 12C-4	0.62	0.77–0.81	139
Segment 10B-6	3.2	0.86–0.89	21.5

The observations suggest that there are some obstacles to achieving the ammonia mixing and equilibration that is necessary to obtain good results from the isotopic method. Isotopic holdover, probably resulting from ammonia binding to system and canister walls, could lead to an underestimation of the ammonia inventory. Based on the ^{15}N holdover ratio for 12C-4, the underestimation is probably less than 10%. On the other hand, the ammonia inventory can be overestimated as a result of the slow mixing of the standard addition canister contents with the extractor vapor (as indicated by the 10B-6 data in Table 5.10). When mixing is slow the sample is exposed to only part of the isotopic ammonia, though the calculations assume exposure to (and equilibration with) all of it. The overestimation of the inventory that results from slow mixing could be larger than the underestimation from ammonia holdover but is difficult to quantify.

6.0 Conclusions and Recommendations

The quantitative results obtained from the RGS for SSTs U-103, S-106, and BY-109 are summarized in Table 6.1. The results support the following conclusions, with evidence from various sources discussed throughout the report:

- When integrated, the local RGS measurements of gas volume fraction in Tank S-106 gave a significantly lower (and those in Tank U-103 a significantly higher) gas inventory than did the BPE method. Two of the tanks sampled in 1996, AW-101 and AN-103, also had RGS-predicted inventories that were lower than those calculated by the BPE method. (However, the RGS and BPE inventories were closely comparable for AN-105 and AN-104.) In general, the tanks whose core profiles show more variation between risers are those whose BPE and RGS inventories are most different. It appears that RGS measurements, which are based on a small number of local samples, must be supplemented with overall tank inventory information (such as barometric pressure response and surface level rise) to estimate gas inventories in high waste-variability tanks.

- The results from the SSTs sampled in 1997 showed that more than 20 vol% of the free gas in the high-solids layer was nitrogen (N_2). The free gases retained in SST wastes can have substantial nonflammable components; this is consistent with findings for the DSTs sampled in 1996.

- Nitrous oxide mole fractions in the SSTs sampled in 1997 ranged from 8% in S-106 to approximately 52% in U-103. Nitrous oxide was calculated to compose less than 1% of the gases in solution.

Table 6.1. Summary of the Retained Gas Sampler Results for 1997

	U-103	S-106 High-Solids Layer		BY-109 Interstitial Liquid Layer
Maximum in-situ gas volume fraction	0.44 ± 0.04 (4 samples, 1 riser)	0.14 ± 0.01 (4 samples, 2 risers)	BY-101 RGS samples were compromised by air inleakage. No RGS results are available for this tank.	0.12 ± 0.01 (3 samples, 2 risers)
Average mole fraction H_2 in free gas	0.22 ± 0.047	0.63 ± 0.063		0.50 ± 0.049
Average mole fraction N_2O in free gas	0.40 ± 0.085	0.11 ± 0.012		0.18 ± 0.018
Average mole fraction N_2 in free gas	0.36 ± 0.076	0.24 ± 0.030		0.29 ± 0.038
Average mole fraction NH_3 in free gas	0.012 ± 0.012	0.0014 ± 0.0002		0.0041 ± 0.0009
Best Estimate Gas Volume (STP m^3)	260 ± 70 (BPE method)	580 ± 190 (BPE method)		140 ± 70 (RGS data)

- Tank U-103 had a very high gas volume fraction (44 vol%) in the topmost core segment that was sampled. This segment was located in a layer of the tank where there also was a high liquid content. Evidence from sample x-rays and the dome space flammable gas measurements during sampling confirmed the high gas fraction and suggested the gas was easily releasable.

- The composition of retained gases in the four SSTs sampled to date (including Tank A-101 from 1996) shows considerable diversity. Tank A-101 contained higher hydrogen mole fractions and ammonia concentrations than any other tank to date. U-103 contained the highest nitrous oxide mole fractions. S-106 had the lowest ammonia concentrations, so low as to be difficult to measure, but its insoluble gas composition was about the same as the compositions of BY-109 and the nonconvective layers of AN-105 and AN-103. No single trend in SST gas retention is immediately apparent.

- RGS measurements showed a significant gas inventory retained below the ILL in Tank BY-109, which was salt-well pumped in 1996.

- Based on RGS calculations, ammonia constitutes more than 99% of the gases in solution. A very small fraction of the total ammonia exists in the form of vapor (gas phase) in the tanks sampled, as in the tanks sampled in 1996.

- The 1997 RGS extraction procedure was changed to include isotopically labeled ammonia ($^{15}NH_3$) to determine the residual sample ammonia (that remaining after gas extraction). The method has not provided the anticipated improvement in ammonia estimation, because of slow ammonia equilibration and mixing and apparent holdover of isotopic ammonia (perhaps sorbed on the system surfaces) from one sample to the next.

- An algorithm has been used to calculate the ammonia that is dissolved in the condensed water in the RGS collection canisters. The dissolved ammonia has consistently been calculated to be about equal to, or somewhat greater than, the ammonia in the vapor phase (which was the only part of the ammonia recognized by the method used in prior work). The new algorithm has removed the factor of 2 to 3 underestimation of extracted ammonia that was known to be present in ammonia estimates made for the tanks sampled in 1996. Some degree of underestimation remains because of the slow equilibration of dissolved ammonia with ammonia vapor under RGS extractor conditions.

- The failure of RGS sampler valves to close led to the loss of samples in FY 1997 as in FY 1996. In addition, waste impenetrability often prevented sample acquisition. Both problems contributed to the failure to obtain BY-101 RGS samples.

- The 1997 sample x-rays were of limited usefulness for density calculation because of variations in exposure and the fact that the necessary air/water standard density profiles were lacking for several samples. The sample densities estimated from the x-rays were generally equal to or less than the densities obtained for adjacent samples by laboratory analysis, in part because the x-ray densities were lowered by gas bubbles in the bulk waste. However, the x-rays gave useful information about the bubble structure in the waste and the volume of waste in the sampler.

- The performance of the RGS continued to be acceptable for measurement of the composition of retained low solubility gases.

The following recommendations are made for future RGS sampling and extraction:

- An in-line mass spectrometer is available for connection to the RGS system and has undergone preliminary testing. We recommend that this equipment undergo complete testing to establish that it does not cause unacceptable errors in the sample composition or gas content and that it measures compositions accurately. If it is proven to be effective, the in-line mass spectrometer should be used to track extractor-side or collector-side compositions. This would help confirm (or disprove) several model assumptions, including complete gas-phase mixing, constancy of gas composition, and ammonia equilibrium.
- Redundant data are needed to support NH_3 analysis. We recommend that after extraction the waste samples be chemically analyzed for ammonia, as a way of cross-checking the RGS estimate of residual ammonia.

7.0 References

7.1 Cited References

AIChE. 1984. *Perry's Chemical Engineers' Handbook*, 6th Ed. Edited by RH Perry, DW Green, and JO Maloney, American Institute of Chemical Engineers. McGraw-Hill Book Company, New York.

Brevick CH. 1994. *Supporting Document for the Historical Tank Content Estimate for U Tank Farm.* WHC-SD-WM-ER-325 Rev. 0, ICF Kaiser Hanford Company, Richland, Washington.

Cannon NS and RC Knight. November 1995. *Retained Gas Sampler System Acceptance Test Report.* WHC-SD-WM-ATR-137 Rev 0, Westinghouse Hanford Company, Richland, Washington.

Cannon NS. 1996. *Retained Gas Sampler System Acceptance Test Report.* WHC-SD-WM-ATR-137 Rev. 1, Westinghouse Hanford Company, Richland, Washington.

Cannon NS. March 1997. *Retained Gas Sampler Interface Volume.* HNF-SD-WM-CN-092, SGN Eurisys Services Corporation, Richland, Washington.

Consort SD, KL Ewer, JW Funk, RG Hale, GA Lisle, and CV Salois. 1996. *Historical Tank Content Estimate for the Northeast Quadrant of the Hanford 200 East Area.* WHC-SD-WM-ER-349 Rev. 1, Westinghouse Hanford Company, Richland, Washington.

Hodgson KM, RP Anantatmula, SA Barker, KD Fowler, JD Hopkins, JA Lechelt, DA Reynolds, DC Hedengren, RE Stout, and RT Winward. 1996. *Evaluation of Hanford Tanks for Trapped Gas.* WHC-SD-WM-ER-526 Rev. 1, Westinghouse Hanford Company, Richland, Washington.

Holman JP. 1978. *Experimental Methods for Engineers.* McGraw-Hill, New York.

Homi CS. August 1995. *Tank 241-S-106 Tank Characterization Plan.* WHC-SD-WM-TP-389 Rev. 0, Westinghouse Hanford Company, Richland, Washington.

Mahoney LA and DS Trent. 1995. *Correlation Models for Waste Tank Sludges and Slurries.* PNL-10695, Pacific Northwest Laboratory, Richland, Washington.

Meyer PA, ME Brewster, SA Bryan, G Chen, LR Pederson, CW Stewart, and G Terrones. 1997. *Gas Retention and Release Behavior in Hanford Double Shell Waste Tanks.* PNNL-11536 Rev. 1, Pacific Northwest National Laboratory, Richland, Washington.

Norton JD and LR Pederson. 1994. *Ammonia in Simulated Hanford Double-Shell Tank Wastes: Solubility and Effects on Surface Tension.* PNL-10173, Pacific Northwest Laboratory, Richland, Washington.

Norton JD and LR Pederson. 1995. *Solubilities of Gases in Simulated Tank 241-SY-101 Wastes.* PNL-10785, Pacific Northwest Laboratory, Richland, Washington.

Prausnitz JM, RN Lichtenthaler, and EG de Azevedo. 1986. *Molecular Thermodynamics of Fluid-Phase Equilibria, 2nd Ed.* Prentice-Hall, Inc., Englewood Cliffs, New Jersey.

Reid RC, JM Prausnitz, and BE Poling. 1987. *The Properties of Gases and Liquids, 4th Ed.* McGraw-Hill, New York.

Remund KM, CM Anderson, and BC Simpson. 1995. *Hanford Single-Shell Tank Grouping Study.* PNL-10749, Pacific Northwest National Laboratory, Richland, Washington.

Shekarriz A. 1994. *Retained Gas Sampler Flow Visualization Guide.* PNL-10138, Pacific Northwest Laboratory, Richland, Washington.

Shekarriz A, DR Rector, LA Mahoney, MA Chieda, JM Bates, RE Bauer, NS Cannon, BE Hey, CG Linschooten, FJ Reitz, and ER Siciliano. 1997. *Composition and Quantities of Retained Gas Measured in Hanford Waste Tanks 241-AW-101, A-101, AN-105, AN-104, and AN-103.* PNNL-11450 Rev. 1, Pacific Northwest National Laboratory, Richland, Washington.

Stewart CW, JM Alzheimer, ME Brewster, G Chen, RE Mendoza, HC Reid, CL Shepard, and G Terrones. 1996a. *In Situ Rheology and Gas Volume in Hanford Double-Shell Waste Tanks.* PNL-11296, Pacific Northwest Laboratory, Richland, Washington.

Stewart CW, ME Brewster, PA Gauglitz, LA Mahoney, PA Meyer, KP Recknagle, and HC Reid. 1996b. *Gas Retention and Release Behavior in Hanford Single-Shell Waste Tanks.* PNNL-11391, Pacific Northwest National Laboratory, Richland, Washington.

Tran TT. 1993. *Thermocouple Status: Single Shell and Double Shell Waste Tanks.* WHC-SD-WM-TI-553 Rev. 0, Westinghouse Hanford Company, Richland, Washington.

Webb BJ. 1994. *Summary Report on the Design of the Retained Gas Sampler System.* WHC-SO-WM-ER-387, Westinghouse Hanford Company, Richland, Washington.

WHC. 1994. *Historical Tank Content Estimate for the Southwest Quadrant of the Hanford 200 West Area.* WHC-SD-WM-ER-352 Rev. 0, Westinghouse Hanford Company, Richland, Washington.

Whitney PD, PA Meyer, NE Wilkins, F Gao, and AG Wood. 1996. *Flammable Gas Data Evaluation Progress Report.* PNNL-11373, Pacific Northwest National Laboratory, Richland, Washington.

Wilkins NE and RE Bauer. 1996. *Test Evaluation of Industrial Hygiene Hand Held Combustible Gas Monitor.* WHC-SD-WM-TRP-256 Rev. 0, Westinghouse Hanford Company, Richland, Washington.

7.2 Bibliography

Schumpe A. 1993. *The Estimation of Gas Solubilities in Salt Solutions.* Chem. Eng. Sci., Vol. 48, p. 153.

Weisenberger S and A Schumpe. 1996. *Estimation of Gas Solubilities in Salt Solutions at Temperatures from 273 K to 363 K.* AIChE J., 42(1):298-300.

Appendix A

RGS Extraction Procedures

Appendix A

RGS Extraction Procedures

During 1997, new experimental methods were explored to improve the measurement of the ammonia content of retained gas sampler (RGS) samples. This exploration necessarily led to procedural changes, which varied enough to require procedural documentation on a sample-by-sample basis. (Note that the system volumes and the procedures that were followed for 1996 RGS samples were different and cannot be safely inferred from 1997 information.) Schematics of the RGS system can be found in Appendix A of Shekarriz et al. (1997).

The laboratory procedure document under which extractions were carried out was Hey (1997). The procedure was revised during 1997; Table A.1 gives the procedure revision that was used for each sample.

A.1 U-103 Sample 7-2

1) Evacuate and leak-check the entire system. Close off the collector side from the extractor side (valve B) and close off the second volume vessel from the extractor vessel and lines (valve R). Close off the second and third J canisters from the collector manifold (valves H2 and H3). Valve the mercury pump (using valve G) so that it is not connected to either the collector or extractor side. Extractor- and collector-side pressures are zero.

Table A.1. Procedures Used for 1997 Extractions

Sample	Procedure Revision
U-103, 7-2	F-0
U-103, 7-5	F-0
U-103, 7-7	F-0
U-103, 7-8	F-0
U-103, 13-4	G-0
S-106, 8-6	G-0
S-106, 8-10	G-0
S-106, 7-3	G-0
S-106, 7-5	G-0
BY-109, 12C-4	H-0
BY-109, 10B-5	H-0
BY-109, 10B-6	H-0

2) Extrude the sample into the extractor vessel (a tare volume of 1290 cc, when the sampler piston is completely closed). At this time the lines of the extractor side of the system are open to the extractor, making an additional volume of 284.5 cc available to the sample gas/vapor. The PQ canister port on the extractor vessel is valved closed, so no volume is contributed by that canister. The extractor-side pressure rises sharply.

3) Open valve R, which opens the second-volume vessel to the extractor vessel and lines. This adds 321.5 cc of volume to that occupied by sample gas/vapor. An additional 51.7 cc of volume is contributed by the PQ canister at a port on the second-volume vessel, which is valved open to the system at this time (valve Q9). The extractor-side pressure steps down.

4) Close valve Q9, taking a PQ grab sample of the gas/vapor in the second volume. No pressure change results.

5) Open valve B. This allows the gas/vapor to expand into the collector-side volume. The additional volume is 31.5 cc (collector manifold) plus 3 cc (volume between valves H1 and J1 in the canister line) plus 88.5 cc (the first J canister). The total volume open to the sample is now 2019 cc (if the volume taken up by the liquids and solids of the sample is ignored). The extractor-side pressure steps down, and the collector-side pressure rises to equal it.

6) Valve the collector side off from the extractor side. No pressure change results. The total volume open to the sample is now 1896 cc (neglecting the sample bulk volume).

7) Close valve J1. This collects the unpumped first J canister. No pressure change results.

8) Open valves H2 and J2. Step 7 has removed a volume of 88.5 cc (the first J canister) from the system and replaced it with 3 cc (volume between valves H2 and J2 in the canister line) plus 90.5 cc (the second J canister). The total volume open to the sample remains at 1896 cc (neglecting the sample bulk volume). The collector pressure steps down by more than half.

9) Use valve G to connect the open mercury pump to the extractor side. The following parts of the system are now connected to the sample: extractor vessel, extractor-side lines, second volume, and open pump (454 cc). The total volume open to the sample is now 2350 cc (neglecting the sample bulk volume). The extractor pressure steps down.

10) Open the collector side to the extractor side once more. The total volume open to the sample is now 2475 cc (neglecting the sample bulk volume). The extractor-side pressure steps down, and the collector-side pressure rises to equal it.

11) Valve the pump off from the extractor side and open it to the collector side. No pressure change results.

12) Close the Hg pump volume to zero, compressing the collector contents. This is the first stroke of the pump on the second J canister. The collector-side volume now consists of only the collector lines and the J canister; the sample is connected to the extractor vessel, lines, and second volume. The collector-side pressure rises sharply. Meanwhile, the extractor-side pressure is rising slightly as vapors leave the sample.

13) Disconnect the pump from both the collector and extractor (valve G). While opening the pump volume, reposition valve G to connect the pump to the extractor lines. The extractor-side pressure steps down, while no change results in the collector-side pressure.

14) Reposition valve G to connect the pump volume to the collector manifold instead of the extractor lines. The collector-side pressure drops sharply. Meanwhile, the extractor-side pressure is rising slightly.

15) Repeat steps 12 through 14 to give a total of 19 strokes.

16) Close valve H2. This collects the pumped second J canister. No pressure change results. The collector-side pressure is that of the peak pumped pressure from the last stroke. The extractor-side pressure is rising slightly.

17) Evacuate the collector side, including the third J canister, all the collector lines, and the pump. On the extractor side, the second volume, extractor lines, and extractor vessel remain open to the sample.

18) Attach the $^{15}NH_3$ standard canister at valve D (with valve C closed), then open valves C and D. The standard enters the extractor side, causing a rapid rise in extractor-side pressure. The extractor-side pressure then drops gradually as the injected ammonia vapor begins to reach equilibrium with the sample ammonia. The volume open to the sample (and the standard) is 1896 cc (neglecting the sample bulk volume and the volume of the standard canister).

19) Close valve D. No pressure change results.

20) Open valve B. This allows the gas/vapor to expand into the collector-side volume and the mercury pump (which is opened to its maximum volume at this time and connected to the collector side). The additional volume is 454 cc (fully open Hg pump) plus 31.5 cc (collector manifold) plus 3 cc (volume between valves H3 and J3 in the canister line) plus 93.3 cc (the third J canister). The total volume open to the sample is now 2478 cc (neglecting bulk sample volume). The extractor-side pressure steps down, and the collector-side pressure rises to equal it.

21) Valve the collector side off from the extractor side. No pressure change results. The total volume open to the sample is now 1896 cc (neglecting the sample bulk volume).

22) Repeat Steps 12 through 14 to pump the third (post-isotopic) canister for a total of 11 strokes.

23) Close valve H3. This collects the pumped third J canister. There is no pressure change. The collector-side pressure is that of the peak pumped pressure from the last stroke. The extractor-side pressure is rising slightly.

24) Carry out the bulk sample volume determination. Close off the collector side and pump from the extractor side. Close off the extractor vessel from the lines and second volume. Add an inert gas to the second volume, and note the pressure (the pressure is measured in the extractor lines, which are connected to the second volume). Open the extractor vessel to the lines and second volume, and note the new pressure. The ratio of pressures and the known tare system volumes allow the unknown bulk sample volume to be calculated.

A.2 U-103 Sample 7-5

1) Evacuate and leak-check the entire system. Close off the collector side from the extractor side (valve B) and close off the second volume vessel from the extractor vessel and lines (valve R). Close off the second and third J canisters from the collector manifold (valves H2 and H3). Valve the mercury pump (using valve G) so that it is not connected to either the collector or extractor side. Extractor- and collector-side pressures are zero.

2) Extrude the sample into the extractor vessel (a tare volume of 1290 cc, when the sampler piston is completely closed). At this time the lines of the extractor side of the system are open to the extractor, making an additional volume of 284.5 cc available to the sample gas/vapor. The PQ canister port on the extractor vessel is valved closed, so no volume is contributed by that canister. The extractor-side pressure rises sharply.

3) Open valve R, which opens the second-volume vessel to the extractor vessel and lines. This adds 321.5 cc of volume to that occupied by sample gas/vapor. The PQ canister was evacuated but is not valved into the system at this time. The extractor-side pressure steps down.

4) Close valve Q9, taking a PQ grab-sample of the gas/vapor in the second volume. No pressure change results.

5) Open valve B. This allows the gas/vapor to expand into the collector-side volume. The additional volume is 31.5 cc (collector manifold) plus 3 cc (volume between valves H1 and J1 in the canister line) plus 39.5 cc (the first J canister) plus 146.98 cc (a grab-sample canister at valve C). The total volume open to the sample is now 2117 cc (if the volume taken up by the liquids and solids of the sample is ignored). The extractor-side pressure steps down, and the collector-side pressure rises to equal it.

6) Valve the collector side off from the extractor side. No pressure change results. The total volume open to the sample is now 1896 cc (neglecting the sample bulk volume).

7) Close valves J1 and D. This collects the unpumped first J canister and the grab-sample canister. No pressure change results.

8) Open valves H2 and J2. Step 7 has removed a volume of 186.5 cc (the first J canister and the grab-sample canister) from the system and replaced it with 3 cc (volume between valves H2 and J2 in the canister line) plus 90.5 cc (the second J canister). The total volume open to the sample remains at 1896 cc (neglecting the sample bulk volume). The collector pressure steps down by more than 80%.

9) Open and then close valve Q9 to take a PQ-canister sample from a port on the second vessel. This temporarily adds 51.7 cc of volume to that available to the gas/vapor, and produces a small step down in extractor-side pressure.

10) Open the collector side to the extractor side once more. The pump is not connected to either side. The total volume open to the sample is now 2021 cc (neglecting the sample bulk volume). The extractor-side pressure steps down, and the collector-side pressure rises to equal it.

11) Use valve G to connect the open mercury pump to the collector side. The following parts of the system are now connected to the sample: extractor vessel, extractor-side lines, second volume, and open pump (454 cc). The total volume open to the sample is now 2475 cc (neglecting the sample bulk volume). The extractor and collector pressures both step down.

12) Valve the collector side off from the extractor side. No pressure change results.

13) Close the Hg pump volume to zero, compressing the collector contents. This is the first stroke of the pump on the second J canister. The collector-side volume now consists of only the collector lines and the J canister; the sample is connected to the extractor vessel, lines, and second volume. The collector-side pressure rises sharply. Meanwhile, the extractor-side pressure is rising slightly as vapors leave the sample.

14) Disconnect the pump from both the collector and extractor (valve G). While opening the pump volume, reposition valve G to connect the pump to the extractor lines. The extractor-side pressure steps down, while no change in the collector-side pressure results.

15) Reposition valve G to connect the pump volume to the collector manifold instead of the extractor lines. The collector-side pressure drops sharply. Meanwhile, the extractor-side pressure is rising slightly.

16) Repeat steps 13 through 15 to give a total of 20 strokes.

17) Close valve H2. This collects the pumped second J canister. No pressure change results. The collector-side pressure is that of the peak pumped pressure from the last stroke. The extractor-side pressure is rising slightly.

18) Carry out the bulk sample volume determination. Close off the collector side and pump from the extractor side. Close off the extractor vessel from the lines and second volume. Add an inert gas to the second volume, and note the pressure (the pressure is measured in the extractor lines, which are connected to the second volume). Open the extractor vessel to the lines and second volume, and note the new pressure. The ratio of pressures and the known tare system volumes allow the unknown bulk sample volume to be calculated.

A.3 U-103 Samples 7-7 and 7-8

1) Evacuate and leak-check the entire system. Close off the collector side from the extractor side (valve B) and close off the second volume vessel from the extractor vessel and lines (valve R). Close off the second and third J canisters from the collector manifold (valves H2 and H3). Valve the mercury pump (using valve G) so that it is not connected to either the collector or extractor side. Extractor- and collector-side pressures are zero.

2) Extrude the sample into the extractor vessel (a tare volume of 1290 cc, when the sampler piston is completely closed). At this time the lines of the extractor side of the system are open to the extractor, making an additional volume of 284.5 cc available to the sample gas/vapor. The PQ canister port on the extractor vessel is valved closed, so no volume is contributed by that canister. The extractor-side pressure rises sharply.

3) Open valve R, which opens the second-volume vessel to the extractor vessel and lines. This adds 321.5 cc of volume to that occupied by sample gas/vapor. An additional volume (52.2 cc for Segment 7, 52 cc for Segment 8) is contributed by the PQ canister attached at a port on the second-volume vessel; the canister is valved open to the system at this time (valve Q9). The extractor-side pressure steps down.

4) Close valve Q9, taking a PQ grab-sample of the gas/vapor in the second volume. No pressure change results.

5) Open valve B. This allows the gas/vapor to expand into the collector-side volume. The additional volume is 31.5 cc (collector manifold) plus 3 cc (volume between valves H1 and J1 in the canister line) plus the volume of the first J canister (40.5 cc for segment 7, 39.2 cc for segment 8). The extractor-side pressure steps down, and the collector-side pressure rises to equal it.

6) Open valve C, which connects a grab-sample canister (146.89 cc for Segment 7, 147.36 cc for segment 8). The extractor-side and collector-side pressures drop.

7) Close valve D. This collects the grab-sample canister. The total volume connected to the sample is now 1971 cc for segment 7, 1970 cc for segment 8. No pressure change results.

8) Use valve G to connect the open mercury pump to the collector side. The following parts of the system are now connected to the sample: extractor vessel, extractor-side lines, second volume, open pump (454 cc), collector lines, canister line, and first J canister. The total volume open to the sample is now 2425 cc for segment 7, 2424 cc for Segment 8 (neglecting the sample bulk volume). The extractor and collector pressures both step down.

9) Valve the collector side off from the extractor side. No pressure change results.

10) Close the Hg pump volume to zero, compressing the collector contents. This is the first stroke of the pump on the first J canister. The collector-side volume now consists of only the collector lines and the J canister; the sample is connected to the extractor vessel, lines, and second volume. The collector-side pressure rises sharply. Meanwhile, the extractor-side pressure is rising slightly as vapors leave the sample.

11) Disconnect the pump from both the collector and extractor (valve G). While opening the pump volume, reposition valve G to connect the pump to the extractor lines. The extractor-side pressure steps down, while no change in the collector-side pressure results.

12) Reposition valve G to connect the pump volume to the collector manifold instead of the extractor lines. The collector-side pressure drops sharply. Meanwhile, the extractor-side pressure is rising slightly.

13) Repeat steps 10 through 12 to give a total of 12 strokes (segment 7) or 13 strokes (segment 8).

14) Close valve J1. This collects the pumped first J canister. No pressure change results. The collector-side pressure is that of the peak pumped pressure from the last stroke. The extractor-side pressure is rising slightly.

15) Open valve H2 and turn valve G to connect the pump volume to the collector manifold. This step removes the volume of the first J canister from the system and replaces it with 3 cc (volume between valves H2 and J2 in the canister line) plus the volume of the second J canister (41.1 cc for segment 7, 146.98 cc for segment 8). The total volume open to the sample remains at 1896 cc (neglecting the sample bulk volume).

16) Repeat steps 10 through 12 to give a total of 20 strokes (segment 7) or 9 strokes (segment 8).

17) Close valve J2. This collects the pumped second J canister. No pressure change results. The collector-side pressure is that of the peak pumped pressure from the last stroke. The extractor-side pressure is rising slightly.

18) Carry out the bulk sample volume determination. Close off the collector side and pump from the extractor side. Close off the extractor vessel from the lines and second volume. Add an inert gas to the second volume, and note the pressure (the pressure is measured in the extractor lines, which are connected to the second volume). Open the extractor vessel to the lines and second volume, and note the new pressure. The ratio of pressures and the known tare system volumes allow the unknown bulk sample volume to be calculated.

A.4 S-106 Samples

All four S-106 RGS samples were handled by the same procedure. To simplify the procedure description, the canister volumes and the number of pump strokes for the various samples are not explicitly stated below; the values appropriate to each canister may be found in Appendix B.

1) Evacuate and leak-check the entire system. Close off the collector side from the extractor side (valve B) and close off the second volume vessel from the extractor vessel and lines (valve R). Close off the second and third J canisters from the collector manifold (valves H2 and H3). Valve the mercury pump (using valve G) so that it is connected to the collector side. Extractor- and collector-side pressures are zero.

2) Extrude the sample into the extractor vessel (a tare volume of 1290 cc, when the sampler piston is completely closed). At this time the lines of the extractor side of the system are open to the extractor, making an additional volume of 284.5 cc available to the sample gas/vapor. The PQ canister port on the extractor vessel is valved closed, so no volume is contributed by that canister. The extractor-side pressure rises sharply.

3) Open valve R, which opens the second-volume vessel to the extractor vessel and lines. This adds 321.5 cc of volume to that occupied by sample gas/vapor. The extractor-side pressure steps down.

4) Open valve B. This allows the gas/vapor to expand into the collector-side volume. The additional volume is 31.5 cc (collector manifold) plus 3 cc (volume between valves H1 and J1 in the canister line) plus the volume of the first J canister plus the volume of the grab canister at valve D plus 454 cc (the open pump). The extractor-side pressure steps down, and the collector-side pressure rises to equal it.

5) Valve the collector side off from the extractor side. No pressure change results. The total volume open to the sample is now 1896 cc (neglecting the sample bulk volume).

6) Close valve J1. This collects the unpumped first J canister. No pressure change results.

7) Open valves H2 and J2. Step 6 has removed the volume of the first J canister from the system and replaced it with 3 cc (volume between valves H2 and J2 in the canister line) plus the volume of the second J canister. The total volume open to the sample remains at 1896 cc (neglecting the sample bulk volume). The collector pressure steps down by more than half.

8) Close the Hg pump volume to zero, compressing the collector contents. This is the first stroke of the pump on the second J canister. The collector-side volume now consists of only the collector lines and the J canister; the sample is connected to the extractor vessel, lines, and second volume. The collector-side pressure rises sharply. Meanwhile, the extractor-side pressure is rising slightly as vapors leave the sample.

9) Disconnect the pump from both the collector and extractor (valve G). While opening the pump volume, reposition valve G to connect the pump to the extractor lines. The extractor-side pressure steps down, while there is no change in the collector-side pressure.

10) Reposition valve G to connect the pump volume to the collector manifold instead of the extractor lines. The collector-side pressure drops sharply. Meanwhile, the extractor-side pressure is rising slightly.

11) Repeat steps 8 through 10 to give the total number of strokes.

12) Close valve H2. This collects the pumped second J canister. No pressure change results. The collector-side pressure is that of the peak pumped pressure from the last stroke. The extractor-side pressure is rising slightly.

13) Evacuate the collector side (including the third J canister, all the collector lines, and the pump) and also the second volume vessel and lines, on the extractor side. On the extractor side, only the extractor vessel remains open to the sample.

14) Attach the $^{15}NH_3$ standard canister at valve D (with valve C closed), then open valves C and D. The standard enters the part of the extractor side that is not connected to the sample, causing a rapid rise in extractor-side pressure.

15) Open the extractor vessel to the rest of the extractor side, including the fully-open pump volume. The extractor-side pressure drops rapidly as a result of expansion, then gradually drops further as the injected ammonia vapor begins to reach equilibrium with the sample ammonia. The volume open to the sample (and the standard) is 2350 cc (neglecting the sample bulk volume and the volume of the standard canister). A delay of up to two hours is allowed at this point for equilibration.

16) Close valve D to disconnect the standard canister. No pressure change results.

17) Open valve B and then connect the pump to the collector side. This allows the gas/vapor to expand into the collector-side volume. The additional volume is 31.5 cc (collector manifold) plus 3 cc (volume between valves H3 and J3 in the canister line) plus the volume of the third J canister. The extractor-side pressure steps down slightly, and the collector-side pressure rises to equal it.

18) Valve the collector side off from the extractor side. No pressure change results. The total volume open to the sample is now 1896 cc (neglecting the sample bulk volume).

19) Repeat Steps 8 through 10 to pump the third (post-isotopic) canister for the total number of strokes.

20) Close valve H3. This collects the pumped third J canister. There is no pressure change. The collector-side pressure is that of the peak pumped pressure from the last stroke. The extractor-side pressure is rising slightly.

21) Carry out the bulk sample volume determination. Close off the collector side and pump from the extractor side. Close off the extractor vessel from the lines and second volume. Add an inert gas to the second volume, and note the pressure (the pressure is measured in the extractor lines, which are connected to the second volume). Open the extractor vessel to the lines and second volume, and note the new pressure. The ratio of pressures and the known tare system volumes allow the unknown bulk sample volume to be calculated.

A.5 BY-109 Sample 12C-4

1) Evacuate and leak-check the entire system. Close off the collector side from the extractor side (valve B) and close off the second volume vessel from the extractor vessel and lines (valve R). Close off the second and third J canisters from the collector manifold (valves H2 and H3). Valve the mercury pump (using valve G) so that it is connected to the collector side. Extractor- and collector-side pressures are zero.

2) Extrude the sample into the extractor vessel (a tare volume of 1290 cc, when the sampler piston is completely closed). At this time the lines of the extractor side of the system are open to the extractor, making an additional volume of 284.5 cc available to the sample gas/vapor. The PQ canister port on the extractor vessel is valved closed, so no volume is contributed by that canister. The extractor-side pressure rises sharply.

3) Open valve R, which opens the second-volume vessel to the extractor vessel and lines. This adds 321.5 cc of volume to that occupied by sample gas/vapor. The extractor-side pressure steps down.

4) Open valve B. This allows the gas/vapor to expand into the collector-side volume. The additional volume is 31.5 cc (collector manifold) plus 3 cc (volume between valves H1 and J1 in the canister line) plus 75.8 cc (the first J canister) plus 74.8 cc (the valve-C grab canister) plus 454 cc (the open mercury pump). The total volume open to the sample is now 2535 cc (if the volume taken up by the liquids and solids of the sample is ignored). The extractor-side pressure steps down, and the collector-side pressure rises to equal it.

5) Valve the collector side off from the extractor side. No pressure change results. The total volume open to the sample is now 1896 cc (neglecting the sample bulk volume).

6) Close valve C. This collects the unpumped grab canister. No pressure change results.

7) Close the Hg pump volume to zero, compressing the collector contents. This is the first stroke of the pump on the first J canister. The collector-side volume now consists of only the collector lines and the J canister; the sample is connected to the extractor vessel, lines, and second volume. The collector-side pressure rises sharply. Meanwhile, the extractor-side pressure is rising slightly as vapors leave the sample.

8) Disconnect the pump from both the collector and extractor (valve G). While opening the pump volume, reposition valve G to connect the pump to the extractor lines. The extractor-side pressure steps down, while no change in the collector-side pressure results.

9) Reposition valve G to connect the pump volume to the collector manifold instead of the extractor lines. The collector-side pressure drops sharply. Meanwhile, the extractor-side pressure is rising slightly.

10) Repeat steps 8 through 10 to give a total of 22 strokes.

11) Close valve H1. This collects the pumped first J canister. No pressure change results. The collector-side pressure is that of the peak pumped pressure from the last stroke. The extractor-side pressure is rising slightly.

12) Open valves H2 and J2 and H3 and J3 and evacuate the collector side and the pump (which is open to the collector side).

13) Carry out the bulk sample volume determination. Close off the collector side and the pump from the extractor side. Close off the extractor vessel from the lines and second volume. Add helium to the second volume, and note the pressure (the pressure is measured in the extractor lines, which are connected to the second volume). Open the extractor vessel to the lines and second volume, and note the new pressure. The ratio of pressures and the known tare system volumes allow the unknown bulk sample volume to be calculated.

14) Attach the $^{15}NH_3$ standard canister at valve D (with valve C closed), substituting it for the grab-sample canister, then open valves C and D. The standard enters the extractor side, causing a rapid rise in extractor-side pressure. The extractor-side pressure then drops gradually as the injected ammonia vapor begins to reach equilibrium with the sample ammonia. The volume open to the sample (and the standard) is 1896 cc (neglecting the sample bulk volume and the volume of the standard canister).

15) Leave the system in this condition for 139 hours, with the extractor vessel mixer running at 3 rpm, so that the standard and the sample can reach equilibrium. (Because valve K was open, some air leaked into the collector during the equilibration period.)

16) Open the collector side (and therefore the pump) to the extractor side. The total volume open to the sample is now 2575 cc (neglecting the sample bulk volume and including the two J canisters, 150.3 cc, and the standard canister, 40.6 cc). The extractor-side pressure steps down, and the collector-side pressure rises to equal it.

17) Valve the extractor side off from the collector side. No pressure change results.

18) Close the Hg pump volume to zero, compressing the collector contents. This is the first stroke of the pump on the second and third J canisters, which are both open and pumped simultaneously. The collector-side volume now consists of only the collector lines and the J canisters; the sample is connected to the extractor vessel, lines, second volume, and standard canister. The collector-side pressure rises sharply. Meanwhile, the extractor-side pressure is rising slightly as vapors leave the sample.

19) Disconnect the pump from both the collector and extractor (valve G). While opening the pump volume, reposition valve G to connect the pump to the extractor lines. The extractor-side pressure steps down, while there is no change in the collector-side pressure.

20) Reposition valve G to connect the pump volume to the collector manifold instead of the extractor lines. The collector-side pressure drops sharply. Meanwhile, the extractor-side pressure is rising slightly.

21) Repeat steps 18 through 20 to give a total of 20 strokes.

22) Close valves H2 and H3. This collects the pumped second and third J canisters. No pressure change results. The collector-side pressure is that of the peak pumped pressure from the last stroke. The extractor-side pressure is rising slightly.

23) Close valve D. This collects the standard canister, which is intended as a sample of the equilibrated extractor-side gas/vapor. No pressure change results.

A.6 BY-109 Sample 10B-5

1) Evacuate and leak-check the entire system. Close off the collector side from the extractor side (valve B) and close off the second volume vessel from the extractor vessel and lines (valve R). Close off the second and third J canisters from the collector manifold (valves H2 and H3). There is no grab-sample canister mounted at valve C. Valve the mercury pump (using valve G) so that it is connected to the collector side. Extractor- and collector-side pressures are zero.

2) Extrude the sample into the extractor vessel (a tare volume of 1290 cc, when the sampler piston is completely closed). At this time the lines of the extractor side of the system are open to the extractor, making an additional volume of 284.5 cc available to the sample gas/vapor. The PQ canister port on the extractor vessel is valved closed, so no volume is contributed by that canister. The extractor-side pressure rises sharply.

3) Open valve R, which opens the second-volume vessel to the extractor vessel and lines. This adds 321.5 cc of volume to that occupied by sample gas/vapor. The extractor-side pressure steps down.

4) Open valve B. This allows the gas/vapor to expand into the collector-side volume. The additional volume is 31.5 cc (collector manifold) plus 3 cc (volume between valves H1 and J1 in the canister line) plus 91.3 cc (the first J canister) plus 454 cc (the open mercury pump). The total volume open to the sample is now 2476 cc (if the volume taken up by the liquids and solids of the sample is ignored). The extractor-side pressure steps down, and the collector-side pressure rises to equal it.

5) Valve the collector side off from the extractor side. No pressure change results. The total volume open to the sample is now 1896 cc (neglecting the sample bulk volume).

6) Close the Hg pump volume to zero, compressing the collector contents. This is the first stroke of the pump on the first J canister. The collector-side volume now consists of only the collector lines and the J canister; the sample is connected to the extractor vessel, lines, and second volume. The collector-side pressure rises sharply. Meanwhile, the extractor-side pressure is rising slightly as vapors leave the sample.

7) Disconnect the pump from both the collector and extractor (valve G). While opening the pump volume, reposition valve G to connect the pump to the extractor lines. The extractor-side pressure steps down, while no change in the collector-side pressure results.

8) Reposition valve G to connect the pump volume to the collector manifold instead of the extractor lines. The collector-side pressure drops sharply. Meanwhile, the extractor-side pressure is rising slightly.

9) Repeat steps 6 through 8 to give a total of 21 strokes.

10) Close valve H1. This collects the pumped first J canister. No pressure change results. The collector-side pressure is that of the peak pumped pressure from the last stroke. The extractor-side pressure is rising slightly.

11) Open valves H2 and J2 and H3 and J3 and evacuate the collector side and the pump (which is open to the collector side).

12) Valve out the second volume and close off the extractor-side lines from the extractor, using valve T.

13) Attach the $^{15}NH_3$ standard canister at valve D (with valve C closed), then open valves C and D. The standard enters the extractor side lines, causing a rapid rise in extractor-side pressure.

14) Open valve T to let the standard into the extractor vessel. The extractor-side pressure drops gradually as the injected ammonia vapor begins to reach equilibrium with the sample ammonia. The volume open to the sample (and the standard) is 1574.5 cc (neglecting the sample bulk volume and the volume of the standard canister).

15) Leave the system in this condition for 91 hours, with the extractor vessel mixer running at 3 rpm, so that the standard and the sample can reach equilibrium.

16) Open the collector side (and therefore the pump) to the extractor side. The total volume open to the sample is now 2272 cc (neglecting the sample bulk volume and including the two J canisters, 182.2 cc, and the standard canister, 27 cc). The extractor-side pressure steps down, and the collector-side pressure rises to equal it.

17) Valve the extractor side off from the collector side. No pressure change results.

18) Close the Hg pump volume to zero, compressing the collector contents. This is the first stroke of the pump on the second and third J canisters, which are both open and pumped simultaneously. The collector-side volume now consists of only the collector lines and the J canisters; the sample is connected to the extractor vessel, lines, second volume, and standard canister. The collector-side pressure rises sharply. Meanwhile, the extractor-side pressure is rising slightly as vapors leave the sample.

19) Disconnect the pump from both the collector and extractor (valve G). While opening the pump volume, reposition valve G to connect the pump to the extractor lines. The extractor-side pressure steps down, while there is no change in the collector-side pressure.

20) Reposition valve G to connect the pump volume to the collector manifold instead of the extractor lines. The collector-side pressure drops sharply. Meanwhile, the extractor-side pressure is rising slightly.

21) Repeat steps 18 through 20 to give a total of 20 strokes.

22) Close valves H2 and H3. This collects the pumped second and third J canisters. No pressure change results. The collector-side pressure is that of the peak pumped pressure from the last stroke. The extractor-side pressure is rising slightly.

23) Close valve D. This collects the standard canister, which is intended as a sample of the equilibrated extractor-side gas/vapor. No pressure change results.

24) Carry out the bulk sample volume determination. Close off the collector side and the pump from the extractor side. Close off the extractor vessel from the lines and second volume. Add helium to the second volume, and note the pressure (the pressure is measured in the extractor lines, which are connected to the second volume). Open the extractor vessel to the lines and second volume, and note the new pressure. The ratio of pressures and the known tare system volumes allow the unknown bulk sample volume to be calculated.

A.7 BY-109 Sample 10B-6

1) Evacuate and leak-check the entire system. Close off the collector side from the extractor side (valve B) and close off the second volume vessel from the extractor vessel and lines (valve R). Close off the second and third J canisters from the collector manifold (valves H2 and H3). Valve the mercury pump (using valve G) so that it is connected to the collector side. Extractor- and collector-side pressures are zero.

2) Extrude the sample into the extractor vessel (a tare volume of 1290 cc, when the sampler piston is completely closed). At this time the lines of the extractor side of the system are open to the extractor, making an additional volume of 284.5 cc available to the sample gas/vapor. The PQ canister port on the extractor vessel is valved closed, so no volume is contributed by that canister. The extractor-side pressure rises sharply.

3) Open valve R, which opens the second-volume vessel to the extractor vessel and lines. This adds 321.5 cc of volume to that occupied by sample gas/vapor. The extractor-side pressure steps down.

4) Open valve B. This allows the gas/vapor to expand into the collector-side volume. The additional volume is 31.5 cc (collector manifold) plus 3 cc (volume between valves H1 and J1 in the canister line) plus 91.6 cc (the first J canister) plus 27 cc (the valve-C grab-sample canister) plus 454 cc (the open mercury pump). The total volume open to the sample is now 2503 cc (if the volume taken up by the liquids and solids of the sample is ignored). The extractor-side pressure steps down, and the collector-side pressure rises to equal it.

5) Close valve C. This collects the unpumped grab canister. No pressure change results.

6) Valve the collector side off from the extractor side. No pressure change results. The total volume open to the sample is now 1896 cc (neglecting the sample bulk volume).

7) Close the Hg pump volume to zero, compressing the collector contents. This is the first stroke of the pump on the first J canister. The collector-side volume now consists of only the collector lines and the J canister; the sample is connected to the extractor vessel, lines, and second volume. The collector-side pressure rises sharply. Meanwhile, the extractor-side pressure is rising slightly as vapors leave the sample.

8) Disconnect the pump from both the collector and extractor (valve G). While opening the pump volume, reposition valve G to connect the pump to the extractor lines. The extractor-side pressure steps down, while no change in the collector-side pressure results.

9) Reposition valve G to connect the pump volume to the collector manifold instead of the extractor lines. The collector-side pressure drops sharply. Meanwhile, the extractor-side pressure is rising slightly.

10) Repeat steps 7 through 9 to give a total of 21 strokes.

11) Close valve H1. This collects the pumped first J canister. No pressure change results. The collector-side pressure is that of the peak pumped pressure from the last stroke. The extractor-side pressure is rising slightly.

12) Open valves H2 and J2 to collect some more of the collector-side gas/vapor into the second J canister. The collector-side pressure drops sharply.

13) Attach 3 new canisters to the collector manifold (at valves J1, J2, and J3) and evacuate the collector side, the pump (which is open to the collector side), and the extractor lines and second volume.

14) Attach the $^{15}NH_3$ standard canister at valve D (with valve C closed), substituting it for the grab-sample canister, then open valves C and D. The standard enters the extractor side lines and second volume, causing a rapid rise in extractor-side pressure.

15) Open valve T to let the standard into the extractor vessel. The extractor-side pressure drops rapidly, by expansion, then gradually as the injected ammonia vapor begins to reach equilibrium with the sample ammonia. The volume open to the sample (and the standard) is 1924 cc (neglecting the sample bulk volume).

16) Leave the system in this condition for 21.5 hours, with the extractor vessel mixer running, so that the standard and the sample can reach equilibrium.

17) Open the collector side (and therefore the pump) to the extractor side. The total volume open to the sample is now 2494 cc (neglecting the sample bulk volume and including the three J canisters, 81 cc, and the standard canister, 27 cc). The extractor-side pressure steps down, and the collector-side pressure rises to equal it.

18) Valve the extractor side off from the collector side. No pressure change results.

19) Close the Hg pump volume to zero, compressing the collector contents. This is the first stroke of the pump on the J canisters, which are all three open and pumped simultaneously. The collector-side volume now consists of only the collector lines and the J canisters; the sample is connected to the extractor vessel, lines, second volume, and standard canister. The collector-side pressure rises sharply. Meanwhile, the extractor-side pressure is rising slightly as vapors leave the sample.

20) Disconnect the pump from both the collector and extractor (valve G). While opening the pump volume, reposition valve G to connect the pump to the extractor lines. The extractor-side pressure steps down, while there is no change in the collector-side pressure.

21) Reposition valve G to connect the pump volume to the collector manifold instead of the extractor lines. The collector-side pressure drops sharply. Meanwhile, the extractor-side pressure is rising slightly.

22) Repeat steps 18 through 20 to give a total of 20 strokes.

23) Close valves H1, H2, and H3. This collects the three pumped J canisters. No pressure change results. The collector-side pressure is that of the peak pumped pressure from the last stroke. The extractor-side pressure is rising slightly.

24) Close valve D. This collects the standard canister, which is intended as a sample of the equilibrated extractor-side gas/vapor. No pressure change results.

25) Carry out the bulk sample volume determination. Close off the collector side and the pump from the extractor side. Close off the extractor vessel from the lines and second volume. Add helium to the second volume, and note the pressure (the pressure is measured in the extractor lines, which are connected to the second volume). Open the extractor vessel to the lines and second volume, and note the new pressure. The ratio of pressures and the known tare system volumes allow the unknown bulk sample volume to be calculated.

A.8 References

Hey BE. 1997. *Retained Gas Sampler Extraction System Operation.* LT-160-101 Rev. F-0, G-0, and H-0. Numatec Hanford Corporation, Richland, Washington.

Shekarriz A, DR Rector, LA Mahoney, MA Chieda, JM Bates, RE Bauer, NS Cannon, BE Hey, CG Linschooten, FJ Reitz, and ER Siciliano. 1997. *Composition and Quantities of Retained Gas Measured in Hanford Waste Tanks 241-AW-101, A-101, AN-105, AN-104, and AN-103.* PNNL-11450 Rev. 1, Pacific Northwest National Laboratory, Richland, Washington.

Appendix B

Laboratory Data and Intermediate Results

Appendix B

Laboratory Data and Intermediate Results

B.1 Tank 241-U-103

As described in Appendix A, gases are extracted from waste samples into "J" canisters and then undergo analysis by mass spectrometry to obtain the mole fraction composition of the extracted gas on a dry basis. (Water vapor is not measured.) The results for Tank U-103 are shown in Table B.1.1.

Table B.1.2 shows the canister (collector-side) conditions that prevailed for Tank U-103 samples. The pressure and temperature of the gas in the J canisters are measured at the time of collection. The collector volume always includes the volume of the canister(s) and, in cases where the collector is pumped down to vacuum after a canister is valved closed, also includes the collector-side line volume. The water vapor pressure is assumed (for unpumped canisters) to be the vapor pressure over the sample because, for unpumped canisters, the collector-side is in direct communication with the sample and is in equilibrium with it. For pumped canisters, the water vapor pressure is that which is in equilibrium with the water in the condensate (an ammonia-in-water solution). The amount of isotopic ammonia added before the last canister is also shown in Table B.1.2, where appropriate, together with the ratio of unlabeled (original) to labeled ammonia measured in the canister that was collected after the isotopic ammonia was added.

Table B.1.1. Mole Percents of Gases Measured in Tank U-103 Dry Gas (obtained by mass spectrometry)

Segment/ Canister	N_2	H_2	N_2O	O_2	CH_4	He
2-J1	36 ± 0.7	22.3 ± 0.5	37.8 ± 0.8	0.167 ± 0.005	0.49 ± 0.02	2.61 ± 0.06
2-J2	34.6 ± 0.7	21.9 ± 0.5	37.9 ± 0.8	0.079 ± 0.004	0.38 ± 0.02	2.63 ± 0.60
2-J3[(a)]	15.6 ± 0.4	8.3 ± 0.2	14.3 ± 0.3	0.94 ± 0.3	0.11 ± 0.02	1.01 ± 0.01
5-J1	27.2 ± 0.6	11.2 ± 0.3	40.5 ± 0.8	0.226 ± 0.006	0.27 ± 0.06	8.3 ± 0.20
5-J2	15.7 ± 0.3	7 ± 0.1	26.9 ± 0.5	0.101 ± 0.002	0.11 ± 0.03	3.69 ± 0.07
7-J1	21.4 ± 0.4	12.2 ± 0.2	17.1 ± 0.3	0.035 ± 0.001	0.28 ± 0.06	4.1 ± 0.08
7-J2	15.1 ± 0.3	8.7 ± 0.2	12.1 ± 0.2	0.045 ± 0.001	0.22 ± 0.05	2.91 ± 0.06
8-J1	16.2 ± 0.3	13.6 ± 0.3	14.1 ± 0.3	0.064 ± 0.001	0.32 ± 0.06	4.26 ± 0.09
8-J2	10.7 ± 0.2	8.8 ± 0.2	9.3 ± 0.2	0.084 ± 0.002	0.2 ± 0.05	2.77 ± 0.06

(a) The isotopic standard was added before this canister; ammonia mole fractions include the ^{15}N standard.

Table B.1.1 (contd)

Segment/ Canister	Ar	Other NOx	C_2H_x	C_3H_x	Other HC	NH_3
2-J1	0.071 ± 0.001	0.01 ± 0.01	0.43 ± 0.04	0 ± 0	0.01 ± 0.01	0.1 ± 0.1
2-J2	0.036 ± 0.002	0.01 ± 0.01	0.40 ± 0.04	0 ± 0	0.03 ± 0.01	2.1 ± 0.6
2-J3[(a)]	0.12 ± 0.01	0.01 ± 0.01	0.09 ± 0.02	0 ± 0	0.03 ± 0.01	59.5 ± 16.4
5-J1	0.039 ± 0.01	0 ± 0	0.17 ± 0.05	0.02 ± 0.01	0.04 ± 0.01	12 ± 3.0
5-J2	0.021 ± 0.001	0 ± 0	0.11 ± 0.05	0.02 ± 0.01	0.04 ± 0.01	46 ± 12
7-J1	0.014 ± 0.001	0 ± 0	0.36 ± 0.04	0 ± 0	0.04 ± 0.01	45 ± 11
7-J2	0.014 ± 0.001	0.1 ± 0.05	0.3 ± 0.04	0 ± 0	0.03 ± 0.01	60 ± 15
8-J1	0.019 ± 0.001	0 ± 0	0.44 ± 0.04	0 ± 0	0.04 ± 0.01	51 ± 13
8-J2	0.021 ± 0.001	0.24 ± 0.04	0.35 ± 0.04	0.01 ± 0.005	0.04 ± 0.01	67 ± 17

(a) The isotopic standard was added before this canister; ammonia mole fractions include the ^{15}N standard.

Table B.1.2. Canister Conditions at the Time of Collection for Tank U-103 Samples

Segment/ Canister	Pressure (kPa)	Collector Volume (cc)	Temperature (°C)	Water Vapor Pressure (kPa)	Sampler Volume (L)	$^{15}NH_3$ Added (μmol)	Ratio of ^{14}N / ^{15}N
2-J1[(b)]	7.76	88.5	26.6	2.14	0.30543		
2-J2	98.16	125	27.0	3.53	0.30543		
2-J3[(a)]	29.56	127.8	27.3	3.20	0.30543	1115	0.437
5-J1[(b)]	5.00	186.48	26.0	2.18	0.30578		
5-J2	82.6	74.4	25.9	2.57	0.30578		
7-J1	90.2	40.5	26.0	2.55	0.30647		
7-J2	83.2	75.6	26.3	2.50	0.30647		
8-J1	81.6	39.2	26.8	2.67	0.30594		
8-J2	32.6	181.48	26.8	3.01	0.30594		

(a) The isotopic standard was added before this canister.
(b) Unpumped canister.

Tables B.1.3 through B.1.5 give the peak collector-side pressures after each stroke of the mercury pump, as well as the extractor-side pressure before each stroke.

Table B.1.3. Pump Cycle Pressures (kPa) for Canister 1 of Each Segment of Tank U-103

Cycle	2-J1		5-J1		7-J1		8-J1	
	collector	extractor	collector	extractor	collector	extractor	collector	extractor
pre-pumping	7.76	7.76	5.00	5.00	5.00	5.00	4.40	4.40
1					28.3	5.00	25.0	4.40
2					44.4	4.47	38.3	4.02
3					54.9	4.21	47.3	3.84
4					62.1	4.06	52.9	3.75
5					67.8	3.95	57.9	3.71
6					72.1	3.89	61.3	3.70
7					76.2	3.84	64.4	3.67
8					79.0	3.80	67.4	3.61
9					82.3	3.75	70.5	3.58
10					84.5	3.71	73.7	3.53
11					87.4	3.68	76.3	3.50
12					90.2	3.65	79.1	3.48
13							81.6	3.43

Table B.1.4. Pump Cycle Pressures (kPa) for Canister 2 of Each Segment of Tank U-103

Cycle	2-J2		5-J2		7-J2		8-J2	
	collector	extractor	collector	extractor	collector	extractor	collector	extractor
pre-pumping	6.1	6.1	4.3	4.3	9.3	3.60	7.3	3.37
1	27.7	6.1	24.9	4.3	48.1	3.60	21.1	3.37
2	43.6	5.49	37.5	3.83	51.8	3.53	23.5	3.33
3	55.3	4.81	46.0	3.57	54.5	3.49	25.3	3.31
4	64.0	4.29	52.2	3.48	56.8	3.48	26.7	3.28
5	70.0	3.94	56.4	3.42	59.1	3.46	27.9	3.28
6	74.3	3.70	59.7	3.38	60.8	3.45	29.1	3.28
7	77.5	3.51	61.7	3.35	62.8	3.43	30.2	3.28
8	80.5	3.37	63.8	3.33	64.6	3.43	31.5	3.27
9	83.2	3.25	66.1	3.30	66.4	3.43	32.6	3.27
10	85.4	3.15	67.3	3.28	68.4	3.41		
11	87.6	3.06	69.0	3.27	69.8	3.41		
12	89.0	2.98	70.6	3.25	71.9	3.40		
13	90.6	2.90	72.2	3.22	73.3	3.40		
14	92.3	2.84	73.7	3.20	74.6	3.39		
15	93.6	2.78	75.4	3.18	76.1	3.38		
16	94.7	2.73	77.3	3.17	77.6	3.38		
17	95.7	2.69	78.9	3.16	79.0	3.37		
18	97.0	2.65	80.4	3.15	81.0	3.37		
19	98.2	2.62	81.4	3.15	81.9	3.36		
20			82.6	3.14	83.2	3.35		

Table B.1.5. Pump Cycle Pressures (kPa) for Canister 3 of Each Segment of Tank U-103

Cycle	2-J3		5-J3		7-J3		8-J3	
	collector	extractor	collector	extractor	collector	extractor	collector	extractor
pre-pump-ing	2.9	2.9						
1	10.2	2.9						
2	16.9	2.93						
3	21.2	2.70						
4	23.8	2.57						
5	25.5	2.50						
6	26.6	2.48						
7	27.3	2.46						
8	28.0	2.46						
9	28.6	2.45						
10	29.0	2.44						
11	29.6	2.44						

Table B.1.6 shows the amounts of gases that are calculated based on the data presented earlier. Only ammonia has a large enough residual (amount left in the extractor side after extraction) to include in the table.

Table B.1.6. Quantities of Gases Found in Tank U-103 Samples

Segment/ Canister	N_2 (µmol)	H_2 (µmol)	N_2O (µmol)	O_2 (µmol)	CH_4 (µmol)	He (µmol)
2-J1	114±8	70±4.9	119±8.2	0.53±0.04	1.55±0.12	8.2±0.6
2-J2	1639±83	1038±54	1796±92	3.7±0.3	18.0±1.3	125±29
2-J3[(a)]	227±77	121±41	208±70	13.7±6.3	1.6±0.61	15±5
2-TOTAL[(a)]	1980±168	1229±100	2123±170	18±6.6	21.2±2.0	148±35
5-J1	73.5±9.0	30.3±3.7	110±13	0.6±0.1	0.73±0.18	22±2.7
5-J2	381±99	170±44	653±170	2.5±0.6	2.7±1.0	90±23
5-TOTAL	454±108	200±48	762±183	3.1±0.7	3.4±1.2	112±26
7-J1	357±45	203±25	285±36	0.6±0.1	4.7±1.2	68±9
7-J2	375±80	216±46	301±64	1.1±0.2	5.5±1.7	72±15
7-TOTAL	732±125	420±72	586±100	1.7±0.3	10.1±2.9	141±24
8-J1	237±35	199±29	206±30	0.94±0.14	4.7±1.1	62±9
8-J2	241±54	198±45	209±47	1.9±0.43	4.5±1.5	62±14
8-TOTAL	478±89	397±74	416±77	2.8±0.6	9.2±2.6	125±23

(a) An isotopic standard and a little inleaked air were added before this canister; the total and residual ammonia exclude the ^{15}N standard.

Table B.1.6 (contd)

Segment/ Canister	Ar (μmol)	Other NOx (μmol)	C_2H_x (μmol)	C_3H_x (μmol)	Other HC (μmol)	NH_3 (μmol)
2-J1	0.22±0.01	0.03±0.03	1.4±0.15	0±0	0.03±0.03	0.32±0.32
2-J2	1.7±0.12	0.47±0.47	18.9±2.1	0±0	1.42±0.48	171±34
2-J3[(a)]	1.7±0.61	0.15±0.15	1.3±0.53	0±0	0.44±0.21	
2-residual						487±152
2-TOTAL[(a)]	3.7±0.74	0.66±0.66	21.6±2.77	0±0	1.89±0.72	659±187
5-J1	0.11±0.03	0±0	0.46±0.15	0.05±0.03	0.11±0.03	32±9
5-J2	0.51±0.13	0±0	2.67±1.4	0.49±0.27	0.97±0.35	3100±445
5-residual						10860±10860
5-TOTAL	0.61±0.16	0±0	3.13±1.54	0.54±0.30	1.08±0.38	13992±11314
7-J1	0.23±0.03	0±0	6.0±1.0	0±0	0.67±0.19	1999±347
7-J2	0.35±0.08	2.5±1.4	7.5±1.9	0±0	0.75±0.29	4065±572
7-residual						16344±16344
7-TOTAL	0.58±0.11	2.5±1.4	13.5±2.9	0±0	1.41±0.48	22408±17263
8-J1	0.28±0.04	0±0	6.4±1.1	0±0	0.59±0.17	2024±255
8-J2	0.47±0.11	5.4±1.5	7.9±2.0	0.23±0.12	0.90±0.30	2015±412
8-residual						8412±8412
8-TOTAL	0.75±0.15	5.4±1.5	14.3±3.1	0.23±0.12	1.49±0.47	12451±9079

(a) An isotopic standard and a little inleaked air were added before this canister; the total and residual ammonia exclude the ^{15}N standard.

Table B.1.7. Mole Percents of Gases in Tank U-103 Dry Insoluble Gas

Segment/ Canister	N_2	H_2	N_2O	O_2	CH_4	He
2-J1	36.0	22.3	37.8	0.2	0.49	2.6
2-J2	35.3	22.4	38.7	0.1	0.39	2.7
2-J3[(a)]	38.5	20.5	35.3	2.3	0.27	2.5
5-J1	30.9	12.7	46.0	0.3	0.31	9.4
5-J2	29.1	13.0	49.8	0.2	0.20	6.8
7-J1	38.9	22.2	31.1	0.1	0.51	7.4
7-J2	37.8	21.8	30.3	0.1	0.55	7.3
8-J1	33.1	27.8	28.8	0.1	0.65	8.7
8-J2	32.4	26.7	28.2	0.3%	0.61	8.4

(a) An isotopic standard and a little inleaked air were added before this canister; the total and residual ammonia exclude the ^{15}N standard.

Table B.1.7 (contd)

Segment/ Canister	Ar	Other NOx	C_2H_x	C_3H_x	Other HC
2-J1	0.07	0.01	0.43	0	0.01
2-J2	0.04	0.01	0.41	0	0.03
2-J3[(a)]	0.30	0.02	0.22	0	0.07
5-J1	0.04	0	0.19	0.02	0.05
5-J2	0.04	0	0.20	0.04	0.07
7-J1	0.03	0	0.65	0	0.07
7-J2	0.04	0.25	0.75	0	0.08
8-J1	0.01	0	0.90	0	0.08
8-J2	0.1	0.73	1.1	0.03	0.12

(a) An isotopic standard and a little inleaked air were added before this canister; the total and residual ammonia exclude the ^{15}N standard.

As discussed in Section 3.3 of the main report, the amount of condensed water and dissolved ammonia in the collector (under pumped conditions) were found by thermodynamic analysis, as were the water and ammonia vapor pressures in the collector. Table B.1.8 contains these variables.

Table B.1.8. Collector Ammonia and Water Contents for Tank U-103 Sample Cycling

Segment/ Canister	Vapor pressure of NH_3 (kPa)	Vapor pressure of water (kPa)	µmoles of condensed NH_3	µmoles of condensed water
2-J1[a]	0.0056	2.14	0	0
2-J2	1.99	3.52	72	7521
2-J3[b]	15.7	3.20	420	3403
5-J1[a]	0.34	2.18	0	0
5-J2	36.8	2.57	1999	7926
7-J1	39.4	2.55	1292	4907
7-J2	48.4	2.50	2595	8700
8-J1	40.2	2.67	1348	5150
8-J2	19.8	3.01	572	3708

(a) This canister was not pumped, so no condensation occurred.
(b) An isotopic standard was added before this canister.

In order to estimate the void fraction and the distribution of gases between the void and slurry phases in each segment, the conditions under which the gas exists must be known. These are given in Table B.1.9 for Tank U-103. The densities were averages of the measured bulk densities in the other (the non-RGS) samples in the cores.[a] The temperatures were based on a profile measured at the T/C tree in riser 1; the profile is shown in Section 4.1. The pressures were derived from hydrostatic head, and are based on the depth of submergence of the segment and the thicknesses and gas-free densities of the waste layers. The solid volume fraction is estimated using 1420 kg/m^3 as the density of solid-free liquid, 1730 kg/m^3 as the density of gas-free slurry, and an assumed 2000 kg/m^3 as the intrinsic (not bulk) density of the solid material.

The water vapor pressure is the pressure in equilibrium with water in the waste; it is calculated using Equation 6.2 and Table 6.2 of Mahoney and Trent (1995), a correlation for water vapor pressure over concentrated homogeneous and non-homogeneous waste simulants. This correlation requires the weight fraction of water in the slurry, which is calculated using the solid volume fraction in the gas-free waste, the solution density, and the weight fraction of water in the solids-free solution. The latter value was set at 0.515, based on data for the drainable liquids in non-RGS samples taken at the same time and in the same cores.[a]

(a) Sasaki L. April 21, 1997. Transmittal from L. Sasaki to LA Mahoney (PNNL) of data collected for the U-103 TCR (document in preparation). Lockheed Martin Hanford Corporation, Richland, Washington.

Table B.1.9. In-Tank Conditions Used for Tank U-103 Phase Distribution Calculations

Segment	Density (kg/m^3)	Temperature (°C)	Pressure (atm)	Solid Volume Fraction	Water Vapor Pressure (atm)
2	1730	27.4	1.06	0.534	0.0072
5	1730	29.7	1.26	0.534	0.0082
7	1730	29.8	1.41	0.534	0.0082
8	1730	29.7	1.48	0.534	0.0082

The average ionic concentrations in the drainable liquid in Tank U-103 are given in Table B.1.10. They were based on non-RGS samples from the same cores.(a)

Table B.1.10. Ionic Concentrations Used For Tank U-103 Phase Distribution Calculations

Ion	gmol/L solution
Na^+	9.72
Al^{3+}	1.14
Fe^{3+}	0.0
Cr^{3+}	0.004
Ni^{2+}	0.003
K^+	0.11
OH^-	5.0
NO_3^-	3.22
NO_2^-	2.96
CO_3^{2-}	0.2
PO_4^{3-}	0.04
SO_4^{2-}	0.04
F^-	0.12
Cl^-	0.56

The Henry's Law constants are necessary to estimate the in-tank phase distribution of gases (see Section 3.5). The intermediate steps in the Henry's Law constant calculation are shown in Table B.1.11. Note that the final Henry's Law constant is in terms of liters of gas-free waste

(a) Sasaki L. June 24, 1997. Transmittal from L. Sasaki to LA Mahoney (PNNL) of data collected for the U-103 TCR (document in preparation). Lockheed Martin Hanford Corporation, Richland, Washington.

Table B.1.11. Henry's Law Constants for Tank U-103 Phase Distribution Calculations

Segment	Condition	N_2	H_2	N_2O	O_2	CH_4	NH_3
2	Schumpe (K in water/K in solution)	122	41.7	83.0	133	146	10.6
	Waste Slurry K (mol/atm L waste)	1.8×10^{-6}	6.3×10^{-6}	9.3×10^{-5}	3.1×10^{-6}	3.2×10^{-6}	1.74
5	Schumpe (K in water/K in solution)	113	40.2	78.2	128	137	10.6
	Waste Slurry K (mol/atm L waste)	1.9×10^{-6}	6.5×10^{-6}	9.3×10^{-5}	3.2×10^{-6}	3.3×10^{-6}	1.56
7	Schumpe (K in water/K in solution)	112	40.1	77.9	127	136	10.6
	Waste Slurry K (mol/atm L waste)	1.9×10^{-6}	6.5×10^{-6}	9.3×10^{-5}	3.2×10^{-6}	3.3×10^{-6}	1.56
8	Schumpe (K in water/K in solution)	113	40.2	78.3	128	137	10.6
	Waste Slurry K (mol/atm L waste)	1.9×10^{-6}	6.5×10^{-6}	9.3×10^{-5}	3.2×10^{-6}	3.3×10^{-6}	1.56

slurry, while the Schumpe model is in terms of kg of water in the salt solution. Both the solid volume fraction and the weight percent of water in the solution are needed to put the Henry's Law constant in its final form. The gases not listed, argon, helium, and the minor gases, were assumed wholly insoluble with Henry's law constants of 10^{-10}.

B.2 Tank 241-S-106

As described in Appendix A, gases are extracted from waste samples into "J" canisters and then undergo analysis by mass spectrometry to obtain the mole fraction composition of the extracted gas on a dry basis. (Water vapor is not measured.) The results, for Tank S-106, are shown in Table B.2.1.

Table B.2.2 shows the canister (collector-side) conditions that prevailed for Tank S-106 samples. The pressure and temperature of the gas in the J canisters are measured at the time of collection. The collector volume always includes the volume of the canister(s) and, in cases where the collector is pumped down to vacuum after a canister is valved closed, also includes the collector-side line volume. The water vapor pressure is assumed (for unpumped canisters) to be the vapor pressure over the sample because, for unpumped canisters, the collector-side is in direct communication with the sample and is in equilibrium with it. For pumped canisters, the water vapor pressure is that which is in equilibrium with the water in the condensate (an ammonia-in-water solution). The amount of isotopic ammonia added before the last canister is also shown in Table B.2.2, together with the ratio of unlabeled (original) to labeled ammonia measured in the canister that was collected after the isotopic ammonia was added.

Table B.2.1. Mole Percents of Gases Measured in Tank S-106 Dry Gas (obtained by mass spectrometry)

Segment/ Canister	N_2	H_2	N_2O	O_2	CH_4	He
3-J1	31.3 ± 0.6	50.2 ± 0.6	7.6 ± 0.2	0.205 ± 0.004	0.33 ± 0.007	10.0 ± 0.2
3-J2	28.8 ± 0.6	51.7 ± 0.6	7.4 ± 0.2	0.104 ± 0.002	0.22 ± 0.04	10.1 ± 0.6
3-J3[(a)]	2.99 ± 0.06	4.35 ± 0.09	0.65 ± 0.01	0.363 ± 0.007	0.2 ± 0.1	0.84 ± 0.02
5-J1	21.3 ± 0.5	51.8 ± 0.5	13.8 ± 0.3	0.1 ± 0.005	0.001 ± 0.001	9.2 ± 0.2
5-J2	18.0 ± 0.4	48.4 ± 0.5	11.5 ± 0.2	0.073 ± 0.004	0.001 ± 0.001	7.0 ± 0.2
5-J3[(a)]	4.07 ± 0.08	4.03 ± 0.08	0.96 ± 0.02	0.92 ± 0.02	0.013 ± 0.002	0.66 ± 0.02
6-J1	25.0 ± 0.5	53.8 ± 0.5	9.7 ± 0.2	0.42 ± 0.02	0.46 ± 0.04	8.6 ± 0.2
6-J2	22.5 ± 0.5	53.5 ± 0.5	8.9 ± 0.2	0.54 ± 0.02	0.28 ± 0.02	8.5 ± 0.2
6-J3[(a)]	1.53 ± 0.03	3.41 ± 0.07	0.8 ± 0.02	0.01 ± 0.005	0.1 ± 0.1	0.52 ± 0.01
10-J1	23.4 ± 0.5	60.3 ± 0.5	10.7 ± 0.2	0.114 ± 0.005	0.216 ± 0.005	5.2 ± 0.1
10-J2	21.6 ± 0.5	58.6 ± 0.5	10.3 ± 0.2	0.03 ± 0.003	0.14 ± 0.005	5.0 ± 0.1
10-J3[(a)]	3.18 ± 0.07	1.41 ± 0.03	0.224 ± 0.004	1.03 ± 0.03	0.01 ± 0.01	0.124 ± 0.004

(a) The isotopic standard was added before this canister; ammonia mole fractions include the ^{15}N standard.

Table B.2.1 (contd)

Segment/ Canister	Ar	Other NOx	C_2H_x	C_3H_x	Other HC	NH_3
3-J1	0.243 ± 0.005	0.01 ± 0.01	0.01 ± 0.01	0.03 ± 0.01	0.02 ± 0.01	0.11 ± 0.05
3-J2	0.223 ± 0.004	0.01 ± 0.01	0.01 ± 0.01	0.04 ± 0.01	0.03 ± 0.01	1.4 ± 0.5
3-J3*	0.039 ± 0.002	0.01 ± 0.01	0.14 ± 0.05	0.01 ± 0.01	0.03 ± 0.01	90.5 ± 23
5-J1	0.05 ± 0.001	0.05 ± 0.05	0.07 ± 0.02	0.04 ± 0.01	0.04 ± 0.01	3.5 ± 0.4
5-J2	0.041 ± 0.002	0.05 ± 0.05	0.07 ± 0.02	0.05 ± 0.01	0.06 ± 0.01	15 ± 3
5-J3*	0.058 ± 0.001	0.01 ± 0.01	0.2 ± 0.1	0.1 ± 0.1	0.11 ± 0.02	88.8 ± 22
6-J1	0.102 ± 0.005	0.1 ± 0.1	0.04 ± 0.01	0.02 ± 0.01	0.02 ± 0.01	1.8 ± 0.5
6-J2	0.089 ± 0.004	0.01 ± 0.005	0.05 ± 0.02	0.02 ± 0.01	0.03 ± 0.01	5.6 ± 2.0
6-J3*	0.016 ± 0.005	0.05 ± 0.05	0.2 ± 0.1	0.1 ± 0.1	0.02 ± 0.01	93.5 ± 23.7
10-J1	0.029 ± 0.003	0.05 ± 0.05	0.027 ± 0.003	0.02 ± 0.01	0.01 ± 0.01	0.1 ± 0.1
10-J2	0.025 ± 0.003	0.02 ± 0.01	0.03 ± 0.01	0.03 ± 0.01	0.01 ± 0.01	4.2 ± 1.0
10-J3*	0.048 ± 0.004	0.01 ± 0.01	0.2 ± 0.1	0.1 ±0.1	0.013 ± 0.006	93.8 ± 23.8

* The isotopic standard was added before this canister; ammonia mole fractions include the ^{15}N standard.

Table B.2.2. Canister Conditions at the Time of Collection for Tank S-106 Samples

Segment/ Canister	Pressure (kPa)	Collector Volume (cc)	Temperature (°C)	Water Vapor Pressure (kPa)	Sampler Volume (L)	$^{15}NH_3$ Added (µmol)	Ratio of ^{14}N / ^{15}N
3-J1[(a)]	3.1	75.8	24.8	1.90	0.3072		
3-J2	30.4	109.92	25.3	3.23	0.3072		
3-J3[(a)]	23.8	109.36	25.7	2.82	0.3072	3059	0.079
5-J1[(b)]	3.0	91.3	24.3	1.46	0.30772		
5-J2	36.5	124	24.3	2.93	0.30772		
5-J3[(a)]	17.7	127.2	24.6	2.74	0.30772	3030	0.414
6-J1[(b)]	2.7	91.6	24.3	1.71	0.30719		
6-J2	24.3	128.5	24.3	3.02	0.30719		
6-J3[(a)]	35.5	124	24.1	2.34	0.30719	3165	0.114
10-J1[(b)]	3.8	88.5	23.4	1.05	0.30682		
10-J2	55.2	125	24.3	3.00	0.30682		
10-J3[(a)]	25.9	127.8	25.6	2.75	0.30682	2918	0.105

(a) The isotopic standard was added before this canister.
(b) Unpumped canister.

Tables B.2.3 through B.2.5 give the peak collector-side pressures after each stroke of the mercury pump, as well as the extractor-side pressure before each stroke.

Table B.2.3. Pump Cycle Pressures (kPa) for Canister 1 of Each Segment of Tank S-106

Cycle	3-J1		5-J1		6-J1		10-J1	
	collector	extractor	collector	extractor	collector	extractor	collector	extractor
pre-pump-ing	3.1	3.1	3.0	3.0	2.7	2.7	3.8	3.8

Table B.2.4. Pump Cycle Pressures (kPa) for Canister 2 of Each Segment of Tank S-106

Cycle	3-J2		5-J2		6-J2		10-J2	
	collector	extractor	collector	extractor	collector	extractor	collector	extractor
pre-pump-ing	3.1	3.1	2.8	2.8	2.7	2.7	3.6	3.6
1	11.9	3.1	10.9	2.8	9.9	2.7	14.7	3.6
2	18.0	2.69	18:8	2.47	14.6	2.30	25.5	3.09
3	21.3	2.46	24.5	2.14	17.4	2.13	33.8	2.48
4	23.1	2.36	28.0	1.95	19.2	2.10	40.5	2.05
5	24.2	2.31	30.1	1.84	20.9	2.02	45.0	1.77
6	25.0	2.27	31.4	1.82	21.5	1.98	47.8	1.60
7	25.7	2.24	32.2	1.83	22.0	1.95	49.5	1.53
8	26.3	2.23	32.7	1.83	22.4	1.95	50.5	1.50
9	26.7	2.20	33.0	1.84	22.5	1.94	51.2	1.49
10	27.1	2.19	33.6	1.84	22.9	1.94	51.8	1.48
11	27.5	2.17	33.9	1.85	23.1	1.94	52.4	1.47
12	27.7	2.17	34.2	1.85	23.1	1.91	52.8	1.47
13	28.0	2.16	34.6	1.85	23.6	1.93	53.1	1.48
14	28.5	2.15	34.8	1.83	23.6	1.93	53.5	1.48
15	28.7	2.16	35.1	1.85	23.8	1.90	53.7	1.48
16	29.1	2.15	35.4	1.83	23.9	1.91	54.1	1.48
17	29.3	2.16	35.6	1.84	24.0	1,91	54.2	1.48
18	29.6	2.15	35.9	1.83	24.2	1.89	54.6	1.47
19	29.8	2.12	36.2	1.82	24.2	1.91	54.9	1.48
20	30.0	2.13	36.3	1.80	24.3	1.93	55.0	1.47
21	30.4	2.13	36.5	1.80			55.2	1.46

Table B.2.5. Pump Cycle Pressures (kPa) for Canister 3 of Each Segment of Tank S-106

Cycle	3-J3		5-J3		6-J3		10-J3	
	collector	extractor	collector	extractor	collector	extractor	collector	extractor
pre-pump-ing	3.1	3.1	1.9	1.9	3.6	3.6	3.8	3.8
1	9.7	3.1	8.1	1.9	16.4	3.6	9.3	3.8
2	14.3	2.80	11.6	1.81	25.6	3.11	18.9	3.25
3	17.3	2.69	13.5	1.77	31.8	2.72	25.9	2.71
4	19.0	2.58	14.5	1.76	35.5	2.44		
5	20.0	2.52	15.4	1.80				
6	20.8	2.44	15.9	1.81				
7	21.3	2.34	16.2	1.82				
8	21.7	2.31	16.6	1.82				
9	22.1	2.29	16.4	1.89				
10	22.5	2.27	16.8	1.84				
11	22.8	2.26	17.1	1.83				
12	23.2	2.22	17.2	1.85				
13	23.5	2.23	17.3	1.86				
14	23.8	2.21	17.5	1.86				
15			17.6	1.85				
16			17.7	1.87				

Table B.2.6 shows the amounts of gases that are calculated based on the data presented earlier. Only ammonia has a large enough residual (amount left in the extractor side after extraction) to include in the table.

Table B.2.6. Quantities of Gases Found in Tank S-106 Samples

Segment/ Canister	N_2 (µmol)	H_2 (µmol)	N_2O (µmol)	O_2 (µmol)	CH_4 (µmol)	He (µmol)
3-J1	34±8	53.9±12.5	8.2±1.9	0.22±0.1	0.35±0.08	10.7±2.5
3-J2	347±15	623±25	89.2±4.2	1.3±0.1	2.65±0.49	122±9
3-J3[(a)]	28±13	41±18	6.1±2.8	3.4±1.5	1.88±1.27	7.9±3.6
3-TOTAL[(a)]	409±36	718±56	104±8.9	4.9±1.6	4.89±1.84	140±15
5-J1	31.5±4.7	76.7±11.4	20.4±3.1	0.15±0.02	0±0	14±2.0
5-J2	303±16	814±42	193±10	1.2±0.09	0.02±0.02	118±7
5-J3[(a)]	32±14	32±14	7.6±3.4	7.3±3.2	0.10±0.05	5.2±2.3
5-TOTAL[(a)]	366±36	922±67	221±17	8.6±3.4	0.12±0.07	137±11
6-J1	24±6	51±13	9.2±2.3	0.40±0.10	0.44±0.12	8.2±2.1
6-J2	249±12	593±26	99±4.9	6.0±0.34	3.1±0.3	94±5
6-J3[(a)]	38±15	85±33	19.9±7.8	0.25±0.16	2.5±2.5	13±5.1
6-TOTAL[(a)]	311+33	729±73	128±15	6.6±0.60	6.0±2.8	115±12
10-J1	62±5	159±12	28.1±2.1	0.30±0.03	0.57±0.04	14±1.0
10-J2	571±23	1550±53	272±10	0.79±0.08	3.7±0.2	132±5
10-J3[(a)]	68±25	30±11	4.8±1.8	22±8.1	0.2±0.2	2.6±1.0
10-TOTAL[(a)]	701±53	1739±76	305±14	23±8.2	4.5±0.45	149±7

(a) An isotopic standard and a little inleaked air were added before this canister; the total and residual ammonia exclude the ^{15}N standard.

Table B.2.6 (contd)

Segment/ Canister	Ar (µmol)	Other NOx (µmol)	C_2H_x (µmol)	C_3H_x (µmol)	Other HC (µmol)	NH_3 (µmol)
3-J1	0.26±0.06	0.01±0.01	0.01±0.01	0.03±0.01	0.02±0.01	0.12±0.06
3-J2	2.7±0.11	0.12±0.12	0.12±0.12	0.48±0.12	0.36±0.12	68±16
3-J3[a]	0.37±0.17	0.09±0.10	1.32±0.76	0.09±0.10	0.28±0.16	
3-residual[a]						241±86
3-TOTAL[a]	3.3±0.34	0.23±0.23	1.45±0.89	0.61±0.24	0.67±0.29	309±10 2
5-J1	0.07±0.01	0.07±0.07	0.10±0.03	0.06±0.02	0.06±0.02	5.2±1.0
5-J2	0.69±0.05	0.84±0.84	1.18±0.34	0.84±0.17	1.01±0.18	530±80
5-J3[a]	0.46±0.20	0.08±0.08	1.58±1.06	0.79±0.86	0.87±0.42	
5-residual[a]						1254±449
5-TOTAL[a]	1.2±0.3	0.99±0.99	2.86±1.43	1.69±1.05	1.94±0.61	1789±529
6-J1	0.10±0.02	0.10±0.10	0.04±0.01	0.02±0.01	0.02±0.01	1.7±0.6
6-J2	1.0±0.06	0.11±0.06	0.55±0.22	0.22±0.11	0.33±0.11	150±38
6-J3[a]	0.40±0.20	1.24±1.24	5.0±3.2	2.49±2.67	0.50±0.32	
6-residual[a]						361±129
6-TOTAL[a]	1.5±0.3	1.45±1.39	5.57±3.40	2.73±2.80	0.85±0.44	513±168
10-J1	0.08±0.01	0.13±0.13	0.07±0.01	0.05±0.03	0.03±0.03	0.3±0.3
10-J2	0.66±0.08	0.53±0.27	0.79±0.27	0.79±0.27	0.26±0.26	244±47
10-J3[a]	1.02±0.38	0.21±0.21	4.3±2.65	2.1±2.27	0.28±0.16	
10-residual[a]						306±109
10-TOTAL[a]	1.8±0.5	0.87±0.60	5±2.92	2.98±2.57	0.57±0.45	550±157

(a) An isotopic standard and a little inleaked air were added before this canister; the total and residual ammonia exclude the ^{15}N standard.

Table B.2.7. Mole Percents of Gases in Tank S-106 Dry Insoluble Gas

Segment/ Canister	N_2	H_2	N_2O	O_2	CH_4	He
3-J1	31.3	50.3	7.6	0.2	0.33	10.0
3-J2	29.2	52.4	7.5	0.1	0.22	10.2
3-J3[(a)]	31.5	45.8	6.8	3.8	2.1	8.8
5-J1	22.1	53.7	14.3	0.1	0.00	9.53
5-J2	21.2	56.9	13.5	0.1	0.0	8.2
5-J3[(a)]	36.3	36.0	8.6	8.2	0.12	5.9
6-J1	25.5	54.8	9.9	0.4	0.47	8.8
6-J2	23.8	56.7	9.4	0.6	0.30	9.0
6-J3[(a)]	23.4	52.2	12.3	0.2	1.5	8.0
10-J1	23.4	60.4	10.7	0.1	0.22	5.2
10-J2	22.5	61.2	10.8	0.0	0.15	5.2
10-J3[(a)]	51.3	22.7	3.6	16.6	0.16	2.0

(a) An isotopic standard and a little inleaked air were added before this canister.

Table B.2.7 (contd)

Segment/ Canister	Ar	Other NOx	C_2H_x	C_3H_x	Other HC
3-J1	0.24	0.01	0.01	0.03	0.02
3-J2	0.23	0.01	0.01	0.04	0.03
3-J3[(a)]	0.41	0.11	1.5	0.11	0.32
5-J1	0.05	0.05	0.07	0.04	0.04
5-J2	0.05	0.06	0.08	0.06	0.07
5-J3[(a)]	0.52	0.09	1.8	0.89	0.98
6-J1	0.10	0.10	0.04	0.02	0.02
6-J2	0.09	0.01	0.05	0.02	0.03
6-J3[(a)]	0.25	0.77	3.1	1.5	0.3
10-J1	0.0	0.05	0.03	0.02	0.01
10-J2	0.0	0.02	0.03	0.03	0.01
10-J3[(a)]	0.8	0.16	3.2	1.6	0.21

(a) An isotopic standard and a little inleaked air were added before this canister.

As discussed in Section 3.3, the amount of condensed water and dissolved ammonia in the collector (under pumped conditions) were found by thermodynamic analysis, as were the water and ammonia vapor pressures in the collector. Table B.2.8 contains these variables.

In order to estimate the void fraction and the distribution of gases between the void and slurry phases in each segment, the conditions under which the gas exists must be known. These are given in Table B.2.9 for Tank S-106. The densities were averages of the measured bulk densities in the other (the non-RGS) samples in the cores.(a) The temperatures were based on a profile measured at the T/C tree in Riser 2; the profile is shown in Section 4.2. The pressures were derived from hydrostatic head, and are based on the depth of submergence of the segment and the thicknesses and gas-free densities of the waste layers. The solid volume fraction is estimated using 1420 kg/m^3 as the density of solid-free liquid, 1780 kg/m^3 as the density of gas-free slurry, and an assumed 2000 kg/m^3 as the intrinsic (not bulk) density of the solid material.

Table B.2.8. Collector Ammonia and Water Contents for Tank S-106 Sample Cycling

Segment/ Canister	Vapor pressure of NH_3 (kPa)	Vapor pressure of water (kPa)	µmoles of condensed NH_3	µmoles of condensed water
3-J1[a]	0.0013	1.90		
3-J2	0.38	3.23	15	7503
3-J3[b]	19.0	2.82	714	4624
5-J1[a]	0.054	1.46		
5-J2	5.03	2.93	198	5573
5-J3[b]	13.3	2.74	478	4096
6-J1[a]	0.018	1.71		
6-J2	1.19	3.02	39	6203
6-J3[b]	31.0	2.34	111	471
10-J1[a]	0.0028	1.05		
10-J2	2.19	3.00	49	4142
10-J3[b]	21.7	2.75	97	561

(a) This canister was not pumped, so no condensation occurred.
(b) An isotopic standard was added before this canister.

(a) Esch R. May 13, 1997. Transmittal from R Esch to LA Mahoney (PNNL) of data collected for the S-106 TCR (document in preparation). Lockheed Martin Hanford Corporation, Richland, Washington.

Table B.2.9. In-Tank Conditions Used for Tank S-106 Phase Distribution Calculations

Segment	Density (kg/m^3)	Temperature (°C)	Pressure (atm)	Solid Volume Fraction	Water Vapor Pressure (atm)
3	1420	25.1	1.14	0	0.017
5	1780	25.7	1.29	0.62	0.057
6	1780	25.8	1.36	0.62	0.058
10	1780	25.9	1.66	0.62	0.057

The water vapor pressure is the pressure in equilibrium with water in the waste; it is calculated using Equation 6.2 and Table 6.2 of Mahoney and Trent (1995), a correlation for water vapor pressure over concentrated homogeneous and non-homogeneous waste simulants. This correlation requires the weight fraction of water in the slurry, which is calculated using the solid volume fraction in the gas-free waste, the solution density, and the weight fraction of water in the solids-free solution. The latter value was set at 0.534, based on data for the drainable liquids in non-RGS samples taken at the same time and in the same cores.(a)

The average ionic concentrations in the drainable liquid in Tank S-106 are given in Table B.2.10. They were based on non-RGS samples from the same cores.(a)

The Henry's Law constants are necessary to estimate the in-tank phase distribution of gases (see Section 3.5). The intermediate steps in the Henry's Law constant calculation are shown in Table B.2.11. Note that the final Henry's Law constant is in terms of liters of gas-free waste slurry, while the Schumpe model is in terms of kg of water in the salt solution. Both the solid volume fraction and the weight percent of water in the solution are needed to put the Henry's Law constant in its final form. The gases not listed, argon, helium, and the minor gases, were assumed wholly insoluble with Henry's law constants of 10^{-10}.

(a) Esch R. May 13, 1997. Transmittal from R Esch to LA Mahoney (PNNL) of data collected for the S-106 TCR (document in preparation). Lockheed Martin Hanford Corporation, Richland, Washington.

Table B.2.10. Ionic Concentrations Used For Tank S-106 Phase Distribution Calculations

Ion	gmol/L solution
Na^+	10.57
Al^{3+}	1.32
Fe^{3+}	0
Cr^{3+}	0.18
Ni^{2+}	0
K^+	0.04
OH^-	5.07
NO_3^-	3.06
NO_2^-	1.46
CO_3^{2-}	0.21
PO_4^{3-}	0.04
SO_4^{2-}	0.09
F^-	0.01
Cl^-	0.19

Table B.2.11. Henry's Law Constants For Tank S-106 Phase Distribution Calculations

Segment	Condition	N_2	H_2	N_2O	O_2	CH_4	NH_3
3	Schumpe (K in water/K in solution)	132	45.7	90.2	139	156	11.9
	Waste Slurry K (mol/atm L waste)	3.8×10^{-6}	1.3×10^{-5}	2.0×10^{-4}	6.9×10^{-6}	6.9×10^{-6}	3.86
5	Schumpe (K in water/K in solution)	130	45.2	88.8	138	153	11.9
	Waste Slurry K (mol/atm L waste)	1.4×10^{-6}	5.0×10^{-6}	7.7×10^{-5}	2.6×10^{-6}	2.6×10^{-6}	1.42
6	Schumpe (K in water/K in solution)	129	45.1	88.5	138	153	11.9
	Waste Slurry K (mol/atm L waste)	1.4×10^{-6}	5.0×10^{-6}	7.7×10^{-5}	2.6×10^{-6}	2.6×10^{-6}	1.41
10	Schumpe (K in water/K in solution)	129	45.1	88.4	137	152	11.9
	Waste Slurry K (mol/atm L waste)	1.4×10^{-6}	5.0×10^{-6}	7.7×10^{-5}	2.6×10^{-6}	2.6×10^{-6}	1.41

B.3 Tank 241-BY-109

As described in Appendix A, gases are extracted from waste samples into "J" canisters and then undergo analysis by mass spectrometry to obtain the mole fraction composition of the extracted gas on a dry basis. (Water vapor is not measured.) The results, for Tank BY-109, are shown in Table B.3.1.

Table B.3.1. Mole Percents of Gases Measured in Tank BY-109 Dry Gas (obtained by mass spectrometry)

Segment/ Canister	N_2	H_2	N_2O	O_2	CH_4	He
4-J1	36.9±0.7	24.9±0.5	15.5±0.3	0.214±0.004	0.7±0.1	9.3±0.2
4-J2[(a)]	20.1±0.4	0.358±0.008	0.775±0.02	8.9±0.2	0.03±0.003	42.3±0.85
5-J1	23.6±0.5	38±0.7	12.8±0.3	0.093±0.002	0.47±0.01	7.4±0.1
5-J2[(a)]	12.2±0.2	10.8±0.2	3.02±0.06	3.53±0.07	0.265±0.065	2±0.04
6-J1	21.4±0.4	47.2±0.9	15±0.3	0.058±0.001	0.73±0.01	4.5±0.09
6-J2[(a)]	9±0.3	12.0±0.208	3.12±0.095	3.04±0.093	0.175±0.008	1.12 ±0.023

(a) The isotopic standard was added before this canister; ammonia mole fractions include the ^{15}N standard. In addition, there was an air leak between canisters J1 and J2 of segment 4, and helium was added to measure the bulk sample volume.

Table B.2.1 (contd)

Segment/ Canister	Ar	Other NOx	C_2H_x	C_3H_x	Other HC	NH_3
4-J1	0.172±0. 003	0.01±0.01	0.5±0.1	0.083±0.002	0.5±0.1	11±3
4-J2[(a)]	0.825 ±0.02	0.01±0.01	0.21±0.04	0.085±0.02	0.515±0.055	26±6
5-J1	0.149±0.003	0.01±0.01	0.42±0.01	0.07±0.01	0.41±0.01	16±3
5-J2[(a)]	0.211±0. 004	0.01±0.01	0.48±0.02	0.1±0.01	1.1±0.1	66±8
6-J1	0.173±0.0 03	0.01±0.01	1.1±0.1	0.09±0.01	0.7±0.07	9±2
6-J2[(a)]	0.198±0.006	0.01±0.01	0.32±0.03	0.183±0.020	1.5±0.2	6 9.3±8

(a) The isotopic standard was added before this canister; ammonia mole fractions include the ^{15}N standard. In addition, there was an air leak between canisters J1 and J2 of segment 4, and helium was added to measure the bulk sample volume.

Table B.3.2 shows the canister (collector-side) conditions that prevailed for Tank BY-109 samples. The pressure and temperature of the gas in the J canisters are measured at the time of collection. The collector volume always includes the volume of the canister(s) and, in cases where

Table B.3.2. Canister Conditions at the Time of Collection for Tank BY-109 Samples

Segment/ Canister	Pressure (kPa)	Collector Volume (cc)	Temperature (°C)	Water Vapor Pressure (kPa)	Sampler Volume (L)	$^{15}NH_3$ Added (μmol)	Ratio of ^{14}N / ^{15}N
4-J1	28.29	110.3	24.3	3.00	0.25079[b]		
4-J2[a]	11.76	184.78	25.9	3.30	0.25079[b]	1959	1.27
5-J1	33.75	125.8	23.5	2.80	0.30354[b]		
5-J2[a]	7.79	216.7	23.9	2.92	0.30354[b]	1178	2.82
6-J1	43.72	126.1	24.2	2.96	0.29559[b]		
6-J2[a]	12.13	115.5	25.5	3.13	0.29559[b]	1137	1.13

(a) The isotopic standard was added before this canister. In addition, there was an air leak between canisters J1 and J2 of segment 4, and helium was added to measure the bulk sample volume.
(b) The sampler volumes have been decreased from nominal values to account for the pistons not being fully retracted. The piston retraction was short by 3.6 in. for segment 4, 0.25 in. for segment 5, and 0.75 in. for segment 6.

the collector is pumped down to vacuum after a canister is valved closed, also includes the collector-side line volume. The water vapor pressure is assumed (for unpumped canisters) to be the vapor pressure over the sample because, for unpumped canisters, the collector-side is in direct communication with the sample and is in equilibrium with it. For pumped canisters, the water vapor pressure is that which is in equilibrium with the water in the condensate (an ammonia-in-water solution). The amount of isotopic ammonia added before the last canister is also shown in Table B.3.2, together with the ratio of unlabeled (original) to labeled ammonia measured in the canister that was collected after the isotopic ammonia was added.

Tables B.3.3 and B.3.4 give the peak collector-side pressures after each stroke of the mercury pump, as well as the extractor-side pressure before each stroke.

Table B.3.3. Pump Cycle Pressures (kPa) for Canister 1 of Each Segment of Tank BY-109

Cycle	4-J1		5-J1		6-J1	
	collector	extractor	collector	extractor	collector	extractor
pre-pump-ing	2.88	2.88	3.17	3.17	3.85	3.85
1	11.85	2.88	12.25	3.17	15.495	3.85
2	16.88	2.545	18.24	2.762	23.115	3.289
3	19.73	2.397	21.98	2.514	28.045	2.935
4	21.22	2.326	24.21	2.4	30.985	2.732
5	22.14	2.297	25.63	2.333	32.775	2.623
6	22.95	2.275	26.67	2.289	34.115	2.547
7	23.24	2.255	27.56	2.255	35.665	2.493
8	24.07	2.244	28.25	2.228	36.665	2.441
9	24.55	2.233	28.88	2.207	37.535	2.401
10	25.02	2.224	29.56	2.192	38.415	2.366
11	25.41	2.22	30.02	2.177	39.045	2.344
12	25.77	2.215	30.44	2.167	39.755	2.324
13	26.1	2.209	30.99	2.181	40.395	2.302
14	26.37	2.205	31.43	2.171	40.905	2.286
15	26.67	2.203	31.88	2.161	41.415	2.272
16	26.97	2.206	32.23	2.162	41.815	2.259
17	27.22	2.203	32.56	2.152	42.285	2.246
18	27.39	2.202	32.82	2.144	42.455	2.246
19	27.67	2.201	33.17	2.137	42.895	2.234
20	27.89	2.202	33.37	2.132	43.375	2.219
21	28.12	2.203	33.75	2.123	43.715	2.206
22	28.29	2.203				

Table B.3.4. Pump Cycle Pressures (kPa) for Canister 2 of Each Segment of Tank BY-109

Cycle	4-J2[a]		5-J2		6-J2	
	collector	extractor	collector	extractor	collector	extractor
pre-pumping	3.72	3.72	1.95	1.98	2.36	2.36
1			3.99	1.98	7.48	2.36
2			5.35	1.912	9.51	2.271
3			6.19	1.858	10.29	2.257
4			6.66	1.836	10.62	2.273
5			6.83	1.833	10.88	2.284
6			7.1	1.836	11.05	2.294
7			7.23	1.84	11.19	2.301
8			7.3	1.845	11.36	2.307
9			7.37	1.849	11.43	2.312
10			7.43	1.852	11.52	2.318
11			7.49	1.854	11.63	2.322
12			7.53	1.856	11.71	2.326
13			7.57	1.859	11.78	2.331
14			7.6	1.861	11.83	2.336
15			7.63	1.864	11.9	2.34
16			7.66	1.865	11.91	2.346
17			7.69	1.866	11.98	2.349
18			7.71	1.867	12.04	2.352
19			7.73	1.869	12.06	2.355
20	11.76	2.587	7.79	1.871	12.13	2.357

(a) The pressure data files for segment 4 were lost; however, logbook entries preserved the beginning and end pressures. These were interpolated between the endpoints to support mass-balance calculations.

Table B.3.5 shows the amounts of gases that are calculated based on the data presented earlier. Only ammonia has a large enough residual (amount left in the extractor side after extraction) to include in the table.

Table B.3.5. Quantities of Gases Found in Tank BY-109 Samples

Segment/ Canister	N_2 (µmol)	H_2 (µmol)	N_2O (µmol)	O_2 (µmol)	CH_4 (µmol)	He (µmol)
4-J1	432±27	292±18	181±11	2.5±0.2	8.2±1.3	109±7
4-J2[(a)]	129±25	2.3±0.4	5.0±1.0	57.3±10.9	0.19±0.04	272±52
4-TOTAL[(a)]	561±51	294±19	186±12	60±11	8.4±1.3	381±59
5-J1	376±22	605±34	204±12	1.5±0.1	7.48±0.43	118±6.5
5-J2[(a)]	53±12	47±10	13±2.9	15.5±3.39	1.16±0.38	8.8±1.9
5-TOTAL[(a)]	429±33	653±45	217±15	17±3.5	8.6±0.8	127±8
6-J1	451±23	996±50	316±16	1.2±0.1	15.4±0.75	95±5
6-J2[(a)]	38±7.7	51±10	13.3±2.7	13.0±2.6	0.75±0.15	4.8±0.9
6-TOTAL[(a)]	490±31	1047±61	330±19	14±2.7	16±0.9	100±6

(a) An isotopic standard and a little inleaked air were added before this canister; the total and residual ammonia exclude the ^{15}N standard. In addition, there was an air leak between canisters J1 and J2 of segment 4, and helium was added to measure the bulk sample volume.

Table B.3.5 (contd)

Segment/ Canister	Ar (µmol)	Other NOx (µmol)	C_2H_x (µmol)	C_3H_x (µmol)	Other HC (µmol)	NH_3 (µmol)
4-J1	2.0±0.12	0.12 ±0.12	5.85±1.22	0.97±0.06	5.85±1.22	288±107
4-J2	5.3±1.0	0.06±0.06	1.35±0.36	0.55±0.17	3.31±0.72	0±0
4-residual[(a)]						2488±577
4-TOTAL[(a)]	7.3±1.1	0.2±0.2	7.2±1.6	1.5±0.2	9.2±1.9	2776±684
5-J1	2.4±0.1	0. 16±0.16	6.69±0.39	1.11±0.17	6.53±0.39	574±175
5-J2	0.93±0.20	0.04±0.04	2 .11±0.47	0.44±0.11	4.83±1.14	0±0
5-residual[(a)]						3322±809
5-TOTAL[(a)]	3.3±0.3	0.2±0.2	8.8±0.9	1.6±0.3	11±2	3895±985
6-J1	3.65±0.18	0.21±0.21	23. 2±2.4	1.90±0.23	14.76±1.63	402±134
6-J2	0.84±0.17	0.04±0.04	1.4±0.3	0.78±0.18	6.4±1.5	0±0
6-residual[(a)]						1285±291
6-TOTAL[(a)]	4.5±0.4	0.3±0.3	25±3	2.7±0.4	21±3	1686±425

(a) An isotopic standard and a little inleaked air were added before this canister; the total and residual ammonia exclude the ^{15}N standard. In addition, there was an air leak between canisters J1 and J2 of segment 4, and helium was added to measure the bulk sample volume.

Table B.3.6. Mole Percents of Gases in Tank BY-109 Dry Insoluble Gas

Segment/ Canister	N_2	H_2	N_2O	O_2	CH_4	He
4-J1	41.5	28.0	17.4	0.2	0.79	10.4
4-J2[(a)]	27.2	0.5	1.0	12.0	0.04	57.2
5-J1	28.1	45.2	15.2	0.1	0.56	8.81
5-J2[(a)]	35.7	31.8	8.9	10.4	0.78	5.88
6-J1	23.5	51.9	16.5	0.1	0.80	4.95
6-J2[(a)]	29.3	39.2	10.2	9.9	0.57	3.64

(a) An isotopic standard and a little inleaked air were added before this canister. In addition, there was an air leak between canisters J1 and J2 of segment 4, and helium was added to measure the bulk sample volume.

Table B.3.6 (contd)

Segment/ Canister	Ar	Other NOx	C_2H_x	C_3H_x	Other HC
4-J1	0.19	0.01	0.56	0.09	0.56
4-J2[(a)]	1.11	0.01	0.28	0.11	0.70
5-J1	0.18	0.01	0.50	0.08	0.49
5-J2[(a)]	0.62	0.03	1.41	0.29	3.24
6-J1	0.19	0.01	1.21	0.10	0.77
6-J2[(a)]	0.64	0.03	1.04	0.60	4.89

(a) An isotopic standard and a little inleaked air were added before this canister. In addition, there was an air leak between canisters J1 and J2 of segment 4, and helium was added to measure the bulk sample volume..

As discussed in Section 3.3, the amount of condensed water and dissolved ammonia in the collector (under pumped conditions) were found by thermodynamic analysis, as were the water and ammonia vapor pressures in the collector. Table B.3.7 contains these variables.

Table B.3.7. Collector Ammonia and Water Contents for Tank BY-109 Sample Cycling

Segment/ Canister	Vapor pressure of NH_3 (kPa)	Vapor pressure of water (kPa)	µmoles of condensed NH_3	µmoles of condensed water
4-J1	2.78	3.00	126	8085
4-J2[a]	2.20	3.30	105	9478
5-J1	4.95	2.80	263	7228
5-J2[a]	3.22	2.92	120	6241
6-J1	3.67	2.96	175	7771
6-J2[a]	6.24	3.13	348	7686
(a) An isotopic standard was added before this canister.				

In order to estimate the void fraction and the distribution of gases between the void and slurry phases in each segment, the conditions under which the gas exists must be known. These are given in Table B.3.8 for Tank BY-109. The densities were averages of the measured bulk densities in the other (the non-RGS) samples in the cores.[a] The temperatures were based on a single measurement. The pressures were derived from hydrostatic head, and are based on the depth of submergence of the segment and the thicknesses and gas-free densities of the waste layers. The solid volume fraction is estimated using 1500 kg/m^3 as the density of solid-free liquid, 1730 kg/m^3 as the density of gas-free slurry, and an assumed 2000 kg/m^3 as the intrinsic (not bulk) density of the solid material.

The water vapor pressure is the pressure in equilibrium with water in the waste; it is calculated using Equation 6.2 and Table 6.2 of Mahoney and Trent (1995), a correlation for water vapor pressure over concentrated homogeneous and non-homogeneous waste simulants. This correlation requires the weight fraction of water in the slurry, which is calculated using the solid volume fraction in the gas-free waste, the solution density, and the weight fraction of water in the solids-free solution. The latter value was set at 0.531, based on data for the drainable liquids in non-RGS samples taken at the same time and in the same cores.[a]

Table B.3.8. In-Tank Conditions Used for Tank BY-109 Phase Distribution Calculations

Segment	Density (kg/m^3)	Temperature (°C)	Pressure (atm)	Solid Volume Fraction	Water Vapor Pressure (atm)
4	1730	30.7	1.26	0.46	0.0105
5	1730	30.7	1.33	0.46	0.0105
6	1730	30.7	1.41	0.46	0.0105

(a) Esch R. July 29, 1997, and August 6, 1997. Transmittals from R Esch to LA Mahoney (PNNL) of data collected for the BY-109 TCR (document in preparation). Lockheed Martin Hanford Corporation, Richland, Washington.

The average ionic concentrations in the drainable liquid in Tank BY-109 are given in Table B.3.9. They were based on non-RGS samples from the same cores.(a)

The Henry's Law constants are necessary to estimate the in-tank phase distribution of gases (see Section 3.5). The intermediate steps in the Henry's Law constant calculation are shown in Table B.3.10. Note that the final Henry's Law constant is in terms of liters of gas-free waste slurry, while the Schumpe model is in terms of kg of water in the salt solution. Both the solid volume fraction and the weight percent of water in the solution are needed to put the Henry's Law constant in its final form. The gases not listed, argon, helium, and the minor gases, were assumed wholly insoluble with Henry's law constants of 10^{-10}.

Table B.3.9. Ionic Concentrations Used for Tank BY-109 Phase Distribution Calculations

Ion	gmol/L solution
Na^+	9.11
Al^{3+}	1.44
Fe^{3+}	0
Cr^{3+}	0.01
Ni^{2+}	0
K^+	0.15
OH^-	5.07
NO_3^-	3.07
NO_2^-	1.80
CO_3^{2-}	0.21
PO_4^{3-}	0.01
SO_4^{2-}	0.01
F^-	0.05
Cl^-	0.13

(a) Esch R. July 29, 1997, and August 6, 1997. Transmittals from R Esch to LA Mahoney (PNNL) of data collected for the BY-109 TCR (document in preparation). Lockheed Martin Hanford Corporation, Richland, Washington.

Table B.3.10. Henry's Law Constants For Tank BY-109 Phase Distribution Calculations

Segment	Condition	N_2	H_2	N_2O	O_2	CH_4	NH_3
4	Schumpe (K in water/K in solution)	84.0	33.3	60.4	95.0	100	10.1
	Waste Slurry K (mol/atm L waste)	3.1×10^{-6}	9.8×10^{-6}	1.5×10^{-4}	5.3×10^{-6}	5.6×10^{-6}	1.99
5	Schumpe (K in water/K in solution)	84.0	33.3	60.4	95.0	100	10.1
	Waste Slurry K (mol/atm L waste)	3.1×10^{-6}	9.8×10^{-6}	1.5×10^{-4}	5.3×10^{-6}	5.6×10^{-6}	1.99
6	Schumpe (K in water/K in solution)	84.0	33.3	60.4	95.0	100	10.1
	Waste Slurry K (mol/atm L waste)	3.1×10^{-6}	9.8×10^{-6}	1.5×10^{-4}	5.3×10^{-6}	5.6×10^{-6}	1.99

B.4 References

Mahoney LA and DS Trent. 1995. *Correlation Models for Waste Tank Sludges and Slurries.* PNL-10695, Pacific Northwest Laboratory, Richland, Washington.

Norton JD and LR Pederson. 1994. *Ammonia in Simulated Hanford Double-Shell Tank Wastes: Solubility and Effects on Surface Tension.* PNL-10173, Pacific Northwest Laboratory, Richland, Washington.

Norton JD and LR Pederson. 1995. *Solubilities of Gases in Simulated Tank 241-SY-101 Wastes.* PNL-10785, Pacific Northwest Laboratory, Richland, Washington.

Schumpe A. 1993. "The Estimation of Gas Solubilities in Salt Solutions." *Chem. Eng. Sci.*, 48:153.

Appendix C

Field Operations Data

M. E. Dahl

Appendix C

Field Operations Data

Field logs, the T-0-080-503 procedure documents for sampling, and other primary sources (found in LMHC's working archive files) provided information about the observations made and methods used to acquire retained gas sampler (RGS) samples from the tanks. This information, which includes time and date, push forces, addition of hydrostatic head fluid, and dose Through the drill string, is given in Tables C.1 Through C.7.

Table C.1. RGS Field Data Summary Sheet for Tank U-103, Riser 7

Sampler Serial Number ********** Cask Serial Number ********** Sample Number XX/XXX/Date	Time and Date of Sampling (Just After Pintle-rod Has Been Pulled) **	Max Force to Unseat Sampler Sampler Removal from Tank - Time and Date	Purge Gas ********** Amount (Type) ********** Time	Amount of Hydrostatic Head Fluid Added	Radiation Dose Reading Through Drill String	Field Ops Notes Downforce
RGS-055 seg 2 C 2015 96-525	1906 hr 1-21-97	111 lb 1919 hr 1-21-97	No purge gas recorded on J-5	1500 mL lithium bromide	1.4 rem\hr	5000 lb
RGS-054 seg 5 C-1036 96-528	0618 hr 1-22-97	105 lb 0636 hr 1-22-97	No purge gas recorded on J-5	1500 mL lithium bromide	1.6 rem\hr	4300 lb
RGS-046 seg 7 69 96-530	1750 hr 1-22-97	118 lb 1810 hr 1-22-97	No purge gas recorded on J-5	1500 mL lithium bromide	1.4 rem\hr	3400 lb
RGS-049 seg 8 IC04-C 96-531	1916 hr 1-21-97	117 lb 1935 hr 1-21-97	No purge gas recorded on J-5	1500 mL litium bromide	1.3 rem\hr	3000 lb
RGS-051 seg 9 C-1049 96-S32	2030 hr 1-21-97	110 lb 2100 hr 1-21-97	No purge gas recorded on J-5	????	230 mrem\hr	2500 lb

Table C.2. RGS Field Data Summary Sheet for Tank U-103, Riser 13

Sampler Serial Number ********** Cask Serial Number ********** Sample Number XX/XXX/Date	Time and Date of Sampling (Just After Pintle-rod Has Been Pulled) **	Max Force to Unseat Sampler Sampler Removal from Tank - Time and Date	Purge Gas ********** Amount (Type) ********** Time	Amount of Hydrostatic Head Fluid Added	Radiation Dose Reading Through Drill String	Field Ops Notes Downforce
RGS-057 seg 4 23 97-020	1319 hr 4-2-97	182 lb 1323 hr 4-2-97	No purge gas recorded on J-5	1500 mL lithium bromide	700 mrem\hr	4000 lb

Table C.3. RGS Field Data Summary Sheet for Tank S-106, Riser 7

Sampler Serial Number ********** Cask Serial Number ********** Sample Number XX/XXX/Date	Time and Date of Sampling (Just After Pintle-rod Has Been Pulled) ** 	Max Force to Unseat Sampler Sampler Removal from Tank - Time and Date	Purge Gas ********** Amount (Type) ********** Time	Amount of Hydrostatic Head Fluid Added	Radiation Dose Reading Through Drill String	Field Ops Notes Downforce
RGS-063 seg 3 10-6 97-40	2000 hr 2-24-97	170 lb 2020 hr 2-24-97	No J-5 Data logged on 2-24-97	1500 mL lithium bromide	1.2 rem\hr	3500 lb
RGS-062 seg 5 69 97-38	0325 hr 2-25-97	171 lb 0355 hr 2-25-97	No J-5 Data logged on 2-25-97	1500 mL lithium bromide	1.2 rem\hr	2800 lb

Table C.4. RGS Field Data Summary Sheet for Tank S-106, Riser 8

Sampler Serial Number ********** Cask Serial Number ********** Sample Number XX/XXX/Date	Time and Date of Sampling (Just After Pintle-rod Has Been Pulled) **	Max Force to Unseat Sampler Sampler Removal from Tank - Time and Date	Purge Gas ********** Amount (Type) ********** Time	Amount of Hydrostatic Head Fluid Added	Radiation Dose Reading Through Drill String	Field Ops Notes Downforce
RGS-044 seg 2 C 2018 97-31	2010 hr 2-12-97	180 lb 2020 hr 2-12-97	No purge gas data	1500 mL lithium bromide	800 mrem\hr	3800 lb
RGS-061 seg 6 68 97-31	0410 hr 2-18-97	180 lb 0420 hr 2-18-97	No purge gas data	1500 mL lithium bromide	900 mrem\hr	2500 lb
RGS-056 seg 10 60 97-35	0313 hr 2-21-97	233 lb 2045 hr 2-21-97	Drill string argon purge done on swing 2-21-97 @ 18:50 hr and 20:00 hr	none	1 rem\hr	1700 lb

Table C.5. RGS Field Data Summary Sheet for Tank S-106, Riser 14

Sampler Serial Number ********** Cask Serial Number ********** Sample Number XX/XXX/Date	Time and Date of Sampling (Just After Pintle-rod Has Been Pulled) **	Max Force to Unseat Sampler Sampler Removal from Tank - Time and Date	Purge Gas ********** Amount (Type) ********** Time	Amount of Hydrostatic Head Fluid Added	Radiation Dose Reading Through Drill String	Field Ops Notes Downforce
RGS-059 seg 2 1004-C 97-051	0956 hr 3-20-97	195 lb 1020 hr 3-20-97	No purge gas data	1500 mL lithium bromide	15 mrem\hr	4000 lb

Notes: RGS samples were planned for riser 13 segments 5, 8 and 12; these segments were not acquired.

Table C.6. RGS Field Data Summary Sheet for Tank BY-109, Riser 10B

Sampler Serial Number ********** Cask Serial Number ********** Sample Number XX/XXX/Date	Time and Date of Sampling (Just After Pintle-rod Has Been Pulled)	Max Force to Unseat Sampler Sampler Removal from Tank - Time and Date	Purge Gas ********** Amount (Type) ********** Time	Amount of Hydrostatic Head Fluid Added	Radiation Dose Reading Through Drill String	Field Ops Notes Downforce
RGS-074 seg 2 23-G 203-02	1805 hr 6-16-97	203 lb 1815 hr 6-16-97	No puge gas data	1500 mL lithium bromide	70 mrem\hr	2600 lb
RGS-073 seg 5 S/N-76 203-05	2013 hr 6-16-97	213 lb 2028 hr 6-16-97	No purge gas data	1500 mL lithium bromide	310 mrem\hr	2000 lb
RGS-068 seg 6 S/N 58 203-6	2058 hr 6-16-97	278 lb 0142 hr 6-17-97	No purge gas data	1500 mL lithium bromide	280 mrem\hr	1800 lb

Table C.7. RGS Field Data Summary Sheet for Tank BY-109, Riser 12C

Sampler Serial Number ********** Cask Serial Number ********** Sample Number XX/XXX/Date	Time and Date of Sampling (Just After Pintle-rod Has Been Pulled) **	Max Force to Unseat Sampler Sampler Removal from Tank - Time and Date	Purge Gas ********** Amount (Type) ********** Time	Amount of Hydrostatic Head Fluid Added	Radiation Dose Reading Through Drill String	Field Ops Notes Downforce
RGS-066 seg 1 18G 2101-4	1039 hr 6-6-97	190 lb 1309 hr 6-6-97	No purge gas data	1488 mL lithium bromide	42 mrem\hr	2700 lb
RGS-070 seg 4 77 201-4	1504 hr 6-12-97	172 lb 1803 hr 6-12-97	No purge gas data	1500 mL lithium bromide	350 mrem\hr	2000 lb

Note: An RGS sample was planned for riser 12C segment 6; this segment was not obtained.

Distribution

No. of Copies

Offsite

2 DOE Office of Scientific and Technical Information

E. K. Barefield
Georgia Institute of Technology
Boggs Chemistry Building
225 North Avenue
Atlanta, GA 30332

M. J. Barnes
Savannah River Site
Aiken, SC 29802

D. O. Campbell
102 Windham Road
Oak Ridge, TN 37830

S. J. Eberlein
Westinghouse Savannah River
241-12H
Aiken, SC 29802

C. W. Forsberg
Oak Ridge National Laboratory
P.O. Box 2008, MS-6495
Oak Ridge, TN 37831-6495

B. C. Hudson
P.O. Box 271
Lindsborg, KS 67456

M. S. Kazimi
Massachusetts Institute
of Technology
Department of Nuclear Engineering
77 Massachusetts Avenue
Cambridge, MA 02139

J. L. Kovach
P.O. Box 29151
70000 Huntley Road
Columbus, OH 43229

No. of Copies

T. S. Kress
102-B Newridge Road
Oak Ridge, TN 37830

T. E. Larson
2711 Walnut St.
Los Alamos, NM 87545

4 Los Alamos National Laboratory
P.O. Box 1663
Los Alamos, NM 87545
Attn: W. L. Kubic K575
C. Unal K575
J. R. White K575

D. Meisel
Argonne National Laboratory
Chemistry Division
9700 S. Cass Avenue
Argonne, IL 60439

D. Pepson
U.S. Department of Energy
Trevion II Building, EM-35
Washington, D.C. 20585-0002

D. A. Powers
Sandia National Laboratory
Nuclear Facilities Safety Department
MS-0744
Albuquerque, NM 87185-0744

W. R. Rossen
University of Texas at Austin
Department of Petroleum/ Geosystems
Engineering
Austin, TX 78712

S. E. Slezak
806 Hermosa NE
Albuquerque, NM 87110

H. Babad
2540 Cordoba Ct.
Richland, WA 99352

No. of Copies

Onsite

6 DOE Richland Operations Office

K. Chen	S7-54
C. A. Groendyke	S7-54
G. W. Hood	S7-73
G. M. Neath	K8-50
J. C. Peschong	S7-54
G. W. Rosenwald	S7-54
C. L. Sohn	S7-51

55 PHMC Team

R. P. Anantatmula	R1-30
S. A. Barker	R2-11
G. S. Barney	T5-12
W. B. Barton	R2-11
R. E. Bauer (10)	S7-14
C. J. Benar	R2-12
R. J. Cash	S7-14
N.S. Cannon	L6-38
A.F. Choho	H6-35
M. L. Dexter	R1-51
J. G. Field	R2-12
K. A. Gasper	G3-21
T. C. Geer	R1-43
J. M. Grigsby	R1-49
B. E. Hey	T6-07
D.C. Hedengren	R2-11
K. M. Hodgson	H0-34
T. A. Hu	R2-12
J. R. Jewett	T6-07
J. Jo	R2-12
G. D. Johnson	S7-15
N. W. Kirch	R2-11
P. F. Kison	T4-07
G. M. Koreski	R2-11
J. G. Kristofzski	R2-12
C. E. Leach	R1-49
J. W. Lentsch	S2-48
C.G. Linschooten	S7-12
L. L. Lockrem	S3-90
J. E. Meacham	S7-14
W. H. Meader	S8-05
G. L. Miller	T6-06
N. J. Milliken	A3-37
J. C. Person	T6-09
R. E. Raymond	S7-12
D. A. Reynolds	R2-11
L.M. Sasaki	R2-12
E. R. Siciliano	HO-31
B. C. Simpson	R2-12
L. M. Stock	S7-14
R. R. Thompson	R2-12
J. E. Van Beek	S2-48
R. J. Van Vleet	A3-34
A. B. Webb	A3-37
N. E. Wilkins	R2-11
A. E. Young	R1-10

44 Pacific Northwest National Laboratory

Z. I. Antoniak	K7-15
J. M. Bates	K7-15
B. O. Barnes	P7-41
S. Q. Bennett	K7-90
J. W. Brothers (10)	K9-20
S. A. Bryan	P7-25
B. C. Bunker	K2-25
J. A. Fort	K7-15
P. A. Gauglitz	P7-41
J. L. Huckaby	K6-80
L. A. Mahoney (10)	K7-15
P. A. Meyer	K7-15
B. J. Palmer	K7-15
L. R. Pederson	K2-44
L.M. Peurrung	P7-41
S. D. Rassat	P7-41
K. P. Recknagle	K7-15
D. R. Rector	K7-15
A. Shekarriz	K7-15
C. W. Stewart	K7-15
G. Terrones	K7-15
Information Release (5)	K6-06